

Neural Correlates of Parkinsonian Syndromes

Der Fakultät für Lebenswissenschaften
der Universität Leipzig
genehmigte
D I S S E R T A T I O N
zur Erlangung des akademischen Grades
doctor rerum naturalium
Dr. rer. nat.

vorgelegt

von Franziska Albrecht, M. Sc.

geboren am 23.10.1990 in Leipzig

Dekan:

Prof. Dr. Tilo Pompe

Gutachter:

Prof. Dr. Rudolf Rübsamen

Prof. Dr. Thilo van Eimerern

Tag der Verteidigung: 4. Oktober 2019

SELBSTSTÄNDIGKEITSERKLÄRUNG GEMÄSS § 7(2) DER PROMOTIONSORDNUNG

Hiermit erkläre ich, Franziska Albrecht, dass ich die vorliegende Arbeit in allen Teilen selbständig verfasst und keine anderen als die angegebenen Quellen und Hilfsmittel (einschließlich elektronischer Medien und Online-Quellen) benutzt habe. Die aus fremden Quellen direkt (als Zitate) oder indirekt (dem Sinn nach) übernommenen Textstellen und Gedanken sind in der Arbeit als solche kenntlich gemacht worden.

Bei der Konzeption der Experimente, der Datenanalyse sowie der Erstellung der Manuskripte wurde ich durch meine Betreuer Matthias L. Schroeter und Karsten Müller und meine Kollegen Tommaso Ballarini und Jane Neumann beraten; die Anteile aller Co-Autoren an den Manuskripten sind gesondert beschrieben. An der geistigen Erstellung dieser Dissertation waren keinerlei weitere Personen beteiligt. Darüber hinaus hat niemand unmittelbar oder mittelbar geldwerte Leistungen für Arbeiten im Zusammenhang mit dem Inhalt der vorliegenden Dissertation erhalten.

Ich versichere hiermit weiterhin, dass weder die gesamte Arbeit noch Teile der Arbeit (oder jegliche andere Art der Prüfungsleistung) in dieser oder ähnlicher Form jemals einer Prüfungsbehörde vorlagen.

Es haben keine früheren erfolglosen Promotionsversuche stattgefunden.

Leipzig, Juli 2019

ACKNOWLEDGMENTS

This PhD thesis would not have been possible without the help and support of many people.

First and foremost, I would like to honor all patients and relatives that made my studies possible. Neurodegenerative diseases are devastating and have a huge impact on quality of life. Hence, it needs patients that dedicate their time to participate in research.

I would like to thank Professor Rudolf Rübsamen at the University of Leipzig for not just teaching me neurobiology during my studies at the university and supervising my thesis but also for supporting me to pursue an academic career.

I am really grateful to Professor Matthias L. Schroeter for supervising me at the Max-Planck-Institute. He supported, helped, and advised me whenever I needed it throughout the course of my doctoral studies. Prof. Schroeter gave me scientific supervision and revised my thesis. He also created an amicable atmosphere in which we can share the passion for research, travel to conferences abroad and interest in animal watching - never forget to be cass-o-wary!

Additionally, I am appreciative of Professor Karsten Müller and Jane Neumann for help me to learn the statistical procedures for analyzing MRI and giving me advices that helped me writing my thesis.

Finally, I would also like to thank all my friends and colleagues of the Cognitive Neuropsychiatry research group and the Neurology department.

Last but not least, I would like to express my gratitude towards my mum for always backing me up and making it possible that I can pursue such a career. I also value the provided work-life balance by Iko.

SUMMARY

Franziska Albrecht

Neural Correlates of Parkinsonian Syndromes

Fakultät für Lebenswissenschaften

Universität Leipzig

Dissertation

Introduction

The incidence and prevalence of neurodegenerative diseases - defined as early loss of specific neurons (Graeber and Moran, 2002) - rises with age (Muangpaisan et al., 2011), representing a major burden in a worldwide aging society. Indeed, 10 to 13 per 100,000 persons yearly are diagnosed with Parkinson's disease (Muangpaisan et al., 2011). Parkinsonian syndromes are often misdiagnosed and mixed up in clinical diagnosis, especially in the early beginning of the disease. Generally, diagnostic decision-making primarily depends on clinical variables. Hence, generalized, quantifiable image-based markers to independently and accurately diagnose patients are missing. In parkinsonian syndromes, if included at all, imaging is used as supportive or exclusion criterion. In other neurodegenerative disease, diagnostic criteria are amended and include recent findings of disease-related brain alterations (Albert et al., 2011; Dubois et al., 2014; Gorno-Tempini et al., 2011; Rascovsky et al., 2011). Parkinson's disease represents the typical appearance of parkinsonian syndromes. Parkinsonism describes the core symptoms of Parkinson's disease: bradykinesia and additionally rest tremor or rigidity. Slowness of movements and a decrease in speed during performance of movements characterizes bradykinesia, rest tremor is described by a shaking when inactive, and rigidity refers to resistance to superficially imposed limb movements (Williams and Litvan, 2013). Further, non-motor symptoms such as mild cognitive impairment, fatigue, and visual hallucinations can be present. Concerning diagnostic decision-making, only dopaminergic imaging is well-established, other imaging biomarkers have not been validated yet, even though they could improve diagnostic accuracy. Stratified into several subgroups, parkinso-

nian syndromes encompass diseases with similar clinical features but varying neuropathologies. This network includes scarce entities such as corticobasal degeneration and progressive supranuclear palsy: atypical parkinsonian syndromes and neurodegenerative diseases, only confirmed by their tau protein-based histopathology. Motor features of postural instability, early falls, and eye-movement impairment indicate progressive supranuclear palsy (McFarland, 2016). A well-known but not yet validated pathognomonic marker is atrophy in the midbrain and cerebellar pedunculi. Recently, clinical diagnostic criteria were amended (Höglinger et al., 2017), only considering 'predominant midbrain atrophy or hypometabolism' as a supportive imaging criterion. Hence, diagnosis of progressive supranuclear palsy mainly depends on clinical evaluation. Corticobasal degeneration is clinically described by corticobasal syndrome. However, only 25% to 56% of corticobasal degeneration cases are predicted ante-mortem (Armstrong et al., 2013). Most frequent motor symptoms in post-mortem proven corticobasal degeneration include limb rigidity and bradykinesia but also cognitive decline and behavioral changes are common (Armstrong et al., 2013). A really specific and peculiar symptom is the alien/anarchic limb phenomenon. About 30% of patients with corticobasal syndrome experience an extremity as rogue or foreign, which performs well-executed but purposeless movements. Identifying disease-specific features of corticobasal degeneration remains ongoing research, restricting the ability to develop definitive clinical criteria foreseeing the pathology. The clinical diagnostic criteria were recently revisited, yet, imaging as a criterion to support diagnosis was not included (Armstrong et al., 2013).

My aim was to investigate objective neuroimaging biomarkers in parkinsonian syndromes, which could be used to increase diagnostic accuracy. I apply three approaches to extract the neural correlates and disease-specific patterns: (1) meta-analysis to find convergence among smaller cohort studies, (2) voxel-based morphometry to identify structural differences between patients and controls, and (3) support-vector machine classification to predict the disease individually. We hypothesized to find disease-specific atrophy that disentangle the parkinsonian syndromes.

Results

Identifying Disease-Specific Patterns by Meta-Analyses. To find convergence of the literature concerning disease-specific patterns with a powerful statistical evaluation, we conducted meta-analyses. We investigated the prototypical neural correlates of 1,767 patients with Parkinson's disease and 210 patients with progressive supranuclear palsy (Study 1 & 2, Albrecht et al. (2018, 2019a)). In Parkinson's disease [18F]-fluorodeoxyglucose - positron emission tomography (FDG-PET) revealed glucose hypometabolism in bilateral inferior parietal cortex and left caudate nucleus. Minor focal gray matter atrophy in the middle occipital gyrus was detected by the means of whole-brain structural magnetic resonance imaging (MRI). In progressive supranuclear palsy meta-analyses identified gray matter atrophy of the midbrain and white matter atrophy of the cerebral/cerebellar pedunculi and midbrain. In Parkinson's disease we evidenced that FDG-PET overcomes MRI as potential biomarker. In progressive supranuclear palsy we validated pathognomonic markers, which can be seen as disease-specific, as we compared results with other published meta-analyses on neurodegenerative diseases. Our studies create a novel conceptual framework to investigate disease-specific alterations for application in clinical routine by data-driven meta-analytic approaches.

Obtaining Disease-Related Regions and Classifying the Disease by Voxel-Based Morphometry and Support-Vector Machine. To individualize diagnostic and treatment protocols, we investigated neural correlates and discriminated disease and clinical syndrome in single patients. Multi-centric group data of patients with the clinical phenotype of corticobasal syndrome and corticobasal syndrome with a unique symptom - alien/ anarchic limb phenomenon - was acquired. 3T T_1 -weighted structural MR images of 25 corticobasal syndrome patients, 8 patients with corticobasal syndrome and alien/ anarchic limb phenomenon, and 25 healthy controls were analyzed. To identify neural underpinnings, we performed voxel-based morphometry: a widely used method to investigate structural alterations like atrophy in patients. A multivariate pattern recognition algorithm - support-vector machine classification - was trained to predict (i) corticobasal syndrome patients and healthy controls and to differentiate (ii)

between patients just having corticobasal syndrome and patients with corticobasal syndrome having alien/ anarchic limb syndrome. Voxel-based morphometry revealed gray matter volume differences between patients and controls in asymmetric frontotemporal and occipital regions, motor areas, and the insulae. The frontoparietal gyrus including the supplementary motor area contralateral to the side of the affected limb was specific for alien/ anarchic limb syndrome. The prediction of the disease among controls was 79.0% accurate. The prediction of the specific syndrome within a disease reached an accuracy of 81.3%. Applying a meta-analytical mask lead to similar stable results (Albrecht et al. (2017)). Because of two classification groups, 50% represents chance level. We reliably classified patients and controls by objective pattern recognition. Moreover, we were able to predict a specific clinical syndrome within a disease, shown even in a small sample.

Discussion

By systematic and quantitative meta-analyses we statistically validated convergence of published results for neurodegenerative diseases. In Parkinson's disease glucose hypometabolism in bilateral inferior parietal cortex and left caudate nucleus is more specific than structural brain atrophy. In progressive supranuclear palsy we verified that midbrain and cerebral/ cerebellar pedunculi atrophy can be seen as disease-characteristic. By applying machine learning we identified diseased and healthy individuals as well as predict a symptom within a clinical syndrome. Additionally for classification, we implemented a meta-analytical mask from a former study, which lead to the same stable results (Albrecht et al. (2017)).

So far, disease diagnosis relies on experts and careful observation of patients and their disease progression. Especially, atypical parkinsonian syndromes are often misdiagnosed in the beginning of the disease course. Correct and also early diagnosis plays a crucial role for treatment-decision and hence symptom relief. A plethora of diagnostic criteria were already updated by including disease-specific brain alterations (Albert et al., 2011; Dubois et al., 2014; Gorno-Tempini et al., 2011; Rascovsky et al., 2011). Diagnostic criteria for Parkinson's disease, progressive supranuclear palsy, and corticobasal degeneration have been revisited recently but only include

the factor of objective medical imaging as supportive or exclusion criteria. Including our proposed regional-atrophy patterns would considerably advance disease diagnosis. Indeed, in frontotemporal lobar degeneration and Alzheimer's disease studies evidence that for both diseases the neuroimaging patterns considerably increased diagnostic accuracy as compared to clinical evaluation (Rascovsky et al., 2002; Dubois et al., 2007; Kipps et al., 2009). Hence, incorporation into diagnostic criteria was advised. The proposed neuroimaging biomarker still need to be validated in independent cohorts and on a single-patient level. An example where imaging criteria have been verified is primary progressive aphasia: diagnostic imaging criteria were proposed by Gorno-Tempini et al. (2011) based on previous neuroimaging studies and later statistically validated by independent meta-analyses (Bisenius et al., 2016). In primary progressive aphasia, imaging-supported diagnosis is even considered as the next level of classification. Hence, patients need to meet clinical criteria plus showing the neuroimaging patterns. Bisenius et al. (2016) confirmed that concerning MRI changes, the neuroimaging criteria are highly distinctive.

Conclusion

My thesis contributes objective disease-specific patterns and their application to better disease diagnosis. For progressive supranuclear palsy we proposed regional atrophy in midbrain and cerebral/ cerebellar pedunculi as specific disease-related pattern, supporting the incorporation into diagnostic criteria. In Parkinson's disease hypometabolism is more sensitive than structural atrophy, nevertheless not disease-specific. By using disease-specific patterns as mask and whole-brain data, we showed stable classification results, discriminating patients from controls and even predicting symptoms within clinical syndromes.

Zusammenfassung

Franziska Albrecht

Neurale Korrelate der Parkinson-Syndrome

Fakultät für Lebenswissenschaften

Universität Leipzig

Dissertation

Einleitung

Inzidenz und Prävalenz neurodegenerativer Erkrankungen, definiert als vorzeitiger Verlust spezifischer Neurone (Graeber and Moran, 2002), steigen mit dem Alter (Muangpaisan et al., 2011). Jährlich werden bei 10 bis 13 von 100.000 Personen die idiopathische Parkinson-Krankheit diagnostiziert (Muangpaisan et al., 2011). Der Parkinsonismus beschreibt die Kardinalsymptome des Parkinson-Syndroms: Bradykinese und zusätzlicher Ruhetremor oder Rigor. Eine Bradykinese ist charakterisiert durch verlangsamte Bewegungen, Ruhetremor beschreibt Zittern bei Inaktivität und Rigor ist eine Art Muskelsteifheit bzw. Starre (Williams and Litvan, 2013). Darüber hinaus können auch nicht-motorische Symptome wie eine leichte kognitive Beeinträchtigung und visuelle Halluzinationen auftreten. Bezüglich der Diagnose ist nur die dopaminerge Bildgebung ein routinemäßig anerkanntes Bildgebungsverfahren. Weitere Bildgebungsmarker wurden bis jetzt noch nicht systematisch validiert, trotz ihres möglichen Potentials die Diagnosegenauigkeit zu erhöhen. Das idiopathische Parkinson-Syndrom stellt die typische und häufigste Erkrankung innerhalb des Spektrums der Parkinson-Syndrome dar. Diese Syndrome werden in Gruppen unterteilt, die ähnliche klinische Eigenschaften teilen, aber in der Neuropathologie variieren. Das Spektrum umfasst seltene Erkrankungen wie die kortikobasale Degeneration und die progressive supranukleäre Blicklähmung. Sie sind atypische Parkinson-Syndrome und neurodegenerative Erkrankungen, welche nur histologisch durch ihre Tau-Protein Pathologie diagnostiziert werden können. Motorische Symptome wie die posturale Instabilität, frühzeitige Stürze und Augenmotorikstörungen weisen auf die progressive supranukleäre Blicklähmung hin (McFarland, 2016). Ein bekannter, aber nicht sys-

tematisch validierter, pathognomonischer Marker ist die Atrophie des Mittelhirns. In die kürzlich revidierten Diagnosekriterien wurde nur eine „prädominante Mittelhirnatrophie oder Hypometabolismus“ als unterstützendes Bildgebungskriterium aufgenommen (Höglinger et al., 2017). Daher beruht die Diagnose der progressiven supranukleären Blicklähmung weiterhin auf der klinischen Einschätzung. Die kortikobasale Degeneration ist klinisch als kortikobasales Syndrom definiert. Es werden nur 25% bis 56% der Fälle kortikobasaler Degeneration tatsächlich ante mortem prädiagnostiziert (Armstrong et al., 2013). Zu den Symptomen post mortem validierter, kortikobasaler Degeneration zählen Rigor der Extremitäten, Bradykinese, aber auch kognitive Beeinträchtigungen und Verhaltensänderungen (Armstrong et al., 2013). Ein spezifisches und außergewöhnliches Symptom stellt das Alien/ anarchische Extremitäten-Phänomen dar. Circa 30% der Patienten mit kortikobasalem Syndrom beschreiben solch eine fremde/ selbstständige Extremität, die zielgerichtete, aber zwecklose Bewegungen ausführt. Auch diese klinischen Kriterien wurden revidiert, wobei jedoch die Bildgebung für die Diagnose unberücksichtigt gelassen wurde (Armstrong et al., 2013). Generell bleibt die Diagnose hauptsächlich von klinisch erfassten Variablen abhängig. Daher gilt es generalisierbare, bildgebende Marker zur objektiven und akkuraten Diagnose zu validieren. Besonders bezüglich der Parkinson-Syndrome ist, wenn überhaupt, die Bildgebung nur als unterstützendes oder Ausschlußkriterium vertreten. Die kürzlich revidierten Kriterien anderer neurodegenerativer Erkrankungen schließen jedoch in die Diagnostik aktuelle Ergebnisse krankheitsspezifischer Hirnveränderungen ein (Albert et al., 2011; Dubois et al., 2014; Gorno-Tempini et al., 2011; Rascovsky et al., 2011). Die vorliegende Arbeit untersucht objektive, neurologische, Bildgebungsmarker, welche die Diagnosegenauigkeit für Parkinson-Syndrome erhöhen könnten. Für die Identifikation neuraler Korrelate und krankheitsspezifischer Muster verwendet diese Arbeit: (1) Metaanalysen, um die Konvergenz zwischen Studien mit kleinen Gruppengrößen zu finden, (2) voxel-basierte Morphometrie, um strukturelle Unterschiede zwischen Patienten und Kontrollen zu identifizieren und (3) Support Vector Machine-Klassifikation, um Erkrankungen individuell zu prädiagnostizieren.

Resultate

Identifikation von krankheitsspezifischen Mustern mittels Metaanalysen: Durch Metaanalysen evaluierten wir statistisch die Konvergenz der Literatur zu krankheitsspezifischen Mustern. Anhand multimodaler Bildgebung wurden die neuronalen Korrelate von 1.767 Patienten mit idiopathischem Parkinson und 210 Patienten mit progressiver supranukleärer Blicklähmung analysiert (Study 1 & 2, Albrecht et al. (2018, 2019a)). Für die idiopathische Parkinson-Krankheit zeigte die [18F]-Fluorodeoxyglucose-Positronen-Emissions-Tomographie (FDG-PET) einen Glucosehypometabolismus im bilateralen inferioren parietalen Kortex und linken Nucleus caudatus. Nur eine geringfügige Atrophie der grauen Substanz konnte im mittleren occipitalen Gyrus durch die strukturelle Magnetresonanztomographie (MRT) festgestellt werden. Die Analyse für die progressive supranukleäre Blicklähmung zeigte eine Atrophie in der grauen Substanz im Mittelhirn und der weißen Substanz des Mittelhirns und zerebralen/ zerebellären Pedunculi. Die Ergebnisse zeigen, dass bei der idiopathischen Parkinson-Krankheit FDG-PET sensitiver als das MRT ist und somit das erstere Potential für die Biomarkersuche bietet. Für die progressive supranukleäre Blicklähmung validierten wir bekannte pathognomonische Marker. Diese können als krankheitsspezifisch gelten, da wir unsere Resultate mit anderen publizierten Metaanalysen neurodegenerativer Erkrankungen abglichen. Anhand datengetriebene Metaanalysen entwerfen wir ein neues Konzept zur Identifikation krankheitsspezifischer Muster für die klinische Applikation.

Investigation krankheitsspezifischer Regionen und Krankheitsklassifikation mittels voxel-basierter Morphometrie und Support Vector Machine -Analysen: Für individualisierte Diagnostik und Behandlungsstrategien untersuchten wir die neuronalen Korrelate und prädizierten Erkrankungen und deren Syndrome mittels multi-zentrischer Daten von Patienten mit kortikobasalem Syndrom und mit zusätzlich einem außergewöhnlichen Symptom, dem Alien/ anarchische Extremitäten-Phänomen. 3T T_1 -gewichtete strukturelle MRT Bilder von 25 Patienten mit kortikobasalem Syndrom, 8 Patienten mit kortikobasalem Syndrom plus Alien/ anarchische Extremitäten Phänomen wurden mit 25 gesunden Kontrollen verglichen. Zur Identifikation neuraler Korrelate führten wir eine voxel-basierte Morh-

pometrie -Analyse durch: Eine valide Methode um strukturelle Veränderungen zu untersuchen, z.B. Atrophie bei Patienten. Ein multivariates Mustererkennungsverfahren, die Support Vector Machine-Klassifikation, wurde trainiert für die Prädiktion von (i) kortikobasalem Syndrom und Kontrollen und um zwischen Patienten mit kortikobasalem Syndrom mit und ohne Alien/ anarchische Extremitäten-Phänomen zu differenzieren. Die voxelbasierte Morphometrie-Analyse ergab Differenzen im grauen Substanzvolumen zwischen Patienten und Kontrollen in frontotemporalen und occipitalen Arealen, motorischen Arealen und der Insel. Spezifisch für Patienten mit Alien/ anarchische Extremitäten-Phänomen war, kontralateral zur Syndromseite, der frontotemporale Gyrus inklusive des supplementär-motorischen Kortex. Die Prädiktion der Erkrankung erreichte eine Genauigkeit von 79.0%. Die Prädiktion des Syndromes innerhalb der Erkrankung erzielte Resultate bis zu 81.3% Genauigkeit. Die zusätzliche Verwendung einer krankheitsspezifischen Maske aus Metaanalysen führte zu ähnlich stabilen Resultaten (Appendix, Albrecht et al. (2017)). Aufgrund der Klassifikation von jeweils zwei Gruppen, liegt das Zufallsniveau bei 50%. Mit dieser Studie unterschieden wir zuverlässig Patienten von Kontrollen durch objektive Mustererkennungsverfahren. Weiterhin zeigten wir, dass sogar die Prädiktion eines Syndromes einer Erkrankung möglich ist.

Diskussion

Durch quantitative Metaanalysen konnten wir die Konvergenz publizierter Studien für neurodegenerative Erkrankungen statistisch validieren. Für die idiopatische Parkinson-Krankheit ist eine Reduktion des Glukosehypometabolismus im inferioren parietalen Kortex und dem linken Nucleus caudatus spezifischer als die strukturelle Hirnatrophie. Für die progressive supranukleäre Blicklähmung verifizierten wir Atrophie des Mittelhirns und der zerebralen/ zerebellären Pedunculi als krankheitsspezifisch. Mittels maschinellem Lernens differenzierten wir Patienten von Kontrollen und prädizierten ein Symptom einer Erkrankung. Die zusätzliche krankheitsspezifische Maske aus den Ergebnissen vorhergehender Metaanalysen führte zu den gleichen stabilen Resultaten (Appendix, Albrecht et al. (2017)). Krankheitsdiagnosen stützen sich primär immer noch auf Experten und die genaue Observation des Krankheitsverlaufes. Ins besondere atypische

Parkinson-Syndrome werden häufig zu Beginn der Krankheit fehldiagnostiziert. Die Korrekte und frühzeitige Diagnose spielt eine essentielle Rolle für die Therapieentscheidung und den Krankheitsverlauf. Die Mehrheit der Diagnosekriterien wurde schon revidiert und bezieht objektive, krankheitsspezifische Hirnveränderungen ein (Albert et al., 2011; Dubois et al., 2014; Gorno-Tempini et al., 2011; Rascovsky et al., 2011). Die Diagnostik für die idiopathische Parkinson-Krankheit, die progressive supranukleäre Blicklähmung und die kortikobasale Degeneration wurden revidiert, betrachten die medizinische Bildgebung jedoch nur als unterstützendes oder Ausschlusskriterium. Die Berücksichtigung unserer vorgeschlagenen regionalen Muster könnte wesentlich zur Validierung der Krankheitsdiagnose beitragen. Studien zur frontotemporalen lobären Degeneration und der Alzheimer-Krankheit zeigen, dass im Vergleich zur rein klinischen Diagnose, die Genauigkeit seit der Integration der neurologischen Bildgebung anstieg (Rascovsky et al., 2002; Dubois et al., 2007; Kipps et al., 2009). Folglich wäre die Inklusion der Bildgebung auch in die Diagnostik anderer neurodegenerativer Erkrankungen in Betracht zu ziehen. Jedoch benötigen unsere vorgeschlagenen, bildgebenden Marker eine Verifizierung in externen, unabhängigen Kohorten und Einzelfallanalysen. Ein Exempel für die Validierung bildgebender Diagnostik zeigt die primär progrediente Aphasie: Kriterien wurden vorgeschlagen von Gorno-Tempini et al. (2011) basierend auf Resultaten von Bildgebungsstudien und daraufhin statistisch validiert durch objektive Metaanalysen (Bisenius et al., 2016). Hier stellt die bildgebungsgestützte Diagnose sogar ein höheres Niveau der Genauigkeit der Klassifikation dar. Demzufolge erfüllen diagnostizierte Patienten die klinischen Kriterien und zusätzlich die neurologischen Bildgebungskriterien. Bisenius et al. (2016) bestätigen, dass die Bildgebungskriterien bezüglich der Hirnveränderungen im MRT eine hohe Unterscheidungskraft aufweisen.

Konklusion

Die vorliegende Arbeit hat zum Ziel objektive, krankheitsspezifische Muster und deren Applikation zur verbesserten Diagnostik beizutragen. Für die progressive supranukleäre Blicklähmung schlagen wir die regionale Atrophie im Mittelhirn und den zerebralen/ zerebellären Pedunculi als krankheitsrelevante Veränderung vor, welche die Einbindung in die Diagnosekriterien

nahelegen. Für die idiopatische Parkinson-Krankheit ergaben die Resultate, dass der regionale Hypometabolismus sensitiver ist als strukturelle Veränderungen. Dieser Hypometabolismus ist aber nicht spezifisch genug für die Unterscheidung zu anderen neurodegenerativen Erkrankungen. Weiterhin konnten wir mit Masken krankheitsspezifischer Muster und unter Einschluss des gesamten Gehirns stabile Klassifikationsresultate für das kortikobasale Syndrom erzielen. Diese ermöglichen die Differenzierung zwischen Patienten und Kontrollen und sogar die Prädiktion von Syndromen innerhalb einer Erkrankung.

BIBLIOGRAPHISCHE DARSTELLUNG

Franziska Albrecht

Neural Correlates of Parkinsonian Syndromes

Fakultät für Lebenswissenschaften

Universität Leipzig

Dissertation

110 Seiten, 55 Literaturangaben, 0 Abbildungen, 3 Tabellen

The thesis investigated objective neuroimaging biomarkers in parkinsonian syndromes, which could be applied to increase diagnostic accuracy. To find convergence of the literature concerning disease-specific patterns in Parkinson's disease and progressive supranuclear palsy, we conducted meta-analyses. In Parkinson's disease glucose hypometabolism was revealed in bilateral inferior parietal cortex and left caudate nucleus and focal gray matter atrophy in the middle occipital gyrus. In progressive supranuclear palsy we identified gray matter atrophy in the midbrain and white matter atrophy in the cerebral/cerebellar pedunculi and midbrain. In sum, in Parkinson's disease hypometabolism outperforms atrophy and in progressive supranuclear palsy we validated pathognomonic markers as disease-specific. Our studies create a novel framework to investigate disease-specific regional alterations for use in clinical routine. Further, we investigated neural correlates by voxel-based morphometry and discriminated disease and clinical syndrome by multivariate pattern recognition in single patients with corticobasal syndrome and corticobasal syndrome with a unique syndrome - alien/ anarchic limb phenomenon. We found gray matter volume differences between patients and controls in asymmetric frontotemporal/ occipital regions, motor areas, and insulae. The frontoparietal gyrus including the supplementary motor area contralateral to the side of the affected limb was specific for alien/ anarchic limb phenomenon. The prediction of the disease among controls was 79.0% accurate. The prediction of the specific syndrome within a disease reached an accuracy of 81.3%. In conclusion, we reliably classified patients and controls by objective pattern recognition. Moreover, we were able to predict a specific clinical syndrome within a disease, paving the way to individualized disease prediction.

Contents

SELBSTSTÄNDIGKEITSERKLÄRUNG	I
ACKNOWLEDGMENTS	II
SUMMARY	III
ZUSAMMENFASSUNG	VIII
BIBLIOGRAPHISCHE DARSTELLUNG	XIV
CONTENTS	XVI
1 GENERAL INTRODUCTION	1
1.1 Parkinsonian Syndromes	2
1.2 Parkinson's Disease	2
1.2.1 Diagnostic Criteria	3
1.3 Progressive Supranuclear Palsy	4
1.3.1 Diagnostic Criteria	5
1.4 Corticobasal Degeneration	5
1.4.1 Diagnostic Criteria	7
1.5 Imaging Biomarkers	7
1.6 Current Thesis	9
1.6.1 Motivation and Framework	9
1.6.2 Research Questions	9
2 GENERAL MATERIALS AND METHODS	12
2.1 Magnetic Resonance Imaging	12
2.2 Analytical Methods	13
2.2.1 Meta-Analysis	13
2.2.2 Voxel-Based Morphometry	14
2.2.3 Support-Vector Machine Classification	15
2.3 Multi-Centric Data	16
2.4 Clinical Assessment	17
3 Study 1	18
4 Study 2	29

<i>CONTENTS</i>	XVI
5 Study 3	41
6 Study 4	50
7 Study 5	57
8 DISCUSSION	73
8.1 Main Findings	73
8.2 Statistical Approaches to Find Imaging Biomarker	76
8.3 Brain Alterations and their Utility as Imaging Biomarker	77
8.4 Limitations	78
8.5 Contributions of the Current Thesis and Future Directions	79
9 REFERENCES	81
APPENDIX	XVIII
LIST OF AUTHORSHIP	XXVII
CURRICULUM VITÆ	XXXVIII

1 GENERAL INTRODUCTION

Healthy living and aging are one of the major challenges for our society. Worldwide demographic changes lead to an increased occurrence of neurodegenerative diseases (Saba, 2015). Neurodegenerative diseases - defined as the precipitate loss of specific neurons (Graeber and Moran, 2002) - have in common that incidence and prevalence are rising with age (Muangpaisan et al., 2011). In particular, Alzheimer's disease, idiopathic Parkinson's disease, and Amyotrophic Lateral Sclerosis are the most frequent occurring neurodegenerative diseases (Graeber and Moran, 2002). For example, the incidence rate of Parkinson's disease varies from 10 to 13 per 100,000 persons yearly (Muangpaisan et al., 2011). Of note, this only includes the typical appearance of parkinsonian syndromes, idiopathic Parkinson's disease, which encompasses 63% of parkinsonism cases. Hence, idiopathic Parkinson's disease only represents one entity of a whole group of parkinsonian syndromes. Parkinsonian syndromes have in common several clinical features but differ regarding their underlying pathologies. Up to now, histopathological examination remains gold standard for a definite discrimination and diagnosis. Belonging to this network are also scarce entities such as corticobasal degeneration (CBD) and progressive supranuclear palsy (PSP). CBD and PSP are atypical parkinsonian syndromes and neurodegenerative diseases, which can only be confirmed by histopathological examination. Reported to be associated with various clinical syndromes, the classical clinical phenotypes are corticobasal syndrome (CBS) and Richardson syndrome (RS) respectively. As aforementioned there are overlaps with other diseases belonging to the group of parkinsonian syndromes making it a special interest to separate CBS and PSP from different syndromes and pathologies. Parkinsonian syndromes are often misdiagnosed and mixed up in clinical diagnosis, especially in the early beginning of the disease. In general, diagnosis primarily depends on clinical variables. Thus, generalized, quantifiable image-based markers to independently and accurately diagnose patients are of high interest and needed. The following is an introduction to the topic of parkinsonian syndromes and related research outcomes.

1.1 Parkinsonian Syndromes

The group of parkinsonian syndromes can be stratified into typical (idiopathic Parkinson's disease), acquired (posttraumatic), hereditary (genetic), and atypical parkinsonism. The pattern of atypical parkinsonism includes the rare, fast progressing illnesses of PSP, Lewy-body disease, multiple-system atrophy, and CBD. All of them show special symptoms but are likely to be misdiagnosed or confounded as Parkinson's diseases or even as another atypical parkinsonism. Moreover, the parkinsonian syndromes are further distinguished by their underlying histopathology. Wrong folding or accumulation of proteins is the major cause leading to a proteinopathy. CBD and PSP are tau-based, while Parkinson's disease, multiple-system atrophy, and Lewy-body disease are alpha synuclein-based pathologies. Due to similarities of symptoms to other diseases associated with the deposition of microtubule-associated tau, it is of special interest to separate CBD and PSP from different tau-based pathologies (tauopathies).

1.2 Parkinson's Disease

"An Essay on The Shaking Palsy" (Parkinson, 1987) was the inception of the disease, which is now named after its discoverer James Parkinson. Parkinson's disease (PD) is mainly characterized as a motor disease but amended diagnostic criteria point out the increasing importance of non-motor features (Postuma et al., 2015). Nevertheless, the hallmark of PD remains parkinsonism described by bradykinesia and additionally rest tremor or rigidity. Patients with bradykinesia suffer from slowness of movements as well as a decrease in speed during performance of movements. Rest tremor means a shaking that is present when inactive, vanishes when moving but increases during mental tasks (Williams and Litvan, 2013). The term rigidity refers to a rise in muscle tone causing a resistance to superficially imposed limb movements. Additionally, non-motor symptoms range from mild cognitive impairment over fatigue to visual hallucinations and significantly increase the burden on the patients quality of life (Poewe et al., 2017). Non-motor symptoms do not only accompany PD, they antedate the disease years before as so called prodromal PD stages: rapid eye movement sleep behavior disorder, depression, anxiety, daytime sleepiness, and smell disturbance.

Concerning pathology, the neuropathological criteria for PD describe morphological changes in the substantia nigra pars compacta assessed by neuronal loss and Lewy pathology identified by alpha-synuclein immunohistochemistry (Dickson et al., 2009). On a molecular level, PD is characterized by dopaminergic depletion due to nigrostriatal degeneration. Treatment of the disease connects this fact and mainly relies on pharmacological dopamine substitution. Here, PD is quite exceptional among the neurodegenerative diseases: symptoms and quality of daily living can be sustained for a long time of the disease course. Nevertheless, medication can manage the symptoms but neither slow down progression nor heal the disease at all.

1.2.1 Diagnostic Criteria

The recent clinical diagnostic criteria by the Movement Disorder Society are summarized in Table 1 (Postuma et al., 2015). Note that neuroimaging is only mentioned as an exclusion criterion.

Table 1. Diagnostic Criteria of Parkinson's Disease (PD) adapted from Postuma et al. (2015).

- **Essential criterion: Parkinsonism**
 - Bradykinesia plus either rest tremor or rigidity
- **Clinically Established Parkinson's disease**
 - None of exclusion criteria: cerebellar abnormalities, supranuclear gaze palsy, parkinsonian features restricted to the lower limbs, no response to high-dose dopaminergic therapy, or normal neuroimaging of dopaminergic system
 - Two supportive criteria: response to dopaminergic therapy, dopaminergic-induced dyskinesia, rest tremor of a limb, olfactory loss or cardiac sympathetic denervation
 - No red flags: rapid progression of gait impairment, no progression of motor symptoms, early bulbar dysfunction, respiratory dysfunction, frequent falls, bilateral symmetric parkinsonism or lack of non-motor features (sleep dysfunction, psychiatric dysfunction or autonomic dysfunction)
- **Clinically Probable Parkinson's disease**
 - None of exclusion criteria
 - Presence of red flags counterbalanced by supportive criteria: 1 red flag + at least 1 supportive criterion or 2 red flags + at least 2 supportive criteria

1.3 Progressive Supranuclear Palsy

Occurring in 5 to 10 per 100,000 persons, progressive supranuclear palsy (PSP) belongs to the spectrum of rare atypical parkinsonian syndromes (Levin et al., 2016). PSP was firstly reported in a small case series by Steele, Richardson, and Olszewski in 1964. The authors already identified vertical supranuclear gaze palsy and neuronal loss in the brain stem as core signs for this rapidly progressing disease. Interestingly, nearly all cases were examined histopathologically, which revealed a shrinkage of the midbrain and cerebellar pedunculi; nowadays still considered as pathognomonic markers of PSP.

Central motor characteristics of PSP include postural instability, early falls, and eye-movement disturbances; differentiating it from other neurodegenerative diseases (McFarland, 2016). Note that PSP responds poorly to dopaminergic treatment making it an important difference to PD (Williams and Litvan, 2013). Another feature discriminating PSP from PD is the absence of severe autonomic dysfunctions. PSP further affects non-motor domains leading to dementia, emotional lability, depression or slowed speech (McFarland, 2016).

The underlying pathology, also referred to as PSP, is known for the accumulation of microtubule-associated protein tau with four microtubule-binding side repeats, neurofibrillary tangles, astrocytic tufts, and oligodendrocytic coils (Hoeglinger et al. 2017). Like other atypical parkinsonian syndromes, a definite diagnosis of PSP can only be confirmed postmortem. Among evaluated PSP-tauopathy patients, 10% to 30% do not present the classic clinical phenotype of Richardson syndrome (PSP-RS) (Williams and Litvan, 2013). Hence, the amended diagnostic criteria recognize that the histopathology of PSP is linked to several other clinical phenotypes (Höglinger et al., 2017). Beside the typical representation of PSP-RS, other phenotypes mimicking PD (PSP-parkinsonism) or CBS (PSP-CBS) are acknowledged. Even though diagnostic criteria were recently revisited, PSP diagnosis remains primary dependent on clinical evaluation. Indeed, imaging is only considered as a supportive criterion, i.e. 'predominant midbrain atrophy or hypometabolism' (Höglinger et al., 2017).

1.3.1 Diagnostic Criteria

Table 2 summarizes the recent clinical diagnostic criteria for PSP by the International Parkinson and Movement Disorder Society-endorsed PSP Study Group (Höglinger et al., 2017). These criteria consider the core features of PSP and rely on different levels of functional domains. For diagnosing the clinical phenotypes of PSP, criteria are further stratified.

Table 2. Diagnostic criteria of progressive supranuclear palsy-Richardson syndrome (PSP-RS) adapted from Höglinger et al. (2017).

- **Highest certainty**

- Vertical supranuclear gaze palsy
- Repeated unprovoked falls within 3 years
- Progressive gait freezing within 3 years
- Speech/language disorder

- **Mid certainty**

- Slow velocity of vertical saccades
- Tendency to fall on the pull-test within 3 years
- Parkinsonism, akinetic-rigid, predominantly axial, and dopaminergic resistant
- Frontal cognitive/behavioral presentation

- **Lowest certainty**

- Frequent macro square wave jerks or “eyelid opening apraxia”
- More than two steps backward on the pull-test within 3 years
- Parkinsonism, with tremor and/or asymmetric and/or dopaminergic responsive
- Corticobasal syndrome

1.4 Corticobasal Degeneration

In 1968, corticobasal degeneration (CBD) was first referred to it as ‘corticonigral degeneration with neuronal achromasia’ in a case study of 3 patients having a progressive neurologic disorder (Rebeiz et al., 1968). All patients showed clinical characteristics of a decrease in speed and alienation during voluntary movements as well as superimposed involuntary movements. Rebeiz et al. presented patients with a lateralization of motor symptoms at the beginning of the disease; severe cognitive impairments

were not noticed until death. Subsequently, patients were also histopathologically evaluated showing asymmetrical gray matter loss in frontoparietal regions. Changes on cellular level such as loss of neurons, gliosis, and swollen cell bodies were further observed. The study of Rebeiz et al. describes the clinical and histopathological features of CBD unaware of the fact that nowadays it is common to distinguish the disorder by the clinical phenotype (corticobasal syndrome, CBS) and the associated histopathology (CBD).

CBS is considered as an orphan disease, only occurring in about 1 per 100,000 individuals, and represents the classical clinical phenotype of CBD (Levin et al., 2016). In a 2013 review, Armstrong et al. summarized that over 37% of CBD cases show CBS as clinical syndrome. Nevertheless, CBD can also be linked to other clinical syndromes: behavioral variant frontotemporal dementia, primary progressive aphasia, posterior cortical atrophy, a type of dementia with histopathology similar to Alzheimer's disease, and Richardson syndrome (Boeve, 2011). On the other hand, also CBS can be associated with different pathologies such as Alzheimer's disease, Creutzfeldt-Jakob disease, Pick's disease, PSP, Lewy-body disease, and frontotemporal lobar degeneration. CBD, as the typical underlying pathology, is defined by widespread deposition of hyperphosphorylated 4-repeat tau in neurons and glia (Dickson et al., 2002). High variety of symptoms makes a diagnosis of CBD challenging. In only 25% to 56% of patients, CBD is predicted ante-mortem (Armstrong et al., 2013). Identifying phenotypes and specific features of CBD is an ongoing problem restricting the ability to develop definitive clinical criteria foreseeing the pathology.

Although CBS/CBD is firstly considered as a motor disease, there are also major changes in behavior and general cognition. Concerning the motor symptoms, limb rigidity and bradykinesia are the most frequent features seen in later post-mortem proven CBD (Armstrong et al., 2013). 85% of patients develop limb rigidity and 76% bradykinesia during the disease course. Other less frequent motor features include postural instability that often leads to falls, myoclonus (brief muscle twitching), dystonia (continuous muscle contraction leading to abnormal postures), and tremor (rhythmic muscle contraction and relaxation), which are observed in 20% of the cases. With regard to higher cortical features, symptoms such as apraxia, speech impairment, behavioral/ cognitive changes, and alien/ anarchic limb

phenomenon are linked to CBD. 57% of CBD patients are suffering from apraxia meaning that they are unable to fulfill skillful motor movements (Armstrong et al., 2013). Interestingly, this deficit cannot be explained by dysfunctions in motor or sensory system (Zadikoff and Lang, 2005). A really scarce and peculiar feature is the alien/anarchic limb phenomenon. About 30% of patients show these signs of a limb, recognized as foreign, which can perform purposeless movements or interrupt movements. Other features include speech impairments like aphasia, which are seen in about 52% of cases or cognitive decline, which is shown in 70% of CBD patients. Although the disease has been known since nearly 50 years, disentangling the interplay of the clinical syndrome and histopathology is still a matter for research.

1.4.1 Diagnostic Criteria

Recently, Armstrong et al. (2013) published new consensus criteria for evaluating CBS and predicting CBD. In her work Armstrong et al. suggested to use the term CBD only for pathology-proven cases. This leads to the fact that a clinical diagnosis can only be probable or possible CBD. Diagnostic criteria to evaluate cases of CBD phenotype CBS are summarized in Table 3.

1.5 Imaging Biomarkers

Since the emergence of neuroimaging during the 1980's, researcher took advantage of medical imaging. Medical neuroimaging can be used as a window into the brain identifying structures with physical alterations, lesions, and damages. These features yield the potential to be disease-specific and hence can be transformed into imaging biomarkers. Understanding the emergence of diseases started with analyzing neuroimaging data by single case descriptions of patients or lesion studies. Researchers and doctors tried to understand the functions of altered brain regions-of-interest. Later on statistical analysis methods came into play to provide a mathematical validation to investigate regions-of-interest and the whole brain by the means of voxels – the smallest unit of an imaging analysis. This

Table 3. Diagnostic criteria of corticobasal syndrome (CBS) adapted from Armstrong et al. (2013)

- **Probable Corticobasal Syndrome**
 - Two of:
 - * 1. Limb rigidity or akinesia
 - * 2. Limb dystonia
 - * 3. Limb myoclonus
 - Plus two of:
 - * 4. Orobuccal or limb apraxia
 - * 5. Cortical sensory deficit
 - * 6. Alien/ anarchic limb phenomenon
- **Possible Corticobasal Syndrome**
 - At least one of:
 - * 1. - 3.
 - Plus one of:
 - * 4. - 6.

further paved the way for methods like voxel-based morphometry analyses to compare groups and derive specific regions of differences. With this method differences between patients and healthy controls, basically atrophy, can be assessed. Regions that were identified as disease-related can be used in clinical trials as imaging biomarker for disease identification or for neuromodulation therapies like treatment prediction (Ballarini et al., 2019). Indeed, several neurodegenerative diseases already benefit from the incorporation of imaging biomarkers to support clinical diagnosis. Magnetic resonance imaging (MRI) and amyloid as well as [18F]-fluorodeoxyglucose positron emission tomography have been integrated in the current diagnostic criteria for mild cognitive impairment and Alzheimer's disease (Albert et al., 2011; Dubois et al., 2014). Moreover, for primary progressive aphasia imaging-supported diagnosis has been successfully introduced and subsequently validated by meta-analysis in independent cohorts (Gorno-Tempini et al., 2011; Bisenius et al., 2016). Multimodal imaging, i.e. structural and metabolic changes, is considered for diagnosis and identification of phenotypes. Note that also for behavioral variant frontotemporal lobar degeneration disease-characteristic imaging biomarkers have been successfully applied: frontal and/or anterior temporal alterations can be detected by MRI, computed tomography, positron emission tomography

or single-photon emission computed tomography (Rascovsky et al., 2011). Hence, my aim was to investigate the utility and applicability of objective neuroimaging biomarkers in parkinsonian syndromes, which could be applied to support diagnosis. In my thesis I apply three approaches to extract the neural correlates and disease-specific patterns: (1) meta-analysis to find convergence among smaller cohort studies, (2) voxel-based morphometry to identify structural differences between patients and controls, and (3) support-vector machine classification to predict the disease individually.

1.6 Current Thesis

1.6.1 Motivation and Framework

The close cooperation with the Clinic for Cognitive Neurology of the University Clinic of Leipzig and working with patients has sensitized me what is needed and necessary in daily clinical assessment. The thesis aims at contributing objective tools to improve diagnoses and treatment of neurodegenerative diseases in clinical routine. We took advantage of the integration of MR imaging into clinical routine and extracted patterns to enable an objective image assessment for accurate disease diagnosis. So far, diagnosis of parkinsonian syndromes remains primarily clinical. Diagnostic criteria for PD, PSP, and CBS have been amended recently but include the factor of objective medical imaging as supportive or exclusion criteria. Other neurodegenerative disease are exemplary regarding the application of neuroimaging as diagnostic criteria, e.g Alzheimer's disease or primary progressive aphasia (Gorno-Tempini et al., 2011; Dubois et al., 2014). In line with that, we investigate the neural correlates of PD, PSP, and CBS as well as predict such syndromes individually, paving the way to personalized disease identification.

1.6.2 Research Questions

The current thesis investigates disease-specific markers to classify parkinsonian syndromes. Aiming at a powerful, detailed description and disentanglement of clinical features as well as neurodegenerative patterns of PD, CBS, and PSP we perform several different approaches.

Firstly, we conducted quantitative and systematic meta-analyses across

voxel-based morphometry studies to identify disease-specific patterns to disentangle parkinsonian syndromes, which are clinically hard to distinguish. The resulting patterns contribute to objectify disease identification, understand these diseases by serving as masks for imaging biomarker or subsequent machine learning analyses. We investigated convergence of the literature regarding neural signatures of PD (Study 1, Albrecht et al. (2018)) and PSP (Study 2, Albrecht et al. (2019a)). For disease-specificity, we qualitatively and quantitatively compared the results with other published meta-analyses on neurodegenerative diseases. We hypothesized in PSP atrophy is mostly focused on midbrain regions and in PD anterior cerebral regions.

Secondly, we performed a study on multi-centric data of CBS patients from the Research Consortium for Frontotemporal Lobar Degeneration Germany (FTLD Consortium) (Study 3, Albrecht et al. (2019b)). Investigating a rare occurring disease such as CBS, multi-centric data is advantageous for the analysis. We performed a voxel-based morphometry analysis to detect regional gray matter volume differences and a machine learning approach to predict the disease itself and a related syndrome. Further, the machine learning approach was used to test the application and accuracy of a disease-specific mask, which was obtained from our recent meta-analysis (Appendix, Albrecht et al. (2017)). Results pave the way to individualized disease and syndrome prediction. We hypothesized to find similar results as in our meta-analysis of CBS: asymmetrical gray matter loss in the left frontal lobe (Appendix, Albrecht et al. (2017)).

Additionally to my main projects, I was engaged in two other projects investigating PD, which I have not described in detail in my thesis. One study predicted the treatment response to dopaminergic medication in a cohort of patients with PD from our cooperation with the Charles University in Prague (Study 4, Ballarini et al. (2019)). We investigated how age, disease duration, and treatment dose/ length influence accuracy as well as responsiveness. Voxel-based morphometry was applied to assess structural differences and support-vector machine classification to foresee individual treatment response. The other study in cooperation with the Charles University in Prague investigated the relationship between memory deficits in PD and hippocampus alterations by neuroimaging and neuropsychological assessments (Study 5, Bezdicek et al. (2019)). Two concepts that could

explain memory impairment in PD were tested and underlying differences in functional connectivity of different hippocampal subfields were analyzed.

Overall, with this thesis I aim to establish an overview over parkinsonian syndromes, their prototypical networks, and identify patterns, which may objectively support diagnosis.

2 GENERAL MATERIALS AND METHODS

In the following section I will explain general methods, which all of my studies during my PhD have in common.

2.1 Magnetic Resonance Imaging

Over the past decade rapid developments in imaging the brain have occurred. Especially in neuroscience, neuroimaging has become an important method to investigate the brain's structure and functions non-invasively. One method has gained special attention, namely the technique of magnetic resonance imaging (MRI) since it can be applied in diagnostic/clinical and basic research settings. MRI uses hydrogen atoms to visualize different types of brain tissue under changing physiological conditions and provides high spatial resolution (Bear et al., 2009). In research, MRI has provided abundant information about the areas of cognitive and sensory processes in the human brain. Further, MR images can also visualize lesions in the brain due to the fact that tumors and inflammation increase the amount of extracellular water (Bear et al., 2009).

The underlying principle is based on quantification of hydrogen atoms in body water. Physically a hydrogen atom can exist in two states: either high-energy state or low-energy state. Both states are abundant in the brain. By applying electromagnetic waves, energy is added to the atoms. These in turn will absorb this energy and gain a higher state of energy, which is called resonant frequency. Turning off these electromagnetic fields lead atoms to return to their lower state and emit a signal of their own special frequency. Signals are collected by a radio receiver, whereas stronger signals reflect greater amounts of hydrogen atoms. Further, MRI scanners use a varying magnetic field to give emitted waves a spatial coding. One side of the magnet has a stronger field, where high-frequency signals of the hydrogen protons are located. Hence, low-frequency waves are located on the weaker side. During the measurement the gradient of the magnet is arranged to different angles relative to the brain. Altering the magnetic field causes a relaxation of the spin of the hydrogen atoms and a shift back to their original states (Cohen and Sweet, 2011).

Due to the fact that the recovering process happens along different spatial dimensions one can distinguish between two options. A spatial distri-

bution along the longitudinal axis is referred to as T_1 relaxation. On the contrary, the phase coherence loss of the spin at the transverse axis corresponds to T_2 relaxation. Further, T_1 is correlated with the enthalpy of the atoms spin and T_2 with the entropy (Cohen and Sweet, 2011). Both approaches differ in their resolution and also sensitivity of tissue type. Most of brain scans assessing atrophy are T_1 -weighted. The whole procedure results in an image visualizing tissue, which actually depicts the distribution of hydrogen atoms.

2.2 Analytical Methods

2.2.1 Meta-Analysis

Meta-analysis were applied to identify disease-specific brain regions for imaging biomarkers. It is defined as "use of statistical methods in a systematic review to integrate the results of included studies" (Moher et al., 2009). This approach creates larger samples, thus leading to higher statistical power to validate convergence of published results. Especially in rare diseases, it is a powerful technique to investigate consistencies in disease features.

Assuring validity and quality, meta-analyses are conducted according to the guidelines of PRISMA (preferred reporting items for systematic reviews and meta-analyses) (Moher et al., 2009). To ensure a standard to report different types of results, Moher et al. (2009) provide a flow diagram and checklist leading to a good scientific practice, transparency, and reproducibility. According to PRISMA statement, literature search and selection should be performed by two investigators separately and discussed afterwards. Literature search engines like PubMed from the National Center for Biotechnology Information (NCBI) are queried by combining different tags. Additionally, inclusion criteria are set for selection: (1) peer-reviewed, (2) whole-brain studies, (3) diagnosis according to established diagnostic criteria, (4) original studies, (5) comparison with age-matched healthy controls, and (6) results normalized to a stereotactic space.

To analyze convergence of literature in the respective diseases, anatomic likelihood estimate meta-analysis method (ALE) (Fox et al., 2005; Laird et al., 2011, 2005; Turkeltaub et al., 2002) and seed-based D mapping (SDM) (Radua and Mataix-Cols, 2009) can be applied. Applying two meth-

ods enables double-validation and leads to robust results, ready for suggestion of disease-specificity. The methods were firstly invented for meta-analyses of functional imaging studies with psychological stimulation of participants. Later, this approach has been extended to imaging studies investigating atrophy (Sacher et al., 2012; Schroeter and Neumann, 2011; Schroeter et al., 2007, 2008). With this analysis one is addressing the question, which brain regions show a higher convergence of atrophy across studies than it would be the case in a random relationship.

In general the underlying algorithm transforms extracted peaks into probability distributions around these peaks. The distribution estimation for each included study is based on empirical estimates of between-subject variability and according to the number of subjects of each study. As a result maps of the single studies are recreated. In an analysis of random-effects, values in the modeled map are afterward combined across studies and tested against the null hypothesis of a random spatial distribution between modeled maps. With this step regions are identified where empirical values are higher than could be expected by chance. The resulting map is thresholded with a customized threshold to reveal statistically significant atrophic regions. For double-validation results of both methods can be overlaid in a conjunction analysis; only revealing clusters significant in both approaches.

2.2.2 Voxel-Based Morphometry

To compare different whole-brain MRI scans the method of voxel-based morphometry (VBM) is widely used. This technique is an unbiased approach for a comprehensive assessment of structural brain alterations. Basis of VBM is a voxel-wise contrast of local gray or white matter values between subjects or also groups (e.g. healthy controls and patients) (Ashburner and Friston, 2000).

An important step in processing MRI images is merging to a particular stereotactic space. Stereotactic space refers to a 3-dimensional coordinate system of the brain to locate certain areas despite of individual differences in structure. Nowadays, the stereotactic space of Montreal Neurology Institute and Hospital (MNI) is the reference standard. In order to define a more representative brain of the population a large amount of 'normal' brains were scanned and averaged here to create a brain template with a respec-

tive coordinate system. Creating this new template included a two-step procedure: (1) in 250 normal MRI scans various landmarks were defined manually and (2) another 55 images were registered to this atlas by an automatic linear registration technique (Rorden and Brett, 2000). Both, the manually and computed brain matches were used to create the MNI 305 atlas. It consists of 239 male and 66 female right handed subjects with an average age of 23.4 (\pm 4.1) (Rorden and Brett, 2000). To spatially normalize to the same stereotactic space, each image is registered to the same standardized template brain. However, not all cortical areas are matched perfectly; there is only a correction for global shape differences. An exact overlay would diminish all regional concentration differences. Gray matter, white matter, and cerebrospinal fluid are segmented while normalizing the images. During normalization it is possible that regional atrophy might disappear. To compensate this, data can be modulated by multiplying the gray matter value after warping the images to the template with the Jacobian determinant. Hence, modulation spatially compensates for deformation. Gray matter is then used for further processing and smoothed. This step ensures a normal distribution of the data and seeds assumptions for subsequent statistical analyses. Using this data tests performing voxel-wise parametric statistics can be run to compare different groups. This technique results in a statistical parametric map displaying regions where concentration of gray matter is significantly different to contrasted group. Such so called univariate approaches lead to a massive number of tests in these regions and voxels (50,000–350,000) (Woo et al., 2017).

2.2.3 Support-Vector Machine Classification

Machine learning can identify brain patterns, which discriminate patients from healthy subjects and establish objective features of underlying disease pathology (Woo et al., 2017). We applied support-vector machine classification (SVM), a multivariate method taking into account multiple dependencies across the whole-brain, to find a function separating classes of data in a multidimensional space (Klöppel et al., 2008; Arbabshirani et al., 2017).

Basically, SVM has two outcomes: a classification result and a weight map. The first provides the answer whether groups are distinguishable or

not. The second provides a map containing the relative contribution of the individual features (Schrouff and Mourao-Miranda, 2018). Linear machine learning weight maps have no applicable unit and provide not directly a surrogate of information about the neural correlates. Thus, in a prediction model of patients and controls weights do not necessarily symbolize atrophy. They rather display the distance from the separating function, meaning the features that yielded the highest predictive value to distinguish between the groups. To reach high classification accuracy, cross-validation using the 'leave-one-subject-out' approach can be implemented into the model. Classification is done several times and at each iteration a patient and a healthy subject is left out when building the classifier. Subsequently, it is checked if both remaining data sets are classified correctly. Specificity and sensitivity of the classification are calculated by the number of correctly classified patients and healthy subjects. It has been shown that SVM is robust against scanner differences, which makes it suitable for multi-centric trials (Klöppel et al., 2008; Franke et al., 2010).

2.3 Multi-Centric Data

The Max-Planck-Institute for Human Cognitive and Brain Sciences and the Clinic of Cognitive Neurology at the University of Leipzig are taking part in the Research Consortium for Frontotemporal Lobar Degeneration Germany (FTLD Consortium) (Otto et al., 2011). This project was sponsored by the German Federal Ministry of Education and Research as part of the competence network for neurodegenerative dementias. The FTLD Consortium is a network consisting of several study centers, which includes clinical centers and centers for translational research. Study sites are spread over whole Germany and Italy; the consortium's headquarter is located in Ulm.

Research consortia and multi-center trials have numerous advantages: fast recruitment of necessary number of patients - especially in rare diseases, higher statistical power due to large sample-sizes, and variance between study center cohorts reflect the real setting. Each clinical center contributes to the project and is allowed to use the comprehensive collected data from all centers. On the other hand, an efficient coordination is indispensable to ensure a high reliability and quality of data. It is important that all study sites follow the same recruitment criteria, study protocols,

and follow-ups. Hence, standard operating procedure protocols are implemented since data quality is depending on the material, equipment, and competence of the collaborators of the study center. All in all, advantages of multi-centric data acquisition are predominant. For Study 3 (Albrecht et al., 2019b), CBS patients and healthy control subjects' data were acquired from the database of the FTLD Consortium Germany.

2.4 Clinical Assessment

For grading disease severity of patients, several tests are administered to assess cognitive deficits and motor impairment. To quantify cognitive impairment, the Mini-Mental State Examination (MMSE) (Folstein et al., 1975) is widely applied. Main target are patients with Alzheimer's dementia, since there are no effects in healthy elderly or patients with personality disorder (Folstein et al., 1975). The MMSE shows a high validity and retest reliability by multiple test dates and examiners. Hence, there are no practicing effects, which enables application to serially document cognitive changes. Patients with cognitive deficits cooperate well only for short time periods, thus the MMSE requires only five to ten minutes (Folstein et al., 1975). The test focuses on cognitive aspects of mental functions, excluding questions depending on mood or mental experiences. First part requires vocal responses of patients addressing orientation, memory, and attention. In the second part, patients have to practice naming and follow verbal or written commands by writing a sentence and copying a geometrical shape.

Clinical features and disease progression of parkinsonian syndromes are assessed by the Unified Parkinson Disease Rating Scale (UPDRS) (Fahn, 1987). The UPDRS is consisting of several parts evaluating different domains from daily living difficulties to behavior, and motor impairment. For clinical studies particularly the motor score of the UPDRS is reported (UPDRS-III) as it points out the severity of motor symptoms. This part of the test examines several motor domains of a patient: speech, facial expressions, gait, postural stability, and movements of extremities. Questions are completed, if possible, by the patient otherwise by the caregiver.

3 STUDY 1

FDG-PET hypometabolism is more sensitive than MRI atrophy in Parkinson's disease: A whole-brain multimodal imaging meta-analysis



FDG-PET hypometabolism is more sensitive than MRI atrophy in Parkinson's disease: A whole-brain multimodal imaging meta-analysis



Franziska Albrecht^{a,*,1}, Tommaso Ballarini^{a,1}, Jane Neumann^{a,c,d}, Matthias L. Schroeter^{a,b}

^a Max Planck Institute for Human Cognitive and Brain Sciences, Leipzig, Germany

^b Clinic of Cognitive Neurology, University of Leipzig & FTLD Consortium Germany, Leipzig, Germany

^c Leipzig University Medical Center, IFB Adiposity Diseases, Leipzig, Germany

^d Department of Medical Engineering and Biotechnology, University of Applied Science, Jena, Germany

ARTICLE INFO

Keywords:

Parkinson's disease
Meta-analysis
MRI
FDG-PET
DTI

ABSTRACT

Recently, revised diagnostic criteria for Parkinson's disease (PD) were introduced (Postuma et al., 2015). Yet, except for well-established dopaminergic imaging, validated imaging biomarkers for PD are still missing, though they could improve diagnostic accuracy.

We conducted systematic meta-analyses to identify PD-specific markers in whole-brain structural magnetic resonance imaging (MRI), [18F]-fluorodeoxyglucose-positron emission tomography (FDG-PET) and diffusion tensor imaging (DTI) studies. Overall, 74 studies were identified including 2323 patients and 1767 healthy controls. Studies were first grouped according to imaging modalities (MRI 50; PET 14; DTI 10) and then into subcohorts based on clinical phenotypes. To ensure reliable results, we combined established meta-analytical algorithms - anatomical likelihood estimation and seed-based *D* mapping - and cross-validated them in a conjunction analysis.

Glucose hypometabolism was found using FDG-PET extensively in bilateral inferior parietal cortex and left caudate nucleus with both meta-analytic methods. This hypometabolism pattern was confirmed in subcohort analyses and related to cognitive deficits (inferior parietal cortex) and motor symptoms (caudate nucleus). Structural MRI showed only small focal gray matter atrophy in the middle occipital gyrus that was not confirmed in subcohort analyses. DTI revealed fractional anisotropy reductions in the cingulate bundle near the orbital and anterior cingulate gyri in PD.

Our results suggest that FDG-PET reliably identifies consistent functional brain abnormalities in PD, whereas structural MRI and DTI show only focal alterations and rather inconsistent results. In conclusion, FDG-PET hypometabolism outperforms structural MRI in PD, although both imaging methods do not offer disease-specific imaging biomarkers for PD.

1. Introduction

Among neurodegenerative diseases, Parkinson's disease (PD) is the second most common disorder with annually 5–35 new cases per 100,000 persons (Poewe et al., 2017). In the last two decades, research on PD has shed new light on its clinical characterization and pathogenesis. However, the most often used diagnostic criteria were published back in 1992 by the Parkinson's Disease Society Brain Bank (PDSBB) (Hughes et al., 1992). These are based on the clinical observation of the parkinsonian syndrome, defined as bradykinesia plus one of rigidity, tremor at rest or postural instability, combined with

fulfilling both exclusion and supportive positive prospective criteria, such as levodopa responsiveness and asymmetry of the motor impairment (Hughes et al., 1992). Beyond motor-symptoms, PD may show also non-motor manifestations, such as sleep disorder, anosmia, constipation, hallucinations, and cognitive impairment possibly leading to dementia (Poewe et al., 2017; Schapira et al., 2017). This is shifting the conceptualization of PD from a pure dopaminergic motor syndrome to a multisystem and multi-neurotransmitter one (Titova et al., 2017). The recently updated PD diagnostic criteria by the Movement Disorder Society have already included the current clinical knowledge of PD research, comprising non-motor features, thus increasing diagnostic

* Corresponding author at: Max Planck Institute for Human Cognitive and Brain Sciences, Stephanstr. 1A, 04103 Leipzig, Germany.

E-mail addresses: falbrecht@cbs.mpg.de (F. Albrecht), tommaso@cbs.mpg.de (T. Ballarini), neumann@cbs.mpg.de (J. Neumann), schroet@cbs.mpg.de (M.L. Schroeter).

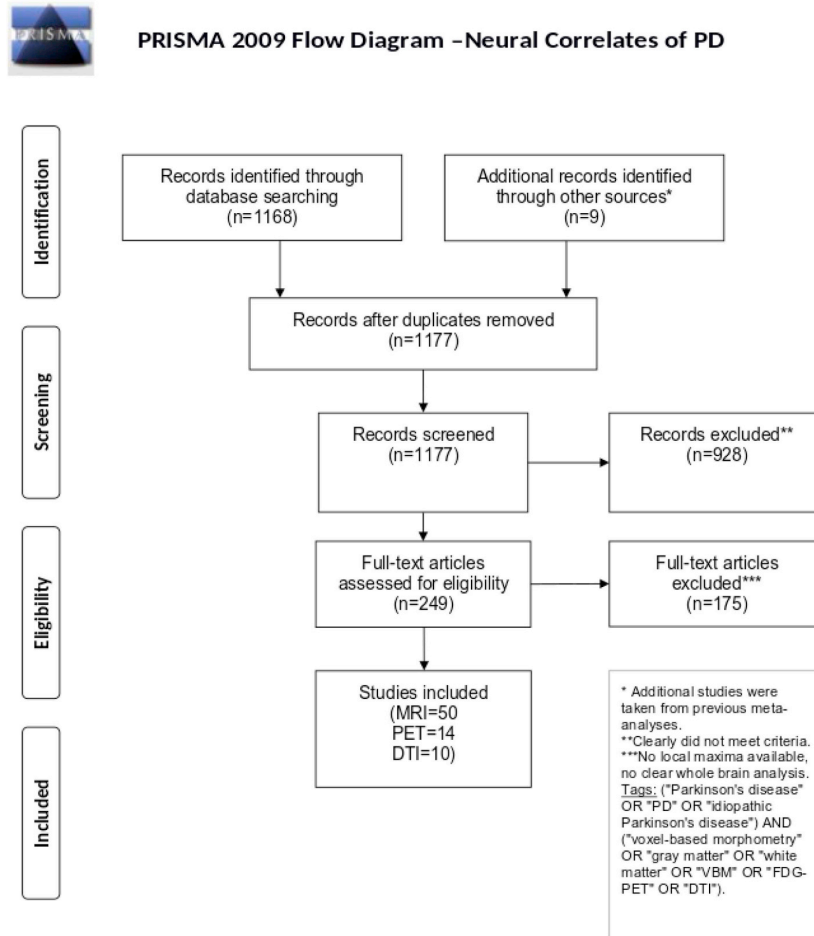
¹ Joined first authorship.

<https://doi.org/10.1016/j.nicl.2018.11.004>

Received 25 April 2018; Received in revised form 1 November 2018; Accepted 10 November 2018

Available online 15 November 2018

2213-1582/ © 2018 The Authors. Published by Elsevier Inc. This is an open access article under the CC BY-NC-ND license (<http://creativecommons.org/licenses/by-nc-nd/4.0/>).



Adapted from: Moher D, Liberati A, Tetzlaff J, Altman DG, The PRISMA Group (2009). Preferred Reporting Items for Systematic Reviews and Meta-Analyses: The PRISMA Statement. *PLoS Med* 6(6): e1000097. doi:10.1371/journal.pmed.1000097

For more information, visit www.prisma-statement.org.

Fig. 1. PRISMA statement flow diagram. Flow of information through different phases of the systematic literature search identifying the neural correlates of Parkinson's disease. Image modified according to the PRISMA statement (Moher et al., 2009).

accuracy (Postuma et al., 2015). Nevertheless, the diagnosis is still predominantly based on clinical symptoms. Indeed, the only brain biomarker mentioned, i.e. normal presynaptic dopaminergic function as detected by molecular imaging, is used as an exclusion criterion for PD (Postuma et al., 2015). A recent meta-analysis has already provided a synthesis of studies investigating presynaptic dopamine function in PD (Kaasinen and Vahlberg, 2017). No other imaging biomarkers have been included so far for the diagnosis of PD, although they could be crucial to improve the diagnostic accuracy. In this respect, Alzheimer's disease research is exemplary. Indeed, magnetic resonance imaging (MRI) and amyloid and [18F]-fluorodeoxyglucose (FDG) positron emission tomography (PET) have been successfully integrated in the most recent diagnostic criteria for mild cognitive impairment, as a pre-stage, and Alzheimer's disease (Albert et al., 2011; Dubois et al., 2014). Along the same line, disease-specific imaging biomarkers have been also proposed for other neurodegenerative diseases, such as fronto-temporal lobar degeneration or primary progressive aphasia (Gorno-Tempini et al., 2011; Rascovsky et al., 2011). The identification of PD-

specific imaging biomarkers based on MRI or FDG-PET imaging could provide a useful tool to improve the differential diagnosis, for example in comparison to atypical parkinsonism.

Up to date, many studies have tried to identify new imaging biomarkers for PD (Lehericy et al., 2017; Lotankar et al., 2017; Postuma and Berg, 2016). Recent qualitative reviews about multimodal biomarkers in PD suggested diffusion tensor imaging (DTI) as preferably useful for diagnosis and staging of PD (Lehericy et al., 2017; Tuite, 2017). Indeed, a pattern recognition algorithm (support vector machine classification) using DTI data of the substantia nigra has proved to yield high accuracy (up to 97.5%) in differentiating PD from healthy subjects and other parkinsonian syndromes (Haller et al., 2012). Also other MRI- and FDG-PET-based measures have been investigated by many studies. However, due to the large variability between study settings and analysis methods, the reported results are heterogeneous and consequently they are considered as still developing methods for PD assessment (Lehericy et al., 2017; Lotankar et al., 2017; Postuma and Berg, 2016). In order to provide an unbiased overview of the up-to-date literature,

free from a priori hypotheses, we decided to focus our meta-analysis on whole-brain studies applying structural MRI, FDG-PET or DTI imaging. For a complete account of the literature, the reader can refer to the references in the Supplementary material. To further disentangle the effects of different clinical phenotypes, we stratified our findings into several clinical subcohorts. Our aim was to identify a robust and replicable neural signature of PD that can be used in the research and clinical settings. To this end, we systematically applied quantitative data-driven meta-analyses on multimodal neuroimaging data to identify prototypical neural networks involved in PD and to extract disease-specific imaging biomarkers. Moreover, we aimed to compare the different imaging modalities by directly contrasting them. However, given the limited number of DTI studies performing whole-brain analysis, this comparison could be performed only between MRI and FDG-PET. Of note, to cross-validate our results, we used a unique approach integrating two meta-analytical algorithms.

2. Materials and methods

2.1. Study selection

Literature search and study selection were performed according to the Preferred Reporting Items for Systematic reviews and Meta-Analyses (PRISMA) statement (www.prisma-statement.org), to assure high quality and reproducibility. First, we searched PubMed for studies published until November 2016 and matching the following keywords: (“Parkinson’s disease” OR “PD” OR “idiopathic Parkinson’s disease”) AND (“voxel-based morphometry” OR “gray matter” OR “white matter” OR “VBM” OR “FDG-PET” OR “DTI”). Only studies satisfying the following criteria were further considered: (1) original and peer-reviewed study, (2) established diagnostic criteria for PD diagnosis², (3) whole-brain neuroimaging analysis, (4) comparison with age-matched healthy controls, and (5) result coordinates reported in stereotactic reference systems, e.g. Talairach or Montreal Neurological Institute (MNI). To prevent any a priori assumptions, region-of-interest analyses and case studies were excluded. The selection is summarized in the PRISMA flowchart (Fig. 1). Both literature search and study selection were independently performed by two investigators (FA and TB).

FDG-PET and structural voxel-based morphometry MRI (MRI-VBM) studies were numerous enough to be stratified into subcohorts. Specifically, three subcohorts were created according to the PD patients’ clinical characteristics: (1) an inclusive group comprising all PD patients irrespective of their clinical features (e.g. cognitive impairment or visual hallucinations) (PD-All), (2) a subgroup including only PD patients with cognitive impairment, defined as Mild Cognitive Impairment or dementia (PD-Cog), (3) a subgroup of patients with only PD motor symptoms without specific cognitive or behavioral deficits (PD-Motor). Additional subanalyses were run on structural MRI studies reporting gray matter increases in PD as compared to controls (PD-Inc) and white matter changes in PD (PD-WM). Furthermore, white matter changes were also investigated in DTI fractional anisotropy studies.

2.2. Statistical analyses

2.2.1. Demographic and clinical features

The following variables were extracted across studies: age, gender, Mini-Mental State Examination (MMSE), disease duration, Hoehn&Yahr stage, and Unified Parkinson’s Disease Rating Scale motor score (UPDRS-III). Summary statistics (i.e. means and standard deviations) were computed across all the studies (MRI + PET + DTI), as well as separately for the clinical subgroups (i.e. PD-All, PD-Motor, PD-Cog, and PD-Inc) and imaging modalities (Table 1). Group comparisons by means of Kruskal-Wallis tests were conducted to statistically assess differences in the extracted variables across different imaging cohorts. Multiple statistical tests were Bonferroni corrected with $\alpha = 0.01$.

2.2.2. Meta-analysis

Statistical analyses were performed with two different software packages to obtain robust, reliable results and to validate the results of each individual technique. Anatomical Likelihood Estimation (ALE) and Seed-based D Mapping (SDM) approaches are implemented in GingerALE (v2.3.6) (Eickhoff et al., 2012) and SDM (v5.1.41) (Radua and Mataix-Cols, 2009) (Table-e11 summarizes characteristics of both methods).

First, we applied the SDM approach (Radua and Mataix-Cols, 2012; Radua et al., 2014). In brief, the extracted maxima from the literature are used to build a statistical map for each study. A value is assigned to each voxel in the map depending on its proximity to the reported coordinates of interest, so that the closer the voxel, the higher its value. In the case of voxels that lie in the proximity of more than one coordinate, the values are linearly summed. To avoid the issue of studies reporting coordinates in close proximity, a multilevel kernel density analysis is implemented to limit the values to a maximum. Then, pooling the individual maps together, a mean meta-analytical map is computed, in which the value of a voxel is defined as the proportion of studies reporting a coordinate around that voxel. Finally, the resulting map is tested against a whole-brain null distribution of the meta-analytical values (Radua and Mataix-Cols, 2009). Of note, the SDM software does not provide a built-in function for multiple comparison correction. Accordingly, we performed false discovery rate (FDR) correction of the uncorrected *p*-values using the SDM FDR online calculator.

For SDM analyses, the extracted coordinates of gray matter density, metabolic or fractional anisotropy changes and the corresponding *z*-scores were used. In case of reported *t*-values, a *t*-to-*z* conversion was performed (www.sdmproject.com/utilities/?show=Statistics). Coordinates were converted into MNI space by the software. The null distribution was computed with 100 randomizations and an anisotropic kernel. The first threshold was set at $p < .001$ uncorrected. In addition, to test the stability of the results, a jack-knife approach was applied, i.e. removing one study at a time and running the analysis again. We thus report only clusters present in at least 80% of the jack-knife folds for the PD-All analysis and the full range (1–100%) for the subanalyses on limited number of studies. Notably, the SDM software takes into account the sample size differences between the included studies and it allows also the inclusion of studies with negative findings.

Secondly, the same meta-analysis was run by means of the ALE method (Eickhoff et al., 2012; Laird et al., 2009). In summary, each coordinate is set as the center of a Gaussian probability distribution, whose width is corrected according to the sample size of the corresponding study. Then, all the Gaussian distributions are summed in one statistical map that is tested voxel-wise against the null hypothesis of an equal spatial distribution of the foci. Thus, regions with ALE values higher than expected by chance are identified.

We converted Talairach coordinates into MNI space with Lancaster transformation as implemented in GingerALE. The statistical threshold at the voxel-level was set at $p < .001$ uncorrected as in SDM. Results were considered significant after Family-Wise Error (FWE) correction at the cluster level ($p < .05$). In contrast to SDM, studies reporting negative findings cannot be included in the ALE meta-analysis and were thus discarded. Furthermore, to enable direct comparison of FDG-PET and MRI-VBM results, we run a contrast analysis between the two modalities on the PD-all cohort. This analysis, which statistically assesses differences between two modalities, is only implemented in GingerALE and was performed with standard parameters, i.e. uncorrected voxel-level threshold at $p < .001$ and 10,000 permutations.

Finally, to facilitate the comparison of results of both meta-analytical approaches, we created an overlap image combining them (SDM \cap ALE). This conjunction analysis revealed clusters that were significant by both algorithms. In the following results and discussion sections we focus on brain changes in PD that were consistently identified by SDM and ALE meta-analyses. This highlights the most reliable findings that are independent from the specifics of the applied meta-analytical method.

Table 1
Summarized subjects' demographics.

Cohort	Modality	Cohorts		Age (years)	Disease duration (years)	MMSE	UPDRS-III	Hoehn and Yahr
		N total (N in studies with null-findings, %)	Patients					
PD-All	FDG-PET	19 (3, 15.8%)	295 (46, 15.6%)	65.9 ± 4.9	8.4 ± 4.6	26.1 ± 5.0	29.8 ± 20.5	2.7 ± 0.9
	MRI	65 (18, 27.7%)	1767 (475, 26.9%)	66.0 ± 5.8	7.1 ± 4.5	25.2 ± 7.9	18.6 ± 10.9	1.5 ± 1.0
	DTI	11 (3, 27.3%)	212 (74, 34.9%)	62.5 ± 4.6	5.4 ± 2.6	28.1 ± 1.7	32.5 ± 17.0	1.8 ± 0
	Combined	95 (21, 22.1%)	2274 (595, 26.2%)	65.6 ± 5.5	7.2 ± 4.4	25.7 ± 7.0	22.4 ± 14.9	1.9 ± 1.1
PD-Motor	FDG-PET	13 (3, 23.1%)	240 (46, 19.2%)	64.8 ± 4.6	7.3 ± 4.2	26.1 ± 5.2	30.1 ± 23.0	2.5 ± 0.9
	MRI*	42 (13, 31.0%)	1177 (368, 31.3%)	64.5 ± 5.5	6.8 ± 2.8	27.8 ± 1.2	24.0 ± 7.2	2.1 ± 0.4
	Combined	55 (16, 29.1%)	1417 (414, 29.2%)	64.6 ± 5.2	7.0 ± 3.3	27.3 ± 3.2	25.7 ± 13.6	2.2 ± 0.6
PD-Cog	FDG-PET	5 (0, 0%)	92 (0, 0.0%)	69.0 ± 5.1	10.7 ± 5.7	20.7 ± 7.4	20.9 ± 8.8	3.3 ± 0.4
	MRI	11 (1, 9.1%)	256 (36, 14.1%)	71.1 ± 3.1	7.6 ± 3.9	24.0 ± 4.3	29.7 ± 7.3	2.7 ± 0.8
	Combined	15 (1, 6.7%)	348 (36, 10.3%)	70.4 ± 3.8	8.7 ± 4.7	23.4 ± 4.7	27.3 ± 8.3	2.9 ± 0.8
PD-WM	MRI	4/6 (2, 33.3%)	139 (64, 46.0%)	63.8 ± 2.5	7.0 ± 3.0	28.5 ± 0.8	22.6 ± 6.4	2.2 ± 0.7
PD-Inc	MRI	5 (0, 0%)	57 (0, 0.0%)	59.5 ± 7.5	8.1 ± 4.6	26.0 ± NA ⁽¹⁾	22.2 ± 0.8	2.1 ± 0.1

Note: Data shown as mean ± standard deviation. Cohorts reporting null findings were subsequently excluded in our meta-analysis. *The MRI meta-analyses led to non-significant results for the PD-Motor cohort, hence we do not elaborate on the results. ⁽¹⁾Only one study reported a value. Abbreviations: DTI diffusion tensor imaging, MMSE Mini-Mental State Examination, MRI magnetic resonance imaging, NA not reported, PD-All all Parkinson's disease patients, PD-Cog Parkinson's disease patients with cognitive impairment, PD-Motor Parkinson's disease patients with motor impairment, PD-WM white matter atrophy in Parkinson's disease, FDG-PET [18F]-fluorodeoxyglucose-positron emission tomography, UPDRS-III motor score of Unified Parkinson Disease Rating Scale.

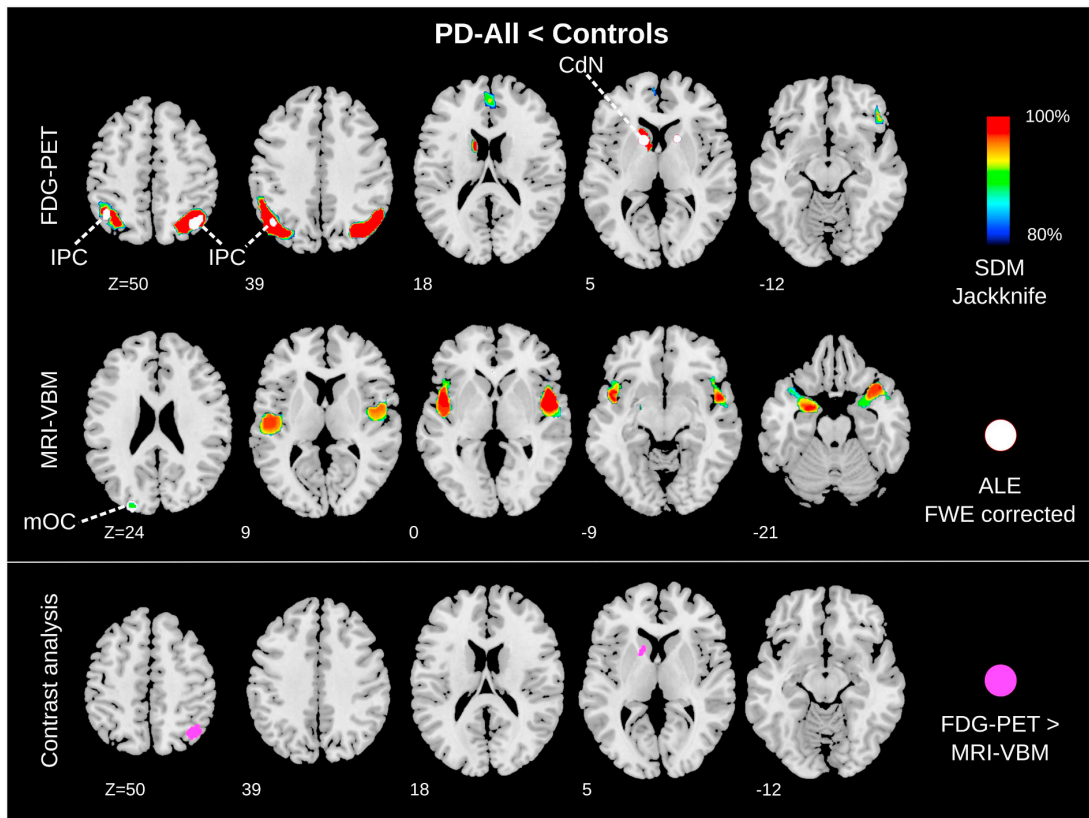


Fig. 2. Hypometabolism and atrophy in Parkinson's disease (PD) patients compared to controls. Upper rows: Meta-analysis of FDG-PET (249 PD/186 controls) and MRI-VBM (1292 PD/1014 controls) studies. The SDM/ALE conjunction highlights brain regions consistently found in both analyses. Anatomical regions are highlighted only for these consistent results. Bottom row: The contrast analysis shows significant regions for the contrast FDG-PET > MRI-VBM. Images shown in neurological convention in MNI space.

Abbreviations: ALE Anatomical Likelihood Estimation, CdN caudate nucleus, FDG-PET [18F]-fluorodeoxyglucose-positron emission tomography, FWE Family-Wise Error rate, IPC inferior parietal cortex, mOC middle occipital cortex, MRI-VBM voxel-based morphometry analysis of magnetic resonance imaging, PD-All cohort of all PD patients, SDM Seed-based D mapping.

3. Results

3.1. Included studies

The PRISMA (Moher et al., 2009) flowchart, describing the selection procedure, is displayed in Fig. 1. The overall meta-analysis included 2323 PD patients and 1767 healthy controls. Out of the total 74 studies, 50 implemented structural MRI (VBM), including 1816 PD patients. Fourteen FDG-PET studies investigated 295 patients and ten whole-brain DTI studies comprised 212 patients. Only studies reporting significant findings are displayed in Table e-1. Notably, negative findings (i.e. no difference comparing patients and controls) were reported in 14 (28% out of all) MRI studies, 3 (21.4%) FDG-PET, and 3 (30%) DTI studies (Table e-2). As for the clinical subgroups, Table 1 displays the number of subjects in each category stratified by imaging modalities.

3.2. Demographic and clinical characteristics

Considering significant studies, Table 1 displays means and standard deviations of descriptive variables for the entire sample, the clinical subgroups, and the imaging modalities. Overall, the mean age of PD patients was 65.6 ± 5.5 years (MRI 66.0 ± 5.8 ; PET 65.9 ± 4.9 ; DTI 62.5 ± 4.6) with a good balance between males and females (m/f) 927/728 (MRI 711/561; PET 107/92; DTI 82/56). Disease duration was on average 7.2 ± 4.4 years (MRI 7.1 ± 4.5 ; PET 8.4 ± 4.6 ; DTI 5.4 ± 2.6).

Kruskal-Wallis tests showed no significant differences across imaging modalities for age ($\chi^2 = 3.0$), disease duration ($\chi^2 = 1.9$), and severity (UPDRS-III $\chi^2 = 5.9$, MMSE $\chi^2 = 1.2$), guaranteeing a well-matched analysis with balanced variables. For disease severity assessed with the Hoehn & Yahr scale there was a significant difference between the groups ($\chi^2 = 9.0$, $df = 2$, $p = .011$). The results should be interpreted with care, though, as 46% of the included studies did not report and/or assess Hoehn & Yahr stage, 39% did not report MMSE, and 19% did not report UPDRS-III. Accordingly, studies' comparability in UPDRS-III scores seems to be more valid than the difference in Hoehn & Yahr stages. Note that only two studies (Watanabe et al., 2013; Yarnall et al., 2014) used the MDS-UPDRS scale (Goetz et al., 2008) instead of the UPDRS scale (Fahn, 1987).

3.3. Meta-analysis on the PD-All cohort

Overlapping results of SDM and ALE were deemed significant and are here reported. The PD-All < Controls comparison revealed significant glucose hypometabolism in the entire PD cohort in the bilateral inferior parietal cortex and in the left caudate nucleus, independently of the meta-analytical approach implemented (Fig. 2, top row, and Table 2, e-3, e-4). The conjunction analysis of the PD-All < Controls contrast revealed small focal gray matter atrophy in the middle occipital gyrus (Fig. 2, middle row, and Table 2, e-5, e-6).

3.4. Contrast analyses

The contrast analysis between FDG-PET and MRI-VBM showed only significant findings in the FDG-PET > MRI-VBM contrast. Namely, FDG-PET compared to MRI-VBM revealed brain changes in the left caudate nucleus and right superior parietal cortex/precuneus (Fig. 2, bottom row Table e-10).

3.5. Meta-analysis on subcohorts

The results of the meta-analysis of the subcohorts are displayed in Fig. 3.

PD-Cog: Glucose metabolism was reduced in the bilateral inferior parietal cortex and in the right orbitofrontal cortex with both meta-analytical algorithms in the PD-Cog < Controls comparison, i.e. in PD

patients with cognitive deficits (Fig. 3 and Table e-3, e-4). Conversely, the conjunction analysis of SDM and ALE for the structural MRI meta-analysis showed no overlap. ALE detected atrophy in left hippocampus only, while using SDM atrophy was seen in left insula, putamen, claustrum, and right putamen, as well as in the globus pallidus (Fig. 3, left side, Table e-5, e-6).

PD-Motor: The conjunction analysis on FDG-PET results revealed consistent glucose hypometabolism in the PD-Motor < Controls comparison, i.e. PD patients with solely motor impairment, in the left caudate nucleus, a motor structure. For structural MRI (Fig. 3, right side, and Table e-3, e-4), the ALE meta-analyses did not provide significant results for the PD-Motor cohort.

PD-Inc: Right side of Fig. 3 and Table e-5 and e-6 display findings of higher gray matter density in PD compared to controls (PD-Inc > Controls). An overlap between SDM and ALE was found in basal ganglia, i.e. caudate nucleus, putamen, globus pallidus, and thalamus.

White matter (DTI): DTI studies revealed lower fractional anisotropy in PD compared to controls with consistent results for SDM and ALE in the cingulate bundle close to the orbital and anterior cingulate gyri (Fig. 3, bottom row, and Table e-7, e-8).

White matter (MRI-VBM): The conjunction analysis revealed white matter atrophy in superior longitudinal fasciculus, internal capsule, and extreme/external capsule in the vicinity of the right putamen and globus pallidus in PD compared to controls. White matter atrophy was further found in the superior occipitofrontal fasciculus, corpus callosum, corona radiata, external and internal capsule surrounding the left caudate nucleus (Fig. 3, bottom row, and Table e-5, e-6).

4. Discussion

In summary, our multimodal meta-analysis across whole-brain imaging studies revealed that FDG-PET glucose hypometabolism is more consistently associated with PD as compared to brain atrophy as identified by MRI-VBM. Moreover, the meta-analysis on the subcohorts provides an interesting initial glimpse into specific neural signatures of different PD clinical phenotypes and into white matter changes in PD.

4.1. FDG-PET hypometabolism is more specific than MRI-VBM structural changes in PD

We hypothesize that the reason behind the dissociation between FDG-PET and MRI-VBM results lies in the different PD-related brain changes captured by the two techniques. Indeed, structural MRI analyzed with VBM identifies morphological brain abnormalities (Ashburner and Friston, 2000), while FDG-PET is a proxy of early neuronal injury and synaptic dysfunction. Such functional brain alterations may antedate morphological changes by several years, as in the case of Alzheimer's disease or Huntington's disease (Mosconi, 2013; Tang et al., 2013). Indeed, FDG-PET studies have shown Alzheimer's disease-related brain hypometabolism in cognitively intact subjects at genetic risk (i.e. $\epsilon 4$ homozygous carriers) several years before disease onset (Reiman et al., 1996). Similarly, multimodal imaging studies, combining FDG-PET and structural MRI to investigate presymptomatic genetic Alzheimer's disease, have shown that hypometabolism precedes and exceeds atrophy in the early identification of brain abnormalities (Gordon et al., 2018; Mosconi et al., 2006). In line with that, metabolic changes were shown to be more sensitive to progression of the disease than structural changes in preclinical Huntington's disease mutation carriers (Tang et al., 2013). Thus, in analogy with Alzheimer's disease and Huntington's disease, FDG-PET might be a more accurate biomarker for subtle brain abnormalities in PD. Of note, cohorts in FDG-PET and MRI-VBM studies did not differ regarding age, disease duration, and disease severity, making respective biases unlikely. Although differences in Hoehn & Yahr stage were evident, this comparison was less reliable due to multiple missing data.

Since functional brain changes seem to be more relevant for PD

Table 2
Results for the PD-All cohort.

Cluster #	Volume (mm ³)	ALE Value	x	y	z	Region
Local maxima of ALE analyses in FDG-PET						
1	1424	0.022737322	-14	12	4	Left caudate body
2	1416	0.015668042	-42	-56	50	Left inferior parietal lobule
		0.015623625	-44	-62	36	Left middle temporal gyrus
3	1336	0.023226662	38	-64	48	Right precuneus
4	856	0.017095294	16	12	4	Right caudate body
Local maxima of ALE analyses in MRI						
1	976	0.0337	-24	-90	24	Left middle occipital gyrus
Cluster #	Voxels	SDM-Z	x	y	z	Region
Local maxima of SDM analyses in FDG-PET						
1	2217	-4.015	-50	-62	38	Left angular gyrus
2	2070	-3.528	34	-72	38	Right middle occipital gyrus
3	568	-2.894	0	46	20	Left superior medial frontal gyrus
4	466	-3.185	-6	14	4	Left caudate nucleus
5	186	-2.804	46	30	-12	Right inferior frontal gyrus
6	45	-2.590	-44	46	-2	Left middle frontal gyrus
7	43	-2.695	14	12	2	Right anterior thalamic projections
8	28	-2.509	46	26	28	Right inferior frontal gyrus
9	27	-2.506	62	-32	-12	Right middle temporal gyrus
10	26	-2.508	14	-94	16	Right cuneus cortex
11	25	-2.537	60	-50	-6	Right middle temporal gyrus
12	22	-2.574	8	-90	2	Right calcarine fissure
Local maxima of SDM analyses in MRI						
1	1952	-3.304	-24	-2	-18	Left amygdala
2	1804	-3.345	50	2	2	Right Rolandic operculum
3	33	-2.746	-24	-90	24	Left superior occipital gyrus

Clusters below an effect-size estimate (SDM) threshold $p < .001$ and an anatomical likelihood estimate (ALE) threshold $p < .05$ FWE are listed. Coordinates are in MNI space.

assessment, also resting-state functional MRI (rs-fMRI) could be employed to investigate the neural signature of PD. Indeed, recent meta-analyses on rs-fMRI studies in PD revealed functional alterations in patients compared to controls in both motor (i.e. supplementary motor areas, left putamen and premotor cortex) and non-motor (i.e. bilateral inferior parietal and supramarginal gyri) networks (Pan et al., 2017; Tahmasian et al., 2017). This result aligns with our FDG-PET findings, pointing out that functional changes both inside and outside the motor network, namely in the inferior parietal cortex, might represent a crucial hallmark of PD that has been neglected so far. Indeed, the inferior parietal cortex is a higher order associative region that plays an important role in various mechanisms ranging from language (e.g. selecting gestures, verbal integration of complex contexts like sentences) to spatial orientation (e.g. processing personal space, localization of objects) as well as motor functions (e.g. tactile reception of complex movements and interaction with objects) (Culham and Kanwisher, 2001). There is even evidence of mirror neurons in the inferior parietal cortex, which encode goals of motor acts (Rizzolatti et al., 2009). Impairment in this region can lead to the well-described effect of spatial hemineglect and further to dysfunction in autobiographical memory, as in the case of Alzheimer's disease, and visual disorientation or mislocalization (Berryhill et al., 2007; Culham and Kanwisher, 2001; Schroeter et al., 2009).

Moreover, we found consistent hypometabolism in the PD-all cohort in the left caudate nucleus, a core structure in the basal ganglia network that, together with the putamen, serves as input structure for nigrostriatal projections (Fallon, 1988). Of note, the conjunction analysis showed a consistent hypometabolism in the left, but not right, caudate nucleus. Different reasons may account for this finding. First, majority of patients with PD present and progress in their parkinsonism unilaterally. In the recent diagnostic criteria by Postuma et al. (2015) bilateral motor symptoms at onset are even considered as a red flag to exclude the diagnosis of PD. Second, SDM additionally identified the right caudate nucleus as compromised by PD, suggesting that our

unilateral finding may have been due to statistical power effects or the differences in algorithms.

Moreover, the result of a consistent caudate hypometabolism in the PD-motor subgroup, but not in the PD-Cog subgroup, is to a certain extent surprising. On the one hand, several previous studies have drawn a link between caudate nuclei function and cognitive deficits – mainly executive functions (Grahn et al., 2008) – in PD with and without dementia (Apostolova et al., 2010; Polito et al., 2012). On the other hand, motor symptoms, particularly rigidity and bradykinesia, are generally associated with dysfunctions in the posterior putamen that shows an earlier and faster decline in dopamine function as compared to the caudate nucleus (Pavese and Brooks, 2009). However, an interesting observation comes from a dual-tracer PET study from Holtbernd et al. (2015) that investigated the relationship between dopaminergic dysfunction and glucose metabolism in a large PD cohort. The study reports significant correlations between dopamine function in the caudate nucleus and the expression of both motor- and cognition-related metabolic patterns in PD, while dopaminergic activity in the putamen was related only to the expression of the motor-related PD pattern. This result supports the role of the posterior putamen in PD motor impairment, while the involvement of the caudate nucleus seems to be implicated in both cognitive and motor symptoms. Of note, many of the studies showing involvement of the putamen in PD by means of FDG-PET applied spatial covariance analysis and reported relative increases in glucose metabolism in the putamen (Eckert et al., 2007). This approach is intrinsically different from the univariate voxel-based statistics implemented by the FDG-PET studies that were object of the present meta-analytical work.

Notably, the subcohort analyses on the FDG-PET data revealed that glucose hypometabolism in cortical associative parietal regions is mainly related to cognitive impairment in PD, while hypometabolism in the caudate nucleus is more strongly associated with the motor phenotype. This might indicate that functional changes outside the basal ganglia are more associated with the presence of cognitive deficits in

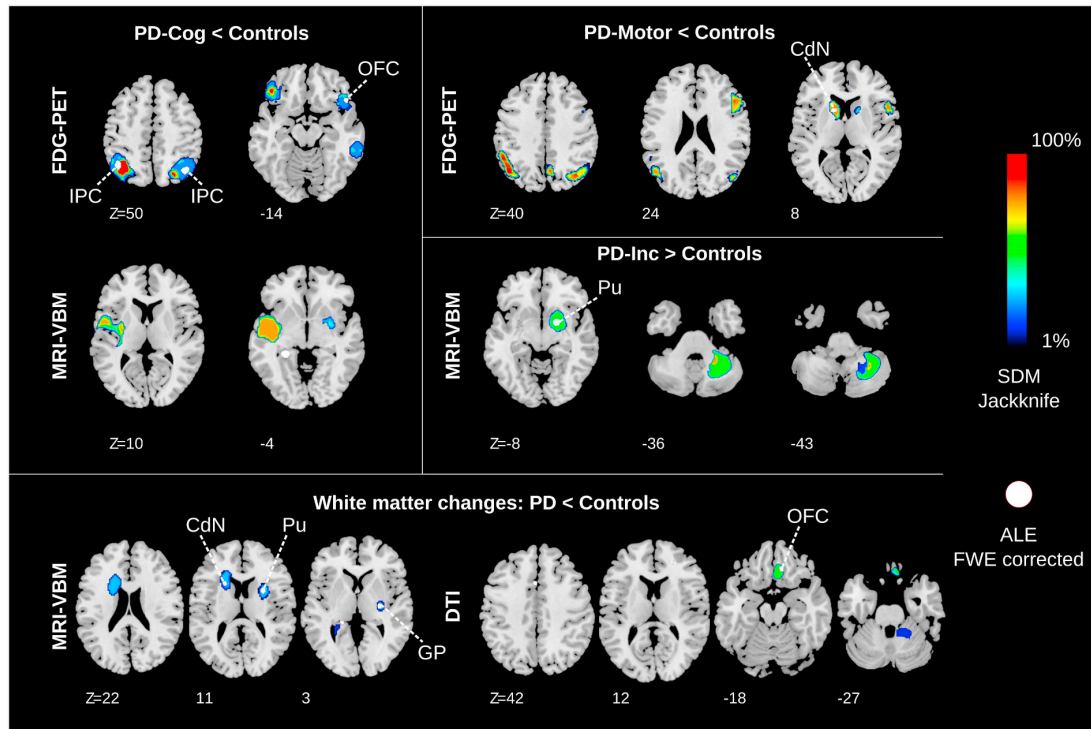


Fig. 3. Hypometabolism and atrophy across Parkinson's disease (PD) clinical subgroups and white matter changes comparing PD to controls. The $SDM \cap ALE$ conjunction highlights brain regions consistently found in both analysis algorithms. Anatomical regions are highlighted only for these consistent results. Images shown in neurological convention in the MNI space.

Abbreviations: ALE Anatomical Likelihood Estimation, CdN projections surrounding caudate nucleus, DTI diffusion tensor imaging, FDG-PET [18F]-fluorodeoxyglucose-positron emission tomography, FWE Family-Wise Error rate, GP projections surrounding globus pallidus, IPC inferior parietal cortex, MRI-VBM voxel-based morphometry analysis of magnetic resonance imaging, OFC orbitofrontal cortex, PD-Cog PD with cognitive impairment, PD-Motor PD with only motor symptoms, PU putamen/projections surrounding putamen, SDM Seed-based D mapping.

PD, as previously suggested (Huang et al., 2007; Lopes et al., 2017). Hypometabolism in parietal associative areas is also a hallmark of Alzheimer's disease, thus limiting the specificity of our finding as PD biomarker (Schroeter et al., 2009). Also the caudate nucleus, due to its connectivity with prefrontal regions, may play a role in the emergence of cognitive dysfunction in PD beside motor deficits (Brück et al., 2000). Disease specificity of glucose hypometabolism in this brain region for PD is not guaranteed as it has also been reported in behavioral variant frontotemporal dementia and nonfluent/agrammatic variant of primary progressive aphasia (synonymous with progressive non-fluent aphasia) (Bisenius et al., 2016; Schroeter et al., 2014).

Remarkably, five out of the 14 FDG-PET studies reported hypermetabolism in PD as compared to controls, but no significant result was found applying the meta-analytical procedure. Relative metabolic increases in the putamen, globus pallidus, pons and cerebellum have been consistently reported as a crucial feature of the PD-related spatial covariance pattern (Eckert et al., 2007). However, the identification of real FDG-PET hypermetabolism in PD has been questioned, as increased glucose metabolism could be the result of the intensity normalization procedure applied in PET analysis. For example, Borghammer et al. (2009) showed that regional (i.e. mainly subcortical) metabolic increases in PD as compared to controls might artifactually emerge as a consequence of global mean normalization when lower global values characterize the patient group. A comparable finding has been reported for Alzheimer's disease and frontotemporal lobar degeneration (Dukart et al., 2011). However, (Ma et al., 2009) reported that global values in early PD stages are identical to those of healthy controls and that subcortical metabolic increases also correlate with clinical measures. In

our meta-analysis, studies reporting hypermetabolism in PD, especially in subcortical structures, applied global mean normalization, while none of the studies that used either normalization to white matter, cerebellum, pons or absolute FDG-PET measures found increased metabolism. This fact might support the assumption of artefactual increases in metabolism due to normalization to the global mean, although other reasons are still possible. Table e-9 reports different intensity normalization procedures for FDG-PET studies.

Finally, our meta-analysis considered whole-brain FDG-PET studies generally applying univariate statistics to compare patients and controls. A consistent body of literature on multivariate network analysis has also demonstrated the usefulness of FDG-PET (Eidelberg, 2009). Several studies identified the so-called *PD-related covariance pattern (PDRP)* that distinguishes PD patients from healthy controls (Niethammer and Eidelberg, 2012). This metabolic pattern has high accuracy (sensitivity 84%, specificity 97%) in differentiating PD from atypical parkinsonism, is modulated by treatment and is predictive for disease progression (Niethammer and Eidelberg, 2012; Tang et al., 2010). This supports the relevance of functional brain changes as PD biomarkers, which in future might be improved by focusing analyses on the prototypical networks identified in our meta-analyses.

4.2. MRI-VBM changes in PD are heterogeneous and unspecific

In contrast with FDG-PET, we did not find a specific consistent pattern of structural brain changes in PD as detected by whole-brain MRI-VBM analysis. This was also apparent in the contrast analyses where we obtained significant differences only for the FDG-

PET > MRI-VBM contrast. The PD-all < controls comparison revealed only minor atrophy in the middle occipital gyrus. Similarly to our study, also previous meta-analyses investigating structural changes in PD showed only minor and heterogeneous changes (Pan et al., 2012; Shao et al., 2014; Shao et al., 2015; Yu et al., 2015). Furthermore, the high number of MRI-VBM studies reporting null findings for the patients vs. controls comparison indicates that gray matter changes in PD are unspecific and heterogeneous. Additionally, the neuropathological criteria for PD only describe morphological changes in the substantia nigra pars compacta and Lewy pathology as specific pathological signatures of PD even in late phases of the disease (Dickson et al., 2009). Concerning the subcohort analyses, both the meta-analyses in PD with solely motor (PD-Motor) and additional cognitive symptoms (PD-Cog) did not reveal consistent results between the two meta-analytical approaches. This further confirms the inadequacy of atrophy and structural MRI in PD. Notwithstanding, implementing structural MRI could be more useful in the diagnostic workout when guided by a priori hypothesis (e.g. focusing on the substantia nigra) and applying recent technical MRI improvements, such as relaxometry, magnetization transfer, and neuromelanin-sensitive imaging (Lehericy et al., 2012). In addition, more sophisticated machine learning approaches have been proposed for the detection of morphometric PD imaging biomarker, providing high accuracy in differentiating PD patients and controls (Peng et al., 2017).

Surprisingly, we found higher gray matter volume in the right lentiform nucleus and thalamus in PD compared to controls. According to Braak's staging model of disease spreading, the degeneration of the thalamic nuclei is a PD hallmark (Braak et al., 2003). The higher gray matter volume might be a compensatory mechanism to counteract the reduction of inhibitory input to the thalamus (Lin et al., 2013). Indeed, it has been proposed that PD leads to a reduction of the inhibitory input from the globus pallidus and the substantia nigra to the thalamus and a consequent derangement of the thalamic excitatory output to the cortex.

4.3. White matter changes: preliminary evidence

Voxel-wise white matter changes were investigated with both MRI-VBM and DTI. The former revealed widespread white matter changes, while the latter indicated the cingulate bundle near the orbital and anterior cingulate gyri as more affected. These findings are in line with the non-motor symptoms of PD. Orbitofrontal gyri are involved in sniffing and smelling (Sobel et al., 1998). Notably, olfactory dysfunction is one of the earliest features of prodromal PD, preceding disease onset by years to decades (Postuma et al., 2015). The anterior cingulate cortex has been associated with behavioral symptoms in PD (Tekin and Cummings, 2002). However, generalizability of these findings is undetermined by the small number of studies in the analysis. As aforementioned, combining the knowledge from histopathological findings and in vivo brain imaging could provide a more accurate PD biomarker. Indeed, DTI studies that focused on the substantia nigra have shown high accuracy in discriminating PD patients from healthy controls (Cochrane and Ebmeier, 2013).

4.4. Limitations of the study

This is, to our knowledge, the largest whole-brain meta-analysis comparing PD patients and controls and the only multimodal study combining MRI, FDG-PET, and DTI. The replicability of our findings is assured by the combination of independent meta-analytical algorithms. Nevertheless, we recognize some limits. First, all included studies lack PD histopathological confirmation, as studies on autopsy-proven cases are extremely rare. Second, methodological and technical differences exist among the included studies, e.g. in field-strength of MR scanners, processing protocols, or data modulation. However, the impact of these differences on our results is limited since the meta-analytical algorithms only take maxima into account and not the cluster size that is more

affected by this heterogeneity. Additionally, our study could not disentangle the influence of pharmacological treatment on PD and the disease process itself, because almost all studies investigated medicated subjects. The aim of our meta-analysis was to identify PD-specific imaging biomarkers to support the diagnosis in the earliest disease stages. However, most of the included studies were performed with patients who have had the disease for several years (mostly in intermediate disease phase), making sub-meta-analyses for early PD unfeasible. We believe that defining biomarkers on subjects in moderate disease stages and applying them at earlier time points, i.e. in *de-novo* patients or even in pre-symptomatic subjects, is a valid approach. This research strategy has been successfully applied in the case of Alzheimer's disease (see for example Bateman et al., 2012; Mosconi et al., 2004; Whitwell et al., 2007). Finally, we remark once again the exploratory nature of the subcohort analysis given the limited number of included studies. Accordingly, future validation of the meta-analysis in independent cohorts is necessary. Specificity and sensitivity of the suggested PD-specific brain regions for differential diagnosis should be validated in large, preferably multicenter, and independent patient cohorts. This approach has already been successfully applied to other neurodegenerative diseases such as Alzheimer's disease and frontotemporal lobar degeneration (Dukart et al., 2013; Dukart et al., 2011). As for the DTI studies, we recognize that the choice of focusing on whole-brain investigations reduced the number of included studies and penalized the results of its diagnostic accuracy. Indeed, as aforementioned, the in vivo tractography of the projections of the substantia nigra provided promising results in classifying patients with PD (Haller et al., 2012).

5. Conclusion

This multimodal and cross-validation meta-analysis aimed at exploring potential imaging biomarkers for PD beyond dopaminergic imaging. The novelty of the meta-analysis is to statistically validate convergence of published results and hence draw solid conclusions with a higher statistical power than single studies. Consistent glucose hypometabolism was found in bilateral inferior parietal cortex and left caudate nucleus combining both meta-analytical methods. Glucose hypometabolism in PD was confirmed in subcohort analyses and related to cognitive deficits (inferior parietal cortex) and motor symptoms (caudate nucleus). Structural MRI showed only small focal gray matter atrophy in the middle occipital gyrus that could not be confirmed in subcohort analyses. DTI revealed fractional anisotropy reduction in the cingulate bundle in the vicinity of the orbital and anterior cingulate gyri in PD. Our meta-analysis suggests that, when applying data-driven whole-brain analysis to neuroimaging data, functional changes as assessed by FDG-PET better characterize PD as compared to structural alterations investigated by MRI-VBM and DTI. Results suggest focusing the search of PD imaging biomarkers on functional rather than structural brain abnormalities. To date neither atrophy nor glucose hypometabolism offer disease-specific imaging biomarkers for PD as the latter regionally overlaps with other neurodegenerative diseases.

Financial disclosure

This study has been supported by the Parkinson's Disease Foundation (Grant No. PDF-IRG-1307), the Michael J Fox Foundation (Grant No. MJFF-11362), the German Federal Ministry of Education and Research (BMBF; Grant number FKZ 01GI1007A; German FTLD consortium), German Research Foundation (DFG, SCHR 774/5-1), and the International Max Planck Research School (IMPRS) NeuroCom by the Max Planck Society. Jane Neumann is supported by the Federal Ministry of Education and Research (BMBF), Germany (FKZ: 01EO1001).

Authors' roles

- 1) Research project: A. Conception: FA, TB, MLS
- B. Organization: FA, TB.
- C. Execution: FA, TB.
- 2) Statistical Analysis: A. Design: FA, TB, MLS.
- B. Execution: FA, TB.
- C. Review and Critique: FA, TB, JN, MLS.
- 3) Manuscript: A. Writing of the first draft: FA, TB
- B. Review and Critique: FA, TB, JN, MLS.

Appendix A. Supplementary data

Table e-1 (All included studies reporting significant findings), Table e-2 (Studies reporting null findings included in the SDM analyses), Table e-3 (FDG-PET maxima ALE), Table e-4 (FDG-PET maxima SDM), Table e-5 (MRI maxima ALE), Table e-6 (MRI maxima SDM), Table e-7 (DTI maxima ALE), Table e-8 (DTI maxima SDM), Table e-9 (Intensity normalization procedures in FDG-PET studies), Table e-10 (Local maxima of contrast analysis), Table e-11 (Differences between ALE and SDM).

References

- Albert, M.S., ST, DeKosky, Dickson, D.F., Dubois, B., Feldman, H., Fox, N.C., Gamst, A., Holtzman, D.M., Jagust, W.J., Petersen, R.C., Snyder, P.J., Carrillo, M.C., Thies, B., Phelps, C.H., 2011. The Diagnosis of Mild Cognitive Impairment Due to Alzheimer's Disease: Recommendations from the National Institute on Aging-Alzheimer's Association Workgroups on Diagnostic Guidelines for Alzheimer's Disease.
- Apostolova, L.G., Beyer, M., Green, A.E., Hwang, K.S., Morra, J.H., Chou, Y.Y., Avedissian, C., Aarsland, D., Janvin, C.C., Larsen, J.P., 2010. Hippocampal, caudate, and ventricular changes in Parkinson's disease with and without dementia. *Mov. Disord.* 25, 687–695.
- Ashburner, J., Friston, K.J., 2000. Voxel-based morphometry – the methods. *NeuroImage* 11, 805–821.
- Bateman, R.J., Xiong, C., Benzinger, T.L., Fagan, A.M., Goate, A., Fox, N.C., Marcus, D.S., Cairns, N.J., Xie, X., Blazey, T.M., 2012. Clinical and biomarker changes in dominantly inherited Alzheimer's disease. *N. Engl. J. Med.* 367, 795–804.
- Berryhill, M.E., Phuong, L., Picasso, L., Cabeza, R., Olson, I.R., 2007. Parietal lobe and episodic memory: bilateral damage causes impaired free recall of autobiographical memory. *J. Neurosci.* 27, 14415–14423.
- Bisenius, S., Neumann, J., Schroeter, M.L., 2016. Validating new diagnostic imaging criteria for primary progressive aphasia via anatomical likelihood estimation meta-analyses. *Eur. J. Neuro.* 23, 704–712.
- Borghammer, P., Cumming, P., Aanerud, J., Gjedde, A., 2009. Artefactual subcortical hyperperfusion in PET studies normalized to global mean: lessons from Parkinson's disease. *NeuroImage* 45, 249–257.
- Braak, H., Del Tredici, K., Rub, U., de Vos, R.A., Jansen Steur, E.N., Braak, E., 2003. Staging of brain pathology related to sporadic Parkinson's disease. *Neurobiol. Aging* 24, 197–211.
- Brück, A., Portin, R., Lindell, A., Laihinne, A., Bergman, J., Haaparanta, M., Solin, O., Rinne, J.O., 2000. Positron Emission Tomography Shows that Impaired Frontal Lobe Functioning in Parkinson's Disease Is Related to Dopaminergic Hypofunction in the Caudate Nucleus.
- Cochrane, C.J., Ebmeier, K.P., 2013. Diffusion tensor imaging in parkinsonian syndromes: a systematic review and meta-analysis. *Neurology* 80, 857–864.
- Culham, J.C., Kanwisher, N.G., 2001. Neuroimaging of cognitive functions in human parietal cortex. *Curr. Opin. Neurobiol.* 11, 157–163.
- Dickson, D.W., Braak, H., Duda, J.E., Duyckaerts, C., Gasser, T., Halliday, G.M., Hardy, J., Leverenz, J.B., Del Tredici, K., Wszolek, Z.K., Litvan, I., 2009. Neuropathological assessment of Parkinson's disease: refining the diagnostic criteria. *Lancet Neurol.* 8, 1150–1157.
- Dubois, B., Feldman, H.H., Jacova, C., Hampel, H., Molinuevo, J.L., Blennow, K., DeKosky, S.T., Gauthier, S., Selkoe, D., Bateman, R., Cappa, S., Crutch, S., Engelborghs, S., Frisoni, G.B., Fox, N.C., Galasko, D., Habert, M.O., Jicha, G.A., Nordberg, A., Pasquier, F., Rabinovici, G., Robert, P., Rowe, C., Salloway, S., Sarazin, M., Epelbaum, S., de Souza, L.C., Vellas, B., Visser, P.J., Schneider, L., Stern, Y., Scheltens, P., Cummings, J.L., 2014. Advancing research diagnostic criteria for Alzheimer's disease: the IWG-2 criteria. *Lancet Neurol.* 13, 614–629.
- Dukart, J., Mueller, K., Horstmann, A., Barthel, H., Moller, H.E., Villringer, A., Sabri, O., Schroeter, M.L., 2011. Combined evaluation of FDG-PET and MRI improves detection and differentiation of dementia. *PLoS One* 6, e18111.
- Dukart, J., Mueller, K., Barthel, H., Villringer, A., Sabri, O., Schroeter, M.L., Alzheimer's Disease Neuroimaging Initiative, 2013. Meta-analysis based SVM classification enables accurate detection of Alzheimer's disease across different clinical centers using FDG-PET and MRI. *Psychiatry Res.* 212, 230–236.
- Eckert, T., Tang, C., Eidelberg, D., 2007. Assessment of the progression of Parkinson's disease: a metabolic network approach. *Lancet Neurol.* 6, 926–932.
- Eickhoff, S.B., Bzdok, D., Laird, A.R., Kurth, F., Fox, P.T., 2012. Activation likelihood estimation meta-analysis revisited. *NeuroImage* 59, 2349–2361.
- Eidelberg, D., 2009. Metabolic brain networks in neurodegenerative disorders: a functional imaging approach. *Trends Neurosci.* 32, 548–557.
- Fahn, S., 1987. Unified Parkinson's disease rating scale. In: *Recent Developments in Parkinson's Disease Volume II*. Macmillan Healthcare Information, pp. 153.
- Fallon, J.H., 1988. Topographic organization of ascending dopaminergic projections. *Ann. N. Y. Acad. Sci.* 537, 1–9.
- Goetz, C.G., Tilley, B.C., Shaftman, S.R., Stebbins, G.T., Fahn, S., Martinez-Martin, P., Poewe, W., Sampaio, C., Stern, M.B., Dodel, R., Dubois, B., Holloway, R., Jankovic, J., Kulisevsky, J., Lang, A.E., Lees, A., Leurgans, S., LeWitt, J.J., Nyenhuis, D., Olanow, C.W., Rascol, O., Schrag, A., Teresi, J.A., van Hilten, J.J., LaPelle, N., Movement Disorder Society UPDRS Revision Task Force, 2008. Movement Disorder Society-sponsored revision of the Unified Parkinson's Disease Rating Scale (MDS-UPDRS): scale presentation and clinimetric testing results. *Mov. Disord.* 23, 2129–2170.
- Gordon, B.A., Blazey, T.M., Su, Y., Hari-Raj, A., Dincer, A., Flores, S., Christensen, J., McDade, E., Wang, G., Xiong, C., Cairns, N.J., Hassenstab, J., Marcus, D.S., Fagan, A.M., Jack Jr., C.R., Hornbeck, R.C., Paumier, K.L., Ances, B.M., Berman, S.B., Brickman, A.M., Cash, D.M., Chhatwal, J.P., Correia, S., Forster, S., Fox, N.C., Graft-Radford, N.R., la Fougere, C., Levin, J., Masters, C.L., Rossor, M.N., Salloway, S., Saykin, A.J., Schofield, P.R., Thompson, P.M., Weiner, M.M., Holtzman, D.M., Raichle, M.E., Morris, J.C., Bateman, R.J., Benzinger, T.L.S., 2018. Spatial patterns of neuroimaging biomarker change in individuals from families with autosomal dominant Alzheimer's disease: a longitudinal study. *Lancet Neurol.* 17, 241–250.
- Gorno-Tempini, M.L., Hillis, A.E., Weintraub, S., Kertesz, A., Mendez, M., Cappa, S.F., Ogar, J.M., Rohrer, J.D., Black, S., Boeve, B.F., Manes, F., Dronkers, N.F., Vandenberghe, R., Rascovsky, K., Patterson, K., Miller, B.L., Knopman, D.S., Hodges, J.R., Mesulam, M.M., Grossman, M., 2011. Classification of primary progressive aphasia and its variants. *Neurology* 76, 1006–1014.
- Grahn, J.A., Parkinson, J.A., Owen, A.M., 2008. The cognitive functions of the caudate nucleus. *Prog. Neurobiol.* 86, 141–155.
- Haller, S., Badoud, S., Nguyen, D., Garibotto, V., Lovblad, K.O., Burkhard, P.R., 2012. Individual detection of patients with Parkinson disease using support vector machine analysis of diffusion tensor imaging data: initial results. *AJNR Am. J. Neuroradiol.* 33, 2123–2128.
- Holtbernd, F., Ma, Y., Peng, S., Schwartz, F., Timmermann, L., Kracht, L., Fink, G.R., Tang, C.C., Eidelberg, D., Eggers, C., 2015. Dopaminergic correlates of metabolic network activity in Parkinson's disease. *Hum. Brain Mapp.* 36, 3575–3585.
- Huang, C., Mattis, P., Tang, C., Perrine, K., Carbon, M., Eidelberg, D., 2007. Metabolic brain networks associated with cognitive function in Parkinson's disease. *NeuroImage* 34, 714–723.
- Hughes, A.J., Ben-Shlomo, Y., Daniel, S.E., Lees, A.J., 1992. What features improve the accuracy of clinical diagnosis in Parkinson's disease: a clinicopathologic study. *Neurology* 42 (6), 1142.
- Kaasinen, V., Vahlberg, T., 2017. Striatal dopamine in Parkinson disease: a meta-analysis of imaging studies. *Ann. Neurol.* 82, 873–882.
- Laird, A., Eickhoff, S., Kurth, F., Fox, P., Uecker, A., Turner, J., Robinson, J., Lancaster, J., Fox, P., 2009. ALE meta-analysis workflows via the BrainMap database: progress towards a probabilistic functional brain atlas. *Front. Neuroinform.* 3.
- Lehericy, S., Sharman, M.A., Dos Santos, C.L., Paquin, R., Gallea, C., 2012. Magnetic resonance imaging of the substantia nigra in Parkinson's disease. *Mov. Disord.* 27, 822–830.
- Lehericy, S., Vaillancourt, D.E., Seppi, K., Monchi, O., Rektorova, I., Antonini, A., McKeown, M.J., Masellis, M., Berg, D., Rowe, J.B., Lewis, S.J.G., Williams-Gray, C.H., Tesson, A., Siebner, H.R., International Parkinson and Movement Disorder Society (IPMDS) Neuroimaging Study Group, 2017. The role of high-field magnetic resonance imaging in parkinsonian disorders: pushing the boundaries forward. *Mov. Disord.* 32, 510–525.
- Lin, C.H., Chen, C.M., Lu, M.K., Tsai, C.H., Chiou, J.C., Liao, J.R., Duann, J.R., 2013. VBM reveals brain volume differences between Parkinson's disease and essential tremor patients. *Front. Hum. Neurosci.* 7, 247.
- Lopes, R., Delmaire, C., Defebvre, L., Moonen, A.J., Duits, A.A., Hofman, P., Leentjens, A.F., Dujardin, K., 2017. Cognitive phenotypes in Parkinson's disease differ in terms of brain-network organization and connectivity. *Hum. Brain Mapp.* 38, 1604–1621.
- Lotankar, S., Prabhavalkar, K.S., Bhatt, L.K., 2017. Biomarkers for Parkinson's disease: recent advancement. *Neurosci. Bull.* 33, 585–597.
- Ma, Y., Tang, C., Moeller, J.R., Eidelberg, D., 2009. Abnormal regional brain function in Parkinson's disease: truth or fiction? *NeuroImage* 45, 260–266.
- Moher, D., Liberati, A., Tetzlaff, J., Altman, D.G., PRISMA-Group, 2009. Preferred reporting items for systematic reviews and meta-analyses: the PRISMA statement. *BMJ* 339, b2535.
- Mosconi, L., 2013. Glucose metabolism in normal aging and Alzheimer's disease: methodological and physiological considerations for PET studies. *Clin. Transl. Imag.* 1.
- Mosconi, L., Perani, D., Sorbi, S., Herholz, K., Nacmias, B., Holthoff, V., Salmon, E., Baron, J.-C., De Cristofaro, M., Padovani, A., 2004. MCI conversion to dementia and the APOE genotype: a prediction study with FDG-PET. *Neurology* 63, 2332–2340.
- Mosconi, L., Sorbi, S., de Leon, M.J., Li, Y., Nacmias, B., Myoung, P.S., Tsui, W., Ginestroni, A., Bessi, V., Fayyaz, M., Caffarra, P., Pupi, A., 2006. Hypometabolism exceeds atrophy in presymptomatic early-onset familial Alzheimer's disease. *J. Nucl. Med.* 47, 1778–1786.
- Niethammer, M., Eidelberg, D., 2012. Metabolic brain networks in translational neurology: concepts and applications. *Ann. Neurol.* 72, 635–647.
- Pan, P.L., Song, W., Yang, J., Huang, R., Chen, K., Gong, Q.Y., Zhong, J.G., Shi, H.C., Shang, H.F., 2012. Gray matter atrophy in behavioral variant frontotemporal dementia: a meta-analysis of voxel-based morphometry studies. *Dement. Geriatr. Cogn. Disord.* 33, 141–148.

- Pan, P., Zhang, Y., Liu, Y., Zhang, H., Guan, D., Xu, Y., 2017. Abnormalities of regional brain function in Parkinson's disease: a meta-analysis of resting state functional magnetic resonance imaging studies. *Sci. Rep.* 7, 40469.
- Pavese, N., Brooks, D.J., 2009. Imaging neurodegeneration in Parkinson's disease. *Biochim. Biophys. Acta (BBA) - Mol. Basis Dis.* 1792, 722–729.
- Peng, B., Wang, S., Zhou, Z., Liu, Y., Tong, B., Zhang, T., Dai, Y., 2017. A multilevel-ROI-features-based machine learning method for detection of morphometric biomarkers in Parkinson's disease. *Neurosci. Lett.* 651, 88–94.
- Poewe, W., Seppi, K., Tanner, C.M., Halliday, G.M., Brundin, P., Volkman, J., Schrag, A.E., Lang, A.E., 2017. Parkinson disease. *Nat. Rev. Dis. Primers* 3, 17013.
- Polito, C., Berti, V., Ramat, S., Vanzi, E., De Cristofaro, M.T., Pellicanò, G., Mungai, F., Marini, P., Formiconi, A.R., Sorbi, S., 2012. Interaction of caudate dopamine depletion and brain metabolic changes with cognitive dysfunction in early Parkinson's disease. *Neurobiol. Aging* 33, 206.e229–206.e239.
- Postuma, R.B., Berg, D., 2016. Advances in markers of prodromal Parkinson disease. *Nat. Rev. Neurol.* 12, 622–634.
- Postuma, R.B., Berg, D., Stern, M., Poewe, W., Olanow, C.W., Oertel, W., Obeso, J., Marek, K., Litvan, I., Lang, A.E., Halliday, G., Goetz, C.G., Gasser, T., Dubois, B., Chan, P., Bloem, B.R., Adler, C.H., Deuschl, G., 2015. MDS clinical diagnostic criteria for Parkinson's disease. *Mov. Disord.* 30, 1591–1601.
- Radua, J., Mataix-Cols, D., 2009. Voxel-wise meta-analysis of grey matter changes in obsessive-compulsive disorder. *Br. J. Psychiatry* 195, 393–402.
- Radua, J., Mataix-Cols, D., 2012. Meta-analytic methods for neuroimaging data explained. *Biol. Mood Anxiety Disord* 2, 6.
- Radua, J., Rubia, K., Canales-Rodríguez, E.J., Pomarol-Clotet, E., Fusar-Poli, P., Mataix-Cols, D., 2014. Anisotropic kernels for coordinate-based meta-analyses of neuroimaging studies. *Front. Psychol.* 5, 13.
- Rascovsky, K., Hodges, J.R., Knopman, D., Mendez, M.F., Kramer, J.H., Neuhaus, J., van Swieten, J.C., Seelaer, H., Dopper, E.G., Onyike, C.U., Hillis, A.E., Josephs, K.A., Boeve, B.F., Kertesz, A., Seeley, W.W., Rankin, K.P., Johnson, J.K., Gorno-Tempini, M.L., Rosen, H., Priloleau-Latham, C.E., Lee, A., Kipps, C.M., Lillo, P., Piguet, O., Rohrer, J.D., Rossor, M.N., Warren, J.D., Fox, N.C., Galasko, D., Salmon, D.P., Black, S.E., Mesulam, M., Weintraub, S., Dickerson, B.C., Diehl-Schmid, J., Pasquier, F., Deramecourt, V., Leber, F., Pijnenburg, Y., Chow, T.W., Manes, F., Grafman, J., Cappa, S.F., Freedman, M., Grossman, M., Miller, B.L., 2011. Sensitivity of revised diagnostic criteria for the behavioural variant of frontotemporal dementia. *Brain* 134, 2456–2477.
- Reiman, E.M., Caselli, R.J., Yun, L.S., Chen, K., Bandy, D., Minoshima, S., Thibodeau, S.N., Osborne, D., 1996. Preclinical evidence of Alzheimer's disease in persons homozygous for the epsilon 4 allele for apolipoprotein E. *N. Engl. J. Med.* 334, 752–758.
- Rizzolatti, G., Fabbri-Destro, M., Cattaneo, L., 2009. Mirror neurons and their clinical relevance. *Nat. Clin. Pract. Neurol.* 5, 24.
- Schapira, A.H.V., Chaudhuri, K.R., Jenner, P., 2017. Non-motor features of Parkinson disease. *Nat. Rev. Neurosci.* 18, 435–450.
- Schroeter, M.L., Stein, T., Maslowski, N., Neumann, J., 2009. Neural correlates of Alzheimer's disease and mild cognitive impairment: a systematic and quantitative meta-analysis involving 1351 patients. *NeuroImage* 47, 1196–1206.
- Schroeter, M.L., Laird, A.R., Chwiesko, C., Deuschl, C., Schneider, E., Bzdok, D., Eickhoff, S.B., Neumann, J., 2014. Conceptualizing neuropsychiatric diseases with multimodal data-driven meta-analyses - the case of behavioral variant frontotemporal dementia. *Cortex* 57, 22–37.
- Shao, N., Yang, J., Li, J., Shang, H.F., 2014. Voxelwise meta-analysis of gray matter anomalies in progressive supranuclear palsy and Parkinson's disease using anatomic likelihood estimation. *Front. Hum. Neurosci.* 8, 63.
- Shao, N., Yang, J., Shang, H., 2015. Voxelwise meta-analysis of gray matter anomalies in Parkinson variant of multiple system atrophy and Parkinson's disease using anatomic likelihood estimation. *Neurosci. Lett.* 587, 79–86.
- Sobel, N., Prabhakaran, V., Desmond, J.E., Glover, G.H., Goode, R.L., Sullivan, E.V., Gabrieli, J.D., 1998. Sniffing and smelling: separate subsystems in the human olfactory cortex. *Nature* 392, 282–286.
- Tahmasian, M., Eickhoff, S.B., Giehl, K., Schwartz, F., Herz, D.M., Drzezga, A., van Eimeren, T., Laird, A.R., Fox, P.T., Khazaie, H., Zarei, M., Eggers, C., Eickhoff, C.R., 2017. Resting-state functional reorganization in Parkinson's disease: an activation likelihood estimation meta-analysis. *Cortex* 92, 119–138.
- Tang, C.C., Poston, K., Eckert, T., Feigin, A., Frucht, S., Gudesblatt, M., Dhawan, V., Lesser, M., Vonsattel, J.-P., Fahn, S., Eidelberg, D., 2010. Differential diagnosis of parkinsonism: a metabolic imaging study using pattern analysis. *Lancet Neurol.* 9 (2), 149–158.
- Tang, C.C., Feigin, A., Ma, Y., Habeck, C., Paulsen, J.S., Leenders, K.L., Teune, L.K., van Oostrom, J.C.H., Guttman, M., Dhawan, V., Eidelberg, D., 2013. Metabolic network as a progression biomarker of premanifest Huntington's disease. *J. Clin. Invest.* 123, 4076–4088.
- Tekin, S., Cummings, J.L., 2002. Frontal-subcortical neuronal circuits and clinical neuropsychiatry: an update. *J. Psychosom. Res.* 53, 647–654.
- Titova, N., Padmakumar, C., Lewis, S.J.G., Chaudhuri, K.R., 2017. Parkinson's: a syndrome rather than a disease? *J. Neural Transm. (Vienna)* 124, 907–914.
- Tuite, P., 2017. Brain magnetic resonance imaging (MRI) as a potential biomarker for Parkinson's disease (PD). *Brain Sci.* 7.
- Watanabe, H., Senda, J., Kato, S., Ito, M., Atsuta, N., Hara, K., Tsuboi, T., Katsuno, M., Nakamura, T., Hirayama, M., Adachi, H., Naganawa, S., Sobue, G., 2013. Cortical and subcortical brain atrophy in Parkinson's disease with visual hallucination. *Mov. Disord.* 28, 1732–1736.
- Whitwell, J.L., Przybelski, S.A., Weigand, S.D., Knopman, D.S., Boeve, B.F., Petersen, R.C., Jack Jr., C.R., 2007. 3D maps from multiple MRI illustrate changing atrophy patterns as subjects progress from mild cognitive impairment to Alzheimer's disease. *Brain* 130, 1777–1786.
- Yarnall, A.J., Breen, D.P., Duncan, G.W., Khoo, T.K., Coleman, S.Y., Firbank, M.J., Nombela, C., Winder-Rhodes, S., Evans, J.R., Rowe, J.B., Mollenhauer, B., Kruse, N., Hudson, G., Chinnery, P.F., O'Brien, J.T., Robbins, T.W., Wesnes, K., Brooks, D.J., Barker, R.A., Burn, D.J., ICICLE-PD Study Group, 2014. Characterizing mild cognitive impairment in incident Parkinson disease: the ICICLE-PD study. *Neurology* 82, 308–316.
- Yu, F., Barron, D.S., Tantiwongkosi, B., Fox, P., 2015. Patterns of gray matter atrophy in atypical parkinsonism syndromes: a VBM meta-analysis. *Brain Behav.* 5, e00329.

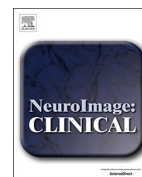
4 STUDY 2

Atrophy in midbrain and cerebral/cerebellar pedunculi is specific for progressive supranuclear palsy - a cross-validation whole-brain meta-analysis



Contents lists available at ScienceDirect

NeuroImage: Clinical

journal homepage: www.elsevier.com/locate/ynicl

Atrophy in midbrain & cerebral/cerebellar pedunculi is characteristic for progressive supranuclear palsy – A double-validation whole-brain meta-analysis



Franziska Albrecht^{a,*}, Sandrine Bisenius^a, Jane Neumann^{a,b,c}, Jennifer Whitwell^d, Matthias L. Schroeter^{a,e}

^a Max Planck Institute for Human Cognitive and Brain Sciences Leipzig, Germany

^b Department of Medical Engineering and Biotechnology, University of Applied Science, Jena, Germany

^c Leipzig University Medical Center, IFB Adiposity Diseases, Germany

^d Department of Radiology, Mayo Clinic, Rochester, MN, United States

^e Clinic of Cognitive Neurology, University of Leipzig & FTLN Consortium Germany, Germany

ARTICLE INFO

Keywords:

Imaging biomarker
Cerebral pedunculi
Cerebellar pedunculi
Meta-analysis
Midbrain
Progressive supranuclear palsy
Anatomical likelihood estimation
Seed-based D mapping

ABSTRACT

Objective: Progressive supranuclear palsy (PSP) is an atypical parkinsonian syndrome characterized by vertical gaze palsy and postural instability. Midbrain atrophy is suggested as a hallmark, but it has not been validated systematically in whole-brain imaging.

Methods: We conducted whole-brain meta-analyses identifying disease-related atrophy in structural MRI. Eighteen studies were identified ($N = 315$ PSP, 393 controls) and separated into gray or white matter analyses (15/12). All patients were diagnosed according to the National Institute of Neurological Disorders and Stroke and the Society for PSP (NINDS-SPSP criteria, Litvan et al. (1996a)), which are now considered as PSP-Richardson syndrome (Höglinger et al., 2017). With overlay analyses, we double-validated two meta-analytical algorithms: anatomical likelihood estimation and seed-based D mapping. Additionally, we conducted region-of-interest effect size meta-analyses on radiological biomarkers and subtraction analyses differentiating PSP from Parkinson's disease.

Results: Whole brain meta-analyses revealed consistent gray matter atrophy in bilateral thalamus, anterior insulae, midbrain, and left caudate nucleus. White matter alterations were consistently detected in bilateral superior/middle cerebellar pedunculi, cerebral pedunculi, and midbrain atrophy. Region-of-interest meta-analyses demonstrated that midbrain metrics generally perform very well in distinguishing PSP from other parkinsonian syndromes with strong effect sizes. Subtraction analyses identified the midbrain as differentiating between PSP and Parkinson's disease.

Conclusions: Our meta-analyses identify gray matter atrophy of the midbrain and white matter atrophy of the cerebral/cerebellar pedunculi and midbrain as characteristic for PSP. Results support the incorporation of structural MRI data, and particularly these structures, into the revised PSP diagnostic criteria.

1. Introduction

Progressive supranuclear palsy (PSP) is a gradually progressive, atypical parkinsonian syndrome characterized by vertical gaze palsy and prominent postural instability with backward falls from disease onset on (Litvan et al., 1996a). Commonly applied diagnostic criteria were proposed by the National Institute of Neurological Disorders and Stroke and the Society for PSP (NINDS-SPSP criteria) in 1996 (Litvan

et al., 1996a, 1996b). To fulfill the diagnostic criteria for possible PSP, patients' age of onset should be > 40 years. Additionally, postural instability leading to falls, accompanied by slower vertical saccades, or vertical gaze palsy alone is required for diagnosis. Probable PSP is diagnosed, when a patient shows all of the aforementioned features. Certainty of the underlying tauopathy can only be confirmed by histopathology - the remaining gold standard for diagnosis (Litvan et al., 1996b). Despite advances in research, the evaluation of atypical

* Corresponding author at: Max Planck Institute for Human Cognitive and Brain Sciences, Stephanstr. 1A, 04103 Leipzig, Germany.

E-mail addresses: falbrecht@cbs.mpg.de (F. Albrecht), bisenius@cbs.mpg.de (S. Bisenius), neumann@cbs.mpg.de (J. Neumann), Whitwell.Jennifer@mayo.edu (J. Whitwell), schroet@cbs.mpg.de (M.L. Schroeter).

<https://doi.org/10.1016/j.nicl.2019.101722>

Received 24 September 2018; Received in revised form 13 February 2019; Accepted 15 February 2019

Available online 19 February 2019

2213-1582/ © 2019 The Authors. Published by Elsevier Inc. This is an open access article under the CC BY-NC-ND license (<http://creativecommons.org/licenses/by-nc-nd/4.0/>).

parkinsonian syndromes has remained primarily dependent on clinical diagnostics. Disease-specific, brain imaging, biomarkers have been introduced to increase diagnostic validity of neurodegenerative diseases, for example, in frontotemporal lobar degeneration and primary progressive aphasia (Bisenius et al., 2016; Gorno-Tempini et al., 2011; Rascovsky et al., 2011; Schroeter et al., 2014). In terms of potential biomarkers, previous PSP studies have focused on the local boundary shift integral, longitudinal diffusion changes, or measurements of the midbrain/cerebellum (Kato et al., 2003; Longoni et al., 2011; Oba et al., 2005; Paviour et al., 2006; Slowinski et al., 2008; Zhang et al., 2016). The aforementioned metrics of midbrain and cerebellum were mainly investigated in small cohorts. During the analysis phase of the present study, the diagnostic criteria for PSP were updated in an attempt to increase diagnostic confidence by including neuroimaging measures as supportive and exclusion criteria, highlighting the timeliness of our report. Clinical diagnostic criteria were further improved by including more detailed diagnosis and acknowledging the several phenotypes of PSP. The amended criteria propose that former diagnosis according to Litvan et al. (1996a) relates to the phenotype of PSP-Richardson syndrome. Indeed, diagnostic criteria by Litvan et al. (1996a) have been shown to be 95–100% specific, validated by pathological examination (Höglinger et al., 2017). In the new criteria, in particular the use of midbrain atrophy or hypometabolism and/or postsynaptic, striatal, dopaminergic degeneration (Höglinger et al., 2017) has been suggested. Whitwell et al. (2017) published a qualitative review of radiological biomarkers, supporting midbrain and cerebellar pedunculi as specific to PSP even in the early phases of disease. However, it is important to prove the reliability of those disease patterns in quantitative whole-brain analyses.

We investigated the neural correlates of PSP to validate pathognomonic signs and further identify possible imaging biomarkers with systematic and quantitative meta-analyses; a thorough and powerful data-driven approach (Bisenius et al., 2016; Schroeter et al., 2014). The meta-analysis focused on whole-brain voxel-based morphometry (VBM) studies that applied structural magnetic resonance imaging (MRI) in PSP. By including only whole-brain studies, we prevented possible vicious circles if only expected brain regions are examined. We investigated disease-associated atrophy separately in gray and white matter in PSP compared with controls. Two widely acknowledged meta-analytical approaches, anatomical likelihood estimation (ALE) (Eickhoff et al., 2012) and anisotropic effect size seed-based *D* mapping (SDM) (Radua and Mataix-Cols, 2009; Radua et al., 2014), were applied and double-validated against each other. Overlay analyses were used to confirm the findings of the individual approaches, by assessing the degree of overlap. This provided reliable results and enabled us to identify a robust, disease-characteristic imaging biomarker. To investigate disease-specificity we run subtraction analyses to compare PSP with related diseases, i.e. Parkinson's disease (Albrecht et al., 2018). We hypothesized atrophy in PSP of white matter in the midbrain and gray matter in the midbrain, thalamus, and insulae (Shao et al., 2014; Shi et al., 2013; Yu et al., 2015). Additionally we performed a supportive region-of-interest effect size meta-analysis on the disease-specific imaging marker studies identified by (Whitwell et al., 2017).

2. Materials and methods

2.1. General study selection

The meta-analysis was conducted according to the PRISMA guidelines (www.prisma-statement.org) and Müller et al. (2018). Two authors (FA, SB) independently searched the PubMed database with the following search strategy: (“progressive supranuclear palsy” OR “Steele-Richardson-Olszewski syndrome”) AND (voxel* OR gray matter OR VBM). Studies were included if they: (1) were peer-reviewed, (2) used established diagnostic criteria, (3) were original work, (4) made comparisons with age-matched healthy controls, (5) reported results

normalized to a stereotactic space (Talairach or the Montreal Neurological Institute's (MNI)), and (6) took a whole-brain approach. Region-of-interest analyses, small volume corrected peaks, and case studies were discarded to prevent any regional a priori assumptions. As we did not find enough [¹⁸F]-fluorodeoxyglucose positron emission tomography (FDG-PET) or diffusion tensor imaging (DTI) studies fulfilling our criteria, we limited analysis to structural MRI, investigating gray and/or white matter atrophy. The literature search was performed between February and May 2016, reviewing all studies regardless of their publication date. We contacted corresponding authors to request local maxima not reported in their original publications and obtained data (Burciu et al., Premi et al., and Hughes et al.). The corresponding author of Burciu et al. confirmed by email that they used the NINDS-SPS criteria for diagnosis.

2.2. Statistical analyses

2.2.1. Whole-brain ALE & SDM meta-analyses

To obtain robust and reliable neural correlates of PSP, we applied two separate meta-analysis methods, enabling confirmation of the results of each individual technique. Our methods included the widely used approaches of ALE and SDM (Eickhoff et al., 2012; Radua and Mataix-Cols, 2009). For in depth details and differences between the methods see Table e-1. In brief, we first applied SDM (v4.31) (Radua and Mataix-Cols, 2009; Radua et al., 2014). SDM involves rebuilding effect size and variance maps for each study using t-scores and the extracted local maxima (i.e. points of difference between patients and controls). Each map consists of voxels with assigned values depending on their proximity to reported maxima coordinates. Voxels close to reported coordinates have higher values. If voxels lie in the proximity of more than one coordinate, the values are summed. Effect sizes from peaks close to each other are calculated by a weighted average. From these study-specific effect size and variance maps, SDM calculates a mean meta-analytical map, taking between study variability into account. The between study variability is defined as the weighted inverse of the variance of the difference of the studies. The resulting map is tested, voxel-wise, against a null distribution of the meta-analytical values. Analyses were performed on 500 permutations with an anisotropic kernel of 1.0. Results are reported and displayed at $p < 0.001$, uncorrected for multiple comparisons, because SDM does not correct the brain mask for the number of statistical tests by default. However, to correct the resulting values for multiple comparisons, probabilities were put into the web-converter of SDM (false discovery rate (FDR) correction) (Hochberg and Benjamini, 1990) and are reported in the Supplement (Table e-3). Note that this only provides a peak-based FDR correction for multiple comparisons. To examine the robustness of the main meta-analytical output, jack-knife analyses were carried out by removing one study at a time and repeating the analysis. Clusters present in $> 90\%$ of iterations are marked as such in Table e-3.

Secondly, we ran meta-analyses using ALE (GingerALE 2.3.6) (2012). This technique transforms the study-specific extracted peaks, of difference between patients and controls, into Gaussian probability distributions surrounding the coordinates. Coordinates reported in the Talairach stereotactic space were transformed into the stereotactic MNI space using the Lancaster transform implemented in GingerALE (Lancaster et al., 2007). The estimation of the width of these Gaussian probability distributions is adapted for each study using the number of included subjects based on empirical estimates of between-subject and between-template variability. The resulting ALE maps are then combined, across studies, and tested against the null hypothesis of a random spatial distribution between the modeled maps. We first analyzed the data at $p < 0.001$, uncorrected for multiple comparisons, to ensure comparability with SDM. Thereafter, we corrected the ALE results with FDR, as was done with SDM (Figure e-2) (Laird et al., 2005). FDR is the only method implemented in ALE and SDM, but they use different algorithms.

Table 1

Studies included in the whole-brain meta-analyses identifying the neural correlates of progressive supranuclear palsy with structural magnetic resonance imaging.

Study	PSP (N)	HC (N)	Age (years)	Gender (male/ female)	Disease Duration (years)	MMSE	UPDRS-III	Notes	Criteria
Gray matter studies									
Boxer et al., 2006	15	80	70.9 ± 6.9	9/6	4.8 ± 1.7	24.0 ± 3.2	NR	a,b	Litvan
Brenneis et al., 2004	12	12	67.5 ± 6.6	NR	2.7 ± 0.9	NR	38.9 ± 10.9	a,b	Litvan
Burciu et al., 2015	20	20	67.8 ± 7.1	10/10	2.6 ± NR	NR	39.0 ± 14.5	a,b,*	Litvan
Cordato et al., 2005	21	23	70.3 ± 6.4	14/7	4.0 ± 2.8	25.4 ± 3.2	23.1 ± 10.1	a,b	Litvan
Ghosh et al., 2012	23	22	71.1 ± 8.6	14/9	2.5	NR	33.8 ± 15.7	a,b,*	Litvan
Giordano et al., 2013	15	15	68.9 ± 1.2	8/7	3.2 ± 1.3	21.2 ± 1.2	38.3 ± 4.0	a,b,*	Litvan
Kamiya et al., 2013	16	21	71.4 ± 6.0	10/6	NR	NR	NR	b	Litvan
Lagarde, 2015	21	18	65.5 ± 6.5	8/13	4.4 ± 1.7	25.8 ± 2.7	NR	a,b*	Litvan
Lehericy et al., 2010	10	9	66.9 ± 6.4	6/4	4.3 ± 1.0	27.0	30.0	a,b	Litvan
Padovani et al., 2006	14	14	73.0 ± 5.6	7/7	3.1 ± 1.0	25.8 ± 2.7	22.1 ± 8.9	a,b	Litvan
Piattella et al., 2015	16	16	68.1 ± 5.9	9/7	3.1 ± NR	24.3 ± 3.9	27.0 ± 3.9	a,b,*	Litvan
Premi et al., 2016	32	32	73.5 ± 6.9	17/15	6.9 ± 3.5	24.9 ± 3.9	NR	b	Litvan
Sandhya et al., 2014	10	8	NR	9/1	NR	NR	NR	a,b,*	Litvan
Takahashi et al., 2011	16	20	64.6 ± 6.4	11/5	NR	21.0 ± 4.4	NR	b	Litvan
Whitwell et al., 2013	16	20	72.1 ± 4.6	8/8	4.1 ± NR	25.8 ± 2.7	52.9 ± 12.6	b,*	Litvan
Total GM	£257	£334	69.4 ± 2.8	140/105	3.9 ± 1.2	24.5 ± 2.0	33.9 ± 9.7		
White matter studies									
Boxer et al., 2006	15	80	70.9 ± 6.9	9/6	4.8 ± 1.7	24.0 ± 3.2	NR	a,b	Litvan
Brenneis et al., 2004	12	12	67.5 ± 6.6	NR	2.7 ± 0.9	NR	38.9 ± 10.9	a,b	Litvan
Burciu et al., 2015	20	20	67.8 ± 7.1	10/10	2.6 ± NR	NR	39.0 ± 14.5	a,b,*	Litvan
Cordato et al., 2005	21	23	70.3 ± 6.4	14/7	4.0 ± 2.8	25.4 ± 3.2	23.1 ± 10.1	a,b	Litvan
Ghosh et al., 2012	23	22	71.1 ± 8.6	14/9	2.5	NR	38.3 ± 4.0	a,b,*	Litvan
Hughes et al., 2014	13	15	68.0 ± 6.8	9/4	4.3 ± 3.1	26.9 ± 2.9	29.2 ± 14.3	b,*	Litvan
Lagarde, 2013	19	18	65.9 ± 6.5	7/12	4.5 ± 1.8	25.5 ± 2.7	NR	a,b,*	Litvan
Lehericy et al., 2010	10	9	66.9 ± 6.4	6/4	4.3 ± 1.0	27.0	30.0	a,b	Litvan
Price, 2004	12	12	65.3 ± 5.8	7/5	4.8 ± 1.7	27.0 ± 3.3	20.4 ± 8.7	a,b	Litvan
Sakurai et al., 2015	33	32	78.0 ± 6.0	20/13	4.8 ± 2.6	NR	NR		Litvan
Takahashi et al., 2011	16	20	64.6 ± 6.4	11/5	NR	21.0 ± 4.4	NR	b	Litvan
Whitwell et al., 2017	16	20	72.1 ± 4.6	8/8	4.1 ± NR	25.8 ± 2.7	52.9 ± 12.6	b,*	Litvan
Total WM	£210	£265	69.0 ± 3.7	115/99	4.1 ± 0.8	25.3 ± 2.0	34.0 ± 10.5		
Total GM + WM	£315	£393	69.2 ± 3.2	176/127	4.0 ± 1.0	24.9 ± 2.0	33.9 ± 9.7		

Gender, age, disease duration, MMSE and UPDRS scores are specified for patients (mean ± standard deviation). All MRI studies used 1.5 T (except for * = 3 T). Disease duration mean scores were calculated without Gosh et al. because they reported data as median. Abbreviations: GM gray matter, HC healthy controls, MMSE mini-mental state examination, N number of subjects, NR not reported, PSP progressive supranuclear palsy, UPDRS-III motor score of unified Parkinson's disease rating scale, WM white matter. a corrected for multiple comparisons, b modulated

Thirdly, separate conjunction analyses were performed for gray and white matter by superimposing the results of SDM and ALE, revealing the most consistent atrophic regions. To overcome the potential bias the different FDR algorithms may introduce, we used the results at $p < 0.001$ uncorrected.

Finally, to investigate disease-specificity of the results, we ran subtraction analyses comparing the present results with the findings of our recently published meta-analysis on Parkinson's disease (For further information please refer to Albrecht et al., 2018). We used the results at $p < 0.001$ uncorrected from the present analysis and the white and gray matter MRI cohort of the Parkinson's disease meta-analysis (cohort with Parkinson's disease only). Data were analyzed in GingerALE with 10,000 randomizations at $p < 0.001$ uncorrected. Again, we corrected the ALE results applying FDR afterwards. Results are shown for the contrasts of PSP - Parkinson's disease for gray and white matter.

To reveal differences in age, gender, disease duration, Mini-Mental-State Examination (MMSE), and the motor score of the Unified Parkinson's Disease Rating Scale (UPDRS-III) between the gray and white matter cohorts, we performed Pearson's χ^2 and unpaired Student's t -tests in R with a significance threshold at $p < 0.05$.

2.2.2. Region-of-interest effect size meta-analyses

As supportive analyses, we performed an effect size meta-analysis on the biomarker studies provided by the systematic review of (Whitwell et al., 2017). To include recently published studies, two authors searched the Pubmed database applying the same search tags as Whitwell and colleagues (October 2017–March 2018). Analyses were performed on studies reporting three metrics: midbrain area, midbrain-pons area ratio, and the MR Parkinsonism Index (MRPI), a midbrain to

pons and middle to superior cerebellar pedunculus ratio. Data were analyzed with metafor in R (Viechtbauer, 2010) and normalized by calculating the standardized mean difference (Hedges' g), with 95% confidence intervals as an effect size estimate. A random-effects model was applied to account for both within- and between-study variance. Between-study heterogeneity was assessed using Q -statistics and I^2 estimate.

2.3. Potential sources of bias and error

To avoid biasing the results toward specific brain areas, only quantitative and automated whole-brain studies were included for the whole-brain meta-analyses; region-of-interest studies were excluded. To eliminate age as a confounding variable, we only included comparisons with age-matched controls. Studies comparing PSP with other neurodegenerative diseases were further excluded. In line with the PRISMA recommendations, two investigators performed the literature search independently and discussed discrepancies (FA, SB). SDM and ALE algorithms are able to balance analyses by taking the sample size of each included study into account, thereby equalizing the contributions of each study. It may be the case that only studies finding atrophy in PSP patients were published and others finding null results were not, leading to a publication bias. While we cannot rule this out completely it does seem unlikely as the effect sizes in the published studies tend to be large and the proportion of patients showing quite severe atrophy has been extremely high.

2.4. Data availability statement

Data and analysis methods are shared at request for purposes of replicating procedures and results.

3. Results

3.1. Whole-brain meta-analyses

3.1.1. Study characteristics

A total of 18, gray and white matter, MRI studies, with 315 patients and 393 healthy controls, were included (Table 1, Figure e-1). Some studies reported both measures, leading to the inclusion of 12 white matter and 15 gray matter patient cohorts consisting of 257 and 210 patients respectively. Unpaired Student's *t*-tests indicated no significant difference between the mean values of the white and gray matter samples concerning age ($t = 0.28, p = 0.78$), disease duration ($t = -0.04, p = 0.97$), and severity of clinical symptoms using MMSE scores ($t = -0.84, p = 0.41$), and UPDRS-III scores ($t = -0.02, p = 0.99$). Furthermore, Pearson's χ^2 test showed no significant differences in gender distribution ($\chi^2 = 0.41, p = 0.52$). There were also no significant differences in standard deviations between the samples regarding age ($t = -0.83, p = 0.42$), disease duration ($t = -0.44, p = 0.67$), and severity of clinical symptoms using MMSE scores ($t = -0.26, p = 0.80$), and UPDRS-III scores ($t = -0.35, p = 0.74$).

All included studies reported decreased gray/white matter volume or density. There were no reports of gray/white increases found in the literature. Moreover, all studies used exactly the same clinical diagnostic criteria (Litvan et al., 1996a), avoiding a potential vicious circle as no imaging biomarker was included. Out of 315 patients, the majority was diagnosed with PSP-Richardson syndrome according to the new criteria by Höglinger et al. (2017). Note that a maximum of 19 patients (Burciu et al., 2015) may have been diagnosed with PSP-parkinsonism additionally, although they fulfill the Litvan criteria for PSP. Hence, in the following, we refer the naming of our cohort to PSP as proposed by the Litvan criteria.

3.1.2. Seed-based *D* mapping analysis

The upper part of Fig. 1 and Table e-2 illustrate the consolidated neural correlates of PSP identified by SDM meta-analysis. The analysis

across structural MRI studies revealed regional gray matter atrophy convergence bilaterally in the inferior and middle frontal and superior temporal gyri, adjacent to the insulae, in the putamen, caudate nuclei, midcingulate cortex, thalamus, and midbrain. White matter convergence occurred bilaterally in the corpus callosum, thalamus, cerebral and superior cerebellar pedunculi, and right middle cerebellar pedunculus.

3.1.3. Anatomical likelihood analysis

The bottom part of Fig. 1 and Table e-3 display the results of the ALE meta-analysis in PSP. The analysis revealed gray matter atrophy convergence in the paracingulate and anterior cingulate gyri, insulae, inferior frontal gyrus, superior parietal lobule, thalamus, caudate nuclei, and cerebellum. White matter regions consistently found were the midbrain, pyramid, pons, thalamus, and cerebral and superior cerebellar pedunculi. FDR correction of the ALE meta-analysis confirmed involvement of the anterior insula and thalamus for gray matter and midbrain for white matter (see Supplement, Figure e-2).

3.1.4. Overlap analysis

Finally, we performed an overlap analysis by superimposing the results of the two separate approaches meta-analyzing PSP (Fig. 2). The results for gray matter revealed that clusters in the bilateral thalamus, bilateral anterior insulae, midbrain, and left caudate nucleus were consistently identified as affected by PSP. The results for white matter analysis revealed consistent converged atrophy bilaterally in the superior and middle cerebellar pedunculi, cerebral pedunculi, midbrain, and right thalamus.

3.1.5. Subtraction analysis

We performed a subtraction analysis to directly compare disease-specificity of the aforementioned results by integrating white and gray matter atrophy of PSP and Parkinson's disease patients. The Parkinson's disease cohort consist of 809 patients from 29 gray matter studies and 75 patients from four white matter studies (Fig. 3, Table e-5). Gray matter atrophy differed between PSP and Parkinson's disease in the thalamus bilaterally as well as the left insula and claustrum, both surviving multiple comparisons correction. Concerning white matter, subtracting Parkinson's disease from PSP revealed the midbrain. Note that the white matter analysis did not survive FDR correction, which may have been due to underpowered analysis.

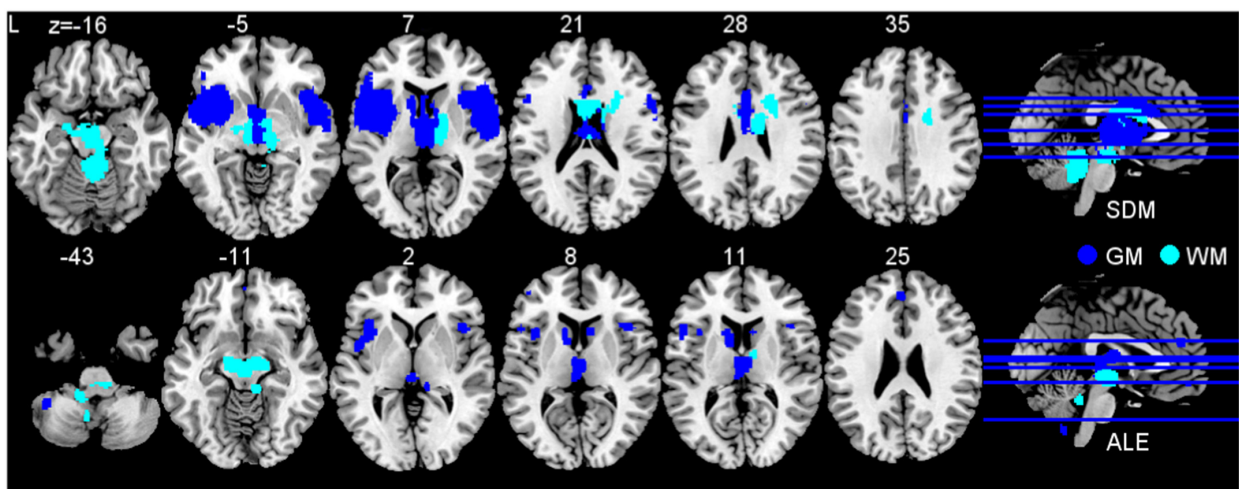


Fig. 1. Brain regions consistently associated with progressive supranuclear palsy. Analysis of gray matter (GM, dark blue) included 257 patients contrasted to 334 healthy subjects. White matter analysis (WM, light blue) included 210 patients contrasted to 265 healthy subjects. Upper image shows effect size estimates (seed-based *D* mapping, SDM) and bottom image anatomical likelihood estimate (ALE) meta-analyses. Abbreviation: L left. (For interpretation of the references to color in this figure legend, the reader is referred to the web version of this article.)

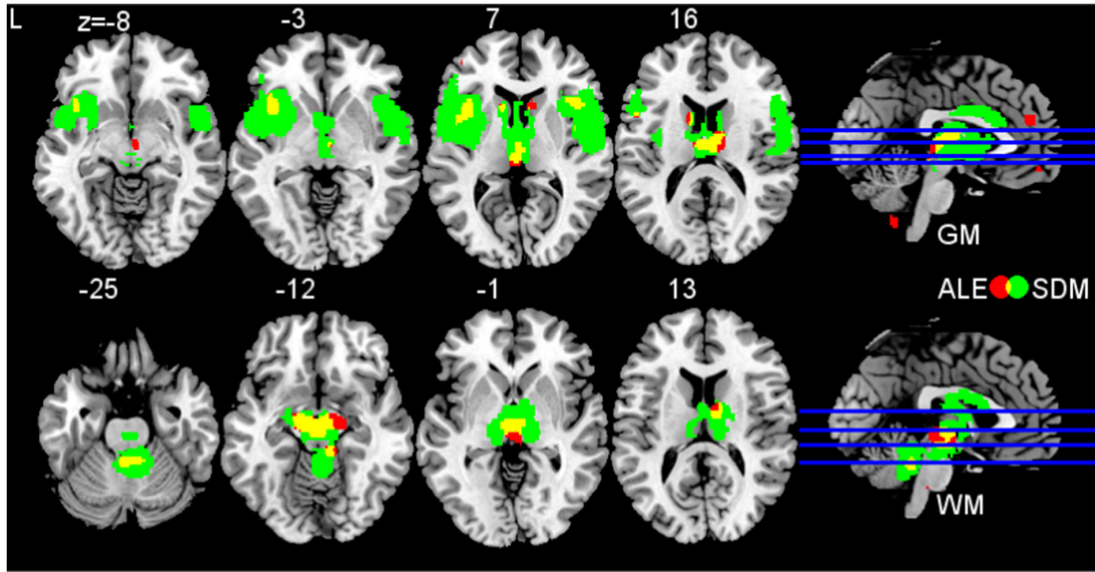


Fig. 2. Overlap analysis. Overlay analysis for impaired brain regions in progressive supranuclear palsy as revealed by anatomical likelihood estimate (ALE) and effect size estimates (seed-based D mapping, SDM) meta-analyses. Results of ALE are shown in red. Results of SDM are shown in green. Yellow clusters indicate overlap of both analyses (ALE and SDM). Upper image displays gray matter (GM) atrophy, bottom image displays white matter (WM) atrophy. Abbreviation: L left. (For interpretation of the references to color in this figure legend, the reader is referred to the web version of this article.)

3.2. Region-of-interest effect size meta-analyses

3.2.1. Study characteristics

Our literature search identified one study (Kim et al., 2017) that we included additionally to the studies already summarized by (Whitwell et al., 2017) in their systematic review. Study details and demographics are specified in Table-e6 in the Supplement. In total, 15 studies, including 246 patients and 173 healthy controls reported midbrain metrics in three neurodegenerative diseases: PSP (15 cohorts, age = 69.8 ± 3.6 years, disease duration = 3.3 ± 0.8 years), Parkinson's disease (14 cohorts, age = 66.6 ± 6.7 , disease duration = 6.3 ± 2.4), and multiple system atrophy (5 cohorts, age = 64.7 ± 4.3 , disease duration = 5.6 ± 1.6). The cohort of PSP patients in the region-of-interest effect size meta-analyses did not differ in age ($t = 0.50$, $p = 0.62$) or gender distribution ($\chi^2 = 0.77$, $p = 0.38$) compared to the PSP cohort of the whole-brain meta-analyses. Note that disease duration ($t = -2.10$, $p = 0.04$) was slightly higher in the PSP cohort of the whole-brain meta-analyses.

3.2.2. Effect size meta-analyses

All random-effects models revealed significant results, highlighting that midbrain metrics generally perform very well in distinguishing PSP from multiple system atrophy and Parkinson's disease with strong effect sizes (Fig. 4). Note that inter-study heterogeneity was overall quite large. Midbrain area measurements yielded smallest between-study heterogeneity in our study as well as largest effect size ($I^2 = 73.8\%$, Hedges' $g = -2.79$). The highest between-study heterogeneity but still high effect size was observed in midbrain-pons area ratio studies ($I^2 = 90.7\%$, Hedges' $g = -1.64$). Notably, even multiple system atrophy and PSP were distinguished by using midbrain-pons ratio with a high effect size (Hedges' $g = -2.37$). MRPI also yielded a large effect size but a high between-study heterogeneity ($I^2 = 89.9\%$, Hedges' $g = 2.10$) in distinguishing PSP from Parkinson's disease. These results emphasize the importance of our work in validating and replicating these patterns in whole brain with quantitative statistical methods.

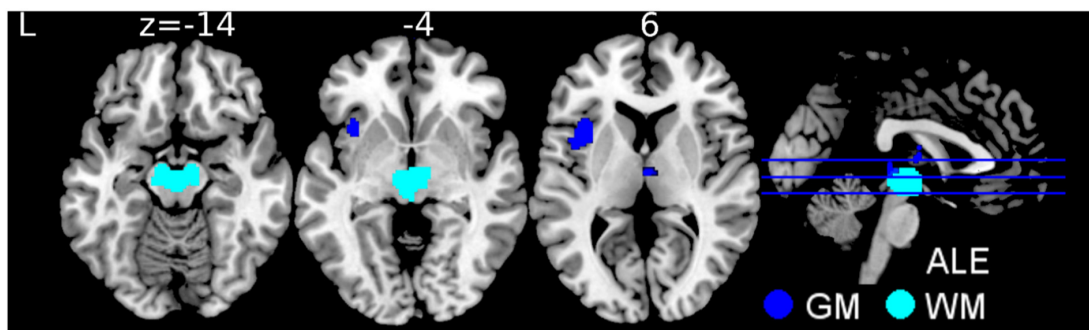


Fig. 3. Brain regions consistently associated with progressive supranuclear palsy in comparison to Parkinson's disease. Analysis of gray matter (GM, dark blue) included 257 patients with PSP contrasted to 809 patients with PD. White matter analysis (WM, light blue) included 210 patients with PSP contrasted to 75 patients with PD. Image shows subtraction anatomical likelihood estimate (ALE) meta-analyses. Abbreviation: L left, PD Parkinson's disease, PSP progressive supranuclear palsy. (For interpretation of the references to color in this figure legend, the reader is referred to the web version of this article.)

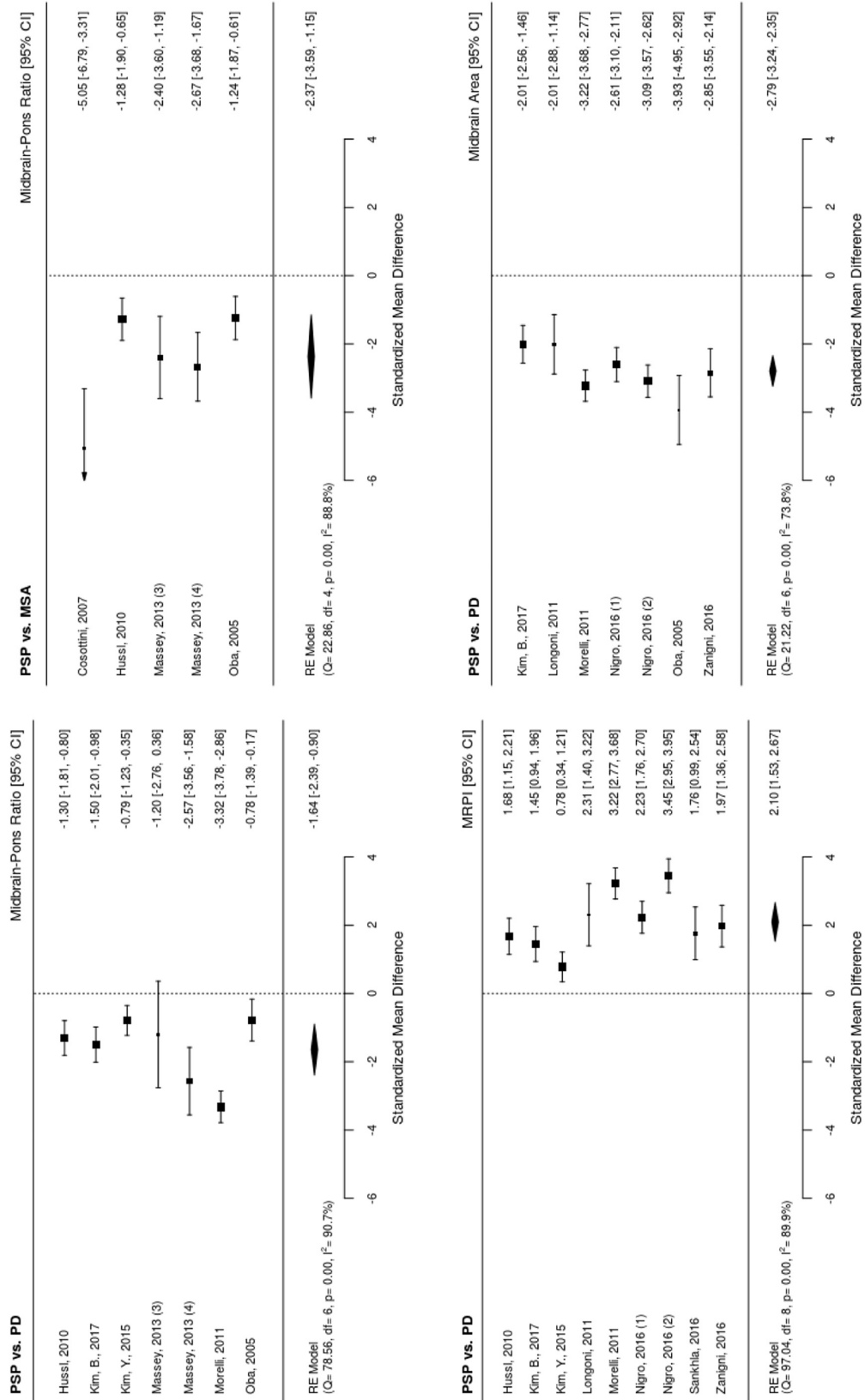


Fig. 4. Effect size (Hedges' g) meta-analyses of radiological biomarkers of progressive supranuclear palsy (PSP) based on Whitwell et al. (2017) and additional literature search. (1) Measurement using 1.5 Tesla, (2) measurement using 3 Tesla, (3) pathologically confirmed, and (4) clinically diagnosed groups. Abbreviation: CI confidence interval, df degrees of freedom, RE random effects, PD Parkinson's disease, MSA multiple system atrophy, MRPI Magnetic Resonance Parkinsonism Index.

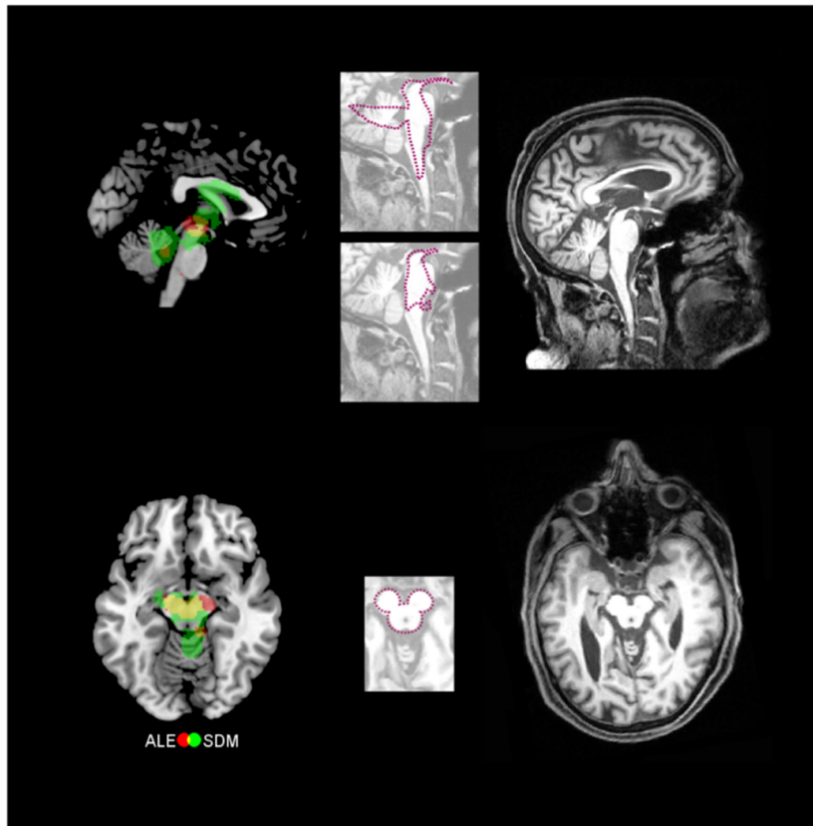


Fig. 5. Meta-analyses confirm proposed pathognomonic imaging markers of progressive supranuclear palsy (PSP). Left column shows meta-analytic results (green seed-based D mapping – SDM – analysis, red anatomical likelihood estimation analysis – ALE –, and yellow overlay). Right column depicts individual examples of corresponding structural magnetic resonance images of individual PSP patients with midbrain atrophy. Images in the middle are the silhouettes of a penguin, a hummingbird, and Mickey Mouse projected onto these patients' brain images. (For interpretation of the references to color in this figure legend, the reader is referred to the web version of this article.)

4. Discussion

To our knowledge, we report the largest most powerful data-driven whole-brain meta-analyses of the neural correlates of PSP to date. The analyses included 315 patients and 393 healthy controls. To help ensure high validity and specificity, all included patients were diagnosed by the same clinical diagnostic criteria, by Litvan et al. (1996a). In the aforementioned criteria imaging biomarkers are not implemented, which avoids a biased and circular design. According to the new PSP criteria (Höglinger et al., 2017), these patients would be referred to as PSP-Richardson syndrome. Note, however, that time criteria are different between both diagnostic systems, that our cohort might have included a minority of subjects with PSP-Parkinsonism additionally to PSP-Richardson syndrome (see Results, 3.1.1), and that one has to be generally very careful in translating old into new clinical criteria see Bisenius et al. (2016 for a related discussion on primary progressive aphasia).

Including only whole-brain studies in our meta-analysis guaranteed a data-driven approach. Notably, the overlap analysis between the two meta-analytical methods revealed gray matter atrophy in four regions in PSP: the bilateral thalamus, bilateral anterior insulae, midbrain, and left caudate nucleus. Concerning white matter atrophy, an overlap of the two methods was observed in the bilateral superior/middle cerebral and cerebellar pedunculi, midbrain, and right thalamus in PSP. Subtraction analysis differentiating PSP from Parkinson's disease confirmed the midbrain as specific for PSP.

Although previous meta-analyses of gray and white matter atrophy have been conducted for PSP, studies investigated either gray or white matter alterations alone and relied on a single meta-analytical algorithm (Shao et al., 2014; Shi et al., 2013; Yang et al., 2014; Yu et al., 2015). Remarkably, these meta-analyses may have been biased by

systematic errors introduced by flawed multiple comparison correction analysis tools, as has been stated recently by (Eickhoff et al., 2016) for former GingerALE software versions. Despite using distributions that contained errors in the FDR calculation, the results are still quite consistent with our own (Yang et al., 2014; Yu et al., 2015).

The present meta-analysis improves on previous studies in several ways. First, we used a novel approach, combining and double-validating two independent meta-analytical techniques to increase validity of our biomarker findings. Second, we included the largest cohort of PSP patients studied to date. Third, we investigated changes in gray and white matter with exactly the same methods to enable comparability of results. Finally, our meta-analyses support region-specific atrophy as an imaging biomarker for PSP – a move toward the inclusion of MRI in the diagnostic workflow for PSP.

4.1. Validating pathognomonic imaging markers for PSP with meta-analyses

Thinning of regions of the midbrain has been suggested as a pathognomonic marker of PSP; previously identified in small cohorts by precisely measuring the diameters of the pons, midbrain, and superior/middle cerebellar pedunculi (Kato et al., 2003; Longoni et al., 2011; Oba et al., 2005; Slowinski et al., 2008). A recent multi-centric volumetric and manual morphometry study has endorsed this view, demonstrating that the midsagittal area and the anterior-posterior diameter of the midbrain distinguishes between PSP and other parkinsonian syndromes (Moller et al., 2017). Previous findings describe three different pathognomonic signs, typically found in PSP patients. First, the 'hummingbird sign' reflects a thinning of the anterior part of the midbrain tegmentum (Kato et al., 2003). The second characteristic feature called the 'penguin silhouette sign' relates to an

atrophy in the shapes of midbrain tegmentum and pons (Oba et al., 2005). The hummingbird and the penguin silhouette signs are apparent in mid-sagittal MRI scans. Another feature, the ‘Mickey Mouse sign’, describes selective atrophy of the midbrain tegmentum, with relative preservation of the tectum and cerebral pedunculi (Schott, 2007). Axial MRI scans of PSP patients reveal this sign. We were able to lend support to these pathognomonic markers with a large cohort (Fig. 5) by revealing white matter loss in the midbrain (specifically the tectum and parts of the tegmentum such as cerebellar pedunculi, red nucleus, and substantia nigra). The Mickey Mouse sign seems less specific, according to our data, because atrophy spread to the cerebral pedunculi (Fig. 5). Due to the algorithm, assumptions concerning the exact neuroanatomical substrates of meta-analyses should be interpreted with caution. Nevertheless, our confidence is increased by the fact that both meta-analytical algorithms across whole-brain studies revealed midbrain atrophy. By replicating previously observed atrophy patterns in a large meta-analytical study, using multiple approaches, we provide further evidence supporting the use of these signs as a diagnostic tool for PSP.

4.2. Atrophy in the midbrain and cerebral/cerebellar pedunculi is disease-characteristic for PSP as compared to other neurodegenerative diseases

Through the conjunctive overlay of the two meta-analytic approaches, we identified gray matter atrophy in PSP patients in the midbrain, thalamus, insulae, and caudate nuclei compared to controls. White matter atrophy was found in the midbrain, thalamus, cerebral pedunculus and superior/middle cerebellar pedunculi. To assess the potential disease-specificity of these patterns we compared our findings to other whole-brain meta-analyses of neurodegenerative diseases qualitatively (Table 2) and quantitatively (Table e-5, Fig. 4). A direct statistical comparison of PSP with another neurodegenerative disease, i.e. Parkinson's disease (Albrecht et al., 2018), revealed that PSP differs in white matter midbrain atrophy. This highlights again the importance

of the midbrain in PSP, especially in distinguishing closely related diseases. Gray matter was significantly impaired in PSP compared to Parkinson's disease in the thalamus and insula. Note that in qualitative comparisons, gray matter loss in the insulae, caudate nuclei, and thalamus has been recently reported in several other neurodegenerative diseases. Hence, these patterns are neither specific to PSP nor other neurodegenerative diseases.

As also illustrated in Table 2 white matter atrophy in the midbrain has not been observed in other neurodegenerative diseases and thus is suggested as a pathognomonic signature of PSP. PSP shows also severe gray matter atrophy distributed over the whole midbrain indicating disease-relatedness in this comparison. Although gray matter atrophy was detected in ALE meta-analyses in the red nucleus in multiple system atrophy (Shao et al., 2015), it was restricted to this brain region. Moreover, white matter atrophy in the cerebral or superior/middle cerebellar pedunculi seems to be characteristic for PSP as we did not find any other evidence in the literature. Missing effects in the cerebral and cerebellar pedunculi in our meta-analytical subtraction analysis might be related to the small number of white matter studies investigating Parkinson's disease. Although, one might assume cerebellar pedunculi atrophy in amyotrophic lateral sclerosis/motor neuron disease, a recent meta-analysis of DTI data rejects such an assumption (Li et al., 2012b). White matter atrophy in the thalamus/adjacent white matter structures seem to be characteristic for PSP as compared to other meta-analyses of Parkinson's disease and Alzheimer's disease (Albrecht et al., 2018; Li et al., 2012a; Yin et al., 2015). As studies on white matter are rare, greatly limiting meta-analytical assessment, disease-specificity should be interpreted with care. Nonetheless, our meta-analyses suggest that gray matter loss in the midbrain and white matter atrophy in the midbrain, cerebral pedunculus, superior/middle cerebellar pedunculi, and thalamus may serve as a disease-characteristic signature for PSP, quantitatively and qualitatively compared to related diagnoses. Further meta-analyses might apply the same methods and

Table 2

Meta-analytical evidence for biomarker specificity of regional atrophy in progressive supranuclear palsy as measured with structural magnetic resonance imaging.

Anatomical region		Thalamus	Midbrain	Insula	Cerebellar & cerebellar pedunculi	Caudate nucleus
Neurodegenerative disease	Study					
Gray matter						
Parkinson's disease	(Shao et al., 2014; Shao et al., 2015, Albrecht et al., 2018)	-	-	-	-	-
Atypical Parkinson's syndromes						
Corticobasal degeneration & syndrome	(Yu et al., 2015; Albrecht et al., 2017)	+	-	-	-	+
Progressive supranuclear palsy	(Present study, Shao et al., 2014; Yu et al., 2015; Shi et al., 2013)	+	+	+	-	+
Multiple system atrophy	(Shao et al., 2015)	+	+	+	-	-
Lewy body dementia	(Zhong et al., 2014)	-	-	+	-	-
Alzheimer's disease	(Schroeter and Neumann, 2011; Schroeter et al., 2009; Yang et al., 2012a)	+	-	+	-	-
Behavioral variant frontotemporal dementia	(Schroeter et al., 2014; Schroeter and Neumann, 2011; Schroeter et al., 2008; Schroeter et al., 2007; Pan et al., 2012)	-	-	+	-	+
Primary progressive aphasia						
Nonfluent/agrammatic variant (progressive non-fluent aphasia)	(Bisenius et al., 2016; Schroeter and Neumann, 2011; Schroeter et al., 2007)	-	-	+	-	-
Semantic variant (semantic dementia)	(Bisenius et al., 2016; Schroeter and Neumann, 2011; Schroeter et al., 2007; Yang et al., 2012b)	-	-	-	-	-
Logopenic variant (logopenic aphasia)	(Bisenius et al., 2016)	-	-	-	-	-
White matter						
Parkinson's disease	(Albrecht et al., 2018)	-	-	-	-	+
Atypical Parkinson's syndromes						
Progressive supranuclear palsy	(Present study, Yang et al., 2014)	+	+	-	+	-
Alzheimer's disease	(Yin et al., 2015; Li et al., 2012a)	-	-	-	-	-

Meta-analyses were conducted by calculating either anatomical likelihood estimates (ALE) or effect-size signed differential mapping (SDM) in the gray or white matter.

parameters to compare several diseases and assess disease-specificity quantitatively by comparing disease patterns with subtraction analyses.

During the course of the present investigation the diagnostic criteria were revised by the Movement Disorder Society-endorsed, P.S.P. Study Group (Höglinger et al., 2017). In this context, (Whitwell et al., 2017) reviewed radiological biomarkers. Our argumentation is in line with their qualitative review. The researchers identified the MRPI, a mid-brain to pons and middle to superior cerebellar pedunculus ratio, measured from structural MRI scans, as a supportive criterion even for early clinical diagnosis. Our region-of-interest effect size analyses based on Whitwell et al.'s review demonstrate large effect sizes for distinguishing PSP from Parkinson's disease and multiple system atrophy. Our dual-approach meta-analytic assessment with a large PSP sample is consistent with these recent developments, supporting the use of these particular regions in diagnosing PSP.

It is clearly necessary to validate the applicability of these disease-related MRI biomarkers for individual diagnosis in single patients before being transferable to clinical routine, for example by support vector machine classification for single-patient neurodegenerative disease discrimination (Bisenius et al., 2017; Dukart et al., 2013; Meyer et al., 2017). In an atlas-based MRI volumetry study, high classification accuracy for PSP versus other parkinsonian syndromes (86%) was indeed driven by atrophy in the midbrain and cerebellar pedunculi (Huppertz et al., 2016). Another MRI study suggests that disease-characteristic regions extracted from meta-analyses can outperform whole-brain approaches in identifying PSP by increasing classification accuracy from 80% to 85% (Mueller et al., 2017). Furthermore, combining structural MRI with DTI in support vector machine classification can increase classification results to 100% accurate (Cherubini et al., 2014). One may conclude that our meta-analytically extracted disease-specific atrophy pattern is ready for application as an imaging biomarker for PSP.

4.3. Study limitations

Our study identified consistent findings of atrophy in PSP, but we recognize some limitations. MRI studies on autopsy-proven cases of PSP are extremely rare (Table 1), hence, we could not validate clinical syndromes with histopathology (Albrecht et al., 2017). Furthermore, we could not disentangle the clinical syndromes seen in PSP as too few studies reported those data. Our meta-analyses had to be limited to MRI studies, because insufficient number of studies applied FDG-PET or DTI. We recommend including other imaging modalities and longitudinal data in the future (Bisenius et al., 2016; Schroeter et al., 2014; Schroeter and Neumann, 2011). The accuracy of the disease-specific patterns needs further validation in multi-centric, independent patient cohorts, which provide clinical imaging data, surrogate markers for histopathology from serum/cerebrospinal fluid or post-mortem examination. Researchers have already applied this successfully in Alzheimer's disease (Klöppel et al., 2008). Due to the lack of combined white matter and gray matter meta-analyses, direct statistical investigation of the results was only possible between PSP and Parkinson's disease. Note that SDM results are only peak-based FDR corrected for multiple comparisons, which should be preferably replaced by cluster- or voxel-based corrections in the future like it is already available for GingerALE.

4.4. Conclusion

We conducted a comprehensive, systematic, and quantitative meta-analysis investigating the neural correlates of PSP. Patients were all diagnosed applying the same diagnostic criteria of Litvan et al. (1996a), which is now referred to as PSP-Richardson syndrome according to Höglinger et al. (2017). By combining two commonly used meta-analytical algorithms, we identified consistent results validating well-known pathognomonic signs in whole-brain imaging to support the

diagnosis of PSP. Results suggest gray matter atrophy in the midbrain and white matter atrophy in the cerebral pedunculus, superior/middle cerebellar pedunculi, and midbrain as imaging biomarkers for diagnosis of PSP ante-mortem. Further, subtraction analyses of meta-analyses of related neurodegenerative diseases could strengthen the disease-specificity of midbrain atrophy by quantitatively comparing atrophy patterns. Taken together, our results are completely consistent with the recent move toward the inclusion of MRI data in the diagnostic workflow for PSP.

Conflict of interest

The authors declare that they have no conflict of interest. All financial disclosures are mentioned in the Acknowledgements.

Acknowledgements

This study has been supported by the Parkinson's Disease Foundation (PDF-IRG-1307), the Michael J Fox Foundation (MJFF-11362), the German Federal Ministry of Education and Research (BMBF; FKZ 01GI1007A; German FTLD consortium), the German Research Foundation (DFG, SCHR 774/5-1), the National Institutes of Health (NIH, R01-NS89757), and the International Max Planck Research School (IMPRS) NeuroCom by the Max Planck Society. Jane Neumann is supported by the Federal Ministry of Education and Research Germany (BMBF, FKZ: 01EO1001), and the German Research Foundation (DFG-SFB1052).

Authors' roles

1. Research project:

- A. Conception: F. Albrecht, M. Schroeter.
- B. Organization: F. Albrecht, M. Schroeter
- C. Execution: F. Albrecht, S. Bisenius, J. Neumann, M. Schroeter

2. Statistical Analysis:

- A. Design: F. Albrecht, J. Neumann, M. Schroeter.
- B. Execution: F. Albrecht, S. Bisenius.
- C. Review and Critique: F. Albrecht, J. Neumann, J. Whitwell, M. Schroeter

3. Manuscript Preparation:

- A. Writing of the first draft: F. Albrecht.
- B. Review and Critique: F. Albrecht, S. Bisenius, J. Neumann, J. Whitwell, M. Schroeter.

Appendix A. Supplementary data

Supplementary data to this article can be found online at <https://doi.org/10.1016/j.nicl.2019.101722>.

References

- Albrecht, F., Bisenius, S., Morales Schaack, R., Neumann, J., Schroeter, M.L., 2017. Disentangling the Neural Correlates of Corticobasal Syndrome and Corticobasal Degeneration with Systematic and Quantitative ALE Meta-Analyses. (npj Parkinson's Disease 3, 12).
- Albrecht, F., Ballarini, T., Neumann, J., Schroeter, M.L., 2018. FDG-PET hypometabolism is more sensitive than MRI atrophy in Parkinson's disease: a whole-brain multimodal imaging meta-analysis. *NeuroImage Clin Epub ahead of print*.
- Bisenius, S., Neumann, J., Schroeter, M.L., 2016. Validating new diagnostic imaging criteria for primary progressive aphasia via anatomical likelihood estimation meta-analyses. *Eur. J. Neurol.* 23, 704–712.
- Bisenius, S., Mueller, K., Diehl-Schmid, J., Fassbender, K., Grimmer, T., Jessen, F., Kassubek, J., Kornhuber, J., Landwehrmeyer, B., Ludolph, A., Schneider, A., Anderl-Straub, S., Stuke, K., Danek, A., Otto, M., Schroeter, M.L., group, F.T.s., 2017. Predicting primary progressive aphasias with support vector machine approaches in structural MRI data. *Neuroimage Clin.* 14, 334–343.
- Boxer, A.L., Geschwind, M.D., Belfor, N., et al., 2006. Patterns of brain atrophy that

- differentiate corticobasal degeneration syndrome from progressive supranuclear palsy. *Arch. Neurol.* 63 (1), 81–86.
- Brenneis, C., Seppi, K., Schocke, M., Benke, T., Wenning, G.K., Poewe, W., 2004. Voxel based morphometry reveals a distinct pattern of frontal atrophy in progressive supranuclear palsy. *J. Neurol. Neurosurg. Psychiatry* 75 (2), 246–249.
- Burciu, R.G., Ofori, E., Shukla, P., Planetta, P.J., Snyder, A.F., Li, H., Hass, C.J., Okun, M.S., McFarland, N.R., Vaillancourt, D.E., 2015. Distinct patterns of brain activity in progressive supranuclear palsy and Parkinson's disease. *Mov. Disord.* 30, 1248–1258.
- Cherubini, A., Morelli, M., Nistico, R., Salsone, M., Arabia, G., Vasta, R., Augimeri, A., Caligiuri, M.E., Quattrone, A., 2014. Magnetic Resonance Support Vector Machine Discriminates between Parkinson Disease and Progressive Supranuclear Palsy. *Cordato, N.J., Duggins, A.J., Halliday, G.M., Morris, J.G., Pantelis, C., 2005. Clinical deficits correlate with regional cerebral atrophy in progressive supranuclear palsy. Brain* 128, 1259–1266 Pt 6.
- Dukart, J., Mueller, K., Barthel, H., Villringer, A., Sabri, O., Schroeter, M.L., Alzheimer's Disease Neuroimaging, I., 2013. Meta-analysis based SVM classification enables accurate detection of Alzheimer's disease across different clinical centers using FDG-PET and MRI. *Psychiatry Res.* 212, 230–236.
- Eickhoff, S.B., Bzdok, D., Laird, A.R., Kurth, F., Fox, P.T., 2012. Activation likelihood estimation meta-analysis revisited. *Neuroimage* 59, 2349–2361.
- Eickhoff, S.B., Laird, A.R., Fox, P.M., Lancaster, J.L., Fox, P.T., 2016. Implementation errors in the GingerALE software: description and recommendations. *Hum. Brain Mapp.* 38 (1), 7–11.
- Ghosh, B.C., Calder, A.J., Peers, P.V., et al., 2012. Social cognitive deficits and their neural correlates in progressive supranuclear palsy. *Brain* 135, 2089–2102 Pt 7.
- Giordano, A., Tessitore, A., Corbo, D., et al., 2013. Clinical and cognitive correlations of regional gray matter atrophy in progressive supranuclear palsy. *Parkinsonism Relat. Disord.* 19 (6), 590–594.
- Gorno-Tempini, M.L., Hillis, A.E., Weintraub, S., Kertesz, A., Mendez, M., Cappa, S.F., Ogar, J.M., Rohrer, J.D., Black, S., Boeve, B.F., Manes, F., Dronkers, N.F., Vandenberghe, R., Rascovsky, K., Patterson, K., Miller, B.L., Knopman, D.S., Hodges, J.R., Mesulam, M.M., Grossman, M., 2011. Classification of primary progressive aphasia and its variants. *Neurology* 76, 1006–1014.
- Hochberg, Y., Benjamini, Y., 1990. More powerful procedures for multiple significance testing. *Stat. Med.* 9, 811–818.
- Höglinger, G.U., Respondek, G., Stamelou, M., Kurz, C., Josephs, K.A., Lang, A.E., Mollenhauer, B., Müller, U., Nilsson, C., Whitwell, J.L., Arzberger, T., Englund, E., Gelpi, E., Giese, A., Irwin, D.J., Meissner, W.G., Pantelyat, A., Rajput, A., van Swieten, J.C., Troakes, C., Antonini, A., Bhatia, K.P., Bordelon, Y., Compta, Y., Corvol, J.C., Colosimo, C., Dickson, D.W., Dodel, R., Ferguson, L., Grossman, M., Kassubek, J., Krismer, F., Levin, J., Lorenzl, S., Morris, H.R., Nestor, P., Oertel, W.H., Poewe, W., Rabinovici, G., Rowe, J.B., Schellenberg, G.D., Seppi, K., van Eimeren, T., Wenning, G.K., Boxer, A.L., Golbe, L.I., Litvan, I., Movement Disorder Society-endorsed, P.S.P.S.G., 2017. Clinical diagnosis of progressive supranuclear palsy: the movement disorder society criteria. *Mov. Disord.* 32, 853–864.
- Hughes, L.E., Rowe, J.B., Ghosh, B.C., Carlyon, R.P., Plack, C.J., Gockel, H.E., 2014. The binaural masking level difference: cortical correlates persist despite severe brain stem atrophy in progressive supranuclear palsy. *J. Neurophysiol.* 112 (12), 3086–3094.
- Huppertz, H.J., Moller, L., Sudmeyer, M., Hilker, R., Hattingen, E., Egger, K., Amtage, F., Respondek, G., Stamelou, M., Schnitzler, A., Pinkhardt, E.H., Oertel, W.H., Knake, S., Kassubek, J., Hoglinger, G.U., 2016. Differentiation of neurodegenerative parkinsonian syndromes by volumetric magnetic resonance imaging analysis and support vector machine classification. *Mov. Disord.* 31, 1506–1517.
- Kamiya, K., Sato, N., Ota, M., et al., 2013. Diffusion tensor tract-specific analysis of the uncinate fasciculus in patients with progressive supranuclear palsy. *J. Neuroradiol.* 40 (2), 121–129.
- Kato, N., Arai, K., Hattori, T., 2003. Study of the rostral midbrain atrophy in progressive supranuclear palsy. *J. Neurol. Sci.* 210, 57–60.
- Kim, B.C., Choi, S.-M., Choi, K.-H., Nam, T.-S., Kim, J.-T., Lee, S.-H., Park, M.-S., Yoon, W., 2017. MRI measurements of brainstem structures in patients with vascular parkinsonism, progressive supranuclear palsy, and Parkinson's disease. *Neurool. Sci.* 38, 627–633.
- Klöppel, S., Stonnington, C.M., Chu, C., Draganski, B., Scahill, R.I., Rohrer, J.D., Fox, N.C., Jack Jr., C.R., Ashburner, J., Frackowiak, R.S., 2008. Automatic classification of MR scans in Alzheimer's disease. *Brain* 131, 681–689.
- Laird, A.R., Fox, P.M., Price, C.J., Glahn, D.C., Uecker, A.M., Lancaster, J.L., Turkeltaub, P.E., Kochunov, P., Fox, P.T., 2005. ALE meta-analysis: controlling the false discovery rate and performing statistical contrasts. *Hum. Brain Mapp.* 25, 155–164.
- Lancaster, J.L., Tordesillas-Gutierrez, D., Martinez, M., Salinas, F., Evans, A., Zilles, K., Mazziotta, J.C., Fox, P.T., 2007. Bias between MNI and Talairach coordinates analyzed using the ICBM-152 brain template. *Hum. Brain Mapp.* 28, 1194–1205.
- Lehericy, S., Hartmann, A., Lannuzel, A., et al., 2010. Magnetic resonance imaging lesion pattern in Guadeloupean parkinsonism is distinct from progressive supranuclear palsy. *Brain* 133, 2410–2425 Pt 8.
- Li, J., Pan, P., Huang, R., Shang, H., 2012a. A meta-analysis of voxel-based morphometry studies of white matter volume alterations in Alzheimer's disease. *Neurosci. Biobehav. Rev.* 36, 757–763.
- Li, J., Pan, P., Song, W., Huang, R., Chen, K., Shang, H., 2012b. A meta-analysis of diffusion tensor imaging studies in amyotrophic lateral sclerosis. *Neurobiol. Aging* 33, 1833–1838.
- Litvan, I., Agid, Y., Calne, D., Campbell, G., Dubois, B., Duvoisin, R.C., Goetz, C.G., Golbe, L.I., Grafman, J., Growdon, J.H., Hallett, M., Jankovic, J., Quinn, N.P., Tolosa, E., Zee, D.S., 1996a. Clinical research criteria for the diagnosis of progressive supranuclear palsy (Steele-Richardson-Olszewski syndrome): report of the NINDS-SPSP international workshop. *Neurology* 47, 1–9.
- Litvan, I., Hauw, J.J., Bartko, J.J., Lantos, P.L., Daniel, S.E., Horoupian, D.S., McKee, A., Dickson, D., Bancher, C., Tabaton, M., Jellinger, K., Anderson, D.W., 1996b. Validity and reliability of the preliminary NINDS neuropathologic criteria for progressive supranuclear palsy and related disorders. *J. Neuropathol. Exp. Neurol.* 55, 97–105.
- Longoni, G., Agosta, F., Kostic, V.S., Stojkovic, T., Pagani, E., Stosic-Opincal, T., Filippi, M., 2011. MRI measurements of brainstem structures in patients with Richardson's syndrome, progressive supranuclear palsy-parkinsonism, and Parkinson's disease. *Mov. Disord.* 26, 247–255.
- Meyer, S., Mueller, K., Stuke, K., Bisenius, S., Diehl-Schmid, J., Jessen, F., Kassubek, J., Kornhuber, J., Ludolph, A.C., Prudlo, J., Schneider, A., Schuemberg, K., Yakushev, I., Otto, M., Schroeter, M.L., Group, F.T.S., 2017. Predicting behavioral variant frontotemporal dementia with pattern classification in multi-center structural MRI data. *Neuroimage Clin.* 14, 656–662.
- Moller, L., Kassubek, J., Sudmeyer, M., Hilker, R., Hattingen, E., Egger, K., Amtage, F., Pinkhardt, E.H., Respondek, G., Stamelou, M., Moller, F., Oertel, W.H., Knake, S., Huppertz, H.J., Hoglinger, G.U., 2017. Manual MRI morphometry in Parkinsonian syndromes. *Mov. Disord.* 32, 778–782.
- Mueller, K., Jech, R., Bonnet, C., Tintera, J., Hanuska, J., Moller, H.E., Fassbender, K., Ludolph, A., Kassubek, J., Otto, M., Ruzicka, E., Schroeter, M.L., Group, F.T.S., 2017. Disease-specific regions outperform whole-brain approaches in identifying progressive supranuclear palsy: a multicentric MRI study. *Front. Neurosci.* 11, 100.
- Müller, V.I., Cieslik, E.C., Laird, A.R., Fox, P.T., Radua, J., Mataix-Cols, D., Tench, C.R., Yarkoni, T., Nichols, T.E., Turkeltaub, P.E., Wager, T.D., Eickhoff, S.B., 2018. Ten simple rules for neuroimaging meta-analysis. *Neurosci. Biobehav. Rev.* 84, 151–161.
- Oba, H., Yagishita, A., Terada, H., Barkovich, A., Kutomi, K., Yamauchi, T., Furui, S., Shimizu, T., Uchigata, M., Matsumura, K., 2005. New and reliable MRI diagnosis for progressive supranuclear palsy. *Neurology* 64, 2050–2055.
- Padovani, A., Borroni, B., Brambati, S.M., et al., 2006. Diffusion tensor imaging and voxel based morphometry study in early progressive supranuclear palsy. *J. Neurol. Neurosurg. Psychiatry* 77 (4), 457–463.
- Pan, P.L., Song, W., Yang, J., Huang, R., Chen, K., Gong, Q.Y., ... Shang, H.F., 2012. Gray matter atrophy in behavioral variant frontotemporal dementia: a meta-analysis of voxel-based morphometry studies. *Dement. Geriatr. Cogn. Disord.* 33 (2-3), 141–148.
- Paviour, D.C., Price, S.L., Jahanshahi, M., Lees, A.J., Fox, N.C., 2006. Longitudinal MRI in progressive supranuclear palsy and multiple system atrophy: rates and regions of atrophy. *Brain* 129, 1040–1049.
- Piattella, M.C., Upadhyay, N., Bologna, M., et al., 2015. Neuroimaging evidence of gray and white matter damage and clinical correlates in progressive supranuclear palsy. *J. Neurol.* 262 (8), 1850–1858.
- Premi, E., Gualeni, V., Costa, P., et al., 2016. Looking for measures of disease severity in the frontotemporal dementia continuum. *J. Alzheimer's Dis.* 52 (4), 1227–1235.
- Radua, J., Mataix-Cols, D., 2009. Voxel-wise meta-analysis of grey matter changes in obsessive-compulsive disorder. *Br. J. Psychiatry* 195, 393–402.
- Radua, J., Rubia, K., Canales-Rodriguez, E.J., Pomarol-Clotet, E., Fusar-Poli, P., Mataix-Cols, D., 2014. Anisotropic kernels for coordinate-based meta-analyses of neuroimaging studies. *Front. Psychiatry* 5, 13.
- Rascovsky, K., Hodges, J.R., Knopman, D., Mendez, M.F., Kramer, J.H., Neuhaus, J., van Swieten, J.C., Seelehar, H., Dopper, E.G., Onyike, C.U., Hillis, A.E., Josephs, K.A., Boeve, B.F., Kertesz, A., Seeley, W.W., Rankin, K.P., Johnson, J.K., Gorno-Tempini, M.L., Rosen, H., Priloleau-Latham, C.E., Lee, A., Kipps, C.M., Lillo, P., Piguet, O., Rohrer, J.D., Rossor, M.N., Warren, J.D., Fox, N.C., Galasko, D., Salmon, D.P., Black, S.E., Mesulam, M., Weintraub, S., Dickerson, B.C., Diehl-Schmid, J., Pasquier, F., Deramecourt, V., Leber, F., Pijnenburg, Y., Chow, T.W., Manes, F., Grafman, J., Cappa, S.F., Freedman, M., Grossman, M., Miller, B.L., 2011. Sensitivity of revised diagnostic criteria for the behavioural variant of frontotemporal dementia. *Brain* 134, 2456–2477.
- Sakurai, K., Imabayashi, E., Tokumaru, A.M., et al., 2015. The feasibility of white matter volume reduction analysis using SPMS plus DARTEL for the diagnosis of patients with clinically diagnosed corticobasal syndrome and Richardson's syndrome. *Neuroimage Clin.* 7, 605–610.
- Sandhya, M., Saini, J., Pasha, S.A., Yadav, R., Pal, P.K., 2014. A voxel based comparative analysis using magnetization transfer imaging and T1-weighted magnetic resonance imaging in progressive supranuclear palsy. *Ann. Indian Acad. Neurol.* 17 (2), 193–198.
- Schott, J.M., 2007. A neurological MRI menagerie. *Pract. Neurol.* 7, 186–190.
- Schroeter, M.L., Neumann, J., 2011. Combined imaging markers dissociate Alzheimer's disease and frontotemporal lobar degeneration - an ALE meta-analysis. *Front. Aging Neurosci.* 3, 10.
- Schroeter, M.L., Raczka, K., Neumann, J., Von Cramon, D.Y., 2007. Towards a nosology for frontotemporal lobar degenerations—a meta-analysis involving 267 subjects. *Neuroimage* 36 (3), 497–510.
- Schroeter, M.L., Raczka, K., Neumann, J., Von Cramon, D.Y., 2008. Neural networks in frontotemporal dementia—a meta-analysis. *Neurobiol. Aging* 29 (3), 418–426.
- Schroeter, M.L., Stein, T., Maslowski, N., Neumann, J., 2009. Neural correlates of Alzheimer's disease and mild cognitive impairment: a systematic and quantitative meta-analysis involving 1351 patients. *Neuroimage* 47 (4), 1196–1206.
- Schroeter, M.L., Laird, A.R., Chwiesko, C., Deuschl, C., Schneider, E., Bzdok, D., Eickhoff, S.B., Neumann, J., 2014. Conceptualizing neuropsychiatric diseases with multimodal data-driven meta-analyses - the case of behavioral variant frontotemporal dementia. *Cortex* 57, 22–37.
- Shao, N., Yang, J., Li, J., Shang, H.F., 2014. Voxelwise meta-analysis of gray matter anomalies in progressive supranuclear palsy and Parkinson's disease using anatomic likelihood estimation. *Front. Hum. Neurosci.* 8, 63.
- Shao, N., Yang, J., Shang, H., 2015. Voxelwise meta-analysis of gray matter anomalies in Parkinson variant of multiple system atrophy and Parkinson's disease using anatomic likelihood estimation. *Neurosci. Lett.* 587, 79–86.
- Shi, H.C., Zhong, J.G., Pan, P.L., Xiao, P.R., Shen, Y., Wu, L.J., Li, H.L., Song, Y.Y., He,

- G.X., Li, H.Y., 2013. Gray matter atrophy in progressive supranuclear palsy: meta-analysis of voxel-based morphometry studies. *Neurol. Sci.* 34, 1049–1055.
- Slowinski, J., Imamura, A., Uitti, R.J., Pooley, R.A., Strongosky, A.J., Dickson, D.W., Broderick, D.F., Wszolek, Z.K., 2008. MR imaging of brainstem atrophy in progressive supranuclear palsy. *J. Neurol.* 255, 37–44.
- Takahashi, R., Ishii, K., Kakigi, T., Yokoyama, K., Mori, E., Murakami, T., 2011. Brain alterations and mini-mental state examination in patients with progressive supranuclear palsy: voxel-based investigations using f-fluorodeoxyglucose positron emission tomography and magnetic resonance imaging. *Dement. Geriatr. Cogn. Dis. Extra* 1 (1), 381–392.
- Viechtbauer, W., 2010. Conducting meta-analyses in R with the metafor package. *J. Stat. Softw.* 36, 1–48.
- Whitwell, J.L., Duffy, J.R., Strand, E.A., et al., 2013. Neuroimaging comparison of primary progressive apraxia of speech and progressive supranuclear palsy. *Eur. J. Neurol.* 20 (4), 629–637.
- Whitwell, J.L., Hoglinger, G.U., Antonini, A., Bordelon, Y., Boxer, A.L., Colosimo, C., van Eimeren, T., Golbe, L.I., Kassubek, J., Kurz, C., Litvan, I., Pantelyat, A., Rabinovici, G., Respondek, G., Rominger, A., Rowe, J.B., Stamelou, M., Josephs, K.A., Movement Disorder Society-endorsed, P.S.P.S.G., 2017. Radiological Biomarkers for Diagnosis in PSP: Where are we and where do we need to be? *Mov. Disord.* 32 (7), 955–971.
- Yang, J., Pan, P., Song, W., Huang, R., Li, J., Chen, K., ... Shang, H., 2012a. Voxelwise meta-analysis of gray matter anomalies in Alzheimer's disease and mild cognitive impairment using anatomic likelihood estimation. *J. Neurol. Sci.* 316 (1–2), 21–29.
- Yang, J., Pan, P., Song, W., Shang, H.F., 2012b. Quantitative meta-analysis of gray matter abnormalities in semantic dementia. *J. Alzheimers Dis.* 31 (4), 827–833.
- Yang, J., Shao, N., Li, J., Shang, H., 2014. Voxelwise meta-analysis of white matter abnormalities in progressive supranuclear palsy. *Neurol. Sci.* 35, 7–14.
- Yin, R.H., Tan, L., Liu, Y., Wang, W.Y., Wang, H.F., Jiang, T., Radua, J., Zhang, Y., Gao, J., Canu, E., Migliaccio, R., Filippi, M., Gorno-Tempini, M.L., Yu, J.T., 2015. Multimodal voxel-based meta-analysis of white matter abnormalities in Alzheimer's disease. *J. Alzheimers Dis.* 47, 495–507.
- Yu, F., Barron, D.S., Tantiwongkosi, B., Fox, P., 2015. Patterns of gray matter atrophy in atypical parkinsonism syndromes: a VBM meta-analysis. *Brain Behav.* 5, e00329.
- Zhang, Y., Walter, R., Ng, P., Luong, P.N., Dutt, S., Heuer, H., Rojas-Rodriguez, J.C., Tsai, R., Litvan, I., Dickerson, B.C., Tartaglia, M.C., Rabinovici, G., Miller, B.L., Rosen, H.J., Schuff, N., Boxer, A.L., 2016. Progression of microstructural degeneration in progressive Supranuclear palsy and Corticobasal syndrome: a longitudinal diffusion tensor imaging study. *PLoS One* 11, e0157218.
- Zhong, J., Pan, P., Dai, Z., Shi, H., 2014. Voxelwise meta-analysis of gray matter abnormalities in dementia with Lewy bodies. *Eur. J. Radiol.* 83 (10), 1870–1874.

5 STUDY 3

Unraveling corticobasal syndrome and alien limb syndrome with structural brain imaging



Behavioural Neurology

Unraveling corticobasal syndrome and alien limb syndrome with structural brain imaging[☆]

Franziska Albrecht^{a,*}, Karsten Mueller^a, Tommaso Ballarini^a,
 Leonie Lampe^{a,b}, Janine Diehl-Schmid^{c,d}, Klaus Fassbender^{c,e},
 Klaus Fliessbach^{c,f}, Holger Jahn^{c,g}, Robert Jech^o, Jan Kassubek^{c,h},
 Johannes Kornhuber^{c,i}, Bernhard Landwehrmeyer^h, Martin Lauer^{c,j},
 Albert C. Ludolph^h, Epameinondas Lyros^{c,e}, Johannes Prudlo^{c,k},
 Anja Schneider^{c,f}, Matthis Synofzik^{c,l,m}, Jens Wiltfang^{c,n},
 Adrian Danek^{c,p}, Markus Otto^{c,h}, FTLD-Consortium¹ and
 Matthias L. Schroeter^{a,b,c}

^a Max Planck Institute for Human Cognitive and Brain Sciences, Leipzig, Germany

^b Clinic of Cognitive Neurology, University of Leipzig, Germany

^c FTLD Consortium Germany, Germany

^d Department of Psychiatry and Psychotherapy, Technical University of Munich, Germany

^e Clinic for Neurology, Saarland University, Germany

^f Department of Neurodegenerative Diseases and Geriatric Psychiatry, University Bonn, Germany

^g Clinic for Psychiatry and Psychotherapy, University Hospital Hamburg-Eppendorf, Germany

^h Clinic for Neurology, University of Ulm, Germany

ⁱ Department of Psychiatry and Psychotherapy, Friedrich-Alexander-University Erlangen-Nuremberg, Germany

^j Clinic for Psychiatry, Psychosomatic Medicine and Psychotherapy, University Würzburg, Germany

^k Department of Neurology, Rostock University Medical Center, Rostock, Germany & German Center for Neurodegenerative Diseases, Rostock, Germany

^l Department of Neurodegenerative Diseases, Centre for Neurology & Hertie-Institute for Clinical Brain Research, University of Tübingen, Germany

^m German Center for Neurodegenerative Diseases (DZNE), Tübingen, Germany

ⁿ University Medical Center Göttingen, Germany & German Center for Neurodegenerative Diseases (DZNE) Göttingen, Germany

^o Department of Neurology and Center of Clinical Neuroscience, First Faculty of Medicine, Charles University, Prague, Czech Republic

^p Clinic of Neurology, Ludwig Maximilian University of Munich, Germany

ARTICLE INFO

Article history:

Received 10 August 2018

Reviewed 25 September 2018

ABSTRACT

Alien limb phenomenon is a rare syndrome associated with a feeling of non-belonging and disowning toward one's limb. In contrast, anarchic limb phenomenon leads to involuntary but goal-directed movements. Alien/anarchic limb phenomena are frequent in corticobasal

[☆] Statistical Analysis conducted by Franziska Albrecht, M.Sc., Max Planck Institute for Human Cognitive and Brain Sciences.

* Corresponding author. Max Planck Institute for Human Cognitive and Brain Sciences, Stephanstr. 1A, 04103 Leipzig, Germany. E-mail address: fabrecht@cbs.mpg.de (F. Albrecht).

¹ Members of the FTLD-Consortium are listed under the Acknowledgments section.

<https://doi.org/10.1016/j.cortex.2019.02.015>

0010-9452/© 2019 The Authors. Published by Elsevier Ltd. This is an open access article under the CC BY-NC-ND license (<http://creativecommons.org/licenses/by-nc-nd/4.0/>).

Revised 3 December 2018
 Accepted 15 February 2019
 Action editor Stephen Jackson
 Published online 25 February 2019

Keywords:

Alien limb syndrome
 Anarchic limb syndrome
 Corticobasal syndrome
 Diagnosis prediction
 Support vector machine

syndrome (CBS), an atypical parkinsonian syndrome characterized by rigidity, akinesia, dystonia, cortical sensory deficit, and apraxia.

The structure–function relationship of alien/anarchic limb was investigated in multi-centric structural magnetic resonance imaging (MRI) data. Whole-group and single-subject comparisons were made in 25 CBS and eight CBS-alien/anarchic limb patients versus controls. Support vector machine was used to see if CBS with and without alien/anarchic limb could be distinguished by structural MRI patterns.

Whole-group comparison of CBS versus controls revealed asymmetric frontotemporal atrophy. CBS with alien/anarchic limb syndrome versus controls showed frontoparietal atrophy including the supplementary motor area contralateral to the side of the affected limb. Exploratory analysis identified frontotemporal regions encompassing the pre-/and postcentral gyrus as compromised in CBS with alien limb syndrome. Classification of CBS patients yielded accuracies of 79%. CBS-alien/anarchic limb syndrome was differentiated from CBS patients with an accuracy of 81%. Predictive differences were found in the cingulate gyrus spreading to frontomedian cortex, postcentral gyrus, and temporoparietooccipital regions.

We present the first MRI-based group analysis on CBS-alien/anarchic limb. Results pave the way for individual clinical syndrome prediction and allow understanding the underlying neurocognitive architecture.

© 2019 The Authors. Published by Elsevier Ltd. This is an open access article under the CC BY-NC-ND license (<http://creativecommons.org/licenses/by-nc-nd/4.0/>).

1. Introduction

Alien and anarchic limb syndromes (AL) are peculiar phenomena that encompass patients struggling with an extremity experienced as rogue. In 1972, this syndrome was first acknowledged by Brion and his colleagues as ‘main étrangère’ (Brion, 1972). Only in 1991, Della Sala et al. published a first attempt to disentangle alien and anarchic limb syndrome cases, introduced an English terminology and description for the scientific community (Della Sala, Marchetti, & Spinnler, 1991). Alien limb syndrome is characterized by a feeling that the limb is unfamiliar or does not belong, whereas anarchic limb syndrome additionally involves the extremity performing targeted but unintended movements that are recognized as one’s own (Della Sala et al., 1991; Marchetti & Della Sala, 1998; Synofzik, Vosgerau, & Newen, 2008). Alien limb, or posterior variant, seems related to the postcentral gyrus and somatosensory cortex, while anarchic limb, or frontal variant, seems related to the supplementary motor area and medial prefrontal cortex (Hassan & Josephs, 2016; Marchetti & Della Sala, 1998). In the following we generally use the term AL as an umbrella term for both alien and anarchic limb phenomena – in the literature both syndromes are often confounded – but apply the exact terms if referring to the peculiar phenomena. AL can be caused by various diseases, amongst which corticobasal syndrome (CBS) is the most frequent (Graff-Radford et al., 2013). CBS is a rare, atypical parkinsonian syndrome characterized by rigidity, akinesia, dystonia, cortical sensory deficit, and apraxia (Armstrong et al., 2013). Revised diagnostic criteria of CBS consider AL an important diagnostic criterion, seen in 30% of CBS patients. However, the exact anatomical correlates of AL are still a matter of debate.

This multi-center study assessed structural differences in the brains of CBS patients with and without AL. Our sample

consisted of 25 CBS patients, of which eight were diagnosed with AL. In the main analyses we did not distinguish between the subtypes of AL, as it would lead to insufficiently powered analysis. In an additional exploratory pilot analysis, we divided the CBS-AL cohort into four alien and three anarchic limb syndrome patients and compared them to the whole-group of controls to unmask the specific anatomical counterpart. Whole-group analyses were performed using voxel-based morphometry. We investigated whether multivariate pattern recognition (support vector machine) could distinguish between CBS patients and controls and also predict AL in CBS. We hypothesized atrophy in CBS with AL in the supplementary motor area, medial prefrontal cortex, posterior postcentral gyrus, and somatosensory cortex. For the CBS versus healthy controls contrast, we hypothesized atrophy in frontal, parietal, and temporal lobes.

2. Material and methods

2.1. Participants

Multi-centric patients’ data were included from the German Consortium of Frontotemporal Lobar Degeneration (Otto et al., 2011). Detailed information on patients/controls’ demographic data and summarized AL symptoms are listed in Table e1–e3. Specialists of the respective clinics (i.e., neurologists and/or psychiatrists) examined the patients thoroughly according to a standard operating procedure protocol and evaluated diagnosis (here CBS) as well as the occurrence of AL (i.e., ‘alien feeling’ or ‘unintended movements’) among several other clinical symptoms/syndromes to assess whether they fit the inclusion criteria for the FTLD Consortium (Otto et al., 2011). Twenty-five CBS patients were compared with 25 age- and gender-matched healthy controls. The patient

group was subdivided into a cohort of 17 CBS patients without AL (CBS-O) and a cohort of eight CBS patients with AL (CBS-AL). Four patients were diagnosed with alien limb, three with anarchic limb syndrome, and one showed signs of both. Pearson's Chi Squared test (χ^2) and unpaired Student's T-tests indicated no significant differences between the cohorts concerning gender, age, disease duration, and severity of clinical symptoms (Table 1). The study was approved by the local ethics committees (Leipzig:ID137-11-18042011). Participants were fully informed and gave written consent in accordance with the Declaration of Helsinki.

2.2. Data acquisition

T1-weighted structural brain images were acquired at each center using the magnetization-prepared rapid gradient-echo (MP-RAGE) sequence implemented on 3T scanners (Table e-2). Although scanner parameters slightly differ, an F-test in SPM12 (UCL, UK) revealed no significant influence.

2.3. Asymmetry correction in alien/anarchic limb syndrome patients

AL is seen in left and/or right limbs. The most severely affected limb for each subject was designated by clinical features at the time of scanning, but without considering the image. If necessary, images were flipped in the left-right dimension (Whitwell et al., 2010) such that the presumably affected hemisphere, contralateral to syndrome location, was positioned on the right side of the image in all AL patients. This allowed investigation of AL in the same hemisphere across subjects.

2.4. Voxel-based morphometry

Voxel-based morphometry was performed applying the CAT12 toolbox (University of Jena, Germany) with SPM12 (UCL, UK). Images were spatially normalized, segmented, modulated by the amount of non-linear deformation, and smoothed

with a Gaussian kernel of 8-mm full-width at half-maximum. Voxel-wise Student's T-tests were performed to compare, separately, the groups of patients with controls. Covariates were used to control for age, gender, and total intracranial volume. For the main comparison, clusters were detected using a voxel-threshold of $p < .001$ and a family-wise error (FWE) corrected cluster-threshold of $p < .05$. For exploratory analyses, clusters were detected applying an uncorrected voxel-threshold of $p < .001$.

The three patient cohorts (CBS, CBS-O, CBS-AL) were compared with healthy controls in whole-group comparisons. For exploratory pilot analyses, we split the CBS-AL cohort according to either alien ($N = 4$) or anarchic limb ($N = 3$) syndrome. Note that one patient was omitted given that he showed both syndromes (AL-16).

2.5. Support vector machine classification

Support vector machine classification allows the separation of data, by class, in a multidimensional space. We ran a support vector machine attempting to distinguish between CBS patients and controls as well as between CBS-AL and CBS-O using libSVM 3.18 (Chang & Lin, 2011). Classification accuracy was obtained by cross-validation using the "leave-one-subject-out" approach. Specificity and sensitivity were calculated by the number of correctly classified cases in each group. To investigate the reliability of the results the influence of several analysis parameters was inspected (e.g., linear/polynomial kernels). First, feature selection was based on SPM's gray matter tissue probability map, using different minimum gray matter probabilities ranging from 0 to 60% (Table e-5). The SPM map was also interpolated and smoothed with a Gaussian kernel of 8-mm full-width at half-maximum. Second, we used disease-specific regions-of-interest for feature selection. Regions-of-interest were selected according to our recent meta-analysis of CBS (Albrecht, Bisenius, Morales Schaack, Neumann, & Schroeter, 2017) as suggested previously (Bisenius et al., 2017; Meyer et al., 2017; Mueller et al., 2017) and generated using the WFU PickAtlas 3.0 (Lancaster, 1997).

Table 1 – Summarized subjects' demographic and clinical characteristics.

Cohort	Number	Female	Age (years)	Disease duration (years)	Clinical dementia rating score	Clinical dementia rating score-FTLD
Healthy controls	25	11	66.2 ± 10.1			
CBS	25	13	66.7 ± 10.1	3.7 ± 2.8	7.0 ± 4.2	8.4 ± 5.1
CBS-O	17	10	68.2 ± 5.4	4.1 ± 3.2	5.8 ± 3.9	7.1 ± 4.6
CBS-AL	8	3	63.4 ± 7.2	2.8 ± 1.6	9.0 ± 4.1	10.8 ± 5.4
<i>Statistical differences</i>						
Healthy controls versus CBS		$\chi^2 = .08, p = .8$	$t = .20, p = .84$			
Healthy controls versus CBS-O		$\chi^2 = .40, p = .5$	$t = .84, p = .41$			
Healthy controls versus CBS-AL		$\chi^2 = .25, p = .6$	$t = -.85, p = .40$			
CBS-O versus CBS-AL		$\chi^2 = 8.8^{e-32}, p = 1.0$	$t = -1.67, p = .12$	$t = -1.4, p = .18$	$t = 1.8, p = .09$	$t = 1.5, p = .15$
Mean ± standard deviation. Student's T-test was applied to compare numerical variables and χ^2 test to compare categorical variables across groups. CBS corticobasal syndrome, CBS-AL corticobasal syndrome with alien/anarchic limb syndrome, CBS-O corticobasal syndrome without alien limb syndrome, Clinical Dementia Rating Score-FTLD score modified for frontotemporal lobar degeneration.						

2.6. Data availability statement

Study protocol and statistical analysis plan will be shared at request. Data of participants are stored at the FTLDCoalition. Patients' data are bound to maintain confidentiality and, accordingly, are only shared at reasonable request to replicate procedures and analysis of the study.

3. Results

3.1. Whole-group voxel-based morphometry

Fig. 1 and Table e-4 display gray matter volume differences between patients with CBS and healthy controls. In the left hemisphere reduced gray matter volume, for patients, was observed in inferior and middle occipital gyrus, medial temporal gyrus and temporoparietal junction, inferior/middle/superior frontal gyri, insula, and premotor and supplementary motor areas. On the right side, less gray matter was revealed in postcentral gyrus, supramarginal gyrus, inferior frontal gyrus, posterior and anterior insula, and supplementary motor area. Furthermore, right posterior cingulate gyrus, cuneus, and precuneus were affected.

Comparing CBS-O to controls revealed lower gray matter volume in superior temporal gyrus, medial temporal gyrus and temporoparietal junction, middle/inferior frontal gyrus, claustrum and putamen, posterior superior frontal sulcus and middle frontal gyrus/precentral gyrus; all on the left side. Less gray matter volume was also found bilaterally in the insula spreading to the superior temporal gyrus.

Contrasting CBS-AL and controls showed reduced gray matter volume in the posterior insula, superior temporal gyrus, and middle/superior frontal gyrus; all in the left

hemisphere. Lower gray matter volume was observed in the right precuneus, and cingulate gyrus spreading to fronto-medial cortex. Importantly, this included the supplementary motor area contralateral to the AL symptoms.

A direct comparison of CBS-AL and CBS-O did not reveal significant results, but may not have been a sufficiently powered analysis.

Contrasting CBS with alien limb syndrome to controls, lower gray matter volume was found in occipital pole, calcarine cortex, and inferior occipital gyrus; all on the left side (Figure e-1 and Table e-6). On the right side, superior/middle temporal gyrus including temporal pole, precentral/postcentral/supramarginal gyrus, and middle cingulate gyrus were implicated. Note that clusters in left occipital gyrus, right precentral/postcentral/supramarginal gyrus, and right superior/middle temporal gyrus were even apparent when correcting for multiple comparisons (see copper clusters in Figure e-1). The comparison of CBS with anarchic limb and controls showed less gray matter volume in superior parietal lobule/precuneus and parietal operculum/transverse temporal gyrus; all in the left hemisphere. In the right hemisphere, superior/middle/inferior occipital gyrus and posterior insula/putamen were compromised.

3.2. Support vector machine classification

The support vector machine classification could reliably identify CBS versus controls as well as CBS-AL versus CBS-O (Fig. 2 and Table e-5). Classification accuracies for the linear kernel were stable around 70–80%, independent of the gray matter mask. The highest accuracy of the classification of CBS patients and controls was 78.9% using a linear kernel and gray matter mask of 4. Regions contributing to correct classification mirrored areas identified in the univariate group comparison

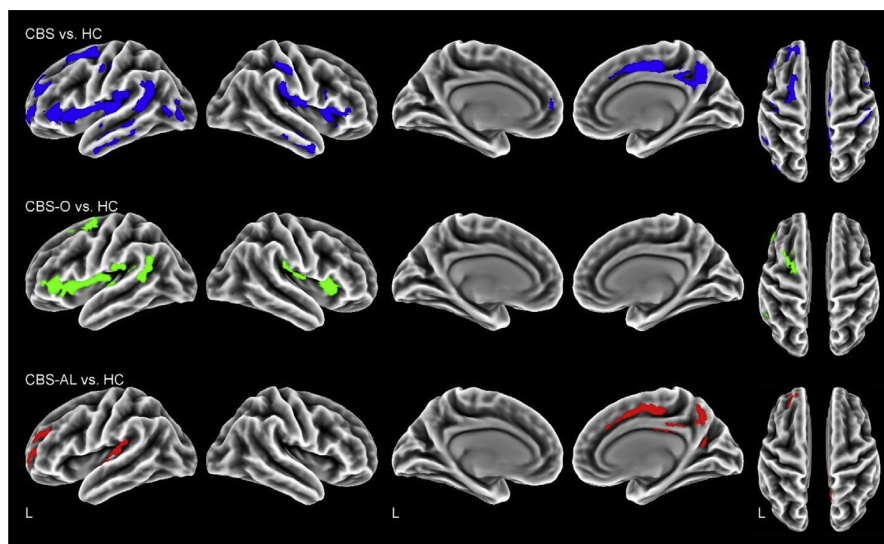


Fig. 1 – Reduced gray matter volume in each corticobasal syndrome (CBS) cohort compared with controls (HC). Clusters are corrected for multiple comparisons, $p < .05$ family-wise error rate (FWE). CBS whole patient cohort, CBS-AL CBS with alien/anarchic limb syndrome, CBS-O CBS without alien limb syndrome, L left.

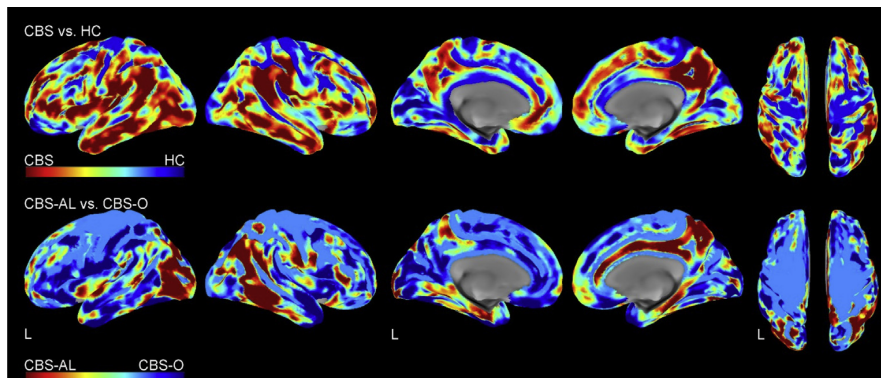


Fig. 2 – Weights of voxels most relevant for individual support vector machine classification between corticobasal syndrome (CBS) versus healthy controls (HC) and CBS with alien limb (CBS-AL) versus CBS without alien/anarchic limb (CBS-O). Note that these weights are relative and have no applicable units. Support vector machine classification was performed with a linear kernel on all voxels within the SPM's gray matter mask (tissue probability $>.4$, top row, tissue probability $>.5$, bottom row).

of the entire CBS group versus controls, as discussed above. Classifying CBS-AL versus CBS-O, resulted in an accuracy of 81.3% when applying a linear kernel and a gray matter mask of .5. Regions predictive of AL included, among others, the cingulate gyrus spreading to frontomedial cortex, postcentral gyrus, and temporoparietooccipital regions, at least partially overlapping with regions of thinner gray matter observed in the univariate comparison CBS-AL versus controls. Using the meta-analytically generated regions-of-interest masks did not improve the results.

4. Discussion

The complete group of CBS patients was characterized by apparent atrophy in frontotemporal and occipital regions, motor areas, and the insulae, in agreement with previous studies (Lee et al., 2011; Whitwell et al., 2010). To our knowledge, no prior study has systematically evaluated syndrome-specific atrophy in CBS with AL. Patients with AL showed apparent atrophy in the insula and frontotemporal gyri compared with healthy controls, and remarkably, also in the supplementary motor area and cingulate cortex contralateral to the symptomatic body side. This pattern was also evident in the entire CBS group although not when the CBS-O was compared with controls. This suggests the difference was driven by the CBS-AL patients.

4.1. Supplementary motor area is a neural correlate for alien/anarchic limb

Although CBS is mainly asymmetric it affects both body sides. Interestingly, AL is reportedly more often seen with left limbs, which would be consistent with neural correlates in the right hemisphere (Graff-Radford et al., 2013). It is speculated that the asymmetry of the functions of the hemispheres explains why certain variants of AL affect only left or right hand. For example Bartolo et al. (2011) report that the right

supplementary motor area is inhibiting both, right and left cortex, while the left supplementary motor area is not dominant and inhibits only contralateral, hence leading to right-sided AL. In Graff-Radford's large cohort, the left extremity was affected in 69% of AL cases. In our sample the prevalence was 50%. One should consider that Graff-Radford's review included cases with various diseases, not only CBS and did not differentiate between alien and anarchic limb phenomena. Their study identified the parietal lobe and its disconnection from other cortical areas as a common correlate for AL, which is in line with our CBS-AL comparison.

Interpreting neural correlates of alien and anarchic limb phenomena is often masked by the fact that in the literature both syndromes are confounded. Disentangling the anatomical counterparts of anarchic limb, studies have identified the supplementary motor area as a crucial brain structure (Frith, Blakemore, & Wolpert, 2000; Hassan & Josephs, 2016; Marchetti & Della Sala, 1998; Schaefer, Heinze, & Galazky, 2013). In line with those findings, our cohort suggests atrophy in the supplementary motor area. Thus, it is hypothesized that an impaired supplementary motor area is necessary for anarchic limb syndrome. The anterior region of the supplementary motor area is internally triggered and activated when movements are imagined and selected (Frith et al., 2000). To initiate the movement the supplementary motor area needs to be inhibited. The inhibition subsequently leads to activation of the primary motor cortex and initiates movement. Damage to this network by atrophy could lead to externally triggered, unintended, movements and disturbed selection of appropriate motor programs, as experienced by anarchic limb syndrome patients. Even visual stimuli of surroundings activate this circuit and motor programs (Sumner & Husain, 2008). Thus, the brain needs to weight several competing motor plans activated by objects in our proximity. Sumner and Husain (2008) summarized in their review that a network of medial frontal areas (including supplementary motor area) and parietal regions inhibit reflexive behavior and mediate competing

motor programs. Indeed, in patients with focal lesions in the supplementary motor area and supplementary eye field, automatic inhibition of subconscious motor activation is impaired, which correlated with the extent of the lesions (Sumner et al., 2007). Hence, automatic inhibition is crucial for flexible and volitional motor control in condition–action associations. Importantly for our results, a case study by McBride, Sumner, Jackson, Bajaj, and Husain (2013) observed disturbed automatic inhibition of primed reactions in the anarchic limb of a CBS patient. In the non-affected limb automatic inhibition remained preserved. This underlines that the hypothesis of automatic inhibition processes facilitating flexible and volitional behavior due to inhibiting unwanted motor plans, primed by surrounding objects, may account for the well-executed and purposeful anarchic limb movements. In the exploratory analyses however, we could not confirm atrophy in the supplementary motor area in anarchic limb syndrome, which may have been an insufficiently powered analysis since it only involved three patients.

Why the affected limb would be experienced as foreign in alien limb syndrome is not clear. One hypothesis is that disruption of parietal circuits leads to dysfunction in self-attribution (Sarva, Deik, & Severt, 2014). Thus, alien limb seems to arise due to a disturbed sense of ownership, but not disturbed sense of agency (Synofzik et al., 2008). Overall, the neural network processing body-ownership comprises the right temporo-parietal junction, right insula, inferior parietal cortex, and premotor cortex (Tsakiris, Longo, & Haggard, 2010). In line with that, Hassan and Josephs (2016) stated in their review that lesions in parietal lobe, i.e., posterior post-central gyrus, posterior primary sensory cortex, and tertiary somatosensory cortex, lead to alien limb syndrome. Notably, we also found these networks involved in the univariate group comparison of CBS-AL and controls as well as in the CBS-AL versus CBS-O classification results. Further, exploratory pilot analyses of the alien limb syndrome cohort confirmed putative atrophy in parietal cortex and postcentral gyrus.

4.2. The role of the cingulate cortex in alien/anarchic limb syndrome

In general, the cingulate cortex and especially its anterior part translates motor intentions into actions and mediates willed control, underlining the important role in motor actions and their cognitive control (Paus, 2001). Further, the anterior cingulate cortex is known for its dense projections from the motor cortex and spinal cord. In healthy conditions, the cingulate cortex implements the selection of actions as well as fights competing motor programs, a crucial part of volitional control.

Contrasting CBS-AL to controls, putative atrophy was also found in the right cingulate cortex, contralateral to the symptoms shown by the patients. In exploratory analyses, we could confirm volume loss in the cingulate cortex in the alien limb syndrome cohort but not in the anarchic limb syndrome cohort. Already, Goldberg, Mayer, and Toglia (1981) hypothesized that the two functional zones of the medial frontal gyrus, i.e., supplementary motor area and cingulate cortex, could be the reason for AL when implicated due to a lesion. Even at this time it was known that both regions are

connected reciprocally as Goldberg further reported. In an early study, Talairach et al. (1973) observed, when stimulating continuously the anterior cingulate cortex in epileptic patients, that they exhibited highly complex motor behavior even adapted to the environmental conditions. This finding already supports the hypothesis that the cingulate cortex plays an important role in high motor integration. Brugger, Galovic, Weder, and Kägi (2015) confirmed involvement of the cingulate cortex in disturbed self-initiated movements in anterior cerebral artery stroke patients with anarchic limb syndrome. The researchers underlined that the medial motor system is essential for volitional motor actions. In their study, they linked especially the pre-supplementary motor area to the signs of anarchic limb syndrome. Another case report of a patient with an ischemic lesion within the right cingulate motor area showed that this leads to anarchic limb-like involuntary movements of the left arm (Brázdíl, Kuba, & Rektor, 2006). This provides a further hint that the cingulate cortex is involved in goal-directed motor behavior, their preparation as well as execution of those action programs.

4.3. Machine learning identifies corticobasal syndrome patients with and without alien/anarchic limb syndrome

The support vector machine analysis was able to distinguish between CBS and controls as well as CBS patients with and without AL, on a single-subject level. Remarkably, multivariate pattern recognition demonstrated much higher predictive power than the univariate group comparison (CBS-AL vs. CBS-O), which did not reveal any significant effects. Although, the putative atrophy in CBS/CBS-AL might be the main contributor to correct classification (if one compares Figs. 1 and 2). This suggests that support vector machine analysis might be applied in the future to support individual diagnosis and perhaps syndrome prediction. This discrepancy might be related to mathematics of the analyses. In voxel-based morphometry univariate relationships are detected voxel-wise across all participants. In support vector machine analysis, multivariate relationships are identified over the whole brain. A previous support vector machine analysis showed that progressive supranuclear palsy, another atypical parkinsonian syndrome, can be distinguished from controls achieving accuracies above 80% (Mueller et al., 2017).

4.4. Study's limitations

Our study identified consistent atrophy and enabled individual classification in CBS with and without AL, but there are also limitations. As our sample is not completely histopathologically validated one cannot draw conclusions concerning the pathology of CBS. It is possible that not all patients had underlying corticobasal degeneration (Armstrong et al., 2013). Our sample of AL patients is also rather small, thus the exploratory analyses to disentangle the neural correlates of AL subtypes should be interpreted with caution. However, as CBS and AL are regarded as orphan diseases, our multi-centric design allowed a reasonable number. Possible biases introduced by the multi-centric approach, including different scanner types/protocols, were minimized by applying strict standard operating procedures and including only 3T MRI. We

did not investigate white matter alterations in CBS patients, thus we cannot account for callosal lesions, which may have led to AL too.

5. Conclusion

This study presents the first MRI-based group analysis of alien and anarchic limb syndrome in CBS. Results may pave the way for individual clinical syndrome prediction, while allowing a better understanding of the underlying brain substrates and neurocognitive architecture.

Author contributions

Franziska Albrecht, study concept and design, analysis and interpretation of data, writing of manuscript.

Matthias L. Schroeter, study concept and design, data acquisition, analysis and interpretation of data, critical revision of manuscript, study supervision.

Karsten Mueller, Tommaso Ballarini, Leonie Lampe, Robert Jech, interpretation of data, critical revision of manuscript.

Adrian Danek, Janine Diehl-Schmid, Jan Kassubek, Bernhard Landwehrmeyer, Albert C. Ludolph, Markus Otto, study design, data acquisition, critical revision of manuscript.

Klaus Fassbender, Klaus Fliessbach, Holger Jahn, Johannes Kornhuber, Martin Lauer, Epameinondas Lyros, Johannes Prudlo, Anja Schneider, Matthias Synofzik, Jens Wiltfang, data acquisition, critical revision of manuscript.

Author disclosures

Franziska Albrecht, Tommaso Ballarini, Adrian Danek, Janine Diehl-Schmid, Klaus Fassbender, Klaus Fliessbach, Holger Jahn, Jan Kassubek, Johannes Kornhuber, Leonie Lampe, Bernhard Landwehrmeyer, Albert C. Ludolph, Martin Lauer, Epameinondas Lyros, Johannes Prudlo, Markus Otto, Karsten Mueller, Anja Schneider, Matthias L. Schroeter, Jens Wiltfang – Report no disclosures relevant to the manuscript.

Matthias Synofzik - Received consulting honoraria from Actelion Pharmaceuticals, unrelated to this study.

Robert Jech – Consultant to Ipsen, Cardion; Advisory Board of Ipsen.

Study funding

This study has been supported by the German Federal Ministry of Education and Research (BMBF) by a grant given to the German FTLD Consortium [grant number FKZ O1G1007A], by the Parkinson's Disease Foundation [grant number PDF-IRG-1307], by the Michael Fox Foundation [grant number 11362], by the German Research Foundation (DFG, SCHR 774/5-1), by the Else Kröner-Fresenius-Stiftung, by the International Max Planck Research School on Neuroscience of Communication: Function, Structure, and Plasticity (IMPRS NeuroCom) by the Max Planck Society, and by the Czech Science Foundation GACR [grant number 16-13323S].

Acknowledgments

The authors thank all patients for participating in this study. We would like to thank Joshua Grant for proofreading and editing the manuscript for non-intellectual content.

Co-investigators

FTLD-Consortium: Sarah Anderl-Straub (Ulm), Katharina Brügggen (Rostock), Marie Fischer (Erlangen), Hans Förstl (TU Muenchen), Anke Hammer (Erlangen), György Homola (Würzburg), Walter Just (Ulm), Johannes Levin (LMU München), Nicolai Marroquin (Ulm), Anke Marschhauser (Leipzig), Magdalena Nagl (Ulm), Timo Oberstein (Erlangen), Maryna Polyakova (Leipzig), Hannah Pellkofer (Göttingen), Tanja Richter-Schmidinger (Erlangen), Carola Rossmeier (TU München), Katharina Schuemberg (Leipzig), Elisa Semler (Ulm), Annika Spottke (Bonn), Petra Steinacker (Ulm), Angelika Thöne-Otto (Leipzig), Ingo Uttner (Ulm), and Heike Zech (Göttingen).

Supplementary data

Supplementary data to this article can be found online at <https://doi.org/10.1016/j.cortex.2019.02.015>.

REFERENCES

- Albrecht, F., Bisenius, S., Morales Schaack, R., Neumann, J., & Schroeter, M. L. (2017). Disentangling the neural correlates of corticobasal syndrome and corticobasal degeneration with systematic and quantitative ALE meta-analyses. *NPJ Parkinson's Disease*, 3(1), 12. <https://doi.org/10.1038/s41531-017-0012-6>.
- Armstrong, M. J., Litvan, I., Lang, A. E., Bak, T. H., Bhatia, K. P., Borroni, B., & Weiner, W. J. (2013). Criteria for the diagnosis of corticobasal degeneration. *Neurology*, 80(5), 496–503. <https://doi.org/10.1212/WNL.0b013e31827f0fd1>.
- Bartolo, M., Zucchella, C., Pichiecchio, A., Pucci, E., Sandrini, G., & Sinforiani, E. (2011). Alien hand syndrome in left posterior stroke [journal article] *Neurological Sciences*, 32(3), 483–486. <https://doi.org/10.1007/s10072-011-0490-y>.
- Bisenius, S., Mueller, K., Diehl-Schmid, J., Fassbender, K., Grimmer, T., Jessen, F., & group, F. T. s. (2017). Predicting primary progressive aphasia with support vector machine approaches in structural MRI data. *Neuroimage Clinical*, 14, 334–343. <https://doi.org/10.1016/j.nicl.2017.02.003>.
- Brázdil, M., Kuba, R., & Rektor, I. (2006). Rostral cingulate motor area and paroxysmal alien hand syndrome. *Journal of Neurology, Neurosurgery & Psychiatry*, 77(8), 992–993. <https://doi.org/10.1136/jnnp.2005.082529>.
- Brion, S. (1972). Troubles du transfert interhémisphérique. A propos de trois observations de tumeurs du corps calleux. Le signe de la main étrangère. *Revista de Neurologia*, 126, 257–266.
- Brügger, F., Galovic, M., Weder, B. J., & Kägi, G. (2015). Supplementary Motor complex and disturbed motor control – a retrospective clinical and lesion analysis of patients after anterior cerebral artery stroke. [original research]. *Frontiers in Neurology*, 6(209). <https://doi.org/10.3389/fneur.2015.00209>.

- Chang, C.-C., & Lin, C.-J. (2011). LIBSVM: a library for support vector machines. *ACM Transactions on Intelligent Systems and Technology (TIST)*, 2(3), 27.
- Della Sala, S., Marchetti, C., & Spinnler, H. (1991). Right-sided anarchic (alien) hand: a longitudinal study. *Neuropsychologia*, 29(11), 1113–1127.
- Frith, C. D., Blakemore, S.-J., & Wolpert, D. M. (2000). Abnormalities in the awareness and control of action. *Philosophical Transactions of the Royal Society of London. Series B: Biological Sciences*, 355(1404), 1771–1788. <https://doi.org/10.1098/rstb.2000.0734>.
- Goldberg, G., Mayer, N. H., & Togliola, J. U. (1981). Medial frontal cortex infarction and the alien hand sign. *Archives of Neurology*, 38(11), 683–686.
- Graff-Radford, J., Rubin, M. N., Jones, D. T., Aksamit, A. J., Ahlskog, J. E., Knopman, D. S., & Josephs, K. A. (2013). The alien limb phenomenon. *Journal of Neurology*, 260(7), 1880–1888. <https://doi.org/10.1007/s00415-013-6898-y>.
- Hassan, A., & Josephs, K. A. (2016). Alien hand syndrome. *Current Neurology and Neuroscience Reports*, 16(8), 73. <https://doi.org/10.1007/s11910-016-0676-z>.
- Lancaster, J. (1997). The Talairach Daemon, a database server for Talairach atlas labels. *Neuroimage*, 5, S633.
- Lee, S. E., Rabinovici, G. D., Mayo, M. C., Wilson, S. M., Seeley, W. W., DeArmond, S. J., & Miller, B. L. (2011). Clinicopathological correlations in corticobasal degeneration. *Annals of Neurology*, 70(2), 327–340. <https://doi.org/10.1002/ana.22424>.
- Marchetti, C., & Della Sala, S. (1998). Disentangling the alien and anarchic hand. *Cognitive Neuropsychiatry*, 3(3), 191–207. <https://doi.org/10.1080/135468098396143>.
- McBride, J., Sumner, P., Jackson, S. R., Bajaj, N., & Husain, M. (2013). Exaggerated object affordance and absent automatic inhibition in alien hand syndrome. *Cortex*, 49(8), 2040–2054. <https://doi.org/10.1016/j.cortex.2013.01.004>.
- Meyer, S., Mueller, K., Stuke, K., Bisenius, S., Diehl-Schmid, J., Jessen, F., & Group, F. T. S. (2017). Predicting behavioral variant frontotemporal dementia with pattern classification in multi-center structural MRI data. *Neuroimage Clinical*, 14, 656–662. <https://doi.org/10.1016/j.nicl.2017.02.001>.
- Mueller, K., Jech, R., Bonnet, C., Tintera, J., Hanuska, J., Moller, H. E., & Group, F. T. S. (2017). Disease-specific regions outperform whole-brain approaches in identifying progressive supranuclear palsy: A multicentric MRI study. *Front Neurosci*, 11, 100. <https://doi.org/10.3389/fnins.2017.00100>.
- Otto, M., Ludolph, A. C., Landwehrmeyer, B., Förstl, H., Diehl-Schmid, J., Neumann, M., & Danek, A. (2011). Konsortium zur Erforschung der frontotemporalen Lobärdegeneration [journal article] *Der Nervenarzt*, 82(8), 1002. <https://doi.org/10.1007/s00115-011-3261-3>.
- Paus, T. (2001). Primate anterior cingulate cortex: where motor control, drive and cognition interface. *Nature Reviews Neuroscience*, 2(6), 417.
- Sarva, H., Deik, A., & Severt, W. L. (2014). Pathophysiology and treatment of alien hand syndrome. *Tremor Other Hyperkinet Movements (New York, N.Y.)*, 4, 241. <https://doi.org/10.7916/D8VX0F48>.
- Schaefer, M., Heinze, H. J., & Galazky, I. (2013). Waking up the alien hand: rubber hand illusion interacts with alien hand syndrome. *Neurocase*, 19(4), 371–376. <https://doi.org/10.1080/13554794.2012.667132>.
- Sumner, P., & Husain, M. (2008). At the edge of consciousness: Automatic motor activation and voluntary control. *Neuroscientist*, 14(5), 474–486. <https://doi.org/10.1177/1073858408314435>.
- Sumner, P., Nachev, P., Morris, P., Peters, A. M., Jackson, S. R., Kennard, C., et al. (2007). Human medial frontal cortex mediates unconscious inhibition of voluntary action. *Neuron*, 54(5), 697–711. <https://doi.org/10.1016/j.neuron.2007.05.016>.
- Synofzik, M., Vosgerau, G., & Newen, A. (2008). I move, therefore I am: a new theoretical framework to investigate agency and ownership. *Consciousness and Cognition*, 17(2), 411–424. <https://doi.org/10.1016/j.concog.2008.03.008>.
- Talairach, J., Bancaud, J., Geier, S., Bordas-Ferrer, M., Bonis, A., Szikla, G., et al. (1973). The cingulate gyrus and human behaviour. *Electroencephalography and Clinical Neurophysiology*, 34(1), 45–52. [https://doi.org/10.1016/0013-4694\(73\)90149-1](https://doi.org/10.1016/0013-4694(73)90149-1).
- Tsakiris, M., Longo, M. R., & Haggard, P. (2010). Having a body versus moving your body: neural signatures of agency and body-ownership. *Neuropsychologia*, 48(9), 2740–2749.
- Whitwell, J. L., Jack, C. R., Jr., Boeve, B. F., Parisi, J. E., Ahlskog, J. E., Drubach, D. A., & Josephs, K. A. (2010). Imaging correlates of pathology in corticobasal syndrome. *Neurology*, 75(21), 1879–1887. <https://doi.org/10.1212/WNL.0b013e3181feb2e8>.

6 STUDY 4

Regional gray matter changes and age predict individual treatment response in Parkinson's disease



Contents lists available at ScienceDirect

NeuroImage: Clinical

journal homepage: www.elsevier.com/locate/ynicl

Regional gray matter changes and age predict individual treatment response in Parkinson's disease



Tommaso Ballarini^a, Karsten Mueller^a, Franziska Albrecht^a, Filip Růžička^{b,d}, Ondrej Bezdicek^b, Evžen Růžička^b, Jan Roth^b, Josef Vymazal^d, Robert Jech^{b,d,1}, Matthias L. Schroeter^{a,c,e,*}

^a Max-Planck Institute for Human Cognitive and Brain Sciences, Leipzig, Germany

^b Department of Neurology, Charles University, First Faculty of Medicine, Prague, Czech Republic

^c Clinic for Cognitive Neurology, University Clinic, Leipzig, Germany

^d Department of Radiology, Na Homolce Hospital, Prague, Czech Republic

^e FTL D Consortium, Germany

ARTICLE INFO

Keywords:

Parkinson's disease
Dopaminergic therapy
Voxel-based morphometry
Support vector machine classification
Predictive models

ABSTRACT

We aimed at testing the potential of biomarkers in predicting individual patient response to dopaminergic therapy for Parkinson's disease. Treatment efficacy was assessed in 30 Parkinson's disease patients as motor symptoms improvement from unmedicated to medicated state as assessed by the Unified Parkinson's Disease Rating Scale score III. Patients were stratified into weak and strong responders according to the individual treatment response. A multiple regression was implemented to test the prediction accuracy of age, disease duration and treatment dose and length. Univariate voxel-based morphometry was applied to investigate differences between the two groups on age-corrected T1-weighted magnetic resonance images. Multivariate support vector machine classification was used to predict individual treatment response based on neuroimaging data. Among clinical data, increasing age predicted a weaker treatment response. Additionally, weak responders presented greater brain atrophy in the left temporoparietal operculum. Support vector machine classification revealed that gray matter density in this brain region, including additionally the supplementary and primary motor areas and the cerebellum, was able to differentiate weak and strong responders with 74% accuracy. Remarkably, age and regional gray matter density of the left temporoparietal operculum predicted both and independently treatment response as shown in a combined regression analysis. In conclusion, both increasing age and reduced gray matter density are valid and independent predictors of dopaminergic therapy response in Parkinson's disease.

1. Introduction

Dopaminergic therapy (DT) has been the foundation of Parkinson's disease therapy for decades. DT is based on two main pharmacological compounds: levodopa (L-3,4-dihydroxyphenylalanine) and dopamine receptor agonists. Despite its extensive application in clinical practice, DT efficacy is influenced by several factors. For example, DT response deteriorates after years of treatment, becoming more intermittent and leading to severe motor and non-motor complications (Connolly and Lang, 2014). Notably, a high individual variability in treatment response is a common finding in clinical practice and it has been often reported in the literature (Constantinescu et al., 2007). In particular, two studies investigated levodopa responsiveness in large series of

autopsy-proven Parkinson's disease cases, showing a suboptimal treatment response in several patients (Hughes et al., 1993; Wenning et al., 2000). However, the sources of heterogeneous DT responses across subjects are still unclear. The aim of the study is to shed light on the potential of clinical and neuroimaging data in predicting clinical response to DT in Parkinson's disease.

2. Materials and methods

2.1. Participants

Thirty patients with Parkinson's disease participated in the study (Hughes et al., 1992) (age = 65.37 ± 7.05 years mean \pm SD; Hoehn&

* Corresponding author at: Max Planck Institute for Human Cognitive and Brain Sciences, Stephanstr. 1A, Clinic for Cognitive Neurology, University Hospital Leipzig, Liebigstr. 16, 04103 Leipzig, Germany.

E-mail address: schroet@cbs.mpg.de (M.L. Schroeter).

¹ These authors contributed equally to the manuscript.

<https://doi.org/10.1016/j.nicl.2018.101636>

Received 14 May 2018; Received in revised form 30 August 2018; Accepted 9 December 2018

Available online 10 December 2018

2213-1582/ © 2018 The Authors. Published by Elsevier Inc. This is an open access article under the CC BY-NC-ND license (<http://creativecommons.org/licenses/by-nc-nd/4.0/>).

Yahr stages I-III; 13 females, disease onset after 45 years of age). Stable DT comprised levodopa either in monotherapy ($N = 5$) or combined with dopamine agonists (pramipexole and ropinirole, respectively $N = 8$ and $N = 17$). Differences in treatment response across DT types were tested with a one-way ANOVA. The assessment of motor symptoms, implemented with the Unified Parkinson's Disease Rating Scale (UPDRS) score III, was performed during medicated (DT-on) and unmedicated states (DT-off) in a randomized order (DT-on first in 16 and DT-off first in 14 patients). For DT-off state, dopamine agonists and levodopa were withdrawn, respectively, at least 72 and 12 h before examination. We considered the difference between the UPDRS-III scores in DT-on and DT-off conditions (i.e. *UPDRS-III-change*) as a proxy for treatment efficacy. The study was authorized by the Ethics Committee of the General University Hospital in Prague, Czech Republic, in line with the Declaration of Helsinki.

2.2. Clinical variables

Correlations between *UPDRS-III-change* and, in turn, age, disease duration, levodopa treatment duration and levodopa equivalent dose were assessed. Note that, for each pair, Pearson's partial correlations ($\alpha = 0.05$) were computed controlling for the remaining variables. Additionally, multivariate regression (enter mode) was conducted including these variables and setting *UPDRS-III-change* as dependent factor.

For MRI analyses, patients were stratified into weak and strong responders, using as cut-off the median *UPDRS-III-change* in our sample (15.50 points). Table 1 displays demographic and clinical characteristics of the groups, and their statistical comparison. Notably, age was significantly higher in the weak responders. Hence, age differences were controlled for in these and the following dichotomous analyses. In addition, to define the clinical significance of the treatment-induced UPDRS-III changes, we compared our results with the cut-off values provided by Shulman et al. (2010) defining minimal, moderate and large clinically important differences (i.e. differences that can be appreciated by the patients themselves). Accordingly, the majority of the patients ($n = 24$) reported large differences, five intermediate and only one minimal. At clinical evaluation, most patients presented with both akinesia/rigidity involvement and tremor. PD phenotypes were further defined according to Jankovic's classification to allow a better comparison with other studies (Jankovic et al., 1990). Three outcomes are possible here: postural instability and gait difficulty (PIGD), tremor dominant (TD) and intermediate. Namely, a ratio score, computed based on the UPDRS-III items in the DT-off state, was used for the

classification: ratio = mean(TD items)/mean(PIGD items). For a list of the items used for computing the mean values for TD and PIGD refer to Table 1 in Stebbins et al. (2013). In our PD cohort, 22 patients had predominant PIGD, 5 TD and 3 intermediate phenotypes. Differences in the distribution of the clinical phenotypes between strong and weak responders were assessed by means of chi-squared test.

2.3. Neuroimaging analysis

T1-weighted MR images (3D-MPRAGE, Magnetization Prepared Rapid Gradient Echo, TR 2.2 s, TE:2.43 ms, inversion time 900 ms, flip angle 8°, matrix 224×224) were acquired on a 3 T MAGNETOM Skyra (Siemens, Erlangen, Germany) at the Radiology Department, Na Homolce Hospital in Prague.

Images were preprocessed with the Computational Anatomy Toolbox (CAT-12). After spatial normalization, gray matter compartment was isolated and 8 mm smoothing was applied. Then, to take into account the effect of age, an age-correction procedure was applied based on data from 30 elderly healthy controls (age = 63.57 ± 8.09 years; 15 females) as previously described (Dukart et al., 2011). Thus, imaging data were normalized for age before all subsequent structural analyses. The efficacy of the procedure was further tested performing a whole-brain correlation analysis between age and gray matter density (GMD) before and after age correction and comparing the z-maps of the two analyses. Individual gray and white matter volumes were entered in the models as covariates.

2.3.1. Univariate analysis

Voxel-based morphometry (Ashburner and Friston, 2000) was run in CAT-12 and SPM (rev.12.6685). Age-corrected GMD images entered a univariate statistical model to compare GMD between weak and strong responders using gray and white matter volumes as covariates. Only clusters surviving $p < .05$ family-wise error (FWE) correction were deemed significant (uncorrected threshold, $p < .005$).

2.3.2. Multivariate analysis

Support vector machine (SVM) classification was applied on age-corrected GMD images using libsvm (release 3.18) in Matlab. This machine learning approach based on multivariate pattern analysis allows testing the prediction accuracy of GMD images for the classification of weak and strong DT responders. The classifier was based on a polynomial kernel and was validated using a leave-one-out cross-validation procedure. Different gray matter probability masks were tested to assure the stability of results. The relative weights, indicating the

Table 1
Demographic and clinical characteristics of Parkinson's disease patients stratified according to dopaminergic treatment response.

	Total	Weak responders	Strong responders	F (df)	p
N	30	15	15	-	-
Age (years)	65.37 \pm 7.05	68.27 \pm 7.56	62.47 \pm 5.28	5.93 (28)	0.021*
Gender (male/female)	17/13	8/7	9/6	-	$\chi^2 = 0.14, p = .71$
Education (years)	14.1 \pm 2.95	13.4 \pm 2.82	14.8 \pm 3	1.10 (27)	0.34
Disease duration (years)	11.4 \pm 3.43	10.87 \pm 3.81	11.93 \pm 3.03	0.78 (27)	0.386
Levodopa duration (years)	8.529 \pm 4.055	8.64 \pm 4.2	8.42 \pm 4.05	0.86 (27)	0.363
Levodopa equivalent dose (mg)	1385.98 \pm 664.75	1155.65 \pm 680.28	1600.97 \pm 582.85	1.84 (27)	0.186
UPDRS-III DT-off	31.03 \pm 10.31	28.27 \pm 10.05	33.80 \pm 10.13	1.48 (27)	0.235
UPDRS-III DT-on	14.77 \pm 7.58	17.20 \pm 8.12	12.33 \pm 6.37	1.73 (27)	0.199
UPDRS-III-change	16.27 \pm 7.06	11.07 \pm 3.73	21.47 \pm 5.59	23.93 (27)	< 0.0001**
UPDRS-IV	4.60 \pm 3.65	3.33 \pm 3.0	5.87 \pm 3.871	2.61 (27)	0.118
NMSS total score	15.10 \pm 19.18	13.53 \pm 20.79	16.67 \pm 18.015	0.50 (27)	0.485
MoCA	25.77 \pm 2.34	25.53 \pm 2.47	26.00 \pm 2.27	0.073 (27)	0.789

Note: Mean \pm SD are shown.

Abbreviations: DT -on medicated state; DT-off unmedicated state; NMSS non-motor symptoms scale; MoCA Montreal Cognitive Assessment; UPDRS Unified Parkinson's Disease Rating Scale (-III motor symptoms; -IV motor complications).

* Significant p-value from ANOVA analysis.

** Significant p-value from ANCOVA analysis controlling for age differences.

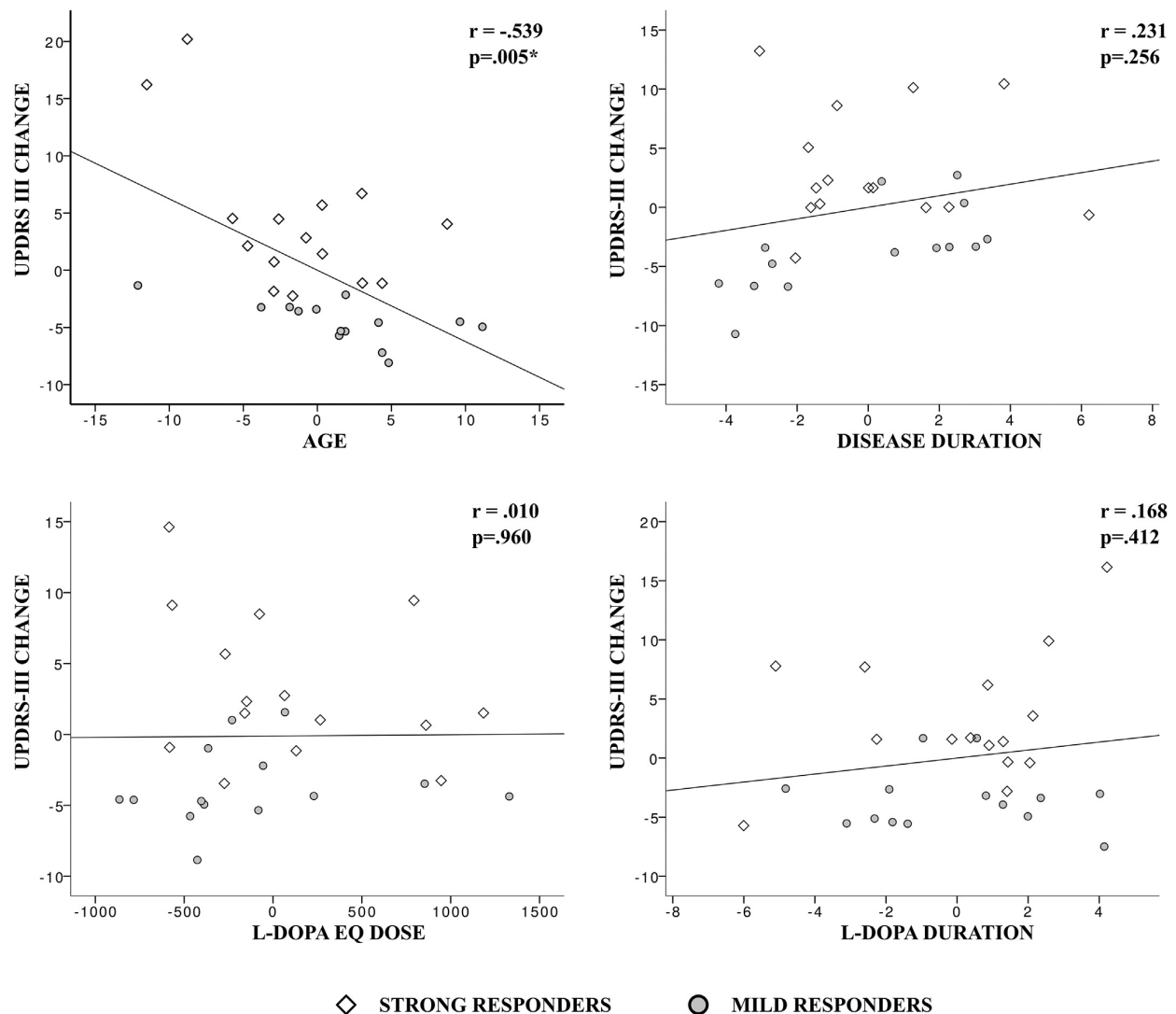


Fig. 1. Partial correlations between clinical variables and *UPDRS-III-change* as proxy for treatment efficacy. Age is the only variable showing a statistically significant negative correlation (i.e. increasing age was associated with weaker treatment response). Pearson correlation coefficients (r) and p -values are displayed. Note that, for each correlation, x and y axes represent the two sets of unstandardized residuals from regressing the variables of interest on the confounding variables. Strong and weak responders, as selected for the neuroimaging analysis, are presented with different symbols.

contribution to the classification of each voxel, were then plotted in the original 3D brain space.

2.4. Disentangling impact of age and imaging parameters on treatment

To disentangle the influence of age and gray matter changes, the SVM model was run on the patients' images also before the age correction procedure. The rationale is that differences in SVM accuracy between pre and post age correction procedure would be attributable to the detrimental aging effect on GMD.

Moreover, to further address the influence of clinical and imaging data on the treatment response, a multivariate linear regression model was run including as predictors age, levodopa dose/duration, disease duration and the average GMD values from the consistent (i.e. overlapping) cluster from the univariate and multivariate analyses, centered on the $x\ y\ z$ MNI coordinates $-33\ -32\ 18$ (represented in orange in Fig. 3).

3. Results

3.1. Clinical variables

The distribution of clinical phenotypes (PIGD, TD and intermediate) was comparable between strong and weak responders ($\chi^2 = 0.715$, $p = .699$). No difference in treatment response was found between different DT types (one-way ANOVA: $F(29) = 0.33$, $p = .723$).

A significant correlation was found between *UPDRS-III-change* and age ($r = -0.539$, $p < .005$). All the other tested correlations did not provide significant results: disease duration ($r = 0.231$, $p < .256$), levodopa treatment duration ($r = 0.168$, $p < .412$) and levodopa equivalent dose ($r = 0.01$, $p < .96$) (Fig. 1).

A multivariate regression model was applied to predict treatment efficacy from age, disease duration, levodopa equivalent dose and levodopa duration. The overall model was significant, $F(4,24) = 4.408$, $p < .008$, with an r^2 of 0.424. However, age was the only significant

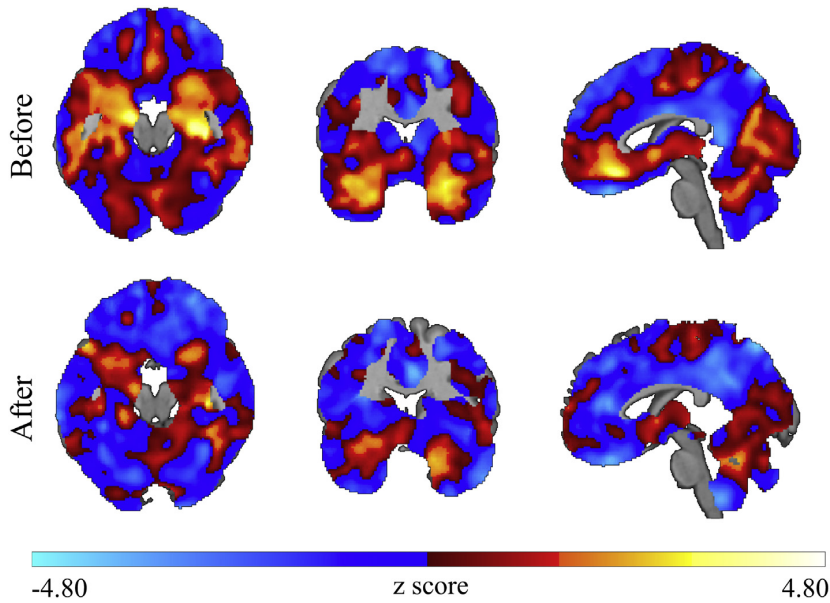


Fig. 2. Efficacy of the age correction procedure following Dukart et al. (2011). Z-maps showing the results of correlation analyses in the patient cohort between age and gray matter density maps before (upper row) and after (bottom row) the applied age-correction procedure. The pattern of negative correlations between age and gray matter density, mainly seen in medial temporal and medial frontal structures, is suppressed after age correction. Images shown in neurological orientation: left of the brain corresponds to the left of the image.

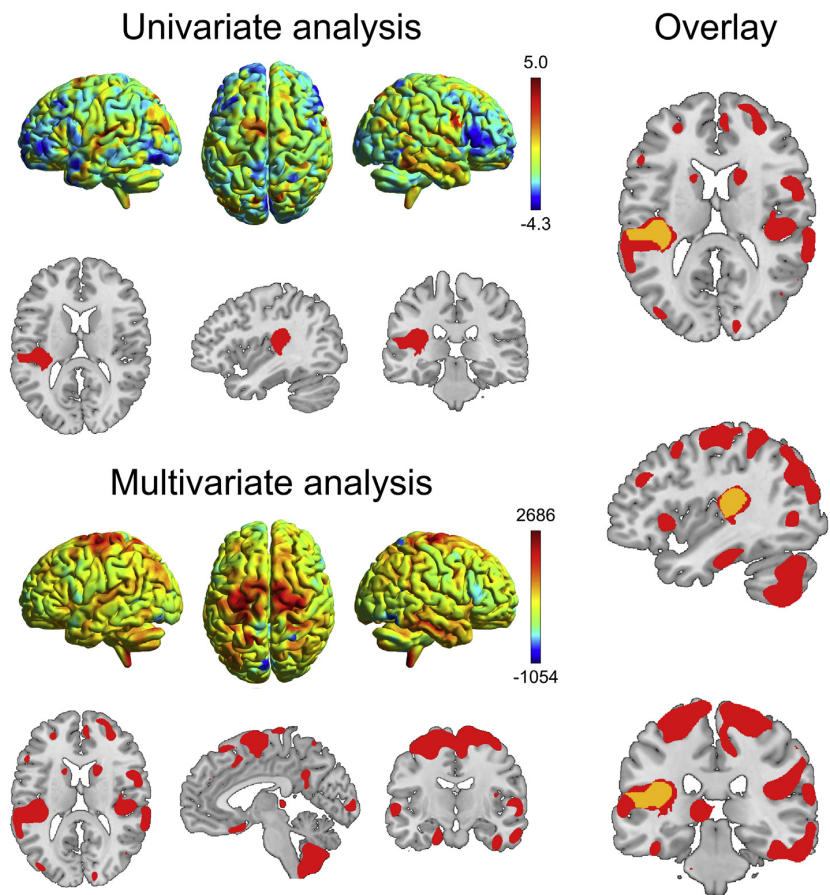


Fig. 3. Results of the univariate and multivariate analyses contrasting weak and strong responders. The 3D rendering shows, respectively, the unthresholded SPM-t map for the weak responders < strong responders univariate SPM comparison (warmer colors indicate lower gray matter density) and the voxel-wise weights obtained from the multivariate support vector machine classification (warmer colors regions contributing to weak responders' classification, arbitrary units). The slice views for the univariate analysis report in red the results surviving the cluster-level correction for multiple comparisons ($p < .05$ FWE), while for the multivariate analyses, the regions showing higher weights for the classification of the weak vs. strong responders are shown. On the right, the overlay between the two thresholded maps is shown in orange. Images shown in neurological orientation: left of the brain corresponds to the left of the image. 3D rendering plotted with BrainNet Viewer 1.61 (<https://www.nitrc.org/projects/bnv/>).

Table 2

Support vector machine (SVM) classification results (weak vs. strong responders) using different gray matter probability masks. Lower gray matter thresholds correspond to more inclusive masks.

Gray matter threshold	Accuracy in weak responders (%)	Accuracy in strong responders (%)	Total accuracy (%)	PPV	NPV
0.01	77.33	70.67	74.00	0.725	0.757
0.1	78.67	70.67	74.67	0.728	0.768
0.2	78.22	70.67	74.44	0.727	0.764
0.3	76.00	72.44	74.22	0.734	0.751
0.4	64.44	73.33	68.89	0.707	0.673
0.5	62.22	73.33	67.78	0.700	0.660

Note: NPV negative predictive value; PPV positive predictive value.

predictor in the model ($p = .005$). Namely, *UPDRS-III-change* decreased of -0.604 points for each additional year of age.

3.2. Neuroimaging analysis

The correlation analysis between age and GMD before the age-correction procedure shows a pattern of negative correlations mainly in medial temporal and medial frontal structures, as expected from a consistent body of literature (Giorgio et al., 2010; Tisserand et al., 2004). After the age correction, this prototypical correlation pattern was mostly suppressed as shown in Fig. 2.

3.2.1. Univariate analysis

Significant lower GMD was found in weak compared to strong responders in the left temporoparietal operculum after age correction (Fig. 3). Observing the unthresholded t-map for the weak < strong responders comparison, a trend towards lower GMD was detected in the right temporoparietal operculum, in supplementary motor area, superior frontal gyrus and cerebellum. The opposite contrast did not reveal significant findings.

3.2.2. Multivariate analysis

The SVM approach, based on whole brain data after age correction, was able to correctly classify 77.33% weak responders and 70.67% strong responders, thus with a total accuracy of 74.0%. Positive and negative predictive values were, respectively, 0.725 and 0.757 (Table 2). The regions that mostly contributed to the classification of weak responders included the supplementary motor and primary motor areas, superior frontal gyrus, the bilateral parietal opercula, and extensively the cerebellum (Fig. 3).

3.3. Disentangling impact of clinical and imaging parameters on treatment

The SVM model applied to the patients' images before the age correction procedure showed a total accuracy of 75.77%, correctly classifying 78.22% weak and 73.33% strong responders. An additional multivariate regression model was calculated to predict treatment efficacy from age and GMD in the left temporoparietal operculum to disentangle the contributions of both relevant factors. This analysis revealed significant effects, $F(5,23) = 6.56$, $p < .001$, with an increased r^2 of 0.588. Significant predictors in the model were both age (standardized $\beta = -0.496$; $p = .009$) and GMD in the left temporoparietal operculum (standardized $\beta = 0.456$; $p = .006$).

4. Discussion

The present findings represent an initial insight into clinical and neuroimaging features that can predict individual DT response in Parkinson's disease. We showed that both increasing age and lower GMD predict a weaker DT response. Of note, weak and strong DT

responders were similarly impaired in the DT-off state, suggesting that treatment response does not depend on motor symptom severity. The relationship between aging and Parkinson's disease has been subject of previous investigations (Levy, 2007). Levy (2007) reported that age, more than disease duration, is associated with a more severe clinical progression. In addition, a previous study showed a negative association between age and the magnitude of DT response in Parkinson's disease (Durso et al., 1993). Taken together, these pieces of evidence are in line with our finding of a poorer treatment response in older Parkinson's disease patients.

Concerning neuroimaging results, structural between-group differences were identified with univariate and multivariate analyses after applying a stringent age-correction procedure. A good agreement was found between the two analytical approaches as exemplified in Fig. 3. Indeed, both revealed pronounced regional gray matter alterations in weak DT responders in the left temporoparietal operculum, compared to strong responders. The parietal operculum is a complex brain structure where different sensorimotor processes take place and, interestingly, it has been previously associated with sensorimotor recovery after moderate to severe strokes within the territory of the internal carotid artery (Hannanu et al., 2017). In addition, the SVM analysis showed also the involvement of the supplementary motor area, primary motor cortex and cerebellum in defining the weak responder group, all crucial regions in the motor pathway. In particular, an impaired activity of the supplementary motor area in Parkinson's disease has been previously associated with motor impairment and, accordingly, attempts to restore its function via transcranial magnetic stimulation showed modest but significant symptoms improvement (Hamada et al., 2008). It is thus reasonable that patients with more severe structural impairment in this area, as suggested by the univariate unthresholded results, present a weaker treatment response.

As for the relationship between age and GMD alterations, the linear regression model including both as predictors of *UPDRS-III change* explained 59% of the variance, as compared to the 42% of the model without imaging metrics. The comparison of standardized beta coefficients showed a similar effect of aging and GMD alterations in predicting the treatment response. This suggests that age and GMD are both significantly and independently contributing to the prediction of treatment response in PD. Additionally, in order to test the modulatory impact of age on GMD-based predictions, the SVM classification was run on the imaging data before and after applying the age correction procedure. This analysis revealed that the performance of the classifier was only minimally improved when images were uncorrected for age differences (overall accuracy pre and post age correction were respectively 75.77% and 74.0%). This again suggests a modest modulatory effect of age on the GMD-based classification, thus indicating that age and GMD are mostly independent predictors of DT treatment response in PD. Consequently, further research would be needed for the identification of mediators of the aging effect on treatment response. For example, it has been proposed that aging might influence neurodegeneration (and possibly treatment response) through the complex interaction between iron and neuromelanine accumulation and loss of dopamine neurons (Zucca et al., 2017).

In conclusion, we provide a new perspective into the issue of heterogeneous individual treatment response in Parkinson's disease. The implementation of SVM classification provides a new approach to the topic and might pave the way to further investigations including larger Parkinson's disease cohorts, atypical parkinsonian syndromes and different neuroimaging data.

Acknowledgement

This work was supported by the Czech Science Foundation (grant number GACR 16-13323S), by the Charles University, Czech Republic (Progres Q27/LF1), by the German Federal Ministry of Education, and Research (BMBF) by a grant given to the German FTLD Consortium

(FKZ O1GI1007A), by the German Research Foundation (DFG, SCHR 774/5-1), by the Parkinson's Disease Foundation (PDF-IRG-1307) and by the Michael J. Fox Foundation (MJFF-11362).

References

- Ashburner, J., Friston, K.J., 2000. Voxel-based morphometry—the methods. *NeuroImage* 11, 805–821.
- Connolly, B.S., Lang, A.E., 2014. Pharmacological treatment of Parkinson disease: a review. *JAMA* 311, 1670–1683.
- Constantinescu, R., Richard, I., Kurlan, R., 2007. Levodopa responsiveness in disorders with parkinsonism: a review of the literature. *Mov. Disord.* 22, 2141–2148 (quiz 2295).
- Dukart, J., Schroeter, M.L., Mueller, K., Alzheimer's Disease Neuroimaging, I., 2011. Age correction in dementia—matching to a healthy brain. *PLoS One* 6, e22193.
- Durso, R., Isaac, K., Perry, L., Saint-Hilaire, M., Feldman, R.G., 1993. Age influences magnitude but not duration of response to levodopa. *J. Neurol. Neurosurg. Psychiatry* 56, 65–68.
- Giorgio, A., Santelli, L., Tomassini, V., Bosnell, R., Smith, S., De Stefano, N., Johansen-Berg, H., 2010. Age-related changes in grey and white matter structure throughout adulthood. *NeuroImage* 51, 943–951.
- Hamada, M., Ugawa, Y., Tsuji, S., Effectiveness of rTms on Parkinson's Disease Study Group, J., 2008. High-frequency rTMS over the supplementary motor area for treatment of Parkinson's disease. *Mov. Disord.* 23, 1524–1531.
- Hannanu, F.F., Zeffiro, T.A., Lamalle, L., Heck, O., Renard, F., Thuriot, A., Krainik, A., Hommel, M., Detante, O., Jaillard, A., Group, I.-H.S., 2017. Parietal operculum and motor cortex activities predict motor recovery in moderate to severe stroke. *Neuroimage Clin.* 14, 518–529.
- Hughes, A.J., Daniel, S.E., Kilford, L., Lees, A.J., 1992. Accuracy of clinical diagnosis of idiopathic Parkinson's disease: a clinico-pathological study of 100 cases. *J. Neurol. Neurosurg. Psychiatry* 55, 181.
- Hughes, A.J., Daniel, S.E., Blankson, S., Lees, A.J., 1993. A clinicopathologic study of 100 cases of Parkinson's disease. *Arch. Neurol.* 50, 140–148.
- Jankovic, J., McDermott, M., Carter, J., Gauthier, S., Goetz, C., Golbe, L., Huber, S., Koller, W., Olanow, C., Shoulson, I., 1990. Variable expression of Parkinson's disease a base-line analysis of the DAT ATOP cohort. *Neurology* 40, 1529.
- Levy, G., 2007. The relationship of Parkinson disease with aging. *Arch. Neurol.* 64, 1242–1246.
- Shulman, L.M., Gruber-Baldini, A.L., Anderson, K.E., Fishman, P.S., Reich, S.G., Weiner, W.J., 2010. The clinically important difference on the unified Parkinson's disease rating scale. *Arch. Neurol.* 67, 64–70.
- Stebbins, G.T., Goetz, C.G., Burn, D.J., Jankovic, J., Khoo, T.K., Tilley, B.C., 2013. How to identify tremor dominant and postural instability/gait difficulty groups with the movement disorder society unified Parkinson's disease rating scale: comparison with the unified Parkinson's disease rating scale. *Mov. Disord.* 28, 668–670.
- Tisserand, D.J., Van Boxtel, M.P., Pruessner, J.C., Hofman, P., Evans, A.C., Jolles, J., 2004. A voxel-based morphometric study to determine individual differences in gray matter density associated with age and cognitive change over time. *Cereb. Cortex* 14, 966–973.
- Wenning, G., Ben-Shlomo, Y., Hughes, A., Daniel, S., Lees, A., Quinn, N., 2000. What clinical features are most useful to distinguish definite multiple system atrophy from Parkinson's disease? *J. Neurol. Neurosurg. Psychiatry* 68, 434–440.
- Zucca, F.A., Segura-Aguilar, J., Ferrari, E., Muñoz, P., Paris, I., Sulzer, D., Sarna, T., Casella, L., Zecca, L., 2017. Interactions of iron, dopamine and neuromelanin pathways in brain aging and Parkinson's disease. *Prog. Neurobiol.* 155, 96–119.

7 STUDY 5

Memory Impairment in Parkinson's Disease: The Retrieval Versus Associative Deficit Hypothesis Revisited and Reconciled

Memory Impairment in Parkinson's Disease: The Retrieval Versus Associative Deficit Hypothesis Revisited and Reconciled

Ondrej Bezdicek
Charles University

Tommaso Ballarini
Max Planck Institute for Human Cognitive and Brain Sciences,
Leipzig, Germany

Herman Buschke
Yeshiva University

Filip Růžička and Jan Roth
Charles University

Franziska Albrecht
Max Planck Institute for Human Cognitive and Brain Sciences,
Leipzig, Germany

Evžen Růžička
Charles University

Karsten Mueller
Max Planck Institute for Human Cognitive and Brain Sciences,
Leipzig, Germany

Matthias L. Schroeter
Max Planck Institute for Human Cognitive and Brain Sciences,
Leipzig, Germany, and Clinic for Cognitive Neurology,
University Clinic, Leipzig, Germany

Robert Jech
Charles University

Objective: Our study explored the retrieval deficit and the associative deficit hypotheses of memory impairments in Parkinson's disease (PD). The former supports a memory deficit mediated by attention/executive dysfunctions, whereas the latter hypothesizes a hippocampal memory impairment in PD. **Method:** We studied 31 controls and 34 PD patients classified as PD with normal cognition (PD-NC; $n = 18$) and PD with mild cognitive impairment (PD-MCI; $n = 16$). To test the retrieval deficit hypothesis, we measured the performance in encoding, retention, and recognition in verbal and visual domains; to test the associative deficit hypothesis, we used a specific associative binding measure. Using resting-state functional-MRI, we compared the functional connectivity of different hippocampal subfields between PD patients and controls, and we related it to memory performance. **Results:** Consistently with the retrieval deficit hypothesis, PD-MCI, and PD-NC, were impaired in free recall encoding and retention in comparison to controls, especially in the visual domain. However, as predicted by the associative deficit hypothesis, PD-MCI and, to a lesser extent, PD-NC, showed also significant associative and binding deficits in cued recall. Notably, PD patients compared to controls did not show structural differences, although they had lower connectivity between the anterior hippocampi and the precuneus/superior parietal cortex. Worse performance in memory was associated with a more severe disruption of the

Ondrej Bezdicek, Department of Neurology and Centre of Clinical Neuroscience, First Faculty of Medicine and General University Hospital, Charles University; Tommaso Ballarini, Max Planck Institute for Human Cognitive and Brain Sciences, Leipzig, Germany; Herman Buschke, Albert Einstein College of Medicine, Yeshiva University; Filip Růžička and Jan Roth, Department of Neurology and Centre of Clinical Neuroscience, First Faculty of Medicine and General University Hospital, Charles University; Franziska Albrecht, Max Planck Institute for Human Cognitive and Brain Sciences; Evžen Růžička, Department of Neurology and Centre of Clinical Neuroscience, First Faculty of Medicine and General University Hospital, Charles University; Karsten Mueller, Max Planck Institute for Human Cognitive and Brain Sciences; Matthias L. Schroeter, Max Planck Institute for Human Cognitive and Brain Sciences, and Clinic for Cognitive Neurology, University Clinic, Leipzig, Germany; Robert Jech, Department of Neurology and Centre of Clinical Neuroscience, First Faculty of Medicine and General University Hospital, Charles University.

This study was supported by the Czech Science Foundation "Micro and Macro-Connectomics of the STN nucleus" grant 16-13323S; "Cognitive Predictors of Neurodegeneration", grant 16-01781S; by Charles University, PROGRES Q27; by the Parkinson's Disease Foundation (PDF-IRG-1307), the Michael J. Fox Foundation (MJFF-11362); and the German Federal Ministry of Education and Research (BMBF) by a grant given to the German FTLD Consortium (Grant FKZ O1GI1007A).

The authors have no financial interests in the Memory Binding Test Czech version and have nothing to disclose.

Correspondence concerning this article should be addressed to Ondrej Bezdicek, Department of Neurology and Centre of Clinical Neuroscience, First Faculty of Medicine and General University Hospital, Charles University, Prague, Kateřinská 30, 128 21 Praha 2, Czech Republic. E-mail: ondrej.bezdicek@gmail.com

hippocampal connectivity. **Conclusions:** The pervasive pattern of memory impairment in PD supports both hypotheses. The interplay between the hippocampus, related to associative memory deficits, and the precuneus, related to attentional control, provides a neural signature that reconciles them.

General Scientific Summary

Our study contributes significant new findings of memory disorder in patients that suffer from both Parkinson's disease and mild cognitive impairment. We tried to coherently reconcile the basic hypotheses for the interpretation of memory impairment in Parkinson's disease: the retrieval deficit and associative deficit hypotheses. Using resting-state functional-MRI, our study reveals the brain mechanisms that enable the development of memory retrieval deficit and associative memory deficit in Parkinson's disease and mild cognitive impairment.

Keywords: memory impairment, mild cognitive impairment, Parkinson's disease, resting-state functional MRI

Supplemental materials: <http://dx.doi.org/10.1037/neu0000503.supp>

Parkinson's disease (PD) is a neurodegenerative disease associated with a heightened risk of cognitive impairment (Aarsland et al., 2017; Muslimović, Post, Speelman, & Schmand, 2005; Pigott et al., 2015; Schrag, Siddiqui, Anastasiou, Weintraub, & Schott, 2017; Williams-Gray, Foltynie, Brayne, Robbins, & Barker, 2007). The underlying pathophysiological changes include compromised dopaminergic neurotransmission in nigro-striatal and fronto-striatal circuitries, and pathological accumulations of α -synuclein in Lewy bodies and β -amyloid plaques in later disease stages (Del Tredici & Braak, 2016; Petrou et al., 2015; Spillantini et al., 1997; Zgaljardic, Borod, Foldi, & Mattis, 2003). To describe and assess cognitive changes, the concept of mild cognitive impairment in PD (PD-MCI) was introduced (Geurtsen et al., 2014; Litvan et al., 2011; Litvan et al., 2012). PD-MCI is defined as a deterioration in cognitive functioning, which is more pronounced than a normal age-associated decline but does not reach the severity of a dementia syndrome (Emre et al., 2007; Litvan et al., 2012). MCI affects 24–35% of patients with PD (Broeders et al., 2013; Janvin, Larsen, Aarsland, & Hugdahl, 2006; Litvan et al., 2011; Pigott et al., 2015). Higher age, longer disease duration with higher disease severity as measured with the Unified Parkinson's disease rating scale motor score (UPDRS-III) are associated with higher probability of MCI (Hoogland et al., 2017). In turn, MCI status increases the hazard of dementia (Hoogland et al., 2017; Muslimović, Schmand, Speelman, & de Haan, 2007; Pagonabarraga & Kulisevsky, 2012; Reid, Hely, Morris, Loy, & Halliday, 2011; Williams-Gray et al., 2013).

An evolving episodic memory impairment in PD is frequent since the early stages of the disease, even though its origin is still under scrutiny and not well understood (Brønneck, Alves, Aarsland, Tysnes, & Larsen, 2011; Cohn, Moscovitch, & Davidson, 2010; Whittington, Podd, & Kan, 2000). Up to now, two main hypotheses were formulated to explain the cause of memory deficits in PD: (a) the retrieval deficit hypothesis and (b) the associative dysfunction hypothesis (Cohn, Giannoylis, De Belder, Saint-Cyr, & McAndrews, 2016; Cohn et al., 2010; Higginson, Wheelock, Carroll, & Sigvardt, 2005; Naveh-Benjamin, 2000). According to the retrieval deficit hypothesis, the typical PD memory profile is due to impaired attention and executive dysfunction that lead to derailed encoding strategies and, as a result, to deficits

in learning and retrieval of items from memory (Costa et al., 2014; Tröster & Fields, 1995; Whittington et al., 2000). This is also mirrored at the brain level by pathophysiological changes in the fronto-striatal networks that are associated with strategic aspects of memory retrieval. The learning/encoding deficit is manifested in flatter learning curves in memory tests and the retrieval deficit in the impaired free recall of single items, especially when the material is poorly organized. On the other hand, recognition memory would be relatively spared (Algarabel et al., 2010; Brønneck et al., 2011; Chiaravalloti et al., 2014; Flowers, Pearce, & Pearce, 1984; Saka & Elibol, 2009). The associative dysfunction hypothesis instead supports the presence of a hippocampal memory disorder in PD that is manifested as impaired recollection when encoding strategies (acquisition of the material) are equated across groups, limiting the load on attention and executive functions (Cohn et al., 2016; Cohn et al., 2010). Indeed, many studies have shown that PD patients perform worse than controls not only in free recall, but also in cued recall, recognition, familiarity, and semantic clustering strategy (Beatty et al., 2003; Brønneck et al., 2011; Buytenhuijs et al., 1994; Chiaravalloti et al., 2014; Edelstyn et al., 2015; Pirogovsky-Turk, Filoteo, Litvan, & Harrington, 2015; Whittington et al., 2000; Whittington, Podd, & Stewart-Williams, 2006). To isolate this specific memory deficit, learning and cued recall methods were introduced to mitigate normal age-related problems in attention, strategic aspects of encoding, and retrieval (Cohn et al., 2016; Grober & Buschke, 1987). Of note, it has been shown that the controlled learning and cued recall verbal memory techniques are especially apt for the differentiation of hippocampal and medial temporal lobe (MTL) involvement in learning and recall (Sarazin et al., 2007; Vyhalek et al., 2014; Zimmerman et al., 2008).

Concerning the neuroimaging correlates of memory deficit in PD, many studies focused on the MTL areas that are known to be implicated in memory encoding and retrieval (Kircher et al., 2008; Miller & D'Esposito, 2012), and especially in recollection (Schacter, Alpert, Savage, Rauch, & Albert, 1996). Morphological changes were documented in the entorhinal cortex, hippocampus, and surrounding MTL areas even in the early PD stages (Biundo et al., 2013; Junqué et al., 2005; Pirogovsky-Turk et al., 2015; Tanner et al., 2015). MTL atrophy in PD and PD with dementia (PD-D) is

milder than in Alzheimer's disease (Laakso et al., 1996; Tam, Burton, McKeith, Burn, & O'Brien, 2005) but correlates with memory performance (Beyer et al., 2013; Brück, Kurki, Kaasinen, Vahlberg, & Rinne, 2004; Pirogovsky-Turk et al., 2015).

Functional architecture changes as measured by resting-state functional MRI (rs-fMRI) provide a novel perspective into the brain and are ideal to investigate neurodegenerative disorders conceptualized as brain disconnection syndromes (Warren, Rohrer, & Hardy, 2012). We, therefore, investigated also the neural substrate of memory in PD-MCI using rs-fMRI to determine whether hippocampal engagement is reduced in PD and whether it correlates with this associative memory measure. To our best knowledge, no previous rs-fMRI study has specifically addressed declarative memory disorders in PD. Conversely, similar investigations in Alzheimer's disease have elucidated memory-related brain network changes, especially focusing on the hippocampal and default mode network connectivity (Chhatwal & Sperling, 2012).

In this article, we evaluate both the retrieval deficit hypothesis, that is, the deficit is due to the impaired free recall of items from memory, and the associative dysfunction hypothesis in PD patients, that is, the deficit is due to the impaired association between items. Therefore, we performed an in-depth assessment of memory function in a group of PD patients (including PD-MCI) and age-matched controls to determine differences in encoding, retrieval, recollection, error scores, and recognition. Specifically, the *retrieval deficit hypothesis* would predict impaired learning and free recall in PD-MCI as compared to controls and relatively spared performance in paired cued recall and recognition, due to equal attentional/executive demands. On the other hand, the *associative dysfunction hypothesis* would also predict a worsening of the performance in PD-MCI compared to controls in the cued paired recall condition, indicating an associative memory deficit in the recollection and relational binding. We investigated both, structural brain images and resting state functional connectivity of medial temporal lobe structures, focusing on the hippocampus, a key region for memory (Koen & Yonelinas, 2014; Squire, 2004). Here we hypothesized significant structural differences between PD patients and controls in the hippocampus and functional connectivity differences associated with the impaired memory performance.

Method

Procedure

Neuropsychological assessment. Both PD patients and controls underwent neuropsychological assessment according to the standard International Parkinson Movement Disorder Society Level II criteria for PD-MCI (Bezdicek, Nikolai, et al., 2017; Bezdicek, Sulc, et al., 2017; Litvan et al., 2012). In addition, an in-depth memory assessment was performed for the present study. The PD-MCI battery consisted of 10 tests in five cognitive domains measuring attention and working memory, executive function, language, visuospatial function, and memory. A complete list of the tests can be found in Supplemental Table S3. Significant group differences in analysis of variance (ANOVA) were found in all the five cognitive domains. PD-MCI was defined when the patient performed at least two tests below $-1.5 SD$ in comparison

to normative data (Bezdicek, Sulc, et al., 2017; Goldman et al., 2013).

Memory assessment (retrieval deficit hypothesis). Rey Auditory Verbal Learning Test (RAVLT). It is a classical and standardized measure that assesses the learning of new material (learning curve represented by Trials 1 to 5 and a total amount of learned material; RAVLT-IRS), retention (delayed recall after 20 min; RAVLT-DR), and recognition memory (a list of 50 words containing all items from Lists A and B and 20 words that are phonemically or semantically similar to those in Lists A and B; RAVLT-Rec; Bezdicek et al., 2014; Ivnik et al., 1990). Brief Visuospatial Memory Test—Revised (BVMTR). A 2×3 matrix containing six simple geometric visual designs is shown to the subjects. The standardized measure is a visuospatial analog of RAVLT consisting of three consecutive trials that yield measures of learning curve a total amount of learned material (BVMTR-IRS), retention/delayed recall (BVMTR-DR), and recognition (BVMTR-Rec; Benedict, 1997).

Associative dysfunction hypothesis. The Experimental Memory Binding Test (MBT) uses controlled learning and cued recall to elicit encoding specificity and maximum retrieval (Buschke, 2014; Papp et al., 2015; Rentz et al., 2013; Tulving & Thomson, 1973). A detailed description of the MBT can be found elsewhere (Buschke, 2014; Buschke et al., 2017). In short, the MBT during cued paired recall requires the subjects to recollect and associatively bind two-word items (e.g., brown and yellow) that are interconnected by a single shared semantic category (i.e., color; associative retrieval and binding measure). In the present study, we used the MBT measures: TIP (total number of items cued recalled in the paired condition, range 0–32) as encoding specificity measure and PIP (the number of pairs cued recalled in the paired condition, range 0–16) as a binding measure for their ability to detect hippocampal episodic memory impairment, which is not compromised by the ubiquity of attention/executive dysfunction in PD (Buschke et al., 2017; Cohn et al., 2016).

Participants

Thirty-four patients diagnosed with sporadic PD (Hughes, Daniel, Kilford, & Lees, 1992) in intermediate or advanced stages and 31 age-matched healthy controls were included in the present study (see Table 1). Other inclusion criteria were age at onset after 45 years of age and stable pharmacological treatment with levodopa in monotherapy or combination with dopamine agonists. The daily levodopa equivalent dose was computed for each patient (Tomlinson et al., 2010). The Unified Parkinson's disease Rating Scale (UPDRS I, II, III and IV) were administered to the patient group. Exclusion criteria were previous or current psychotic symptoms, treatment with antipsychotics, severe cognitive impairment (i.e., MoCA below $-1.5 SD$ according to the Czech normative data; Kopecek et al., 2017), treatment with deep brain stimulation or jejunal infusion of levodopa, and/or presence of any comorbidity potentially interfering with motor or cognitive performance. PD patients and controls did not differ on any of the measured demographic variables (see Table 1). Antidepressants were also administered to eight patients (selective serotonin reuptake inhibitors only in five patients, in combination with serotonin-norepinephrine reuptake inhibitors in two cases and tricyclic antidepressants only in one patient) and three controls (selective serotonin reuptake inhibitors). All subjects gave their informed consent to participate

This document is copyrighted by the American Psychological Association or one of its allied publishers. This article is intended solely for the personal use of the individual user and is not to be disseminated broadly.

Table 1
Demographic, Clinical and Basic Memory Performance Characteristics

Variables (<i>M</i> ± <i>SD</i>)	Controls (<i>n</i> = 31)	PD (<i>n</i> = 34)	PD-NC (<i>n</i> = 18)	PD-MCI (<i>n</i> = 16)	<i>p</i> -value (<i>t</i>) Controls vs PD-NC	<i>p</i> -value (<i>t</i>) Controls vs PD-MCI	<i>p</i> -value (<i>t</i>) PD-NC vs PD-MCI
Age (years)	63.61 ± 7.12	64.21 ± 7.18	63.67 ± 6.90	64.81 ± 7.65	.724	.498	.652
Education (years)	15.08 ± 3.36	14.28 ± 2.66	14.97 ± 2.46	13.50 ± 2.73	.950	.077	.032
NART (IQ)	117.87 ± 12.44	115.68 ± 10.95 [†]	118.83 ± 9.70	112.13 ± 11.47	.876	.103	.081
Race (Caucasian, %)	100	100	100	100	—	—	—
Sex (male, %)	42	58	56	56	.685	.680	.999
PD duration (years)	—	11.82 ± 4.45	11.11 ± 5.27	12.63 ± 3.28	—	—	.179
UPDRS-III "on" state	—	17.82 ± 9.63	16.94 ± 10.14	18.81 ± 9.26	—	—	.501
Hoeft/ahr stage	—	2.04 ± .53	2.06 ± .51	2.03 ± .56	—	—	.942
L-Dopa Equivalent	—	1366.18 ± 666.72	1343.79 ± 744.55	1391.36 ± 590.24	—	—	.646
MoCA	26.81 ± 2.18	25.76 ± 2.52	26.56 ± 1.69	24.88 ± 3.03	.652	.033	.081
BDI-II	6.84 ± 4.89	10.26 ± 4.93	9.50 ± 5.12	11.13 ± 4.73	.100	.011*	.543
RAVLT-IRS	44.23 ± 7.17	40.21 ± 10.99	41.94 ± 7.63	38.25 ± 13.86	.383	.132	.325
RAVLT-DR	9.35 ± 1.92	7.03 ± 3.44	7.78 ± 2.80	6.19 ± 3.97	.017 (.34)	.009* (.38)	.282
RAVLT-Rec	45.94 ± 10.73	42.79 ± 4.90	44.56 ± 3.40	40.81 ± 5.65	.048 (.28)	.001* (.47)	.021 (.40)
BVMT-R-IRS	25.94 ± 4.92	18.53 ± 7.19	21.39 ± 5.20	15.31 ± 7.88	.003* (.43)	<.001* (.61)	.025 (.39)
BVMT-R-DR	10.32 ± 1.54	7.68 ± 3.02	9.00 ± 1.94	6.19 ± 3.37	.010* (.37)	<.001* (.62)	.009* (.45)
BVMT-R-Rec	5.77 ± .43	5.74 ± .51	5.78 ± .43	5.69 ± .60	.977	.772	.779
MBT CR-L1	15.65 ± .61	14.82 ± 1.38	15.06 ± 1.16	14.56 ± 1.59	.090	.007* (.40)	.232
MBT CR-L2	13.68 ± 1.72	12.03 ± 2.65	12.83 ± 1.86	11.13 ± 3.14	.062	.001* (.49)	.147
MBT PIP	13.10 ± 2.15	9.94 ± 4.24	10.94 ± 3.78	8.81 ± 4.55	.033 (.30)	.001* (.50)	.131
MBT TIP	29.03 ± 2.43	25.91 ± 4.41	27.11 ± 2.88	24.56 ± 5.45	.018 (.34)	.001* (.49)	.155

Note. PD (PD-NC + PD-MCI) = Parkinson's disease; PD-MCI = Parkinson's disease with mild cognitive impairment; PD-NC = Parkinson's disease with normal cognition; MoCA = Montreal Cognitive Assessment; BDI-II = Beck Depression Inventory, 2nd ed.; BVMT-R-IRS = Brief Visuospatial Memory Test, revised, immediate recall score the sum of all correct responses given over the three consecutive trials (T1 + T2 + T3; min.-max. 0-36); BVMT-R-DR = the total number of correct words recalled on the delayed recall trial (min.-max. 0-12); BVMT-R-Rec = number of all correctly recognized items in recognition (min.-max. 0-12); NART = National Adult Reading Test Czech version (error scores transformed to IQ); RAVLT-IRS = Rey Auditory Verbal Learning Test immediate recall score, the sum of all correct responses given over the five consecutive trials (T1 + T2 + T3 + T4 + T5; min.-max. 0-50); RAVLT-DR = the total number of correct words recalled on the delayed recall trial (T7; min.-max. 0-15); RAVLT-Rec = number of all correctly recognized items in recognition (min.-max. 0-50); MBT = Memory Binding Test; CR-L1 = number of items cued recalled from List 1 on the MBT; CR-L2 = number of items cued recalled from List 2 on the MBT; PIP = number of pairs cued recalled in the paired condition on the MBT (0-16 pairs); TIP = total number of items cued recalled in the paired condition on the MBT (0-32); *p*-value (two-tailed), Cohen's *r* in parenthesis, based on Mann-Whitney U Test.
[†] *p* = .393 (Controls vs PD). * Statistically significant after Bonferroni correction ($\alpha \leq .016$).

in the study. The study was approved by the Ethics Committee of the General University Hospital in Prague, Czech Republic, and therefore performed in accordance with the ethical standards established in the 1964 Declaration of Helsinki.

Statistical Analyses

The analyses were performed using IBM SPSS 20.0. Considering the nonnormal distribution of MBT scores (after checking the Q-Q plot and Shapiro-Wilk test), we used nonparametric statistics. The association between test scores and age and years of education was evaluated by a Spearman's rho and by a point-biserial correlation for gender. To analyze between-groups differences in the test performance between controls, PD-MCI and PD-NC, we ran Mann-Whitney *U* tests with Bonferroni corrected post hoc comparisons. Specifically, we investigated group differences in RAVLT and BVMT-R for retention (delayed recall), and recognition and in MBT for associative retrieval/binding (cued recall). Differences in the slope of the learning curve in BVMT-R and RAVLT were investigated with a mixed between-within subjects ANOVA. The error patterns were also compared for all the tests (Thomas et al., 2018). In case of between-groups differences in sex, we used χ^2 test for independence with Yates continuity correction. $\alpha \leq .05$ was adopted for statistical significance and effect size was determined using Cohen's (*r*)—.1, small; .3, medium; .5, large (Cohen, 1988)—or partial eta squared (η^2)—.02, small, .13, medium, .26, large. In addition, we used Spearman's correlations to check the relationship between the different memory scores (Supplemental Table S1) and between them and the performance in other cognitive domains (Supplemental Table S2). To assess the differential impact of attention/working memory and visuospatial abilities on the memory tests (since these domains are frequently impaired in PD and might influence the memory performance), linear regression was implemented using as independent variables, Trail Making Test, Part A, Digit Span backward (attention/working memory domain), and a Clock Drawing Test (visuospatial domain) and setting the different memory measures as dependent variables.

Neuroimaging

Data acquisition and preprocessing: Magnetic resonance images were acquired on a 3T MR scanner (Magnetom Skyra, Siemens, Germany). To investigate brain structure, a whole-brain T1-weighted MRI dataset was acquired using a sagittal 3D-MPRAGE (Magnetization Prepared Rapid Gradient Echo) sequence with voxel resolution 1 mm³, TR = 2.2 sec, TE = 2.43 ms, inversion time = 900 ms, matrix = 224 × 224, and flip angle = 8°. To assess functional brain connectivity, resting-state functional MRI (rs-fMRI) was also performed, using T2*-weighted gradient-echo-planar imaging (EPI), flip angle = 90 deg, TR = 2sec, TE = 30ms, voxel size 3*3*3.45 mm, 300 volumes. A T2-weighted sequence (TR = 3.2 sec, TE = 9 ms, resolution = 0.9x0.9x3 mm) was also implemented to exclude confounding pathological brain changes. Because of MRI incompatibility or severe artifacts in MRI images, six patients and six controls had to be discarded from the neuroimaging analysis that included, accordingly, 28 PD patients and 25 controls. The time between MRI and neuropsychological assessments was on average 11 days. Both cognitive mea-

asures and MRI acquisition were performed when the patients were taking their usual dopaminergic medication (i.e., in ON state). Images taken in the ON state were chosen to minimize a possible influence of the motor impairment on neuropsychological performance and head movement during the MRI acquisition.

T1 MRI data were preprocessed in CAT12 toolbox (www.neuro.uni-jena.de/cat12) and SPM12 (www.fil.ion.ucl.ac.uk/spm) within Matlab™ environment (MathWorks, Natick, MA). First, the images were normalized to MNI space, segmented into white matter, gray matter, and cerebrospinal fluid. After that, gray matter density (GMD) images were obtained using modulation that encodes spatial transformations in the actual voxel gray values. Finally, GMD images were further smoothed using a Gaussian kernel of 8 mm full-width at half-maximum. A quality check was performed using quality reports provided in CAT12.

For rs-fMRI data, the functional images were first realigned and slice-time corrected. Then, the unified segmentation approach (Ashburner & Friston, 2005) was implemented to achieve segmentation, bias correction, and normalization through nonlinear warping. As for T1 data, 8 mm smoothing was applied to comply with the requirements of the Gaussian random field theory to correct the statistical analysis for multiple comparisons. We show statistics on the motion parameters of our patients and healthy controls groups. To check for differences in head motion during the MRI acquisition, we computed the mean and maximum frame-wise displacement for each study participant based on the frame-by-frame translation and rotation values (Power, Barnes, Snyder, Schlaggar, & Petersen, 2012). Of note, patients and controls did not differ in head motion as indicated by Student's *t* test (mean FD: $t(df) = -1.173 (51), p = .246$; max FD: $t(df) = -1.638 (51), p = .108$). Information on mean and maximum frame-wise displacement values are shown in the Supplementary Figure S1 in the online supplemental material. Next, to increase the signal to noise ratio and to reduce possible motion-related artifacts, a nuisance regression was performed at the end of the preprocessing using signals from WM and CSF, as well as the head motion parameters.

Statistical Analyses

To identify structural changes in the medial temporal lobe and hippocampus, we applied voxel-based morphometry (VBM; Ashburner & Friston, 2000). The preprocessed GMD images were compared between patients and controls in a two-sample *t* test restricting the analysis within a mask including the hippocampus, the parahippocampal gyrus, and the entorhinal cortex. The statistical design included nuisance covariates to consider the variability in total intracranial volume and age in the statistical analysis.

To investigate the differences in hippocampal resting-state functional connectivity between patients and controls, we applied seed-based connectivity analyses. Namely, three seeds for each hippocampus were defined according to previous research (Chen et al., 2016), anterior (MNI: ±24, -14, -20), middle (MNI: ±26, -26, -12) and posterior subfields (MNI: ±26, -34, -4) of the hippocampus (see Figure 3). Anterior, middle, and posterior subfields correspond, respectively, to the hippocampal head, body, and tail (Chen et al., 2016). Single voxels were used as seeds to maintain specificity for the hippocampal subregions. Here we consider that the smoothing step during the preprocessing had already merged into the seed voxels part of the surrounding signal

intensity. The time-courses were extracted from the preprocessed functional images for patients and controls. Whole-brain correlations were performed in Matlab between the time-courses in the seed voxels and that of all the other voxels in the brain. This produced a correlation map for each subject, in which each voxel contains a value corresponding to its correlation in time with the seed region. After that, individual correlation maps were compared in SPM12 between patients and controls using a two-sample *t* test and entering age as a nuisance covariate. Significant clusters were obtained with $p < .05$ using family wise error correction at cluster-level. When significant results were obtained in the group comparison, a seed-based connectivity analysis from the selected seed was also computed independently for patients and controls, to identify the complete pattern of functional connections with the seed in each group.

When significant differences in hippocampal seed-based connectivity between patients and controls were identified, we investigated their relationship with memory performance. Specifically, we selected the clusters showing a significant difference and tested if the connectivity change between those regions and the corresponding hippocampal seeds was associated with memory scores (i.e., MBT, RAVLT, and BVMT). We extracted the correlation values from the significant clusters using the marsbar toolbox (<http://marsbar.sourceforge.net/>) and correlated them with memory scores using two-tailed nonparametric Spearman's *rho*.

Results

Memory Assessment

Retrieval deficit hypothesis: Learning (learning curve) and encoding. The between groups differences and learning curves are shown in Figures 1 (top, verbal domain; bottom, visual domain) and 2 and Table 1. Overall, based on a mixed between-within subjects ANOVA, the linear slope was significantly steeper during RAVLT Trials 1 to 5 across groups, thus indicating a significant effect for trial ($p < .001$). On the contrary, there was no effect neither for the group factor ($p = .124$) nor the Trial \times Group interaction ($p = .212$), suggesting no difference in the learning curves between groups (Figure 1 top). Regarding BVMT-R Trial 1 to 3, there was a significant effect for trial ($p < .001$) and for group (PD-MCI $<$ PD-NC $<$ controls; $p < .001$) with no significant Trial \times Group interaction ($p = .405$). (Figure 1 bottom).

Retention (delayed recall). We found significant differences with a medium effect size in retention in verbal domain RAVLT-DR in PD-MCI $<$ controls ($r = .38$) and medium effect size in PD-NC $<$ controls ($r = .34$), whereas the PD-MCI versus PD-NC comparison was not significant. Differences in retention in the visual domain were highly significant for all the comparisons, with the large effect size in PD-MCI $<$ controls ($r = .62$) and medium effect size in PD-MCI $<$ PD-NC and PD-NC $<$ controls (Table 1 and Figure 2 C/2 D).

Recognition. We found significant differences with the medium effect size in recognition in the verbal domain in PD-MCI $<$ controls ($r = .47$) and low and medium effect size in PD-MCI $<$ controls and PD-MCI $<$ PD-NC, respectively ($r = .28$ and $.40$). However, in recognition in the visual domain, there were no

significant between-groups differences (Table 1 and Figure 2 E/2F).

Associative dysfunction hypothesis: Retrieval and relational binding (cued recall). There were significant differences with the large effect size in MBT-PIP (binding measure) in PD-MCI $<$ controls ($r = .50$) and with the medium effect size in PD-NC $<$ controls ($r = .30$). We also found a medium effect size in MBT-TIP (encoding specificity measure) in PD-MCI $<$ controls ($r = .49$) and with the medium effect size in PD-NC $<$ controls ($r = .34$) and again no difference between PD-MCI versus PD-NC (Figure 1G/1H and Table 1).

Memory error patterns. PD-MCI made significantly more intrusions with the medium effect size in RAVLT Trial 6 to 8 compared to controls and, also, significantly more intrusions with the medium effect size in the MBT second interference list (MBT CR-L2; Supplemental Table S4 in the online supplemental material). Furthermore, PD-MCI and PD-NC, compared to controls, did also more false positive errors during recognition with large and medium effect size, respectively (Supplemental Table S4). The linear regression analysis showed that performance in attention, working memory and visuospatial functions predicted BVMT-R-IRS and BVMT-R-DR, whereas only working memory was a significant predictor of RAVLT-IRS and only visuospatial functions showed an influence on MBT-TIP (see Table 2).

Neuroimaging Results

Comparing structural brain images between PD patients and healthy controls using the VBM technique, we did not obtain any significant GMD differences in the medial temporal lobe and hippocampus.

Using seed-based connectivity analysis, we obtained significant group differences between PD patients and controls in the functional connectivity of the bilateral anterior hippocampi. Namely, both the left and right anterior hippocampi showed reduced connectivity with the precuneus and the adjacent superior parietal cortex in patients as compared to controls (see Figure 3). The functional connectivity maps between the bilateral anterior hippocampi and the rest of the brain are additionally shown separately for patients and controls in Supplementary Figure S2 in the online supplemental material. No significant results were found neither for the reverse comparison (i.e., controls $>$ PD) nor the middle and posterior hippocampi. Notably, significant nonparametric correlations were found between memory scores and the connectivity of the anterior hippocampus and precuneus/superior parietal cortex. Both the connectivity patterns between the right and left anterior hippocampi and the precuneus/superior parietal cortex correlated significantly with associative retrieval and binding (TIP, PIP) and with retention and learning in visuospatial domain (i.e., BVMT-R-DR and BVMT-R sum of 1–3 trials). Also, the connectivity between the left hippocampus and the superior parietal cortex positively correlated with the performance in the RAVLT-DR (Figure 4 and Table 3).

Discussion

In the present study, we aimed at clearly distinguishing between retrieval versus associative models of declarative memory impairment in nondemented PD to explore the associative dysfunction

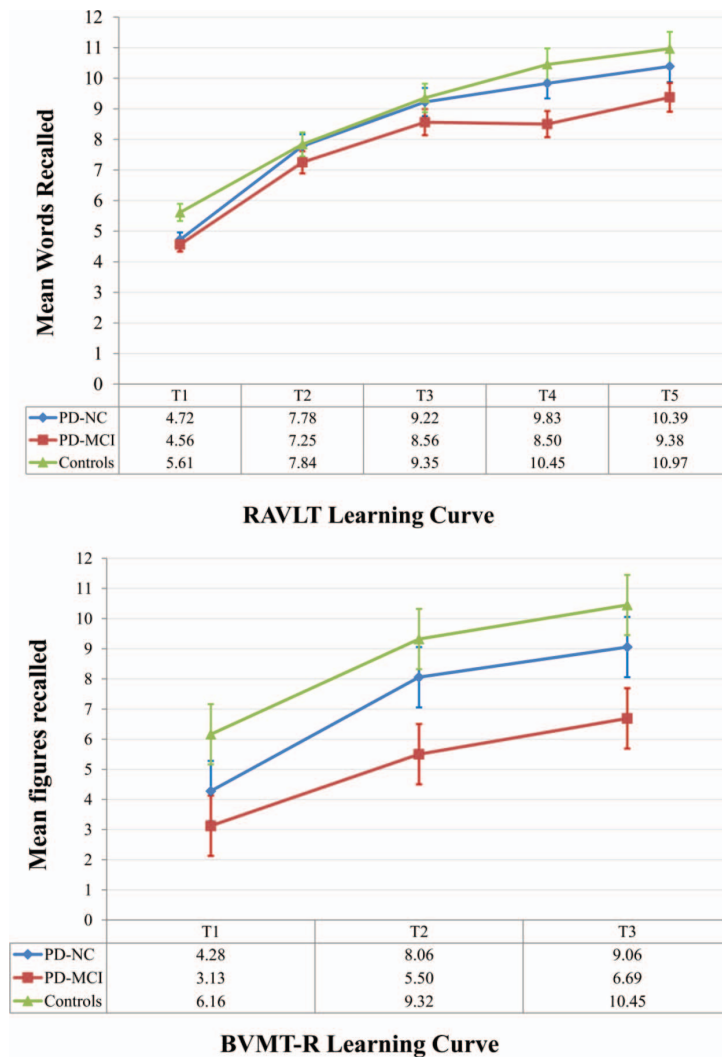


Figure 1. Verbal learning curve (top) and visual learning curve (bottom) in Parkinson's disease patients and controls. RAVLT = Rey Auditory Verbal Learning Test Learning Curve over five trials. The whiskers of the lines graph are $+1$ and -1 SD 's; a mixed between-within subjects analysis of variance (ANOVA) in RAVLT Trial 1 to 5 showed no significant interaction between Trial \times Group status, Wilks' $\lambda = .84$, $F(8, 118) = 1.01$, $p = .212$, partial $\eta^2 = .086$. There was a substantial main effect for trial, Wilks' $\lambda = .12$, $F(4, 59) = 110.38$, $p < .001$, partial $\eta^2 = .882$, with all groups showing an increment in verbal learning. However, the main effect of group status was nonsignificant, $F(2, 62) = 2.16$, $p = .124$, partial $\eta^2 = .065$. BVMT-R = Brief Visuospatial Memory Test, revised, learning curve over three trials. The whiskers of the lines graph are $+1$ and -1 SD 's; a mixed between-within subjects ANOVA in BVMT-R Trial 1 to 3 showed no significant interaction between Trial \times Group status, Wilks' $\lambda = .94$, $F(4, 122) = 1.01$, $p = .405$, partial $\eta^2 = .032$. There was a substantial main effect for trial, Wilks' $\lambda = .21$, $F(2, 61) = 116.83$, $p < .001$, partial $\eta^2 = .793$, with all groups showing an increment in visual learning. The main effect of group status was significant, $F(2, 62) = 17.60$, $p < .001$, partial $\eta^2 = .362$. See the online article for the color version of this figure.

versus retrieval deficit hypotheses (Brønnick et al., 2011; Cohn et al., 2016; Cohn et al., 2010; Costa et al., 2014; Edelstyn et al., 2015; Chiaravalloti et al., 2014; Tröster & Fields, 1995; Whittington et al., 2000). Our results, combining neuropsychological and

neuroimaging data, support to a certain degree both models. Indeed, at the behavioral level, the test performance of PD patients indicates that memory deficit in PD can be both associative (with an impairment in binding of two words) and, concurrently, a

This document is copyrighted by the American Psychological Association or one of its allied publishers. This article is intended solely for the personal use of the individual user and is not to be disseminated broadly.

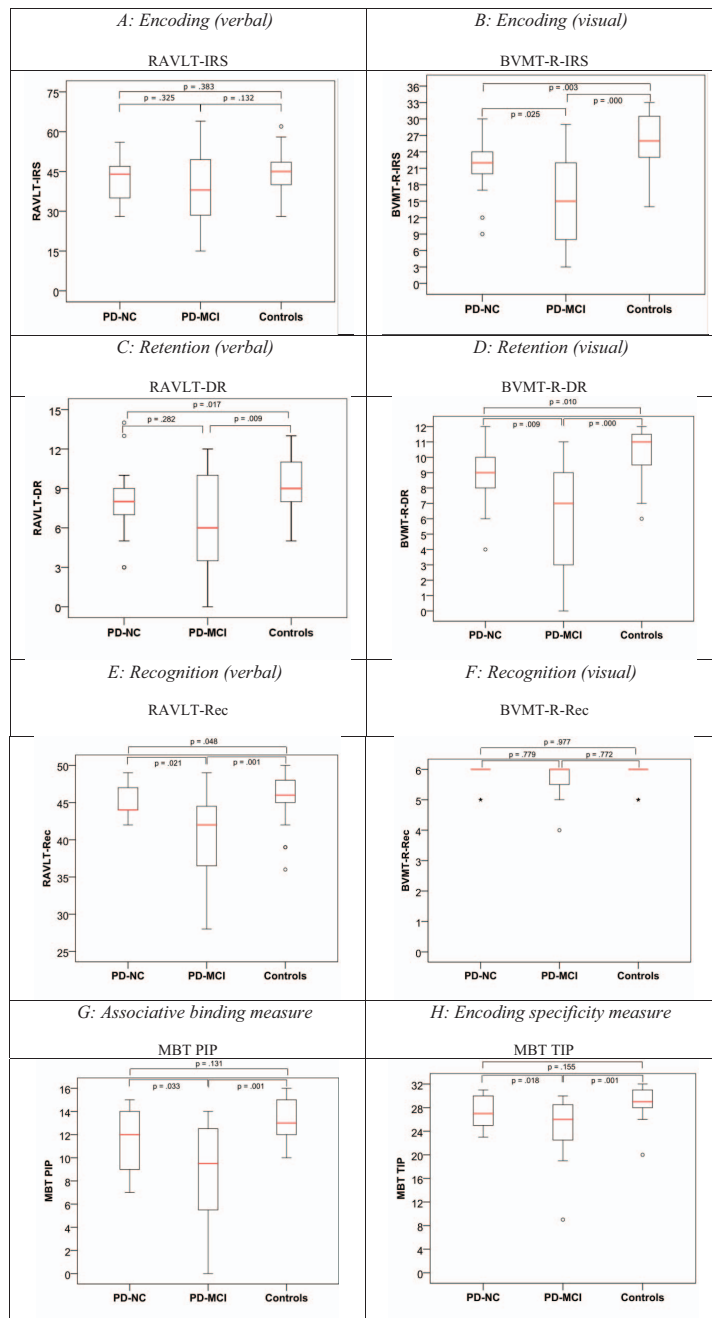


Figure 2. In-depth analysis of memory profiles in Parkinson's disease (PD-NC, $n = 18$; PD-MCI, $n = 16$; controls, $n = 31$). BVMT-R-IRS = Brief Visuospatial Memory Test, revised, immediate recall score; BVMT-R-DR = delayed recall; BVMT-R-Rec = Recognition; RAVLT-IRS = Rey Auditory Verbal Learning Test immediate recall score; RAVLT-DR = Rey Auditory Verbal Learning Test delayed recall; RAVLT-Rec = Rey Auditory Verbal Learning Test recognition; MBT = Memory Binding Test; PIP = number of pairs cued recalled in the paired condition; TIP = total number of items cued recalled in the paired condition. The length of the box is the interquartile range, the whiskers go out to highest and smallest values and the red line across the inside of the box is median. See the online article for the color version of this figure.

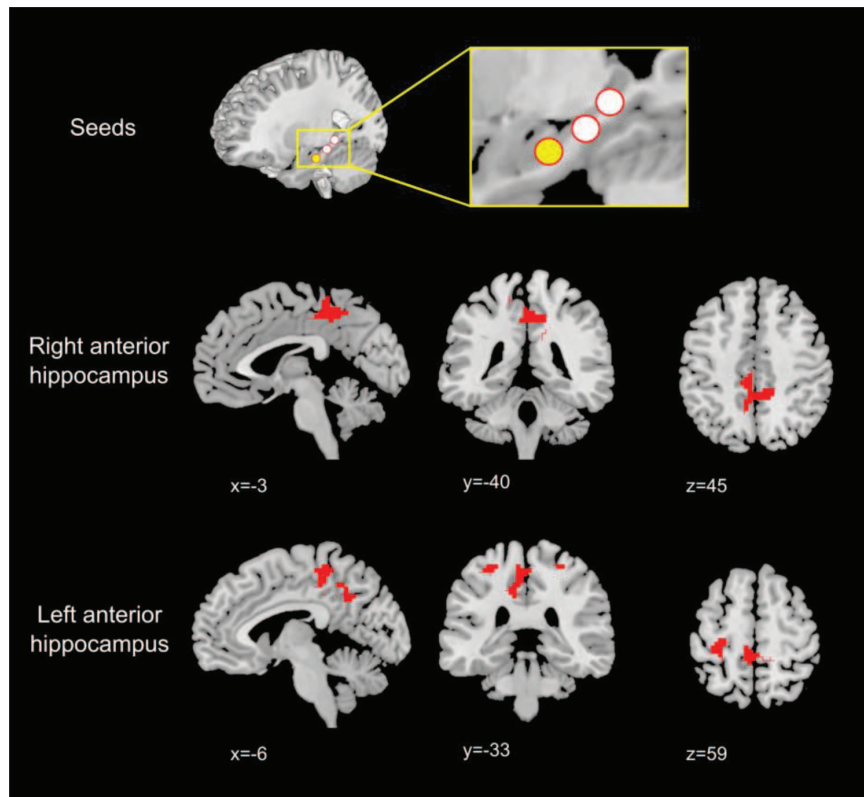


Figure 3. Decreased anterior hippocampal functional connectivity in Parkinson's disease (PD) patients ($n = 28$) compared to controls ($n = 25$). From top to bottom: graphical visualization of seeds in the anterior, middle and posterior hippocampus. Single voxels were used as seeds in the analysis. Significant results were found for the anterior hippocampus (highlighted in yellow). Group comparisons (PD patients < controls) showing diminished connectivity between the right/left anterior hippocampi and the precuneus and superior parietal cortex. Red blobs represent clusters surviving the $p < .05$ FWE correction for multiple comparisons at the cluster level. See the online article for the color version of this figure.

deficit in retrieval (in free recall, retention and recognition) mediated by attention and encoding strategies (preponderantly in the visual domain). At the brain level, this complex framework is mirrored in the functional interplay between the hippocampus and the precuneus.

In contrast to previous studies, we used rigorously determined cognitive phenotypes (PD-MCI and PD-NC) by applying the standard International Parkinson Movement Disorder Society criteria Level II for PD-MCI (Bezdicek, Sulc, et al., 2017; Litvan et al., 2012; Williams-Gray et al., 2007). To disentangle the two hypotheses, we implemented both standardized tools with established psychometric properties in verbal (RAVLT) and visual (BVMT-R) domains and an experimental cued recall technique (MBT) sensitive to hippocampal dysfunction in MCI and PD-MCI (Balthazar, Yasuda, Cendes, & Damasceno, 2010; Bezdicek, Sulc, et al., 2017; Buschke, 2014; Buschke et al., 2017; Cohn et al., 2016; Chang et al., 2010; Edelstyn et al., 2015; Lee et al., 2010). The behavioral test results show a specific, declarative memory impairment profile in basic memory mechanisms in PD-MCI and, to a lesser extent, in

PD-NC. Of note, premorbid intelligence levels and demographic variables were comparable between patients and controls and even between PD-NC versus PD-MCI and controls (see Table 1).

Learning/encoding strategies were significantly impaired in the visual domain, with a gradient PD-MCI < PD-NC < controls, whereas, surprisingly, the between-groups differences were not significant in the verbal domain. Moreover, for both tests investigating visual and verbal domains, we found no interaction between trial and group. This lack of learning slope difference may indicate that encoding strategies are not a major difference between groups. If attention/strategic impairments were contributing to encoding errors, one would predict a flatter slope for at least PD-MCI group. Nevertheless, PD-MCI showed a trend toward a lower, though not significant, learning slope in comparison to other groups, which is consistent with previous research (Brønnick et al., 2011; Chiaravalloti et al., 2014). This differential affliction of learning in visual and verbal domains is interesting because it might indicate that the presentation of visual material to PD patients influence their overall memory performance. Indeed, deficits in visuospatial and

Table 2
Multiple Regression Analysis of All Memory Measures and Visual Attention (TMT-A) and Auditory Attention (DS Backwards) and Visuospatial Measure (CLOX-I) as Predictors

Predictors	ANOVA			TMT-A			DS backwards			CLOX-I		
	Adjusted R^2	F	p -value	β	t	p	β	t	p	β	t	p
RAVLT-IRS	.122	3.975	.012	.05	.36	.723	.35	2.86	.006**	.16	1.26	.210
RAVLT-DR	.060	2.368	.079	-.20	-1.49	.139	.24	1.87	.066	-.76	-.57	.571
RAVLT-Rec	.014	1.298	.283	.05	.38	.704	.18	1.42	.160	.15	1.07	.288
BVMT-R-IRS	.466	19.611	<.001***	-.42	-4.11	<.001***	.32	3.30	.002**	.22	2.22	.030*
BVMT-R-DR	.509	23.147	<.001***	-.52	-5.33	<.001***	.19	2.04	.045*	.25	2.58	.012*
BVMT-R-Rec	.002	.048	.986	.05	.37	.716	.01	.03	.978	.03	.23	.816
MBT PIP	.127	4.101	.010**	-.17	-1.29	.201	.19	1.52	.132	.21	1.64	.106
MBT TIP	.224	7.164	<.001***	-.20	-1.63	.107	.21	1.83	.072	.29	2.38	.021*

Note. ANOVA = analysis of variance; TMT-A = Trail Making Test, Part A; DS = Digit Span; CLOX-I = an unprompted executive clock drawing task; BVMT-R-IRS = Brief Visuospatial Memory Test, revised, immediate recall score the sum of all correct responses given over the three consecutive trials (T1 + T2 + T3; min.-max. 0–36); BVMT-R-DR = the total number of correct words recalled on the delayed recall trial (min.-max. 0–12); BVMT-R-Rec = number of all correctly recognized items in Recognition (min.-max. 0–12); RAVLT-IRS = Rey Auditory Verbal Learning Test immediate recall score, the sum of all correct responses given over the five consecutive trials (T1 + T2 + T3 + T4 + T5; min.-max. 0–50); RAVLT-DR, the total number of correct words recalled on the delayed recall trial (T7; min.-max. 0–15); RAVLT-Rec = number of all correctly recognized items in recognition (min.-max. 0–50); MBT = Memory Binding Test; CR-L1 = number of items cued recalled from List 1 on the MBT; CR-L2 = number of items cued recalled from List 2 on the MBT; PIP = number of pairs cued recalled in the paired condition on the MBT (0–16 pairs); TIP, Total number of Items cued recalled in the Paired condition on the MBT (0–32).

* $p < .05$. ** $p < .01$. *** $p < .001$.

visuo-constructive abilities have frequently been reported in PD-MCI with posterior-cortical defects (Martinez-Horta & Kulisevsky, 2011) and might thus significantly contribute to degrading their performance in the BVMT-R in comparison to RAVLT learning curve. In retention in the verbal domain we found a significant difference between PD-MCI versus controls and PD-NC versus controls, but not between PD-MCI versus PD-NC. The finding is further corroborated by significantly higher verbal intrusion rate between PD-MCI and controls (Brønneck et al., 2011). We found a similar pattern in retention in a visual domain where, additionally, the difference between PD-MCI versus PD-NC was significant. This finding is consistent with a higher affliction of visual than a verbal declarative memory in PD encoding and retention (Lee et al., 2010). In recognition, there was a striking pattern of significant impairment between all groups in verbal but not visual domain (Rodríguez, Algarabel, & Escudero, 2014). However, we believe this is not reflecting a real absence of between-groups differences in visual memory recognition rather a floor effect in BVMT-R Recognition (see the trend in Figure 2 F). PD-MCI compared to controls also indicated more false positive errors with a nonsignificant difference in false negative rate and a trend toward significance in PD-NC versus controls (Higginson et al., 2005). Overall, we see a pattern of declarative memory impairment in learning, retention, with a higher level of intrusions errors, a pattern similar to that observed in the progression of MCI due to Alzheimer's disease (Thomas et al., 2018), and recognition in PD-MCI again with higher intrusion and false positive rates which is accompanied by a similar but milder memory deficit in PD-NC (especially in recognition) consistent with previous research (Brønneck et al., 2011). These results would thus indicate a memory profile to a large degree (especially in the visual domain) consistent with the retrieval deficit hypothesis (Tröster & Fields, 1995). Moreover, the BVMT-R test revealed larger group differences as compared to the RAVLT. The linear regression analysis helps in further understanding the source of this discrepancy.

Indeed, the BVMT-R requires a heavier load not only on visuospatial functions as previously argued but also on attention/working memory functions that were impaired in our sample which is in accordance to the previous literature on PD with cognitive deficits (Martinez-Horta & Kulisevsky, 2011).

Furthermore, we observe a significant difference in the associative binding (MBT-PIP) and in encoding specificity measure (MBT-TIP) between PD-MCI and controls. A similar trend is apparent in PD-NC. Of note, the linear regression analysis did not reveal a significant contribution of attention/working memory to the memory performance in TIP and PIP scores. These results support the associative deficit hypothesis and are consistent with studies showing memory impairment in recollection and relational binding in PD-MCI (Brønneck et al., 2011; Cohn et al., 2010, 2016; Chiaravalloti et al., 2014; Edelstyn et al., 2015; Edelstyn, Mayes, Condon, Tunnicliffe, & Ellis, 2007; Edelstyn, Shepherd, Mayes, Sherman, & Ellis, 2010; Higginson et al., 2005), however, discordant findings that PD patients benefit substantially from cueing also can be found (Costa et al., 2014).

Notably, the neuroimaging results did not show any morphological change in the Schelten's MTL scale of PD patients as compared to controls. This is in contrast with a part of the previous literature that has reported atrophy in the MTL in PD with cognitive deficit and related it to memory performance (Biundo et al., 2013; Junque et al., 2005; Pan et al., 2013; Pirogovsky-Turk et al., 2015; Tanner et al., 2015). However, it has to be mentioned that the identification of consistent atrophy pattern in PD has been challenging so far, often leading to heterogeneous and inconsistent results (Saeed et al., 2017). As for the rs-fMRI analysis, we believe that our findings may reconcile both the associative and the retrieval deficit hypothesis and provide a more coherent account of memory deficits in PD. Lower performance in memory scores was significantly associated with disrupted connectivity between the anterior hippocampi, the precuneus, and superior parietal cortex. The precuneus and the superior parietal cortex have been related to

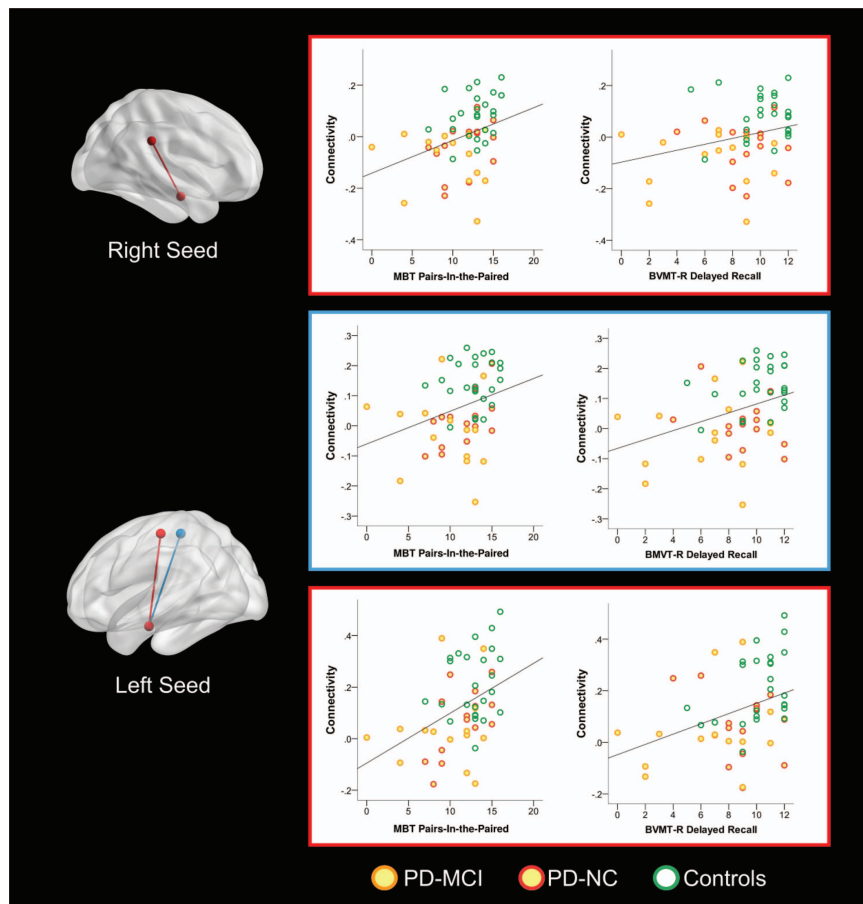


Figure 4. Correlations between bilateral anterior hippocampal functional connectivity changes and memory scores in Parkinson's disease (PD) patients ($n = 28$) and controls ($n = 25$). The 3D brain images schematically display regions showing diminished connectivity in PD patients compared to controls. The peak coordinates of significant clusters from [Figure 3](#) were selected as targets of the anterior hippocampal connections (MNI: 12 –37 29 for the right seed; MNI –30 –28 56 and –6 –34 56 for the left seed). The scatter-plots show positive correlations between higher connectivity (expressed as r coefficients on the y axes) and better memory performance. For simplicity, only selected results are shown, while a full list of the significant correlations with the memory scores can be found in the results section and in [Supplemental Table S1](#) in the online supplemental material. BVMT-R = Brief Visuospatial Memory Test-Revised; MBT = Memory Binding Test; MNI = Montreal Neurological Institute. See the online article for the color version of this figure.

This document is copyrighted by the American Psychological Association or one of its allied publishers. This article is intended solely for the personal use of the individual user and is not to be disseminated broadly.

both attentional control and visuospatial imagery (Cavanna & Trimble, 2006), whereas the hippocampus and, in particular, its anterior subfield, is pivotal in the memory network, by supporting relational memory (Giovanello, Schnyer, & Verfaellie, 2004) and encoding (Lepage, Habib, & Tulving, 1998). The fact that differences between PD patients and controls were found only in the anterior hippocampus might be associated with the functional specialization of the hippocampus along the longitudinal axis (Poppenk, Evensmoen, Moscovitch, & Nadel, 2013).

Based on our findings, we propose that the reduced connectivity in precuneus/superior parietal cortex mainly supports the retrieval deficit hypotheses, where attention plays a crucial role in the encoding and retention phase (Tröster & Fields, 1995). These tasks

are particularly challenging in PD patients when combined with a visual attentional or visuospatial component in the material (cf. BVMT-R-IRS vs. RAVLT-IRS in the encoding and BVMT-R-DR and RAVLT-DR in the retention when retrieving the information). We hypothesize that these primarily attention and orienting to stimuli deficits are leading to bottom-up detrimental effects on memory encoding and might arise as a consequence of cholinergic dysfunction. It has been shown that PD, beyond dopaminergic deficits, might also lead to degeneration of the nucleus basalis of Meynert (NBM) network and subsequent cortical cholinergic deficits (Hall et al., 2014). Accordingly, the reduced connectivity of precuneus to the anterior hippocampus, which also results in a hippocampal deficit in relational binding can be viewed as a result

Table 3

Spearman's Correlations Between Bilateral Anterior Hippocampal Changes in Connectivity and Memory Scores in Parkinson's Disease and Controls

Connectivity	BVMT-R-DR	BVMT-R-IRS	MBT-TIP	MBT-PIP	RAVLT-IRS	RAVLT-DR
Right anterior hippocampus connectivity (TC: 12–37 29)						
<i>rho</i>	.305*	.292*	.357**	.409**	-.159	.126
<i>p</i>	.026	.034	.009	.002	.256	.370
Left anterior hippocampus connectivity 1 (TC: -6–34 56)						
<i>rho</i>	.356**	.382**	.329*	.331*	-.132	.100
<i>p</i>	.009	.005	.016	.016	.348	.474
Left anterior hippocampus connectivity 2 (TC: -30–28 26)						
<i>rho</i>	.424**	.503**	.388**	.429**	.031	.284*
<i>p</i>	.002	.000	.004	.001	.826	.039

Note. MNI coordinates of the target clusters (TC) of the hippocampal connectivity are reported on the left. Correlations shown in Figure 4 are reported in bold. BVMT-R-IRS = Brief Visuospatial Memory Test, revised, immediate recall score the sum of all correct responses given over the three consecutive trials (T1 + T2 + T3; min.–max. 0–36); BVMT-R-DR = the total number of correct words recalled on the delayed recall trial (min.–max. 0–12); RAVLT-IRS = Rey Auditory Verbal Learning Test immediate recall score, the sum of all correct responses given over the five consecutive trials (T1 + T2 + T3 + T4 + T5; min.–max. 0–50); RAVLT-DR = the total number of correct words recalled on the delayed recall trial (T7; min.–max. 0–15); MBT-PIP = number of pairs cued recalled in the paired condition on the MBT (0–16 pairs); TIP = total number of items cued recalled in the paired condition on the MBT (0–32).

* Significant at the .05 level (two-tailed). ** Significant at the .01 level (two-tailed).

of NBM network degeneration with an affliction of the NBM pathway connected to MTL structures (Gratwicke, Jahanshahi, & Foltynie, 2015). These findings support the associative deficit hypothesis (MBT-TIP and severe recognition deficit). The associative deficit is mirrored in the impairment of associative binding (MBT-PIP), independent of visual attentional or visuospatial component (Cohn et al., 2016). Hence the different NBM pathways and their degeneration in PD could shed light on the reduced connectivity in precuneus/superior parietal cortex and between precuneus and anterior hippocampus, thus reconciling both hypotheses from a neural network perspective (Gratwicke et al., 2015).

Of notice is that the reduced hippocampus-precuneus functional connectivity has been reported to be an early sign of Alzheimer's disease (Kim, Kim, & Lee, 2013) and can also be associated with the true nature of cognitive deficit in PD-MCI (Martinez-Horta & Kulisevsky, 2011). Limited evidence in PD comes also from Amboni et al. (2015) who reported a trend between memory and attention/executive scores and the connectivity in the medial prefrontal cortex and from Lebedev et al. (2014), who found that better memory performance correlated with increased prefronto-limbic processing in PD, that is, in orbitofrontal, anterior cingulate, parahippocampal, temporopolar regions (Lebedev et al., 2014). The dissociation between morphological and functional connectivity changes supports the view of PD as a brain disconnection syndrome, in which pathophysiological features lead in the first place to changes in the functional architecture in the brain (Bezdicek et al., 2018; Warren et al., 2012).

However, the relatively small sample size in our study represents a limit, possibly explaining the lack of volumetric between-groups alterations and differences in RAVLT-IRS. Furthermore, we cannot completely exclude, in PD-MCI, that the patients present concomitant PDD + AD pathology because amyloid or tau PET scans or respective biomarkers from the cerebrospinal fluid are not available in the present study (Irwin et al., 2012; Montine et al., 2012). However, we found no differences in Schelten's MTL scale between the groups, indicating no evidence of AD-like structural MRI changes in our sample (Supplemental Table S5 in the online supplemental material).

In conclusion, we propose a comprehensive picture of memory impairment in PD. We reconcile and refine the retrieval deficit and the associative deficit hypotheses regarding the nature of memory impairment in PD coherently, supporting our findings with rigorously defined phenotypes of cognitive impairment in PD and with brain structural and functional connectivity evidence.

References

- Aarsland, D., Creese, B., Politis, M., Chaudhuri, K. R., Ffytche, D. H., Weintraub, D., & Ballard, C. (2017). Cognitive decline in Parkinson disease. *Nature Reviews Neurology*, *13*, 217–231. <http://dx.doi.org/10.1038/nrneuro.2017.27>
- Algarabel, S., Rodríguez, L. A., Escudero, J., Fuentes, M., Peset, V., Pitarque, A., . . . Mazón, J. F. (2010). Recognition by familiarity is preserved in Parkinson's without dementia and Lewy-Body disease. *Neuropsychology*, *24*, 599–607. <http://dx.doi.org/10.1037/a0019221>
- Amboni, M., Tessitore, A., Esposito, F., Santangelo, G., Picillo, M., Vitale, C., . . . Barone, P. (2015). Resting-state functional connectivity associated with mild cognitive impairment in Parkinson's disease. *Journal of Neurology*, *262*, 425–434. <http://dx.doi.org/10.1007/s00415-014-7591-5>
- Ashburner, J., & Friston, K. J. (2000). Voxel-based morphometry—The methods. *NeuroImage*, *11*, 805–821. <http://dx.doi.org/10.1006/nimg.2000.0582>
- Ashburner, J., & Friston, K. J. (2005). Unified segmentation. *NeuroImage*, *26*, 839–851. <http://dx.doi.org/10.1016/j.neuroimage.2005.02.018>
- Balthazar, M. L., Yasuda, C. L., Cendes, F., & Damasceno, B. P. (2010). Learning, retrieval, and recognition are compromised in aMCI and mild AD: Are distinct episodic memory processes mediated by the same anatomical structures? *Journal of the International Neuropsychological Society*, *16*, 205–209. <http://dx.doi.org/10.1017/S1355617709990956>
- Beatty, W. W., Ryder, K. A., Gontkovsky, S. T., Scott, J. G., McSwan, K. L., & Bharucha, K. J. (2003). Analyzing the subcortical dementia syndrome of Parkinson's disease using the RBANS. *Archives of Clinical Neuropsychology*, *18*, 509–520.
- Benedict, R. H. B. (1997). *Brief Visuospatial Memory Test—Revised. Professional manual*. Lutz, FL: Psychological Assessment Resources.
- Beyer, M. K., Bronnick, K. S., Hwang, K. S., Bergsland, N., Tysnes, O. B., Larsen, J. P., . . . Apostolova, L. G. (2013). Verbal memory is associated with structural hippocampal changes in newly diagnosed Parkinson's

- disease. *Journal of Neurology, Neurosurgery & Psychiatry*, 84, 23–28. <http://dx.doi.org/10.1136/jnnp-2012-303054>
- Bezdzicek, O., Ballarini, T., Růžicka, F., Roth, J., Mueller, K., Jech, R., & Schroeter, M. L. (2018). Mild cognitive impairment disrupts attention network connectivity in Parkinson's disease: A combined multimodal MRI and meta-analytical study. *Neuropsychologia*, 112, 105–115. <http://dx.doi.org/10.1016/j.neuropsychologia.2018.03.011>
- Bezdzicek, O., Nikolai, T., Michalec, J., Ruzicka, F., Havrankova, P., Roth, J., . . . Ruzicka, E. (2017). The diagnostic accuracy of Parkinson's disease mild cognitive impairment battery using the Movement Disorder Society Task Force criteria. *Movement Disorders Clinical Practice (Hoboken, N. J.)*, 4, 237–244. <http://dx.doi.org/10.1002/mdc3.12391>
- Bezdzicek, O., Stepankova, H., Moták, L., Axelrod, B. N., Woodard, J. L., Preiss, M., . . . Poreh, A. (2014). Czech version of Rey Auditory Verbal Learning test: Normative data. *Aging, Neuropsychology and Cognition*, 21, 693–721. <http://dx.doi.org/10.1080/13825585.2013.865699>
- Bezdzicek, O., Sulc, Z., Nikolai, T., Stepankova, H., Kopecek, M., Jech, R., & Růžicka, E. (2017). A parsimonious scoring and normative calculator for the Parkinson's disease mild cognitive impairment battery. *The Clinical Neuropsychologist*, 31, 1231–1247. <http://dx.doi.org/10.1080/13854046.2017.1293161>
- Biundo, R., Calabrese, M., Weis, L., Facchini, S., Ricchieri, G., Gallo, P., & Antonini, A. (2013). Anatomical correlates of cognitive functions in early Parkinson's disease patients. *PLoS ONE*, 8(5), e64222. <http://dx.doi.org/10.1371/journal.pone.0064222>
- Broeders, M., de Bie, R. M., Velseboer, D. C., Speelman, J. D., Muslimovic, D., & Schmand, B. (2013). Evolution of mild cognitive impairment in Parkinson disease. *Neurology*, 81, 346–352. <http://dx.doi.org/10.1212/WNL.0b013e31829c5c86>
- Brønneck, K., Alves, G., Aarsland, D., Tysnes, O. B., & Larsen, J. P. (2011). Verbal memory in drug-naïve, newly diagnosed Parkinson's disease. The retrieval deficit hypothesis revisited. *Neuropsychology*, 25, 114–124. <http://dx.doi.org/10.1037/a0020857>
- Brück, A., Kurki, T., Kaasinen, V., Vahlberg, T., & Rinne, J. O. (2004). Hippocampal and prefrontal atrophy in patients with early non-demented Parkinson's disease is related to cognitive impairment. *Journal of Neurology, Neurosurgery & Psychiatry*, 75, 1467–1469. <http://dx.doi.org/10.1136/jnnp.2003.031237>
- Buschke, H. (2014). Rationale of the Memory Binding Test. In L. Nilsson & N. Ohta (Eds.), *Dementia and memory* (pp. 55–71). Hove, UK: Psychology Press.
- Buschke, H., Mowrey, W. B., Ramratan, W. S., Zimmerman, M. E., Loewenstein, D. A., Katz, M. J., & Lipton, R. B. (2017). Memory binding test distinguishes amnesic mild cognitive impairment and dementia from cognitively normal elderly. *Archives of Clinical Neuropsychology*, 32, 29–39.
- Buytenhuijs, E. L., Berger, H. J., Van Spaendonck, K. P., Horstink, M. W., Borm, G. F., & Cools, A. R. (1994). Memory and learning strategies in patients with Parkinson's disease. *Neuropsychologia*, 32, 335–342. [http://dx.doi.org/10.1016/0028-3932\(94\)90135-X](http://dx.doi.org/10.1016/0028-3932(94)90135-X)
- Cavanna, A. E., & Trimble, M. R. (2006). The precuneus: A review of its functional anatomy and behavioural correlates. *Brain: A Journal of Neurology*, 129, 564–583. <http://dx.doi.org/10.1093/brain/awl004>
- Chang, Y. L., Bondi, M. W., Fennema-Notestine, C., McEvoy, L. K., Hagler, D. J., Jr., Jacobson, M. W., . . . the Alzheimer's Disease Neuroimaging Initiative. (2010). Brain substrates of learning and retention in mild cognitive impairment diagnosis and progression to Alzheimer's disease. *Neuropsychologia*, 48, 1237–1247. <http://dx.doi.org/10.1016/j.neuropsychologia.2009.12.024>
- Chen, J., Duan, X., Shu, H., Wang, Z., Long, Z., Liu, D., . . . Zhang, Z. (2016). Differential contributions of subregions of medial temporal lobe to memory system in amnesic mild cognitive impairment: Insights from fMRI study. *Scientific Reports*, 6, 26148. <http://dx.doi.org/10.1038/srep26148>
- Chhatwal, J. P., & Sperling, R. A. (2012). Functional MRI of mnemonic networks across the spectrum of normal aging, mild cognitive impairment, and Alzheimer's disease. *Journal of Alzheimer's Disease*, 31 (Suppl.), S155–167. <http://dx.doi.org/10.3233/jad-2012-120730>
- Chiaravalloti, N. D., Ibarretxe-Bilbao, N., DeLuca, J., Rusu, O., Pena, J., García-Gorostiaga, I., & Ojeda, N. (2014). The source of the memory impairment in Parkinson's disease: Acquisition versus retrieval. *Movement Disorders*, 29, 765–771. <http://dx.doi.org/10.1002/mds.25842>
- Cohen, J. (1988). *Statistical power analysis for the behavioral sciences*. Hillsdale, NJ: Erlbaum.
- Cohn, M., Giannoylis, I., De Belder, M., Saint-Cyr, J. A., & McAndrews, M. P. (2016). Associative reinstatement memory measures hippocampal function in Parkinson's disease. *Neuropsychologia*, 90, 25–32. <http://dx.doi.org/10.1016/j.neuropsychologia.2016.04.026>
- Cohn, M., Moscovitch, M., & Davidson, P. S. (2010). Double dissociation between familiarity and recollection in Parkinson's disease as a function of encoding tasks. *Neuropsychologia*, 48, 4142–4147. <http://dx.doi.org/10.1016/j.neuropsychologia.2010.10.013>
- Costa, A., Monaco, M., Zabberoni, S., Peppe, A., Perri, R., Fadda, L., . . . Carlesimo, G. A. (2014). Free and cued recall memory in Parkinson's disease associated with amnesic mild cognitive impairment. *PLoS ONE*, 9(1), e86233. <http://dx.doi.org/10.1371/journal.pone.0086233>
- Del Tredici, K., & Braak, H. (2016). Review: Sporadic Parkinson's disease: Development and distribution of α -synuclein pathology. *Neuropathology and Applied Neurobiology*, 42, 33–50. <http://dx.doi.org/10.1111/nan.12298>
- Edelstyn, N. M., John, C. M., Shepherd, T. A., Drakeford, J. L., Clark-Carter, D., Ellis, S. J., & Mayes, A. R. (2015). Evidence of an amnesia-like cued-recall memory impairment in nondementing idiopathic Parkinson's disease. *Cortex: A Journal Devoted to the Study of the Nervous System and Behavior*, 71, 85–101. <http://dx.doi.org/10.1016/j.cortex.2015.06.021>
- Edelstyn, N. M., Mayes, A. R., Condon, L., Tunnicliffe, M., & Ellis, S. J. (2007). Recognition, recollection, familiarity and executive function in medicated patients with moderate Parkinson's disease. *Journal of Neuropsychology*, 1, 131–147. <http://dx.doi.org/10.1348/174866407X182565>
- Edelstyn, N. M. J., Shepherd, T. A., Mayes, A. R., Sherman, S. M., & Ellis, S. J. (2010). Effect of disease severity and dopaminergic medication on recollection and familiarity in patients with idiopathic nondementing Parkinson's. *Neuropsychologia*, 48, 1367–1375. <http://dx.doi.org/10.1016/j.neuropsychologia.2009.12.039>
- Emre, M., Aarsland, D., Brown, R., Burn, D. J., Duyckaerts, C., Mizuno, Y., . . . Dubois, B. (2007). Clinical diagnostic criteria for dementia associated with Parkinson's disease. *Movement Disorders*, 22, 1689–1707. <http://dx.doi.org/10.1002/mds.21507>
- Flowers, K. A., Pearce, I., & Pearce, J. M. (1984). Recognition memory in Parkinson's disease. *Journal of Neurology, Neurosurgery & Psychiatry*, 47, 1174–1181. <http://dx.doi.org/10.1136/jnnp.47.11.1174>
- Geurtsen, G. J., Hoogland, J., Goldman, J. G., Schmand, B. A., Troster, A. I., Burn, D. J., & Litvan, I. (2014). Parkinson's disease mild cognitive impairment: Application and validation of the criteria. *Journal of Parkinson's Disease*, 4, 131–137. <http://dx.doi.org/10.3233/jpd-130304>
- Giovanello, K. S., Schnyer, D. M., & Verfaellie, M. (2004). A critical role for the anterior hippocampus in relational memory: Evidence from an fMRI study comparing associative and item recognition. *Hippocampus*, 14, 5–8. <http://dx.doi.org/10.1002/hipo.10182>
- Goldman, J. G., Holden, S., Bernard, B., Ouyang, B., Goetz, C. G., & Stebbins, G. T. (2013). Defining optimal cutoff scores for cognitive impairment using Movement Disorder Society Task Force criteria for mild cognitive impairment in Parkinson's disease. *Movement Disorders*, 28, 1972–1979. <http://dx.doi.org/10.1002/mds.25655>

- Gratwicke, J., Jahanshahi, M., & Foltynie, T. (2015). Parkinson's disease dementia: A neural networks perspective. *Brain: A Journal of Neurology*, *138*, 1454–1476. <http://dx.doi.org/10.1093/brain/awv104>
- Grober, E., & Buschke, H. (1987). Genuine memory deficits in dementia. *Developmental Neuropsychology*, *3*, 13–36. <http://dx.doi.org/10.1080/87565648709540361>
- Hall, H., Reyes, S., Landeck, N., Bye, C., Leanza, G., Double, K., . . . Kirik, D. (2014). Hippocampal Lewy pathology and cholinergic dysfunction are associated with dementia in Parkinson's disease. *Brain*, *137*, 2493–2508.
- Higginson, C. I., Wheelock, V. L., Carroll, K. E., & Sigvardt, K. A. (2005). Recognition memory in Parkinson's disease with and without dementia: Evidence inconsistent with the retrieval deficit hypothesis. *Journal of Clinical and Experimental Neuropsychology*, *27*, 516–528. <http://dx.doi.org/10.1080/13803390490515469>
- Hoogland, J., Boel, J. A., de Bie, R. M. A., Geskus, R. B., Schmand, B. A., Dalrymple-Alford, J. C., . . . the MDS Study Group "Validation of Mild Cognitive Impairment in Parkinson Disease". (2017). Mild cognitive impairment as a risk factor for Parkinson's disease dementia. *Movement Disorders*, *32*, 1056–1065. <http://dx.doi.org/10.1002/mds.27002>
- Hughes, A. J., Daniel, S. E., Kilford, L., & Lees, A. J. (1992). Accuracy of clinical diagnosis of idiopathic Parkinson's disease: A clinicopathological study of 100 cases. *Journal of Neurology, Neurosurgery, and Psychiatry*, *55*, 181–184. <http://dx.doi.org/10.1136/jnnp.55.3.181>
- Irwin, D. J., White, M. T., Toledo, J. B., Xie, S. X., Robinson, J. L., Van Deerlin, V., . . . Trojanowski, J. Q. (2012). Neuropathologic substrates of Parkinson disease dementia. *Annals of Neurology*, *72*, 587–598. <http://dx.doi.org/10.1002/ana.23659>
- Ivnik, R. J., Malec, J. F., Tangalos, E. G., Petersen, R. C., Kokmen, E., & Kurland, L. T. (1990). The Auditory-Verbal Learning Test (AVLT): Norms for ages 55 years and older. *Psychological Assessment: A Journal of Consulting and Clinical Psychology*, *2*, 304–312. <http://dx.doi.org/10.1037/1040-3590.2.3.304>
- Janvin, C. C., Larsen, J. P., Aarsland, D., & Hugdahl, K. (2006). Subtypes of mild cognitive impairment in Parkinson's disease: Progression to dementia. *Movement Disorders*, *21*, 1343–1349. <http://dx.doi.org/10.1002/mds.20974>
- Junqué, C., Ramírez-Ruiz, B., Tolosa, E., Summerfield, C., Martí, M. J., Pastor, P., . . . Mercader, J. M. (2005). Amygdalar and hippocampal MRI volumetric reductions in Parkinson's disease with dementia. *Movement Disorders*, *20*, 540–544. <http://dx.doi.org/10.1002/mds.20371>
- Kim, J., Kim, Y. H., & Lee, J. H. (2013). Hippocampus-precuneus functional connectivity as an early sign of Alzheimer's disease: A preliminary study using structural and functional magnetic resonance imaging data. *Brain Research*, *1495*, 18–29. <http://dx.doi.org/10.1016/j.brainres.2012.12.011>
- Kircher, T., Weis, S., Leube, D., Freymann, K., Erb, M., Jessen, F., . . . Krach, S. (2008). Anterior hippocampus orchestrates successful encoding and retrieval of non-relational memory: An event-related fMRI study. *European Archives of Psychiatry and Clinical Neuroscience*, *258*, 363–372. <http://dx.doi.org/10.1007/s00406-008-0805-z>
- Koen, J. D., & Yonelinas, A. P. (2014). The effects of healthy aging, amnesic mild cognitive impairment, and Alzheimer's disease on recollection and familiarity: A meta-analytic review. *Neuropsychology Review*, *24*, 332–354. <http://dx.doi.org/10.1007/s11065-014-9266-5>
- Kopeček, M., Stepanková, H., Lukavský, J., Ripová, D., Nikolai, T., & Bezdicek, O. (2017). Montreal cognitive assessment (MoCA): Normative data for old and very old Czech adults. *Applied Neuropsychology: Adult*, *24*, 23–29. <http://dx.doi.org/10.1080/23279095.2015.1065261>
- Laakso, M. P., Partanen, K., Riekkinen, P., Lehtovirta, M., Helkala, E. L., Hallikainen, M., . . . Soininen, H. (1996). Hippocampal volumes in Alzheimer's disease, Parkinson's disease with and without dementia, and in vascular dementia: An MRI study. *Neurology*, *46*, 678–681. <http://dx.doi.org/10.1212/WNL.46.3.678>
- Lebedev, A. V., Westman, E., Simmons, A., Lebedeva, A., Siepel, F. J., Pereira, J. B., & Aarsland, D. (2014). Large-scale resting state network correlates of cognitive impairment in Parkinson's disease and related dopaminergic deficits. *Frontiers in Systems Neuroscience*, *8*, 45. <http://dx.doi.org/10.3389/fnsys.2014.00045>
- Lee, J. E., Park, H. J., Song, S. K., Sohn, Y. H., Lee, J. D., & Lee, P. H. (2010). Neuroanatomic basis of amnesic MCI differs in patients with and without Parkinson disease. *Neurology*, *75*, 2009–2016. <http://dx.doi.org/10.1212/WNL.0b013e3181ff96bf>
- Lepage, M., Habib, R., & Tulving, E. (1998). Hippocampal PET activations of memory encoding and retrieval: The HIPER model. *Hippocampus*, *8*, 313–322. [http://dx.doi.org/10.1002/\(SICI\)1098-1063\(1998\)8:4<313::AID-HIPO1>3.0.CO;2-I](http://dx.doi.org/10.1002/(SICI)1098-1063(1998)8:4<313::AID-HIPO1>3.0.CO;2-I)
- Litvan, I., Aarsland, D., Adler, C. H., Goldman, J. G., Kulisevsky, J., Mollenhauer, B., . . . Weintraub, D. (2011). MDS Task Force on mild cognitive impairment in Parkinson's disease: Critical review of PD-MCI. *Movement Disorders*, *26*, 1814–1824. <http://dx.doi.org/10.1002/mds.23823>
- Litvan, I., Goldman, J. G., Tröster, A. I., Schmand, B. A., Weintraub, D., Petersen, R. C., . . . Emre, M. (2012). Diagnostic criteria for mild cognitive impairment in Parkinson's disease: Movement Disorder Society Task Force guidelines. *Movement Disorders*, *27*, 349–356. <http://dx.doi.org/10.1002/mds.24893>
- Martínez-Horta, S., & Kulisevsky, J. (2011). Is all cognitive impairment in Parkinson's disease "mild cognitive impairment"? *Journal of Neural Transmission*, *118*, 1185–1190. <http://dx.doi.org/10.1007/s00702-011-0675-9>
- Miller, B. T., & D'Esposito, M. (2012). Spatial and temporal dynamics of cortical networks engaged in memory encoding and retrieval. *Frontiers in Human Neuroscience*, *6*, 109. <http://dx.doi.org/10.3389/fnhum.2012.00109>
- Montine, T. J., Phelps, C. H., Beach, T. G., Bigio, E. H., Cairns, N. J., Dickson, D. W., . . . the National Institute on Aging, & the Alzheimer's Association. (2012). National Institute on Aging-Alzheimer's Association guidelines for the neuropathologic assessment of Alzheimer's disease: A practical approach. *Acta Neuropathologica*, *123*, 1–11. <http://dx.doi.org/10.1007/s00401-011-0910-3>
- Muslimović, D., Post, B., Speelman, J. D., & Schmand, B. (2005). Cognitive profile of patients with newly diagnosed Parkinson disease. *Neurology*, *65*, 1239–1245. <http://dx.doi.org/10.1212/01.wnl.0000180516.69442.95>
- Muslimović, D., Schmand, B., Speelman, J. D., & de Haan, R. J. (2007). Course of cognitive decline in Parkinson's disease: A meta-analysis. *Journal of the International Neuropsychological Society*, *13*, 920–932. <http://dx.doi.org/10.1017/S1355617707071160>
- Naveh-Benjamin, M. (2000). Adult age differences in memory performance: Tests of an associative deficit hypothesis. *Journal of Experimental Psychology: Learning, Memory, and Cognition*, *26*, 1170–1187. <http://dx.doi.org/10.1037/0278-7393.26.5.1170>
- Pagonabarraga, J., & Kulisevsky, J. (2012). Cognitive impairment and dementia in Parkinson's disease. *Neurobiology of Disease*, *46*, 590–596. <http://dx.doi.org/10.1016/j.nbd.2012.03.029>
- Pan, P. L., Shi, H. C., Zhong, J. G., Xiao, P. R., Shen, Y., Wu, L. J., . . . Li, H. L. (2013). Gray matter atrophy in Parkinson's disease with dementia: Evidence from meta-analysis of voxel-based morphometry studies. *Neurological Sciences*, *34*, 613–619. <http://dx.doi.org/10.1007/s10072-012-1250-3>
- Papp, K. V., Amariglio, R. E., Mormino, E. C., Hedden, T., Dekhytar, M., Johnson, K. A., . . . Rentz, D. M. (2015). Free and cued memory in relation to biomarker-defined abnormalities in clinically normal older adults and those at risk for Alzheimer's disease. *Neuropsychologia*, *73*, 169–175. <http://dx.doi.org/10.1016/j.neuropsychologia.2015.04.034>
- Petrou, M., Dwamena, B. A., Foerster, B. R., MacEachern, M. P., Bohnen, N. I., Müller, M. L., . . . Frey, K. A. (2015). Amyloid deposition in

- Parkinson's disease and cognitive impairment: A systematic review. *Movement Disorders*, 30, 928–935. <http://dx.doi.org/10.1002/mds.26191>
- Pigott, K., Rick, J., Xie, S. X., Hurtig, H., Chen-Plotkin, A., Duda, J. E., . . . Weintraub, D. (2015). Longitudinal study of normal cognition in Parkinson disease. *Neurology*, 85, 1276–1282. <http://dx.doi.org/10.1212/WNL.0000000000002001>
- Pirogovsky-Turk, E., Filoteo, J. V., Litvan, I., & Harrington, D. L. (2015). Structural MRI Correlates of Episodic Memory Processes in Parkinson's Disease Without Mild Cognitive Impairment. *Journal of Parkinson's Disease*, 5, 971–981. <http://dx.doi.org/10.3233/JPD-150652>
- Poppenk, J., Evensmoen, H. R., Moscovitch, M., & Nadel, L. (2013). Long-axis specialization of the human hippocampus. *Trends in Cognitive Sciences*, 17, 230–240. <http://dx.doi.org/10.1016/j.tics.2013.03.005>
- Power, J. D., Barnes, K. A., Snyder, A. Z., Schlaggar, B. L., & Petersen, S. E. (2012). Spurious but systematic correlations in functional connectivity MRI networks arise from subject motion. *NeuroImage*, 59, 2142–2154. <http://dx.doi.org/10.1016/j.neuroimage.2011.10.018>
- Reid, W. G., Hely, M. A., Morris, J. G., Loy, C., & Halliday, G. M. (2011). Dementia in Parkinson's disease: A 20-year neuropsychological study (Sydney Multicentre Study). *Journal of Neurology, Neurosurgery & Psychiatry*, 82, 1033–1037. <http://dx.doi.org/10.1136/jnnp.2010.232678>
- Rentz, D. M., Parra Rodriguez, M. A., Amariglio, R., Stern, Y., Sperling, R., & Ferris, S. (2013). Promising developments in neuropsychological approaches for the detection of preclinical Alzheimer's disease: A selective review. *Alzheimer's Research and Therapy*, 5, 58. <http://dx.doi.org/10.1186/alzrt222>
- Rodriguez, L. A., Algarabel, S., & Escudero, J. (2014). Exploring recollection and familiarity impairments in Parkinson's disease. *Journal of Clinical and Experimental Neuropsychology*, 36, 494–506. <http://dx.doi.org/10.1080/13803395.2014.909386>
- Saeed, U., Compagnone, J., Aviv, R. I., Strafella, A. P., Black, S. E., Lang, A. E., & Masellis, M. (2017). Imaging biomarkers in Parkinson's disease and Parkinsonian syndromes: Current and emerging concepts. *Translational Neurodegeneration*, 6, 8. <http://dx.doi.org/10.1186/s40035-017-0076-6>
- Saka, E., & Elibol, B. (2009). Enhanced cued recall and clock drawing test performances differ in Parkinson's and Alzheimer's disease-related cognitive dysfunction. *Parkinsonism & Related Disorders*, 15, 688–691. <http://dx.doi.org/10.1016/j.parkreldis.2009.04.008>
- Sarazin, M., Berr, C., De Rotrou, J., Fabrigoule, C., Pasquier, F., Legrain, S., . . . Dubois, B. (2007). Amnesic syndrome of the medial temporal type identifies prodromal AD: A longitudinal study. *Neurology*, 69, 1859–1867. <http://dx.doi.org/10.1212/01.wnl.0000279336.36610.f7>
- Schacter, D. L., Alpert, N. M., Savage, C. R., Rauch, S. L., & Albert, M. S. (1996). Conscious recollection and the human hippocampal formation: Evidence from positron emission tomography. *Proceedings of the National Academy of Sciences of the United States of America*, 93, 321–325. <http://dx.doi.org/10.1073/pnas.93.1.321>
- Schrag, A., Siddiqui, U. F., Anastasiou, Z., Weintraub, D., & Schott, J. M. (2017). Clinical variables and biomarkers in prediction of cognitive impairment in patients with newly diagnosed Parkinson's disease: A cohort study. *The Lancet Neurology*, 16, 66–75. [http://dx.doi.org/10.1016/S1474-4422\(16\)30328-3](http://dx.doi.org/10.1016/S1474-4422(16)30328-3)
- Spillantini, M. G., Schmidt, M. L., Lee, V. M., Trojanowski, J. Q., Jakes, R., & Goedert, M. (1997). Alpha-synuclein in Lewy bodies. *Nature*, 388, 839–840. <http://dx.doi.org/10.1038/42166>
- Squire, L. R. (2004). Memory systems of the brain: A brief history and current perspective. *Neurobiology of Learning and Memory*, 82, 171–177. <http://dx.doi.org/10.1016/j.nlm.2004.06.005>
- Tam, C. W., Burton, E. J., McKeith, I. G., Burn, D. J., & O'Brien, J. T. (2005). Temporal lobe atrophy on MRI in Parkinson disease with dementia: A comparison with Alzheimer disease and dementia with Lewy bodies. *Neurology*, 64, 861–865. <http://dx.doi.org/10.1212/01.WNL.0000153070.82309.D4>
- Tanner, J. J., Mareci, T. H., Okun, M. S., Bowers, D., Libon, D. J., & Price, C. C. (2015). Temporal Lobe and Frontal-Subcortical Dissociations in Non-Demented Parkinson's Disease with Verbal Memory Impairment. *PLoS ONE*, 10(7), e0133792. <http://dx.doi.org/10.1371/journal.pone.0133792>
- Thomas, K. R., Eppig, J., Edmonds, E. C., Jacobs, D. M., Libon, D. J., Au, R., . . . the Alzheimer's Disease Neuroimaging Initiative. (2018). Word-list intrusion errors predict progression to mild cognitive impairment. *Neuropsychology*, 32, 235–245. <http://dx.doi.org/10.1037/neu0000413>
- Tomlinson, C. L., Stowe, R., Patel, S., Rick, C., Gray, R., & Clarke, C. E. (2010). Systematic review of levodopa dose equivalency reporting in Parkinson's disease. *Movement Disorders*, 25, 2649–2653. <http://dx.doi.org/10.1002/mds.23429>
- Tröster, A. I., & Fields, J. A. (1995). Frontal cognitive function and memory in Parkinson's disease: Toward a distinction between prospective and declarative memory impairments? *Behavioural Neurology*, 8, 59–74. <http://dx.doi.org/10.1155/1995/167286>
- Tulving, E., & Thomson, D. M. (1973). Encoding specificity and retrieval processes in episodic memory. *Psychological Review*, 80, 352–373. <http://dx.doi.org/10.1037/h0020071>
- Vyhnalek, M., Nikolai, T., Andel, R., Nedelska, Z., Rubinova, E., Markova, H., . . . Hort, J. (2014). Neuropsychological correlates of hippocampal atrophy in memory testing in nondemented older adults. *Journal Alzheimer's Disease*, 42 (Suppl. 3), S81–S90. <http://dx.doi.org/10.3233/jad-132642>
- Warren, J. D., Rohrer, J. D., & Hardy, J. (2012). Disintegrating brain networks: From syndromes to molecular nexopathies. *Neuron*, 73, 1060–1062. <http://dx.doi.org/10.1016/j.neuron.2012.03.006>
- Whittington, C. J., Podd, J., & Kan, M. M. (2000). Recognition memory impairment in Parkinson's disease: Power and meta-analyses. *Neuropsychology*, 14, 233–246. <http://dx.doi.org/10.1037/0894-4105.14.2.233>
- Whittington, C. J., Podd, J., & Stewart-Williams, S. (2006). Memory deficits in Parkinson's disease. *Journal of Clinical and Experimental Neuropsychology*, 28, 738–754. <http://dx.doi.org/10.1080/13803390.590954236>
- Williams-Gray, C. H., Foltynie, T., Brayne, C. E., Robbins, T. W., & Barker, R. A. (2007). Evolution of cognitive dysfunction in an incident Parkinson's disease cohort. *Brain: A Journal of Neurology*, 130, 1787–1798. <http://dx.doi.org/10.1093/brain/awm111>
- Williams-Gray, C. H., Mason, S. L., Evans, J. R., Foltynie, T., Brayne, C., Robbins, T. W., & Barker, R. A. (2013). The CamPaIGN study of Parkinson's disease: 10-year outlook in an incident population-based cohort. *Journal of Neurology, Neurosurgery, and Psychiatry*, 84, 1258–1264. <http://dx.doi.org/10.1136/jnnp-2013-305277>
- Zgaljardic, D. J., Borod, J. C., Foldi, N. S., & Mattis, P. (2003). A review of the cognitive and behavioral sequelae of Parkinson's disease: Relationship to frontostriatal circuitry. *Cognitive and Behavioral Neurology*, 16, 193–210. <http://dx.doi.org/10.1097/00146965-200312000-00001>
- Zimmerman, M. E., Pan, J. W., Hetherington, H. P., Katz, M. J., Verghese, J., Buschke, H., . . . Lipton, R. B. (2008). Hippocampal neurochemistry, neuromorphometry, and verbal memory in nondemented older adults. *Neurology*, 70, 1594–1600. <http://dx.doi.org/10.1212/01.wnl.0000306314.77311.be>

Received March 27, 2018

Revision received August 20, 2018

Accepted August 20, 2018 ■

8 DISCUSSION

Medical imaging, beside other biomarkers, will play an important role in modern clinical diagnosis. Hence, more and more diagnostic criteria of neurodegenerative diseases are amended incorporating recent findings of disease-related brain alterations (Albert et al., 2011; Dubois et al., 2014; Gorno-Tempini et al., 2011; Rascovsky et al., 2011). MRI scanners are nearly available in all clinics and imaging is incorporated into clinical routine for assessing neurodegenerative diseases. Research should take advantage of this and develop diagnostic criteria including medical imaging. Yet, diagnostic decision-making still primarily depends on clinical variables. Hence, we are in need for generalized, quantifiable image-based markers to independently and accurately diagnose patients. Especially in atypical parkinsonian syndromes, imaging is applied only as supportive or exclusion criterion. Hence, objectively assessed MRI variables are needed and expected to lead to more independent, improved medical diagnoses. The task of research is to develop approaches that can be translated into clinical and radiological routine when assessing and diagnosing patients. This will be even more important when treatment and medication based on underlying histopathologies is available. As our society ages we need new approaches to diagnose, monitor progression, and treat diseases. MRI is an outstanding tool in this case: applied for diagnostics and research purposes in in vivo tissue. The following section discusses the results of my projects altogether.

8.1 Main Findings

Our aim was to investigate the neural correlates of parkinsonian syndromes. Conducting data-driven meta-analyses, voxel-based morphometry analysis, and support-vector machine classification of multi-centric MRI data, we identified and applied potential neuroimaging biomarkers in the diseases of Parkinson's disease, progressive supranuclear palsy, and corticobasal syndrome.

Studies 1 & 2: Identifying Disease-Specific Patterns by Meta-Analyses.

First part of the thesis concerned quantitative and systematic meta-analyses

on imaging data, which find convergence of the literature to identify disease-specific patterns to disentangle parkinsonian syndromes. We investigated the prototypical neural correlates of Parkinson's disease (PD) and progressive supranuclear palsy (PSP) (Study 1 & 2, Albrecht et al. (2018, 2019a)). To reveal disease-affected brain regions across studies we double-validated results by applying two widely used meta-analytical algorithms considering only the overlap as significant result. We investigated impaired gray matter, white matter, and metabolism alterations in 1,767 patients with PD and 210 patients with PSP in comparison with healthy controls. In PSP white matter studies converged in the bilateral superior/middle cerebellar pedunculi, cerebral pedunculi, and midbrain and gray matter studies in the midbrain confirming proposed pathognomonic imaging markers. Subtraction analyses directly comparing the aforesaid regions by integrating white and gray matter atrophy of PSP and PD patients underline the disease-specificity of midbrain atrophy by quantitatively comparing atrophy patterns. Furthermore, effect size meta-analyses confirm that midbrain metrics generally perform very well in separating PSP from multiple system atrophy and PD yielding strong effect sizes. On the other hand, in PD meta-analyses, structural MRI showed only minor focal gray matter atrophy in the middle occipital gyrus, indicating that this may not be the optimal method for disease identification when compared to healthy controls. Interestingly, glucose metabolism changes seem to be more specific to PD affecting the bilateral inferior parietal cortex and left caudate nucleus.

Thus, the meta-analytically identified alterations in PSP can be regarded as disease-specific, as we compared results with whole-brain, region-of-interest, and subtraction meta-analyses to other neurodegenerative diseases. In PD, structural MRI revealed inconsistent results. The identified hypometabolism was not unique and is also found in other neurodegenerative diseases like Alzheimer's disease.

Study 3: Obtaining Disease-Related Regions and Classifying the Disease by Voxel-Based Morphometry and Support-Vector Machine. Second part of the thesis focused on multi-centric group data analyses to investigate neural underpinnings and discriminate disease and clinical syndrome in single patients (Study 3, Albrecht et al. (2019b)). In a voxel-based morphometry analysis - a standard tool in detecting volumetric brain

changes - we found gray matter volume differences in asymmetric frontotemporal and occipital regions, motor areas, and the insulae in patients with corticobasal syndrome (CBS). Characteristic for an unique disease-related symptom, alien/ anarchic limb phenomenon, was the frontoparietal gyrus including the supplementary motor area contralateral to the side of the affected limb. A cutting-edge multivariate pattern recognition algorithm – support-vector machine classification – was used to predict patients with the clinical phenotype of CBS and CBS with alien/anarchic limb phenomenon. The support-vector machine distinguished (i) patients with CBS from healthy controls and distinguished (ii) between patients just having CBS and patients with CBS having alien/anarchic limb phenomenon. Whereas the first approach predicts the disease, the second predicts one important and very interesting clinical syndrome individually. The support-vector machine classification was trained using whole-brain structural MRI data and later trained on a disease-specific mask of atrophy pattern obtained by our recent meta-analysis (Appendix, Albrecht et al. (2017)). The prediction of the disease among controls yielded a high accuracy of 79.0%. The prediction of the specific syndrome within a disease reached an accuracy of 81.3%. Applying the meta-analytical mask lead to similar stable results. Due to two groups, 50% represents chance level in both analyses.

Our results highlight that we can identify patients and controls by objective pattern recognition. Furthermore, we were able to reliably predict a specific clinical syndrome within a disease. This was shown even in a small sample of 8 patients. Of note, we successfully applied a disease-specific mask for prediction: discrimination remained stable when adding the meta-analytical mask. This mask was obtained from our recent study, which disentangled the clinical syndrome of CBS and underlying histopathology of corticobasal degeneration with meta-analyses (Appendix, Albrecht et al. (2017)). We stratified the analyses according to clinical syndrome, proven histopathology, and a conjunction of both results. In CBS, we identified gray matter loss in the basal ganglia/thalamus, frontal, parietal, and temporal lobes. CBD was related to atrophy in the thalamus, frontal, temporal, and occipital lobes. A conjunction analysis combined the results of both cohorts by overlaying them. Here, we found the bilateral thalamus, the bilateral posterior frontomedian cortex, posterior midcingulate cortex and pre-/ supplementary motor area, and the left posterior superior and middle

frontal gyrus/ precentral gyrus as affected. After comparing results qualitatively with other meta-analysis of neurodegenerative diseases, we proposed the region of the pre-/ supplementary motor area and posterior mid-cingulate/ frontomedian cortex as an imaging biomarker. Findings of the voxel-based morphometry analysis in CBS are similar to the comprehensive meta-analyses, thus we replicated the suggested imaging biomarker from the meta-analyses. It should be mentioned that histopathological evaluation was only available in one patient, so underlying neurodegeneration could not be confirmed for the whole group. CBS can be associated with various pathologies. Up to now, the multi-centric cohort is clinically evaluated by experienced experts, which should reduce a bias of misdiagnoses. Nevertheless, we cannot exclude the possibility that other pathologies influenced the results. Atrophy in our multi-centric cohort overlaps with frontotemporal lobar degeneration, Alzheimer's disease, PSP, and PD. All aforementioned pathologies can possibly underly CBS. Yet, CBD remains the most frequent pathology of CBS.

8.2 Statistical Approaches to Find Imaging Biomarker

Univariate Approach. Voxel-based morphometry and hence, also meta-analysis are defined as univariate approaches. Only single variables are analyzed to describe the data and its pattern, thus the results are not causes or relationships. We could replicate the resulting regions from the recent meta-analysis of CBS in our voxel-based morphometry analysis. Still, voxel-based morphometry and meta-analysis are different approaches. An important difference is the underlying methodical technique. Meta-analyses integrate single maxima from different studies and do not consider the combined clusters. On the other hand, voxel-based morphometry analyses also consider maxima but from a single study. Results of both analyses are interpreted on cluster- and not on maxima-level. Further, the variance between different studies in meta-analysis is likely to be higher than between single subjects in a voxel-based morphometry analysis. Nevertheless, one can compare and replicate results of both approaches when investigating the same variable, namely brain volume differences.

Multivariate Approach. Machine learning considers multiple variables and whole patterns - so called multivariate approach - leading to a different analyses of the data. Indeed, in Study 3 (Albrecht et al., 2019b) voxel-based morphometry - univariate approach - was not able to detect regional differences of gray matter volume when comparing patients with and without alien/ anarchic limb phenomenon voxel-wise. Only the comparison of healthy controls with patients showed regional gray matter volume differences that underly alien/ anarchic limb phenomenon. Interestingly, support-vector machine classification was able to detect patterns that identify alien/ anarchic limb phenomenon in a group of patients with CBS. The prediction not only of a disease but especially of a syndrome yields the potential to inform about not obviously detectable symptoms or even treatment selection. Furthermore, even the whole concept of disease entities and underlying pathologies can be probed by the means of machine learning. One should also consider that if a classification model performs poor in distinguishing between patients and healthy controls or predicting symptoms, it may also be due to a questionable disease entity model. There are already abundant examples of application of machine learning in the literature. Not only single-disease classification is possible, more clinical utility is gained when these classification models also incorporate often confounded diseases. By the means of [18F]-fluorodeoxyglucose-positron emission tomography it was already shown that an algorithm can even outperform movement disorder specialists in diagnosing PD, multiple system atrophy, and PSP (Tang et al., 2010). Another promising application is treatment prediction leading to a precision medicine approach (Study 4, Ballarini et al. (2019)). Treatment can be customized and even adjusted according to brain signatures of the patients, lowering side effects and unresponsive drug application at all. Further medical applications remain ongoing research.

8.3 Brain Alterations and their Utility as Imaging Biomarker

In general, our results are completely consistent with the recent move toward the incorporation of MRI data in the clinical routine and diagnostic criteria. Nevertheless, the proposed neuroimaging biomarkers still need to be validated in independent cohorts and on a single-patient level. This kind of verification and integration of neuroimaging as a criterion is already suc-

cessfully performed - for example in primary progressive aphasia. Here, diagnostic imaging criteria were proposed by Gorno-Tempini et al. (2011) based on previous neuroimaging studies and later statistically validated by independent meta-analyses (Bisenius et al., 2016). Imaging-supported diagnosis is even considered as the higher certainty level of classification: patients need to meet clinical criteria plus showing the neuroimaging patterns. Furthermore, Bisenius et al. (2016) independently confirmed in a cohort of 396 patients with conjunction and disjunction meta-analyses the specificity of the proposed diagnostic neuroimaging criteria. Note that meta-analytical results suggested to stratify criteria into metabolism and structural changes. Other studies probed in large, independent, multi-center patient cohorts the imaging criteria for frontotemporal lobar degeneration and Alzheimer's disease (Dukart et al., 2013, 2011). By the means of support-vector machine classification and the use of regional brain alterations, both diseases could be reliably distinguished with accuracies up to 100%. Further studies evidence that for both diseases the neuroimaging patterns considerably increase diagnostic accuracy as compared to clinical evaluation (Rascovsky et al., 2002; Dubois et al., 2007; Kipps et al., 2009). For these reasons, incorporation into diagnostic criteria is an advisable step toward higher accuracy of diagnosis.

8.4 Limitations

The thesis was done according to good scientific practice standards. In spite of all our efforts, our studies recognize some limitations. First of all, the included studies in the meta-analyses and our CBS cohort lack in histopathological evaluation, as autopsy confirmation is extremely rare. Hence, we can only infer the underlying neurodegeneration by their typical clinical representation. Second, methodological and technical differences exist among the included studies in the meta-analyses and also among our multi-centric data. Indeed, field-strength of MR scanners, processing protocols, or data modulation differ among the single studies in the meta-analyses. However, the impact of these differences on the results should be minor since within the studies patients and controls have been investigated by the same protocols and scanner. Further, the meta-analytical algorithms only take maxima into account and not the cluster size that is more biased

by this heterogeneity. For the multi-centric data, standard operating procedure protocols ensure comparability of the acquired data minimizing variance. Accordingly, future validation of the results of our analyses in independent cohorts is necessary. Specificity and sensitivity of the suggested disease-specific brain regions for differential diagnosis should be validated in large, preferably multi-center, and independent patient cohorts. This approach has already been successfully applied to other neurodegenerative diseases such as Alzheimer's disease and frontotemporal lobar degeneration (Dukart et al., 2013, 2011). Furthermore, we recognize also some limitations in the utility of machine learning. Overall, the generalizability of the results needs to be proven in independent cohorts and later on a single-patient level to serve as an outcome with diagnostic value. Here, ethical reasons might guide how high the accuracy of a classification model needs to be and how many false positives are allowed for a valid clinical decision-making. On the other hand, models 100% accurate may be unrealistic since also disease diagnosis yet primarily depends on clinical evaluation by specialists. To enhance interpretability of machine learning outcome, it is advantageous to compare results to other analytical approaches such as meta-analyses including samples from various cohorts or voxel-based morphometry.

8.5 Contributions of the Current Thesis and Future Directions

The current PhD thesis investigates the neural correlates of parkinsonian syndromes. We aimed at proposing neuroimaging biomarkers for parkinsonian syndromes and apply them in subsequent analyses. For PSP regional atrophy in midbrain and cerebral/ cerebellar pedunculi can be seen as specific disease-related pattern, supporting the incorporation into diagnostic criteria. On the other hand, in PD hypometabolism is more sensitive than structural atrophy, nevertheless not unique for the disease. By using disease-specific patterns as mask as well as whole-brain data, we were able to distinguish patients with CBS from healthy controls and even predict a syndrome within clinical disease up to 81% accurate.

Still, there are many open questions for future research. Our biomarker builds a cornerstone for better disease diagnosis. Specifically, the prediction of histopathology will be a necessary step in patient's appropriate treat-

ment. Scientists are developing medications targeting the specific pathologic protein causing the neurodegeneration. Therefore, an improvement in ante-mortem diagnosis of each pathology underlying clinical syndromes is essential. To achieve this, it is of particular interest to fuel a standard in serial assessments of clinical, psychological, laboratory, and imaging features to better understand the natural history of parkinsonian syndromes. Especially, in rare atypical parkinsonian syndromes such as CBS and PSP comparable data acquisition is needed to pool data. A first step toward this goal is the diagnosis according to the recently amended consensus criteria (Armstrong et al., 2013; Höglinger et al., 2017; Postuma et al., 2015). Another step is the development of multi-center studies and consortia applying standard operating procedure protocols and enabling comparable datasets. The aforementioned remarks only include some of the challenges future research has to face to accurately diagnose diseases and ease symptoms. In particular, developing a cure for neurodegenerative diseases remains the overall goal.

9 REFERENCES

- M. S. Albert, S. T. DeKosky, D. Dickson, B. Dubois, H. H. Feldman, N. C. Fox, A. Gamst, D. M. Holtzman, W. J. Jagust, R. C. Petersen, et al. The diagnosis of mild cognitive impairment due to alzheimer's disease: Recommendations from the national institute on aging-alzheimer's association workgroups on diagnostic guidelines for alzheimer's disease. *Alzheimer's & dementia*, 7(3):270–279, 2011.
- F. Albrecht, S. Bisenius, R. M. Schaack, J. Neumann, and M. L. Schroeter. Disentangling the neural correlates of corticobasal syndrome and corticobasal degeneration with systematic and quantitative ale meta-analyses. *npj Parkinson's Disease*, 3(1):12, 2017.
- F. Albrecht, T. Ballarini, J. Neumann, and M. L. Schroeter. Fdg-pet hypometabolism is more sensitive than mri atrophy in parkinson's disease: A whole-brain multimodal imaging meta-analysis. *NeuroImage: Clinical*, 2018.
- F. Albrecht, S. Bisenius, J. Neumann, J. Whitwell, and M. L. Schroeter. Atrophy in midbrain & cerebral/cerebellar pedunculi is characteristic for progressive supranuclear palsy—a double-validation whole-brain meta-analysis. *NeuroImage: Clinical*, page 101722, 2019a.
- F. Albrecht, K. Mueller, T. Ballarini, L. Lampe, J. Diehl-Schmid, K. Fassbender, K. Fließbach, H. Jahn, R. Jech, J. Kassubek, J. Kornhuber, B. Landwehrmeyer, M. Lauer, A. C. Ludolph, E. Lyros, J. Prudlo, A. Schneider, M. Synofzik, J. Wiltfang, A. Danek, M. Otto, S. Anderl-Straub, K. Brügggen, M. Fischer, H. Förstl, A. Hammer, G. Homola, W. Just, J. Levin, N. Marroquin, A. Marschhauser, M. Nagl, T. Oberstein, M. Polyakova, H. Pellokofer, T. Richter-Schmidinger, C. Rossmeier, K. Schuemberg, E. Semler, A. Spottke, P. Steinacker, A. Thöne-Otto, I. Uttner, H. Zech, and M. L. Schroeter. Unraveling corticobasal syndrome and alien limb syndrome with structural brain imaging. *Cortex*, 117: 33 – 40, 2019b. doi: <https://doi.org/10.1016/j.cortex.2019.02.015>.
- M. R. Arbabshirani, S. Plis, J. Sui, and V. D. Calhoun. Single subject prediction of brain disorders in neuroimaging: promises and pitfalls. *Neuroimage*, 145:137–165, 2017.
- M. J. Armstrong, I. Litvan, A. E. Lang, T. H. Bak, K. P. Bhatia, B. Borroni, A. L. Boxer, D. W. Dickson, M. Grossman, M. Hallett, et al. Criteria for the diagnosis of corticobasal degeneration. *Neurology*, 80(5):496–503, 2013.
- J. Ashburner and K. J. Friston. Voxel-based morphometry—the methods. *Neuroimage*, 11(6):805–821, 2000.
- T. Ballarini, K. Mueller, F. Albrecht, F. Růžička, O. Bezdicek, E. Růžička, J. Roth, J. Vymazal, R. Jech, and M. L. Schroeter. Regional gray matter changes and age predict individual treatment response in parkinson's disease. *NeuroImage: Clinical*, 21:101636, 2019. ISSN 2213-1582. doi: <https://doi.org/10.1016/j.nicl.2018.101636>. URL <http://www.sciencedirect.com/science/article/pii/S221315821830384X>.

- M. F. Bear, B. Connors, and M. Paradiso. Neuroscience: Exploring the brain. 2007. *Computational and Mathematical Methods in Medicine Gastroenterology Research and Practice Evidence-Based Complementary and Alternative Medicine*, 2014, 2009.
- O. Bezdicek, T. Ballarini, H. Buschke, F. Růžička, J. Roth, F. Albrecht, E. Růžička, K. Mueller, M. L. Schroeter, and R. Jech. Memory impairment in parkinson's disease: The retrieval versus associative deficit hypothesis revisited and reconciled. *Neuropsychology*, 33(3): 391–405, 2019. ISSN 1931-1559(Electronic),0894-4105(Print).
- S. Bisenius, J. Neumann, and M. L. Schroeter. Validating new diagnostic imaging criteria for primary progressive aphasia via anatomical likelihood estimation meta-analyses. *European journal of neurology*, 23(4):704–712, 2016.
- B. F. Boeve. The multiple phenotypes of corticobasal syndrome and corticobasal degeneration: implications for further study. *Journal of Molecular Neuroscience*, 45(3):350, 2011.
- R. A. Cohen and L. H. Sweet. Brain imaging in behavioral medicine and clinical neuroscience: Synthesis. In *Brain imaging in behavioral medicine and clinical neuroscience*, pages 383–393. Springer, 2011.
- D. W. Dickson, C. Bergeron, S. Chin, C. Duyckaerts, D. Horoupian, K. Ikeda, K. Jellinger, P. Lantos, C. Lippa, S. Mirra, et al. Office of rare diseases neuropathologic criteria for corticobasal degeneration. *Journal of Neuropathology & Experimental Neurology*, 61(11):935–946, 2002.
- D. W. Dickson, H. Braak, J. E. Duda, C. Duyckaerts, T. Gasser, G. M. Halliday, J. Hardy, J. B. Leverenz, K. Del Tredici, Z. K. Wszolek, et al. Neuropathological assessment of parkinson's disease: refining the diagnostic criteria. *The Lancet Neurology*, 8(12):1150–1157, 2009.
- B. Dubois, H. H. Feldman, C. Jacova, S. T. DeKosky, P. Barberger-Gateau, J. Cummings, A. Delacourte, D. Galasko, S. Gauthier, G. Jicha, et al. Research criteria for the diagnosis of alzheimer's disease: revising the nincds–adrda criteria. *The Lancet Neurology*, 6(8): 734–746, 2007.
- B. Dubois, H. H. Feldman, C. Jacova, H. Hampel, J. L. Molinuevo, K. Blennow, S. T. DeKosky, S. Gauthier, D. Selkoe, R. Bateman, et al. Advancing research diagnostic criteria for alzheimer's disease: the iwq-2 criteria. *The Lancet Neurology*, 13(6):614–629, 2014.
- J. Dukart, K. Mueller, A. Horstmann, H. Barthel, H. E. Möller, A. Villringer, O. Sabri, and M. L. Schroeter. Combined evaluation of fdg-pet and mri improves detection and differentiation of dementia. *PloS one*, 6(3):e18111, 2011.
- J. Dukart, K. Mueller, H. Barthel, A. Villringer, O. Sabri, M. L. Schroeter, A. D. N. Initiative, et al. Meta-analysis based svm classification enables accurate detection of alzheimer's disease across different clinical centers using fdg-pet and mri. *Psychiatry Research: Neuroimaging*, 212(3):230–236, 2013.

- S. R. Fahn. Unified parkinson's disease rating scale. *Recent development in Parkinson's disease*, 1987.
- M. F. Folstein, S. E. Folstein, and P. R. McHugh. Mini-mental state (mmse) journal of psychiatric research. 1975.
- P. T. Fox, A. R. Laird, and J. L. Lancaster. Coordinate-based voxel-wise meta-analysis: Dividends of spatial normalization. report of a virtual workshop. *Human brain mapping*, 25(1):1–5, 2005.
- K. Franke, G. Ziegler, S. Klöppel, C. Gaser, A. D. N. Initiative, et al. Estimating the age of healthy subjects from t1-weighted mri scans using kernel methods: exploring the influence of various parameters. *Neuroimage*, 50(3):883–892, 2010.
- M. L. Gorno-Tempini, A. E. Hillis, S. Weintraub, A. Kertesz, M. Mendez, S. F. Cappa, J. M. Ogar, J. Rohrer, S. Black, B. F. Boeve, et al. Classification of primary progressive aphasia and its variants. *Neurology*, 76(11):1006–1014, 2011.
- M. B. Graeber and L. B. Moran. Mechanisms of cell death in neurodegenerative diseases: fashion, fiction, and facts. *Brain pathology*, 12(3):385–390, 2002.
- G. U. Höglinger, G. Respondek, M. Stamelou, C. Kurz, K. A. Josephs, A. E. Lang, B. Mollenhauer, U. Müller, C. Nilsson, J. L. Whitwell, et al. Clinical diagnosis of progressive supranuclear palsy: the movement disorder society criteria. *Movement Disorders*, 32(6):853–864, 2017.
- C. Kipps, J. Hodges, T. Fryer, and P. Nestor. Combined magnetic resonance imaging and positron emission tomography brain imaging in behavioural variant frontotemporal degeneration: refining the clinical phenotype. *Brain*, 132(9):2566–2578, 2009.
- S. Klöppel, C. M. Stonnington, C. Chu, B. Draganski, R. I. Scahill, J. D. Rohrer, N. C. Fox, C. R. Jack Jr, J. Ashburner, and R. S. Frackowiak. Automatic classification of mr scans in alzheimer's disease. *Brain*, 131(3):681–689, 2008.
- A. R. Laird, P. M. Fox, C. J. Price, D. C. Glahn, A. M. Uecker, J. L. Lancaster, P. E. Turkeltaub, P. Kochunov, and P. T. Fox. Ale meta-analysis: Controlling the false discovery rate and performing statistical contrasts. *Human brain mapping*, 25(1):155–164, 2005.
- A. R. Laird, S. B. Eickhoff, P. M. Fox, A. M. Uecker, K. L. Ray, J. J. Saenz, D. R. McKay, D. Bzdok, R. W. Laird, J. L. Robinson, et al. The brainmap strategy for standardization, sharing, and meta-analysis of neuroimaging data. *BMC research notes*, 4(1):349, 2011.
- J. Levin, A. Kurz, T. Arzberger, A. Giese, and G. U. Höglinger. Differenzialdiagnose und therapie der atypischen parkinson-syndrome. *Dtsch Arztebl Int*, 113:61–69, 2016.
- N. R. McFarland. Diagnostic approach to atypical parkinsonian syndromes. *Continuum: Lifelong Learning in Neurology*, 22(4 Movement Disorders):1117, 2016.

- D. Moher, A. Liberati, J. Tetzlaff, and D. G. Altman. Preferred reporting items for systematic reviews and meta-analyses: the prisma statement. *Annals of internal medicine*, 151(4): 264–269, 2009.
- W. Muangpaisan, A. Mathews, H. Hori, and D. Seidel. A systematic review of the worldwide prevalence and incidence of parkinson's disease. *Journal of the Medical Association of Thailand*, 94(6):749, 2011.
- M. Otto, A. Ludolph, B. Landwehrmeyer, H. Förstl, J. Diehl-Schmid, M. Neumann, H. Kretzschmar, M. Schroeter, J. Kornhuber, A. Danek, et al. Konsortium zur erforschung der frontotemporalen lobärdegeneration. *Der Nervenarzt*, 82(8):1002, 2011.
- J. Parkinson. An essay on the shaking palsy. *The Journal of neuropsychiatry and clinical neurosciences*, 14(2):223–236, 1987.
- W. Poewe, K. Seppi, C. M. Tanner, G. M. Halliday, P. Brundin, J. Volkmann, A.-E. Schrag, and A. E. Lang. Parkinson disease. *Nature reviews Disease primers*, 3:17013, 2017.
- R. B. Postuma, D. Berg, M. Stern, W. Poewe, C. W. Olanow, W. Oertel, J. Obeso, K. Marek, I. Litvan, A. E. Lang, et al. Mds clinical diagnostic criteria for parkinson's disease. *Movement Disorders*, 30(12):1591–1601, 2015.
- J. Radua and D. Mataix-Cols. Voxel-wise meta-analysis of grey matter changes in obsessive–compulsive disorder. *The British Journal of Psychiatry*, 195(5):393–402, 2009.
- K. Rascovsky, D. Salmon, G. Ho, D. Galasko, G. Peavy, L. Hansen, and L. Thal. Cognitive profiles differ in autopsy-confirmed frontotemporal dementia and ad. *Neurology*, 58(12): 1801–1808, 2002.
- K. Rascovsky, J. R. Hodges, D. Knopman, M. F. Mendez, J. H. Kramer, J. Neuhaus, J. C. Van Swieten, H. Seelaar, E. G. Dopper, C. U. Onyike, et al. Sensitivity of revised diagnostic criteria for the behavioural variant of frontotemporal dementia. *Brain*, 134(9): 2456–2477, 2011.
- J. J. Rebeiz, E. H. Kolodny, and E. P. Richardson. Corticodentatonigral degeneration with neuronal achromasia. *Archives of neurology*, 18(1):20–33, 1968.
- C. Rorden and M. Brett. Stereotaxic display of brain lesions. *Behavioural neurology*, 12(4): 191–200, 2000.
- L. Saba. *Imaging in neurodegenerative disorders*. OUP Oxford, 2015.
- J. Sacher, J. Neumann, T. Fünfstück, A. Soliman, A. Villringer, and M. L. Schroeter. Mapping the depressed brain: a meta-analysis of structural and functional alterations in major depressive disorder. *Journal of affective disorders*, 140(2):142–148, 2012.
- M. L. Schroeter and J. Neumann. Combined imaging markers dissociate alzheimer's disease and frontotemporal lobar degeneration—an ale meta-analysis. *Frontiers in Aging Neuroscience*, 3:10, 2011.

-
- M. L. Schroeter, K. Raczka, J. Neumann, and D. Y. Von Cramon. Towards a nosology for frontotemporal lobar degenerations—a meta-analysis involving 267 subjects. *Neuroimage*, 36(3):497–510, 2007.
- M. L. Schroeter, K. Raczka, J. Neumann, and D. Y. Von Cramon. Neural networks in frontotemporal dementia—a meta-analysis. *Neurobiology of aging*, 29(3):418–426, 2008.
- J. Schrouff and J. Mourao-Miranda. Interpreting weight maps in terms of cognitive or clinical neuroscience: nonsense? In *2018 International Workshop on Pattern Recognition in Neuroimaging (PRNI)*, pages 1–4. IEEE, 2018.
- J. C. Steele, J. C. Richardson, and J. Olszewski. Progressive supranuclear palsy: a heterogeneous degeneration involving the brain stem, basal ganglia and cerebellum with vertical gaze and pseudobulbar palsy, nuchal dystonia and dementia. *Archives of neurology*, 10(4):333–359, 1964.
- C. C. Tang, K. L. Poston, T. Eckert, A. Feigin, S. Frucht, M. Gudesblatt, V. Dhawan, M. Lesser, J.-P. Vonsattel, S. Fahn, et al. Differential diagnosis of parkinsonism: a metabolic imaging study using pattern analysis. *The Lancet Neurology*, 9(2):149–158, 2010.
- P. E. Turkeltaub, G. F. Eden, K. M. Jones, and T. A. Zeffiro. Meta-analysis of the functional neuroanatomy of single-word reading: method and validation. *Neuroimage*, 16(3):765–780, 2002.
- D. R. Williams and I. Litvan. Parkinsonian syndromes. *Continuum: Lifelong Learning in Neurology*, 19(5 Movement Disorders):1189, 2013.
- C.-W. Woo, L. J. Chang, M. A. Lindquist, and T. D. Wager. Building better biomarkers: brain models in translational neuroimaging. *Nature neuroscience*, 20(3):365, 2017.
- C. Zadikoff and A. E. Lang. Apraxia in movement disorders. *Brain*, 128(7):1480–1497, 2005.

Appendix

ARTICLE OPEN

Disentangling the neural correlates of corticobasal syndrome and corticobasal degeneration with systematic and quantitative ALE meta-analyses

Franziska Albrecht¹, Sandrine Bisenius¹, Rodrigo Morales Schaack¹, Jane Neumann^{1,2} and Matthias L. Schroeter^{1,3}

Corticobasal degeneration is a scarce neurodegenerative disease, which can only be confirmed by histopathological examination. Reported to be associated with various clinical syndromes, its classical clinical phenotype is corticobasal syndrome. Due to the rareness of corticobasal syndrome/corticobasal degeneration and low numbers of patients included in single studies, meta-analyses are particularly suited to disentangle features of the clinical syndrome and histopathology. Using PubMed, we identified 11 magnetic resonance imaging studies measuring atrophy in 22 independent cohorts with 200 patients contrasted to 318 healthy controls. The anatomic likelihood estimation method was applied to reveal affected brain regions across studies. Corticobasal syndrome was related to gray matter loss in the basal ganglia/thalamus, frontal, parietal, and temporal lobes. In corticobasal degeneration patients, atrophy in the thalamus, frontal, temporal, and occipital lobes were found. Finally, in a conjunction analysis, the bilateral thalamus, the bilateral posterior frontomedian cortex, posterior midcingulate cortex and premotor area/supplementary motor area, and the left posterior superior and middle frontal gyrus/precentral gyrus were identified as areas associated with both, corticobasal syndrome and corticobasal degeneration. Remarkably, atrophy in the premotor area/supplementary motor area and posterior midcingulate/frontomedian cortex seems to be specific for corticobasal syndrome/corticobasal degeneration, whereas atrophy in the thalamus and the left posterior superior and middle frontal gyrus/precentral gyrus are also associated with other neurodegenerative diseases according to anatomic likelihood estimation method meta-analyses. Our study creates a new conceptual framework to understand, and distinguish between clinical features (corticobasal syndrome) and histopathological findings (corticobasal degeneration) by powerful data-driven meta-analytic approaches. Furthermore, it proposes regional-specific atrophy as an imaging biomarker for diagnosis of corticobasal syndrome/corticobasal degeneration ante-mortem.

npj Parkinson's Disease (2017)3:12; doi:10.1038/s41531-017-0012-6

INTRODUCTION

Recently, Armstrong *et al.*¹ developed new diagnostic criteria underlining the use of the term corticobasal syndrome (CBS) only for clinical representation, whereas the term corticobasal degeneration (CBD) should label pathology-proven cases. CBS, as a scarce clinical phenotype, is associated with its classical histopathology, CBD, but also with other proteinopathies related to tau, amyloid, and transactive response DNA-binding protein.² Diagnostic criteria of CBS associated with CBD include rigidity or akinesia, dystonia or myoclonus of limb, cortical sensory deficit, alien limb phenomena, or orobuccal/limb apraxia.¹ Interestingly, the disease most often affects the hand.³ When considering a patient having probable CBS with the pathology of CBD, four of the mentioned symptoms should be present asymmetrically. The patient should present at least two symptoms, which can be symmetric, for possible CBS. Regarding higher cortical features beside apraxia, the hallmark of CBS, additional cognitive impairments are often described in the literature.^{1, 3}

Patients with CBD show widespread deposition of hyperphosphorylated 4-repeat tau in neurons and glia.⁴ Neuropathologic diagnostic criteria require Gallyas/tau-positive lesions, including neuronal inclusions, threads, coiled bodies, and astrocytic plaques

as well as neuronal loss or additionally ballooned/achromatic neurons. Tau pathology can be found throughout gray and white matter, basal ganglia, diencephalon as well as rostral brainstem, while major lesions are found in superior frontal, pre-central/post-central and superior parietal gyri, the thalamus as well as the caudate nucleus.⁵ Encoded by the microtubule-associated protein tau (*MAPT*) gene, tau is responsible for microtubule assembly and stability. This function is controlled by the status of phosphorylation of tau protein. In the case of pathological dysfunction, binding affinity for microtubules decreases. Based on this tau-histopathology, several clinical phenotypes of CBD may evolve beside the most frequent syndrome CBS.² This complex and highly variable clinical presentation underlines the challenge to accurately diagnose CBD in a living patient and develop specific diagnostic criteria.

Nowadays, physicians and scientists have to face and disentangle this wide range of clinical symptoms and distinct histopathologies leading to a broad clinicopathological heterogeneity. Aiming at a powerful, detailed description and disentanglement of clinical features and neurodegenerative patterns, here we performed a meta-analysis across voxel-based morphometry (VBM) imaging studies, applying structural magnetic

¹Max Planck Institute for Human Cognitive and Brain Sciences, 04103 Leipzig, Germany; ²IFB Adiposity Diseases, Leipzig University Medical Center, 04103 Leipzig, Germany and ³Clinic of Cognitive Neurology, Leipzig Research Center for Civilization Diseases, University of Leipzig & FTLD Consortium Germany, Ulm, Germany
Correspondence: Franziska Albrecht (falbrecht@cbs.mpg.de)

Received: 3 February 2016 Revised: 9 December 2016 Accepted: 18 January 2017
Published online: 31 March 2017

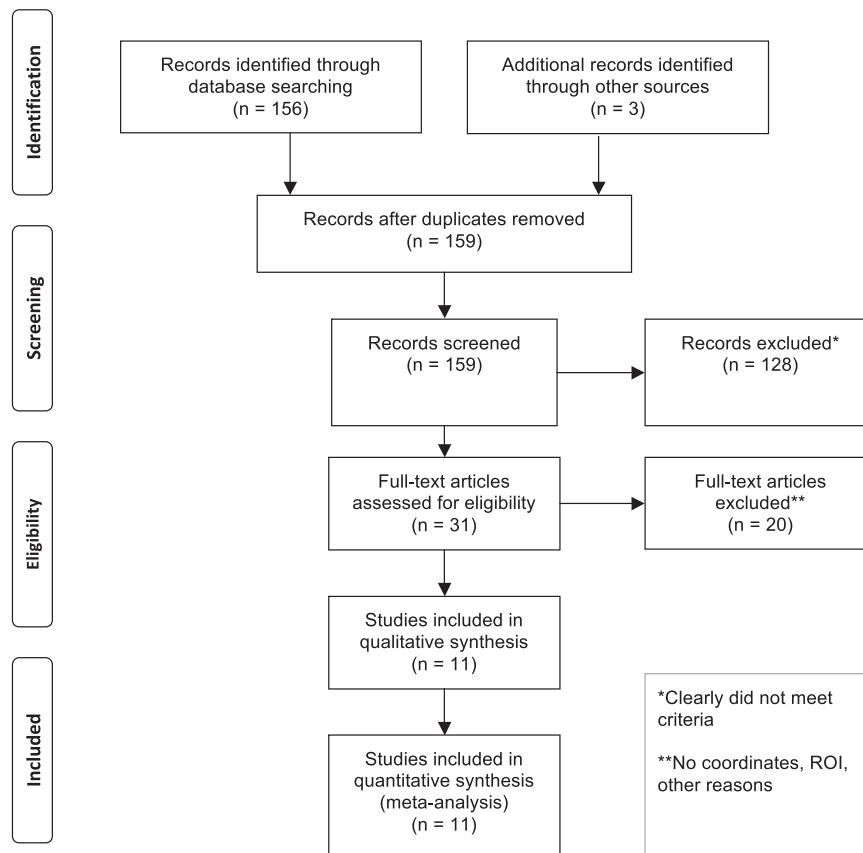


Fig. 1 PRISMA statement flow diagram. Flow of information through different phases of the systematic literature search identifying the neural correlates of CBS and CBD according to the PRISMA statement, as suggested by Moher, Liberati, Tetzlaff and Altman.¹³ ROI region of interest

resonance imaging (MRI) to detect disease-specific atrophy patterns. For the method, we applied anatomical likelihood estimate (ALE) meta-analyses that have been established as a standard tool for identifying prototypical neural correlates of neuropsychiatric diseases.^{6–12} The analysis was conducted separately for the clinical syndrome CBS, and for the (post-mortem) proven histopathology CBD to disentangle the interplay between clinical symptoms and underlying histopathology. Note that this approach enabled a strict dissociation and a subsequent comparison between the neural correlates of CBS and CBD. This distinction will be especially relevant for future treatment strategies aiming at specific proteinopathies.

We hypothesized that in CBS, severe atrophy will be found asymmetrically, mainly in the frontal lobe, due to the asymmetric occurrence of motor symptoms. According to findings in neuropathology, we hypothesized CBD lesions in the thalamus, caudate nucleus, superior frontal regions, regions around pre-central gyri/post-central gyri, and superior parietal regions. In addition to ALE meta-analyses conducted separately in CBS and CBD, we conducted a conjunction analysis to reveal overlapping regions, which is only specific for the disease combination of CBS/CBD.

RESULTS

Figure 1 depicts the flow of information through the different phases of study selection process according to Moher *et al.*¹³ Details of the imaging studies for CBS and CBD that were included

are summarized in Table 1 and Supplementary Table e-1. The meta-analysis integrated 11 MRI studies including 200 patients contrasted to 318 healthy controls. Note that two studies contained more than one cohort, leading to the inclusion of 22 independent patient cohorts. All studies involved reported either decreased gray matter volume or density, and none reported increases in gray matter volume or density in patients compared to control subjects. The CBS patient cohort included 184 patients with mean age of 66.3 ± 4.3 years (mean \pm standard deviation), disease duration of 5.3 ± 2.0 years, and Mini-Mental State Examination (MMSE) score of 21.9 ± 2.8 . The CBD cohort included 34 patients characterized by an age of 64.4 ± 5.9 years, disease duration of 7.0 ± 1.4 years, and a mean value in the MMSE of 23.9 ± 3.2 . Unpaired Student's *t*-tests indicate that there is no significant difference in age ($t = -0.65$, $p = 0.54$), and MMSE scores ($t = 1.20$, $p = 0.27$) between both cohorts. Note that mean disease duration was slightly, but non-significantly, longer in CBD than CBS in agreement with the post-mortem definition of CBD ($t = 1.83$, $p = 0.09$).

The upper part of Fig. 2 and Supplementary Table e-2 illustrate the results of the ALE meta-analysis identifying the neural correlates of CBS. The analysis across MRI studies revealed regional atrophy in the frontal, parietal and temporal lobe, and the basal ganglia/thalamus. More specifically, CBS affects the thalamus, the superior precuneus/postcentral gyrus and the posterior frontomedian cortex, posterior midcingulate cortex and premotor area/supplementary motor area bilaterally. In the right hemisphere, CBS is associated with atrophy in the caudate

Table 1. Studies included in the meta-analyses that identified the neural correlates of CBS and CBD with MRI

Study	Pat. (N)	Clin. Syn.	Hist.	Cont. (N)	Gender (m/f)	Age (years)	Dis. Dur. (years)	MMSE	Diagnosis of Clin. Syn.	Notes
<i>Studies included in the CBS cohort</i>										
Borroni	20	CBS	NE	21	13/7	62.7 ± 8.0	2.0 ± 1.4	25.0 ± 3.6	Lang et al. 1994	a, b
Boxer	14	CBS	NE	80	4/10	64.6 ± 5.9	5.6 ± 1.7	19.2 ± 8.3	(own criteria)	a, b
Gross	6 out of 20	CBS	NE	12	9/11	67.4 ± 9.8	3.9 ± 2.0	22.7 ± 6.2	NR	b, *
Grossman	9	CBS	NE	12	NR	64.0 ± 7.0	3.4 ± 1.5	18.8 ± 7.4	(own criteria)	
Halpern	5 out of 13	CBS	NE	12	7/6	66.8 ± 10.2	4.2 ± 1.7	19.6 ± 5.1	Riley et al. 2000	
Huey	48 (1)	CBS	NE	14	25/23	66.0 ± 9.0	5.0	NR	Boeve et al. 2005	a, b
Koss	5 out of 10	CBS	NE	32	5/5	66.2 ± 8.3	NR	20.9 ± 6.1	Murray et al. 2007, (own criteria)	a, b, *
Pardini	25	CBS	NE	14	12/13	62.0 ± 9.0	4.0 ± 1.8	NR	NR	b
Lee	7 out of 9	CBS	AD	44	5/4	59.2	8.3	18.0	UCSF-MAC	b
	11 out of 14	CBS	CBD		4/10	66.0	6.7	23.9	UCSF-MAC	b
	4 out of 5	CBS	PSP		3/2	69.3	8.1	21.8	UCSF-MAC	b
	3 out of 5	CBS	FTLD-TDP		2/3	72.1	7.9	26.2	UCSF-MAC	b
	3 out of 5	CBS	Mixed (2)		4/1	75.8	5.0	25.0	UCSF-MAC	b
Whitwell	6	CBS	AD	24	2/4	60.0	7.0	26.0	Boeve et al. 2003	a, b
	7	CBS	CBD		1/6	68.0	6.0	20.0	Boeve et al. 2003	a, b
	6	CBS	PSP		3/3	69.0	7.0	27.0	Boeve et al. 2003	a, b
	5	CBS	FTLD-TDP		3/2	71.0	6.0	22.0	Boeve et al. 2003	a, b
Total CBS	184			265	102/110	66.3 ± 4.3	5.3 ± 2.0	21.9 ± 2.8		
<i>Studies included in the CBD cohort</i>										
Lee	3 out of 5	bvFTD	CBD	44	3/2	65.9	7.9	18.5	Neary et al. 1998	b
	11 out of 14	CBS	CBD		4/10	66.0	6.7	23.9	UCSF-MAC	b
	5 out of 7	EM	CBD		2/5	64.4	5.6	25.3	(own criteria)	b
	1	PCA	CBD		0/1	54.8	8.6	27.0	McMonagle et al. 2006	b
	4 out of 5	PNFA	CBD		1/4	71.0	5.6	25.0	Neary et al. 1998, Gorno-Tempini et al. 2004	b
Rankin	3 out of 5	bvFTD	CBD	53	3/2	61.4	7.6	22.0	Neary et al. 1998	a, b
Whitwell	7	CBS	CBD	24	1/6	68.0	6.0	20.0	Boeve et al. 2003	a, b
Total CBD	34			121	14/30	64.4 ± 5.9	7.0 ± 1.4	23.9 ± 3.2		
Total CBS + CBD(3)	200			318	111/124	65.8 ± 4.9	5.7 ± 2.0	22.5 ± 3.1		

Gender, age, disease duration, and MMSE scores are specified for patients (mean ± standard deviation). All MRI studies used 1.5T (except for * = 3T). Clinical data are reported for all patients, whereas in four studies, MRI analyses were performed in a subcohort. Total mean scores were calculated without Rankin and Whitwell because they reported data as median. Data on references of included studies and diagnostic criteria are available in the [Supplementary data](#) (Supplementary Table e-1). Underline signifies the total score.

^a Correction for multiple comparisons
^b modulated

(1) Only 5 CBD cases were proven by pathology. (2) Mixed cases showed features of PSP, CBD and FTLD-TDP mixed with possible AD. (3) CBS-CBD cohorts of Lee and Whitwell were only used once to calculate total CBS + CBD

AD Alzheimer's disease, bvFTD behavioral variant frontotemporal dementia, CBD corticobasal degeneration, CBS corticobasal syndrome, Clin. Syn. clinical syndrome, Con. controls, Dis. Dur. disease duration, EM executive-motor, f female, FTLD-TDP frontotemporal lobar degeneration with TAR DNA-binding protein 43 inclusions, Hist. histopathology, m male, MMSE Mini-Mental State Examination, N number of subjects, NE not examined, NR not reported, Pat. patients, PCA posterior cortical atrophy, PNFA progressive nonfluent aphasia, PSP progressive supranuclear palsy, UCSF-MAC University of California, San Francisco Memory and Aging Center criteria for CBS

nucleus, the anterior superior temporal gyrus, the anterior superior insula, the claustrum, as well as putamen, and the posterior insula. In the left hemisphere, the meta-analysis additionally identified the precentral gyrus, posterior superior frontal sulcus and middle/superior frontal gyrus, a cluster in the inferior frontal junction area/posterior inferior frontal sulcus and precentral gyrus, and one cluster in the inferior postcentral sulcus/superior temporal gyrus.

The results of the ALE meta-analysis that investigated the neural correlates of CBD are displayed in the middle part of Fig. 2 and Supplementary Table e-2. Note that patients with

histopathological CBD included several clinical symptoms beside CBS

(see Table 1). CBS was clinically observed in only 53% (18 out of 34 cases). In general, the analysis across MRI studies revealed atrophy in the thalamus, frontal, temporal and occipital lobes. In detail, post-mortem proved CBD affects the thalamus, and the posterior frontomedian cortex, posterior midcingulate cortex and premotor areas/supplementary motor areas bilaterally. The right hemisphere shows atrophy in the posterior superior frontal sulcus and middle/superior frontal gyrus, while the left hemisphere shows gray matter loss in the medial/lateral occipitotemporal gyrus, the

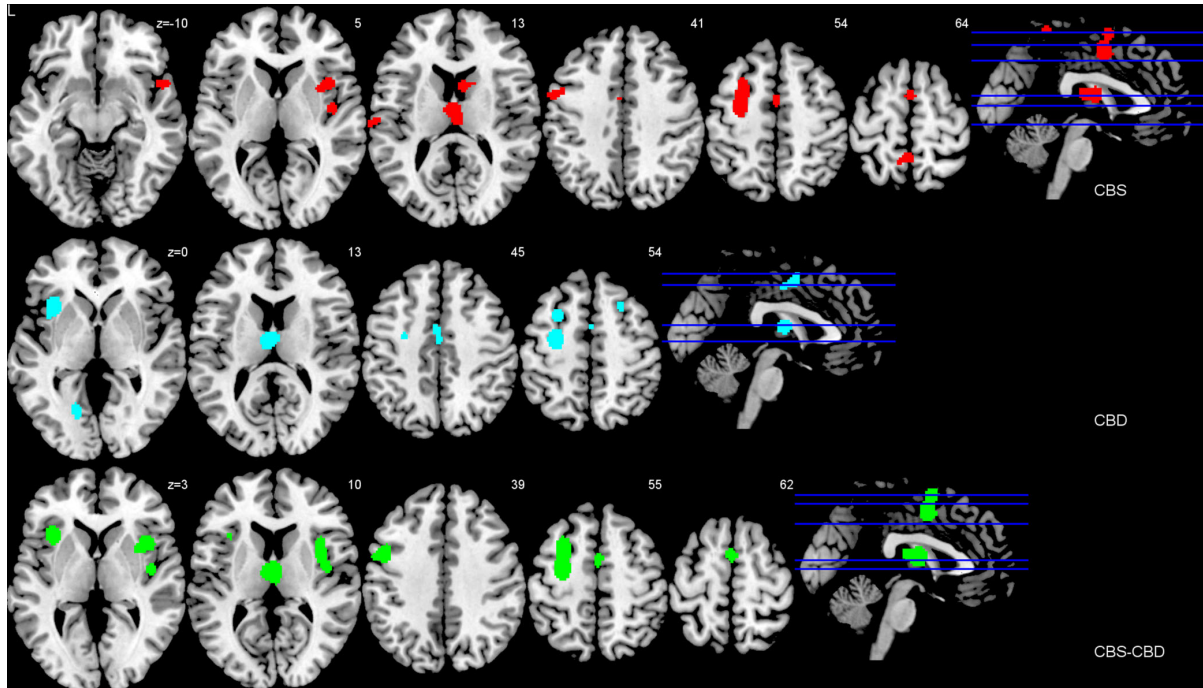


Fig. 2 Impaired regions in CBS and CBD. Impaired brain regions in CBS and CBD in comparison with healthy control subjects—anatomical likelihood estimates meta-analyses. Atrophy was measured by MRI. The CBS analysis (*red*) included 184 patients from 17 cohorts contrasted to 265 healthy subjects. The CBD analysis (*blue*) included 34 patients from seven cohorts contrasted to 121 healthy subjects. The analysis of the combined cohort of CBS and CBD (*white*) included 200 patients contrasted to 318 healthy control subjects. Coordinates are reported in MNI space. *L* left

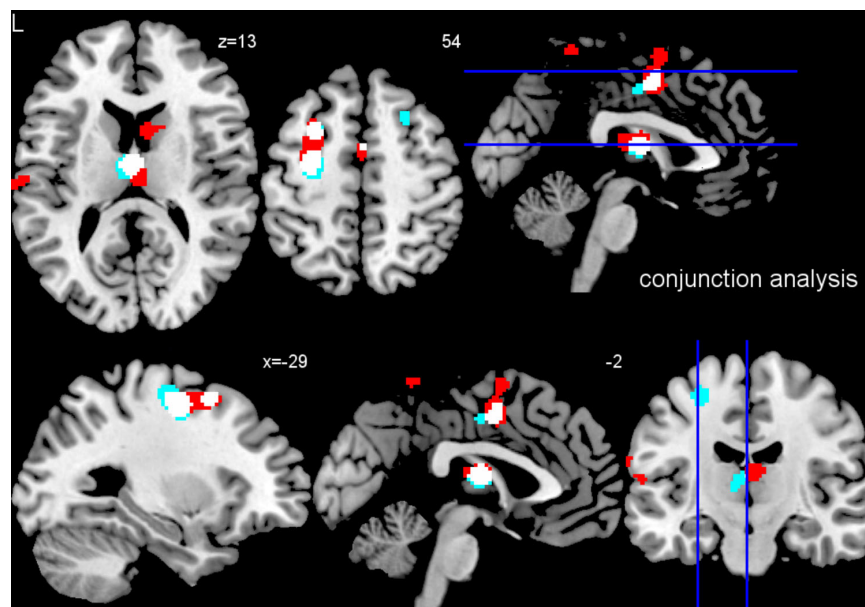


Fig. 3 Conjunction analysis. Conjunction analysis for impaired brain regions in CBS and CBD in comparison with healthy control subjects—anatomical likelihood estimates meta-analyses. White clusters indicate overlap of both meta-analyses (CBS and CBD). Atrophy was measured by MRI. Coordinates are reported in MNI space. *L* left

precentral gyrus, posterior superior frontal sulcus and middle/superior frontal gyrus, the posterior frontal sulcus and middle frontal sulcus, and the anterior insula.

The lower part of Fig. 2 and Supplementary Table e-2 show the results of the ALE meta-analysis combining all CBS and CBD patients. Generally, the results of this analysis revealed that the

Table 2. Meta-analytical evidence for biomarker specificity of regional atrophy in CBS/CBD as measured with MRI

Disease	Study	Anatomical region				
		Thalamus	Bl. fronto-median and midcingulate cortex	Bl. premotor area and supplementary motor area	L. pre-central gyrus	L. superior frontal sulcus and middle frontal gyrus
Parkinson's syndromes						
Parkinson's disease	15, 16	–	–	–	+	+
Atypical Parkinson's syndromes						
CBD and syndrome	Present meta-analysis	+	+(posterior)	+	+	+
Progressive supranuclear palsy	15	+	–	–	+	–
Multiple system atrophy	16	+	–	–	–	–
Lewy body dementia	40*	(–)	(–)	(–)	(–)	(–)
Alzheimer's disease						
Behavioral variant frontotemporal dementia	8–11	–	+(anterior)	–	–	–
Primary progressive aphasia						
Nonfluent/agrammatic variant (progressive non-fluent aphasia)	9, 10, 42	–	–	–	–	+
Semantic variant (semantic dementia)	9, 10, 42, 43	–	–	–	–	–
Logopenic variant (logopenic aphasia)	42	–	–	–	–	–

Meta-analyses were conducted by calculating ALEs in the gray matter. Other methods, such as effect-size signed differential mapping, were not taken into account to avoid a bias of different methods.
*Only one study by Zhong et al.⁴⁰ applying anisotropic effect size version of signed differential mapping (AES-SDM) was included, because no ALE meta-analysis has been available to date.
Bl/ bilateral, L left, NR not reported to date

basal ganglia/thalamus and frontal lobe are affected. In detail, atrophy was again identified in the thalamus, and the posterior frontomedian cortex, posterior midcingulate cortex and premotor areas/supplementary motor areas bilaterally. Further, atrophy was detected in the right insula and claustrum/putamen. Finally, the left hemisphere showed gray matter loss in the inferior frontal junction/posterior inferior frontal gyrus and precentral gyrus, the precentral gyrus/posterior superior frontal sulcus and middle/superior frontal gyrus, and the anterior superior insula.

Finally, a conjunction analysis was performed by overlaying the results of the two separate meta-analyses on CBS and CBD to identify brain regions involved in both, CBS and CBD. Results are displayed in Fig. 3, where white shading indicates overlap of both analyses. The analysis revealed that four clusters (1) in the bilateral thalamus, (2) in the posterior frontomedian cortex/posterior midcingulate cortex and premotor area/supplementary motor area, (3) in the left posterior superior frontal sulcus and middle frontal gyrus/precentral gyrus, and (4) in the left posterior superior frontal sulcus and middle frontal gyrus were consistently atrophic in both cohorts, CBS and CBD.

DISCUSSION

To our knowledge, here we present the first powerful data-driven meta-analyses identifying and comparing the neural correlates of CBS and CBD for MRI measuring atrophy in comparison with healthy control subjects. The design enabled high validity and statistical power by including 200 patients with this rare disease and 318 healthy control subjects. Additionally, the inclusion criterion of whole brain imaging studies for all meta-analyses guaranteed a data-driven approach.

Our results reveal that CBS is characterized by gray matter loss in the basal ganglia/thalamus, frontal, parietal and temporal lobes. In CBD patients, atrophy in the thalamus, frontal, temporal and occipital lobes was found. The latter results on CBD agree with

Dickson *et al.*,⁴ who described histopathologically atrophy and tau-immunoreactive lesions in the superior frontal/parietal, pre- and postcentral gyri, the caudate nucleus, the putamen, and the thalamus in CBD.

Most remarkably, in a conjunction analysis focusing on common brain regions affected by both, CBS and CBD, our study identified four brain areas with significant atrophy: (1) the bilateral anterior thalamus, and (2) the bilateral posterior frontomedian cortex, posterior midcingulate cortex and premotor area/supplementary motor area, and, in the left hemisphere, (3) the posterior superior frontal sulcus and middle frontal gyrus/precentral gyrus, and (4) the left posterior superior frontal sulcus and middle frontal gyrus. As these regions obviously constitute the core hubs for CBS/CBD according to our meta-analyses, we want to discuss them now in more detail. With regard to disease specificity, we will compare results of our ALE meta-analysis with structural MRI ALE meta-analyses of other neurodegenerative diseases (Table 2). Note that the differential diagnosis between CBS/CBD, progressive supranuclear palsy, multiple system atrophy, Lewy body disease, and Parkinson's disease is of paramount interest, as all of these might be associated with an (atypical or typical) Parkinson's syndrome.

Thalamic and left precentral atrophy is not specific for CBS/CBD. Although the thalamus was altered in both, CBS and CBD, changes in thalamic structure do not seem to be an exclusive imaging biomarker for CBS/CBD. Other neurodegenerative diseases, such as Alzheimer's disease, progressive supranuclear palsy, behavioral variant frontotemporal dementia, or Huntington's disease are also characterized by thalamic atrophy.¹⁴ Atrophy in the thalamus was also confirmed in recent ALE meta-analyses in Alzheimer's disease, progressive supranuclear palsy, and multiple system atrophy.^{9, 12, 15, 16} Furthermore, thalamic volume also shrinks in healthy people throughout life independent from and prior to total volume loss.¹⁷

In our conjunction analysis, the region of the left posterior superior frontal sulcus and middle frontal gyrus/precentral gyrus also showed significant atrophy. Remarkably, atrophy was located anterior to the right hand area in the precentral gyrus,¹⁸ fitting well with the clinical finding that the hand is most often impaired in CBS.³ The precentral gyrus encompasses parts of primary motor and premotor cortex. Dorsal premotor regions are responsible for promoting movements and response selection depending on spatial cues.¹⁹ Ventral premotor regions regulate hand movement to manipulate and grasp objects, and contain functions related to cognition such as the comprehension of actions. Goldenberg²⁰ suggested that atrophy in ventral regions of the left hemisphere is correlated with apraxia, in particular imitating hand postures and using or pantomiming the use of mechanical tools. Clinically, CBS is most frequently linked to apraxia²¹—an impairment in higher cortical features concerning skillful motoric movement without motoric deficits per se.

With regard to other neurodegenerative diseases (Table 2), recent meta-analyses also show atrophy in the left middle frontal gyrus in Parkinson's disease, and in the nonfluent/agrammatical variant of primary progressive aphasia, while atrophy in the left precentral gyrus is shown in Parkinson's disease and progressive supranuclear palsy.^{9, 10, 15, 16} This leads to the conclusion that atrophy in these brain regions is not disease-specific for CBS/CBD.

Atrophy in premotor area/supplementary-motor area and posterior midcingulate/frontomedian cortex is specific for CBS/CBD

According to the conjunction analysis, the premotor areas and supplementary motor areas showed atrophy in both CBS and CBD. These regions are essential for linking cognition to action²² and their atrophy can lead to the alien limb phenomenon, which is part of the diagnostic criteria for CBS. Although Parkinson's disease patients display less activation or a loss of neurons in this region,²² ALE meta-analyses have never identified these brain regions as affected by atrophy in other neurodegenerative diseases, including Parkinson's disease (Table 2; in particular^{15, 16}).

Additionally, the conjunction analysis revealed significant gray matter loss in the posterior frontomedian and midcingulate cortex in CBS/CBD. Although former ALE meta-analyses have shown atrophy in behavioral variant frontotemporal dementia in the anterior frontomedian and midcingulate cortex,^{8–11} the respective location was much more posterior in CBS/CBD without any overlap. In sum, atrophy in the premotor area/supplementary motor area and posterior midcingulate/frontomedian cortex seems to be specific for CBS/CBD, suggesting these brain regions as candidates for diagnostic and differential diagnostic imaging biomarkers in CBS/CBD in contrast to other neurodegenerative diseases (Table 2).

Study's limitations

Our study identified consistent findings of gray matter volume changes in CBS and CBD, but it also has its limitations. A main deficit of all included studies is the lack of a common standard in using special diagnostic criteria for evaluating CBS, where some studies used idiosyncratic criteria based on clinical expertise (Table 1). Therefore, slightly differently included clinical symptoms and, at least partly, imprecise diagnoses are possible. However, due to the meta-analytical approach, this confounding effect should be minor and not bias our results decisively. Armstrong *et al.*¹ built a foundation for new consensus criteria, which should be employed in clinical studies to help overcome the problem of not strictly comparable diagnosis. In future, it will be possible to include only studies based on these new criteria in meta-analyses. Due to low incidence and ethical issues, MRI studies on autopsy proven cases of CBD are rare. Hence, results of our CBD analysis should be handled with caution due to the small cohort of patients. CBS/CBD patients are characterized by asymmetrical

atrophy and symptoms. Unfortunately, the original studies did not separate their analyses into patients suffering from left or right-sided clinical symptoms, although Armstrong *et al.* (2013) underlined the importance of symptom laterality in the new diagnostic criteria. Studies just reported local maxima of atrophy from whole CBS/CBD cohorts. Thus, conducting separate meta-analyses for left and right sided CBS was not possible. An important contributing factor could be the preference for using either the right or left hand. We were not able to control for handedness due to unreported data. One should also consider that there are methodological differences between VBM studies, for instance, field-strength of scanners, processing protocols, or data modulation. However, these differences would not have confounded our results, because the ALE method only takes maxima into account and not cluster sizes. During the literature search, we did not find enough ¹⁸F-fluorodeoxyglucose positron emission tomography (FDG-PET) or diffusion tensor imaging (DTI) studies, which reported coordinates in stereotactic space, to conduct meaningful meta-analyses. Thus, our meta-analyses had to be limited to structural MRI atrophy data. We recommend extending meta-analyses to other imaging modalities in the future, when more studies are available. It is well-known that for different imaging modalities regional alterations might be dissociated in time and space.^{8, 12, 23, 24}

Furthermore, specificity and sensitivity of the suggested disease-specific brain regions in differentiation of neurodegenerative diseases like CBS/CBD have to be validated in large, preferably multi-centric, and independent patient cohorts. These patient cohorts should ideally provide information about clinical and imaging data as well as surrogate markers for histopathology from serum and cerebrospinal fluid or even post mortem validation. This approach has already been successfully applied to other neurodegenerative diseases such as Alzheimer's disease and frontotemporal lobar degeneration.^{25, 26} Validating results of ALE meta-analyses in independent cohorts is also necessary due to the fact that these meta-analyses generally include maxima and not cluster sizes of the various imaging studies. Consequently, single studies might have shown that dementia diseases may be regionally more unspecific than the present meta-analyses suggest.

CONCLUSION

The meta-analyses build a foundation for a better disentanglement of the clinical phenotype CBS, and the histopathological type CBD. Results suggest atrophy in the premotor area/supplementary motor area and posterior midcingulate/frontomedian cortex as an imaging biomarker for diagnosis of CBS or CBD ante-mortem.

MATERIALS AND METHODS

General study selection

Assuring validity and quality, the meta-analysis was conducted according to preferred reporting items for systematic reviews and meta-analyses (PRISMA) guidelines¹³ (also see www.prisma-statement.org). To identify adequate studies, PubMed was used applying the following search strategy: (corticobasal degeneration OR CBD OR corticobasal syndrome OR CBS) AND (voxel* OR gray matter OR VBM). Studies were included if they fulfilled the following criteria: (1) peer-reviewed, (2) diagnosis according to established diagnostic criteria, (3) original study, (4) comparison with age-matched healthy control group, (5) results normalized to a stereotactic space such as the Talairach²⁷ or the Montreal Neurological Institute's²⁸ (MNI) reference system and respective coordinates available, (6) whole brain study. Region-of-interest analyses or case studies were excluded to prevent any a priori regional assumptions. Since we did not find enough imaging studies that applied FDG-PET or DTI, which reported coordinates in stereotactic space, studies were limited to structural MRI atrophy data. We concentrated on reporting gray matter

atrophy studies because only two studies analyzed white matter changes. Literature search was performed between November 2014 and January 2015 reviewing all studies regardless of their publication date. During this process, we contacted two study authors and obtained data on maxima from one study.

Statistical analyses

To extract the neural correlates of CBS and CBD, we applied the ALE meta-analysis method.^{29–32} This method was first invented for meta-analyses of functional imaging studies with psychological stimulation of participants (here called activation likelihood estimate). Later, this approach was extended to imaging studies during rest investigating atrophy or hypometabolism.^{6–12}

In 2009, Eickhoff *et al.*³³ presented a revised analysis algorithm. The underlying method transforms extracted peaks into Gaussian probability distributions around these coordinates. The estimation of the width of these Gaussian probability distributions is adapted for each study according to the number of included subjects based on empirical estimates of between-subject and between-template variability. The resulting ALE maps are later combined across studies and tested against the null hypothesis of a random spatial distribution between the modeled maps. In this step, regions where empirical ALE values are higher than those expected by chance are identified. The resulting map is thresholded with a customized threshold to report only cluster that exceed the number of voxels corresponding to 5% possible false positives.

The analyses were performed in BrainMap Ginger ALE 2.3³⁴ using extracted peaks of atrophy in CBS/CBD studies. Coordinates reported in the stereotactic space of Talairach and Tournoux were transformed into the stereotactic MNI space using the Lancaster transform implemented in Ginger ALE 2.3.³⁵ As an error corrector for multiple testing we applied the conservative false discovery rate nonparametric *p*-value threshold (FDR *p*_N) correction^{30, 36} with a threshold of *p* < 0.05. Clusters with a minimum size of 374 mm³ are reported. Recently, Eickhoff, Laird, Fox, Lancaster, and Fox (2016)³⁷ reported about implementation errors in determining thresholds to account for multiple comparisons in older GingerALE software distributions. Note that ALE scores and peak locations are unaffected by these errors. We compare our results to other meta-analyses using also these versions of GingerALE. This way, we ensure homogeneity and comparability to other previous meta-analyses on neurodegenerative diseases. Future studies shall apply the new corrected GingerALE software versions homogeneously for different neurodegenerative diseases.

To disentangle the neural correlates for CBS/CBD specifically, we performed data analyses in three cohorts: (1) cohort of clinically evaluated CBS patients (CBS cohort), (2) cohort of histopathologically proven CBD patients (CBD cohort), and (3) cohort including all CBS and CBD data (CBS + CBD cohort). Additionally, we conducted a conjunction analysis between the results of the separate meta-analyses on CBS and CBD in order to reveal regions that were consistently atrophied in both cohorts.

For purposes of visualization, results were imported into MRICron.³⁸

To reveal possible differences in age, disease duration, and MMSE scores between groups, we performed Student's *t*-tests in R³⁹ with a significance threshold at *p* < 0.05.

Potential bias

Several methods were applied to reduce the risk of bias of single studies and across studies. To overcome the problem of a bias toward specific brain areas, only studies using a quantitative automated whole brain analysis were included. Studies reporting results of region-of-interest approaches were not considered. To exclude any impact of age as a confounding factor on our results, only studies comparing patients with age-matched healthy controls were included into the meta-analysis. Studies investigating brain atrophy compared to other neurodegenerative diseases were also excluded to avoid any bias due to divergent control groups. According to PRISMA statement, two investigators performed literature search and selection separately (FA and RMS). As proposed in Eickhoff's *et al.*³³ new algorithm, the number of patients included in each study was taken into account in data synthesis. This leads to a balanced analysis. Although studies with negative findings might theoretically have been omitted, this publication bias is unlikely, because CBS and CBD patients generally show severe atrophy in comparison with healthy control subjects.

ACKNOWLEDGEMENTS

Sandrine Bisenius is supported by the MaxNetAging Research School of the Max Planck Society. Rodrigo Morales Schaack reports no disclosure. Jane Neumann is supported by the Federal Ministry of Education and Research (BMBF), Germany (FKZ: 01EO1001) and the German Research Foundation (DFG-SFB1052). Matthias L. Schroeter and Franziska Albrecht are supported by the German Federal Ministry of Education and Research (BMBF; Grant No. FKZ 01G1007A, German FTLD consortium), and additionally by the Parkinson's Disease Foundation (Grant No. PDF-IRG-1307) and Michael J Fox Foundation (Grant No. MJFF-11362). Further support for this study was also awarded to Matthias L. Schroeter by LIFE-Leipzig Research Center for Civilization Diseases at the University of Leipzig. LIFE is funded by the European Union, by the European Regional Development Fund (ERFD) and by the Free State of Saxony within the framework of the excellence initiative.

AUTHOR CONTRIBUTIONS

Franziska Albrecht-Study concept and design, acquisition of data, analysis and interpretation, critical revision of the manuscript for important intellectual content. Sandrine Bisenius-Critical revision of the manuscript for important intellectual content. Rodrigo Morales Schaack-Acquisition of data, critical revision of the manuscript for important intellectual content. Jane Neumann – Study analysis and interpretation, critical revision of the manuscript for important intellectual content. Matthias L. Schroeter - Study concept and design, analysis and interpretation, critical revision of the manuscript for important intellectual content, study supervision.

COMPETING INTERESTS

The authors declare that they have no competing interests.

REFERENCES

1. Armstrong, M. J. et al. Criteria for the diagnosis of corticobasal degeneration. *Neurology* **80**, 496–503 (2013).
2. Boeve, B. F. The multiple phenotypes of corticobasal syndrome and corticobasal degeneration: implications for further study. *J. Mol. Neurosci.* **45**, 350–353 (2011).
3. Williams, D. R. & Litvan, I. Parkinsonian syndromes. *Continuum (Minneapolis)* **19**, 1189–1212 (2013).
4. Dickson, D. W. et al. Office of Rare Diseases neuropathologic criteria for corticobasal degeneration. *J. Neuropathol. Exp. Neurol.* **61**, 935–946 (2002).
5. Kouri, N., Whitwell, J. L., Josephs, K. A., Rademakers, R. & Dickson, D. W. Corticobasal degeneration: a pathologically distinct 4R tauopathy. *Nat. Rev. Neurol.* **7**, 263–272 (2011).
6. Glahn, D. C. et al. Meta-analysis of gray matter anomalies in schizophrenia: application of anatomic likelihood estimation and network analysis. *Biol. Psychiatry* **64**, 774–781 (2008).
7. Sacher, J. et al. Mapping the depressed brain: a meta-analysis of structural and functional alterations in major depressive disorder. *J. Affect. Disord.* **140**, 142–148 (2012).
8. Schroeter, M. L. et al. Conceptualizing neuropsychiatric diseases with multimodal data-driven meta-analyses—the case of behavioral variant frontotemporal dementia. *Cortex* **57**, 22–37 (2014).
9. Schroeter, M. L. & Neumann, J. Combined imaging markers dissociate Alzheimer's disease and frontotemporal lobar degeneration—an ALE meta-analysis. *Front. Aging Neurosci.* **3**, 10 (2011).
10. Schroeter, M. L., Raczka, K., Neumann, J. & von Cramon, D. Y. Towards a nosology for frontotemporal lobar degenerations—a meta-analysis involving 267 subjects. *Neuroimage* **36**, 497–510 (2007).
11. Schroeter, M. L., Raczka, K., Neumann, J. & von Cramon, D. Y. Neural networks in frontotemporal dementia—a meta-analysis. *Neurobiol. Aging* **29**, 418–426 (2008).
12. Schroeter, M. L., Stein, T., Maslowski, N. & Neumann, J. Neural correlates of Alzheimer's disease and mild cognitive impairment: a systematic and quantitative meta-analysis involving 1351 patients. *Neuroimage* **47**, 1196–1206 (2009).
13. Moher, D., Liberati, A., Tetzlaff, J. & Altman, D. G. Preferred reporting items for systematic reviews and meta-analyses: the PRISMA statement. *J. Clin. Epidemiol.* **62**, 1006–1012 (2009).
14. Power, B. D. & Looi, J. C. The thalamus as a putative biomarker in neurodegenerative disorders. *Aust. N. Z. J. Psychiatry* **49**, 502–518 (2015).
15. Shao, N., Yang, J., Li, J. & Shang, H. F. Voxelwise meta-analysis of gray matter anomalies in progressive supranuclear palsy and Parkinson's disease using anatomic likelihood estimation. *Front. Hum. Neurosci.* **8**, 63 (2014).
16. Shao, N., Yang, J. & Shang, H. Voxelwise meta-analysis of gray matter anomalies in Parkinson variant of multiple system atrophy and Parkinson's disease using anatomic likelihood estimation. *Neurosci. Lett.* **587**, 79–86 (2015).

17. Van Der Werf, Y. D. et al. Thalamic volume predicts performance on tests of cognitive speed and decreases in healthy aging: a magnetic resonance imaging-based volumetric analysis. *Brain Res. Cogn. Brain Res.* **11**, 377–385 (2001).
18. Yousry, T. A. et al. Localization of the motor hand area to a knob on the precentral gyrus. A new landmark. *Brain* **120**, 141–157 (1997).
19. Chouinard, P. A. & Paus, T. The primary motor and premotor areas of the human cerebral cortex. *Neuroscientist* **12**, 143–152 (2006).
20. Goldenberg, G. Apraxia—The cognitive side of motor control. *Cortex* **57**, 270–274 (2014).
21. Zadikoff, C. & Lang, A. E. Apraxia in movement disorders. *Brain* **128**, 1480–1497 (2005).
22. Nachev, P., Kennard, C. & Husain, M. Functional role of the supplementary and pre-supplementary motor areas. *Nat. Rev. Neurosci.* **9**, 856–869 (2008).
23. Jack, C. R. Jr et al. Hypothetical model of dynamic biomarkers of the Alzheimer's pathological cascade. *Lancet Neurol.* **9**(1), 119–128 (2010).
24. Dukart, J. et al. Alzheimer's disease neuroimaging initiative. Relationship between imaging biomarkers, age, progression and symptom severity in Alzheimer's disease. *Neuroimage Clin.* **3**, 84–94 (2013).
25. Dukart, J. et al. Classification enables accurate detection of Alzheimer's disease across different clinical centers using FDG-PET and MRI. *Psychiatry Res.* **212**, 230–236 (2013).
26. Dukart, J. et al. Combined evaluation of FDG-PET and MRI improves detection and differentiation of dementia. *PLoS One* **6**, e18111 (2011).
27. Talairach, J. & Tournoux, P. Co-planar stereotaxic atlas of the human brain: 3-dimensional proportional system: an approach to cerebral imaging (Thieme, 1988).
28. Evans A. C. et al. 3D statistical neuroanatomical models from 305 MRI volumes. In *IEEE Nuclear Science Symposium and Medical Imaging Conference*. pp. 1813–1817 (IEEE, 1993).
29. Fox, P. T., Laird, A. R. & Lancaster, J. L. Coordinate-based voxel-wise meta-analysis: dividends of spatial normalization. Report of a virtual workshop. *Hum. Brain Mapp.* **25**, 1–5 (2005).
30. Laird, A. R. et al. ALE meta-analysis: controlling the false discovery rate and performing statistical contrasts. *Hum. Brain Mapp.* **25**, 155–164 (2005).
31. Laird, A. R. et al. The BrainMap strategy for standardization, sharing, and meta-analysis of neuroimaging data. *BMC Res. Notes* **4**, 349 (2011).
32. Turkeltaub, P. E., Eden, G. F., Jones, K. M. & Zeffiro, T. A. Meta-analysis of the functional neuroanatomy of single-word reading: method and validation. *Neuroimage* **16**, 765–780 (2002).
33. Eickhoff, S. B. et al. Coordinate-based activation likelihood estimation meta-analysis of neuroimaging data: a random-effects approach based on empirical estimates of spatial uncertainty. *Hum. Brain Mapp.* **30**, 2907–2926 (2009).
34. Fox P. T. et al. *BrainMap GingerALE 2.3*. <http://brainmap.org> (2014).
35. Lancaster, J. L. et al. Bias between MNI and Talairach coordinates analyzed using the ICBM-152 brain template. *Hum. Brain Mapp.* **28**, 1194–1205 (2007).
36. Genovese, C. R., Lazar, N. A. & Nichols, T. Thresholding of statistical maps in functional neuroimaging using the false discovery rate. *Neuroimage* **15**, 870–878 (2002).
37. Eickhoff S. B., Laird A. R., Fox P. M., Lancaster J. L., & Fox P. T. Implementation errors in the GingerALE Software: description and recommendations. *Hum. Brain Mapp.* (2016).
38. Rorden C. *MRIcron*. <http://www.cabiatl.com/micro/mricron> (2015).
39. R-Core-Team. *R: a language and environment for statistical computing*. <http://www.R-project.org> (2013).
40. Zhong, J., Pan, P., Dai, Z. & Shi, H. Voxelwise meta-analysis of gray matter abnormalities in dementia with Lewy bodies. *Eur. J. Radiol.* **83**, 1870–1874 (2014).
41. Yang, J. et al. Voxelwise meta-analysis of gray matter anomalies in Alzheimer's disease and mild cognitive impairment using anatomic likelihood estimation. *J. Neurol. Sci.* **316**, 21–29 (2012).
42. Bisenius, S., Neumann, J. & Schroeter, M. L. Validating new diagnostic imaging criteria for primary progressive aphasia via anatomical likelihood estimation meta-analyses. *Eur. J. Neurol.* **23**, 704–712 (2016).
43. Yang, J., Pan, P., Song, W. & Shang, H. F. Quantitative meta-analysis of gray matter abnormalities in semantic dementia. *J. Alzheimers Dis.* **31**, 827–833 (2012).



This work is licensed under a Creative Commons Attribution 4.0 International License. The images or other third party material in this article are included in the article's Creative Commons license, unless indicated otherwise in the credit line; if the material is not included under the Creative Commons license, users will need to obtain permission from the license holder to reproduce the material. To view a copy of this license, visit <http://creativecommons.org/licenses/by/4.0/>

© The Author(s) 2017

Supplementary Information accompanies the paper on the *npj Parkinson's Disease* website (doi:10.1038/s41531-017-0012-6).

List of Authorship

Nachweis über Anteile der Co-Autoren:

Nachweis über Anteile der Co-Autoren, Franziska Albrecht, Neural Correlates of Parkinsonian Syndromes

Title: FDG-PET hypometabolism is more sensitive than MRI atrophy in Parkinson's disease: A whole-brain multimodal imaging meta-analysis

Journal: NeuroImage: Clinical

Authors: Franziska Albrecht*, Tommaso Ballarini*, Jane Neumann, Matthias L. Schroeter

Anteil Franziska Albrecht* (Erstautor/in):

- Projektidee
- Konzeption
- Analyse und Verarbeitung der Daten
- Schreiben und Revision der Publikation

Anteil Tommaso Ballarini* (Erstautor/in):

- Projektidee
- Konzeption
- Analyse und Verarbeitung der Daten
- Schreiben und Revision der Publikation

Anteil Jane Neumann (Autor/in 2):

- Analyse und Verarbeitung der Daten
- Revision der Publikation

Anteil Matthias L. Schroeter (Senior-Autor/in):

- Projektidee
- Konzeption
- Schreiben und Revision der Publikation

Franziska Albrecht

Matthias L. Schroeter

Nachweis über Anteile der Co-Autoren, Franziska Albrecht, Neural Correlates of Parkinsonian Syndromes

Title: Atrophy in midbrain and cerebral/cerebellar pedunculi is specific for progressive supranuclear palsy - a cross-validation whole-brain meta-analysis

Journal: NeuroImage: Clinical

Authors: Franziska Albrecht, Sandrine Bisenius, Jane Neumann, Jennifer Whitwell, Matthias L. Schroeter

Anteil Franziska Albrecht (Erstautor/in):

- Projektidee
- Konzeption
- Analyse und Verarbeitung der Daten
- Schreiben und Revision der Publikation

Anteil Sandrine Bisenius (Autor/in 2):

- Analyse und Verarbeitung der Daten
- Revision der Publikation

Anteil Jane Neumann (Autor/in 3):

- Analyse und Verarbeitung der Daten
- Revision der Publikation

Anteil Jennifer Whitwell (Autor/in 4):

- Bereitstellung der Daten
- Revision der Publikation

Anteil Matthias L. Schroeter (Senior-Autor/in):

- Projektidee
- Konzeption
- Schreiben und Revision der Publikation

Franziska Albrecht

Matthias L. Schroeter

Nachweis über Anteile der Co-Autoren, Franziska Albrecht, Neural Correlates of Parkinsonian Syndromes

Title: Unraveling Corticobasal Syndrome and Alien Limb Syndrome with Structural Brain Imaging

Journal: Cortex

Authors: Franziska Albrecht, Karsten Mueller, Tommaso Ballarini, Leonie Lampe, Janine Diehl-Schmid, Klaus Fassbender, Klaus Fliessbach, Holger Jahn, Robert Jech, Jan Kassubek, Johannes Kornhuber, Bernhard Landwehrmeyer, Martin Lauer, Albert C. Ludolph, Epameinondas Lyros, Johannes Prudlo, Anja Schneider, Matthis Synofzik, Jens Wiltfang, Adrian Danek, Markus Otto, FTLD-Consortium, Matthias L. Schroeter

Anteil Franziska Albrecht (Erstautor/in):

- Projektidee
- Konzeption
- Analyse und Verarbeitung der Daten
- Schreiben und Revision der Publikation

Anteile Karsten Mueller (Autor/in 2):

- Unterstützung Analyse der Daten
- Revision der Publikation

Anteile Tommaso Ballarini (Autor/in 3):

- Unterstützung Analyse der Daten
- Revision der Publikation

Anteile Leonie Lampe, Janine Diehl-Schmid, Klaus Fassbender, Klaus Fliessbach, Holger Jahn, Robert Jech, Jan Kassubek, Johannes Kornhuber, Bernhard Landwehrmeyer, Martin Lauer, Albert C. Ludolph, Epameinondas Lyros, Johannes Prudlo, Anja Schneider, Matthis Synofzik, Jens Wiltfang, Adrian Danek, Markus Otto, FTLD-Consortium (Autor/in):

- Erhebung und Verarbeitung der Daten

- Revision der Publikation

Anteil Matthias L. Schroeter (Senior-Autor/in):

- Projektidee
- Konzeption
- Erhebung und Verarbeitung der Daten
- Schreiben und Revision der Publikation

Franziska Albrecht

Matthias L. Schroeter

Nachweis über Anteile der Co-Autoren, Franziska Albrecht, Neural Correlates of Parkinsonian Syndromes

Title: Regional gray matter changes and age predict individual treatment response in Parkinson's disease

Journal: NeuroImage: Clinical

Authors: Tommaso Ballarini, Karsten Mueller, Franziska Albrecht, Filip Růžička, Ondrej Bezdicek, Evžen Růžička, Jan Roth, Josef Vymazal, Robert Jech, Matthias L. Schroeter

Anteil Tommaso Ballarini (Erstautor/in):

- Projektidee
- Konzeption
- Analyse und Verarbeitung der Daten
- Schreiben der Publikation

Anteil Karsten Mueller (Autor/in 2):

- Projektidee
- Konzeption
- Analyse der Daten
- Revision der Publikation

Anteil Franziska Albrecht (Autor/in 3):

- Unterstützung Analyse der Daten
- Revision der Publikation

Anteil Filip Růžička (Autor/in 4):

- Konzeption
- Erhebung und Verarbeitung der Daten
- Revision der Publikation

Anteil Ondrej Bezdicek (Autor/in 5):

- Konzeption
- Erhebung und Verarbeitung der Daten
- Revision der Publikation

Anteil Evžen Růžička (Autor/in 6):

- Konzeption
- Revision der Publikation

Anteil Jan Roth (Autor/in 7):

- Konzeption
- Erhebung und Verarbeitung der Daten
- Revision der Publikation

Anteil Josef Vymazal (Autor/in 8):

- Konzeption
- Erhebung und Verarbeitung der Daten
- Revision der Publikation

Anteil Robert Jech (Autor/in 9):

- Konzeption
- Erhebung und Verarbeitung der Daten
- Revision der Publikation

Anteil Matthias L. Schroeter (Senior-Autor/in):

- Konzeption
- Schreiben und Revision der Publikation

Franziska Albrecht

Matthias L Schroeter

Contribution of Coauthors, Franziska Albrecht, Neural Correlates of Parkinsonian Syndromes

Title: Memory Impairment in Parkinson's Disease: The Retrieval Versus Associative Deficit Hypothesis Revisited and Reconciled

Journal: Neuropsychology

Authors: Ondrej Bezdicek, Tommaso Ballarini, Herman Buschke, Filip Růžička, Jan Roth, Franziska Albrecht, Evžen Růžička, Karsten Mueller, Matthias L. Schroeter, Robert Jech

Part Ondrej Bezdicek (First author):

- Project idea and concept
- Collection, analysis, and preparation of data
- Writing and revising manuscript

Part Tommaso Ballarini (Author 2):

- Analysis and preparation of data
- Writing and revising manuscript

Part Herman Buschke (Author 3):

- Project concept
- Revising manuscript

Part Filip Růžička (Author 4):

- Data collection
- Revising manuscript

Part Jan Roth (Author 5):

- Data collection
- Revising manuscript

Part Franziska Albrecht (Author 6):

- Analysis and preparation of data

- Writing and revising manuscript

Part Evžen Růžička (Author 7):

- Project idea and concept
- Revising manuscript

Part Karsten Mueller (Author 8):

- Analysis of data
- Revising manuscript

Part Matthias L. Schroeter (Author 9):

- Revising manuscript

Part Robert Jech (Senior-Author):

- Project idea and concept
- Revising manuscript

Franziska Albrecht

Robert Jech

Curriculum Vitæ

Franziska Albrecht

Curriculum Vitæ

Education

- 2016–2019 **PhD Student**, *International Max Planck Research School on Neuroscience of Communication: Function, Structure, and Plasticity (IMPRS NeuroCom)*, *Max-Planck-Institute for Human Cognitive and Brain Sciences, Group Cognitive Neuropsychiatry & University of Leipzig*, Leipzig.
- 2013–2015 **Master of Science, Neurobiology and Behavior**, *University of Leipzig*, Leipzig.
Specialized in neurobiology, cognitive processes, biological psychology, and behavior.
- 2010–2013 **Bachelor of Science, Biology**, *Martin-Luther University of Halle-Wittenberg*, Halle/ Saale.
Specialized in physiology of humans and animals.
- 2007–2010 **Sixth-Form College**, *Karl-Heine-Schule*, Leipzig, *Qualification: Allgemeine Hochschulreife (General Certificate of Education Advanced Level)*.
Profile technological science/ specialization in engineering.

PhD Thesis

- Title *Neural Correlates of Parkinsonian Syndromes*
- Supervisors **Prof. Dr. Dr. Matthias L. Schroeter**, **Prof. Dr. Karsten Müller**, *Max-Planck-Institute for Human Cognitive and Brain Sciences & Prof. Dr. Rudolf Rübsamen*, *University of Leipzig*
- Description The thesis applies voxel-based morphometry, machine learning, graph theory & quantitative meta-analyses to find disease-characteristic MRI-based neural correlates of parkinsonian syndromes.

Masters Thesis

- Title *Neural Correlates of Atypical Parkinsonian Syndromes*
- Supervisors **Prof. Dr. Dr. Matthias L. Schroeter**, *Max-Planck-Institute for Human Cognitive and Brain Sciences & Prof. Dr. Rudolf Rübsamen*, *University of Leipzig*
- Description The thesis disentangled the neural correlates of an atypical parkinsonian syndrome and its associated underlying histopathology with systematic and quantitative ALE meta-analyses. These correlates were replicated also in an included voxel-based morphometry analysis on multicentric data.

Bachelors Thesis

- Title *Analgesic Effect of Affiliation*
- Supervisors **Joshua A. Grant, PhD**, *Max-Planck-Institute for Human Cognitive and Brain Sciences & Prof. Dr. Hans J. Ferenz*, *University of Halle/ Wittenberg*

Max-Planck-Institute: Stephanstr. 1A, 04103 Leipzig, Germany

Private: Seelenbinderstr. 2, 04159 Leipzig, Germany

☎ +49 341 9940161 • ✉ falbrecht@cbs.mpg.de

🌐 www.cbs.mpg.de/falbrecht •  [Franziska Albrecht](https://www.researchgate.net/profile/Franziska-Albrecht) •  [@FranziAlb](https://twitter.com/FranziAlb)

Description The thesis investigated the influence of affiliation on pain perception. Participants were shown film clips to induce specific feelings. Before and after the film clips, pain tolerance was assessed using the Cold Pressor Task.

Vocational Experience

2013–2016 **Research Assistant**, *Max-Planck-Institute for Human Cognitive and Brain Sciences, Department of Neurology, Collaborative Research Center (CRC 1052) "Obesity Mechanisms"*, Leipzig, Supervisor: Dr. Annette Horstmann.

Responsible for supporting the planning and conducting of experiments (behavioral tests). Including recruitment of participants, analyzing data, as well as administrative and technical preliminary work. Also establishing and doing preliminary work for the groups database.

2012 **Two-month Internship**, *Max-Planck-Institute for Human Cognitive and Brain Sciences, Department of Social Neurosciences*, Leipzig, Supervisor: Joshua A. Grant, PhD.

Responsible for recruitment of participants, running multi-person testing sessions, taking genetic samples, administer several computer-based tasks, and organization/coordination of testing. Extraction and analysis of data from several studies.

Technical Skills

OFFICE: \LaTeX , Visual Basic for Applications, Microsoft Office, LibreOffice, Adobe Illustrator

STATISTIC SOFTWARE: R, SPSS, GingerALE, Seed-based D mapping, FSL, MATLAB, SPM and toolboxes, Cat12, EEGLAB, libSVM

OPERATING SYSTEMS: MacOS X, Linux-Ubuntu, Windows

Workshops

Good Scientific Practice, Academic writing, MATLAB course for beginner and intermediate user, Bayesian statistics, Project and time management.

Reviewer

ACS Chemical Neuroscience.

Grants

2019 **Leibniz TRAVEL**, *Travel grant Research Academy Leipzig for 14th World Congress of Biological Psychiatry, Vancouver, Canada.*

Travel Grant AFI e.V., *Travel grant Alzheimer Forschung Initiative e.V. for 14th World Congress of Biological Psychiatry, Vancouver, Canada.*

2018 **Leibniz TRAVEL**, *Travel grant Research Academy Leipzig for 11th International Conference on Frontotemporal Dementias, Sydney, Australia.*

2017 **Leibniz TRAVEL**, *Travel grant Research Academy Leipzig for 23rd Annual Meeting of the Organization for Human Brain Mapping, Vancouver, Canada.*

Young Fellowship Programme, *Scholarship for WPA XVII World Congress of Psychiatry Conference, Berlin, Germany.*

Talks

- 2019 **'Wenn Oma oder Opa komisch werden'**, *Presentation with Prof. Dr. Dr. Matthias L. Schroeter*, Girls' Day – Mädchenzukunftstag, Max-Planck-Institute for Human Cognitive and Brain Sciences, Leipzig, Germany.
'Predicting diagnosis, symptoms and treatment response in Parkinsonian syndromes', *Presentation within Symposium 'Predicting diagnosis & treatment in neuropsychiatric disorders with pattern recognition algorithms'*, 14th World Congress of Biological Psychiatry (WFSBP 2019 Congress), Vancouver, Canada.
- 2018 **'Sprechmotorische Störungen bei PPA - neurophonetische Methoden und Bildungsanalysen'**, *Invited Colloquium*, Institute of Phonetics and Speech Processing (IPS), Research Group Clinical Neuropsychology (EKN), Ludwig-Maximilians-University München, München, Germany.
- 2017 **61. Jahrestagung der Deutschen Gesellschaft für Klinische Neurophysiologie und Funktionelle Bildgebung (DGKN)**, *Datablitz presentation*, Leipzig, Germany.

Poster

- 2019 **15th Research Festival Leipzig 2019**, Leipzig, Germany.
Brain-In-Depth (BID) 2019, International Symposium on layer-dependent MRI: Modeling Cortical Microstructure, Leipzig, Germany.
14th World Congress of Biological Psychiatry (WFSBP 2019 Congress), Vancouver, Canada.
9th IMPRS NeuroCom Summer School, Leipzig, Germany.
- 2018 **11th International Conference on Frontotemporal Dementias (ICFTD)**, Sydney, Australia.
Molecular Imaging in Neurodegeneration in Cologne: From Molecules to System Failure: A translational synopsis across the neurodegenerative disease spectrum (MINC Symposium 2018), Köln, Germany.
8th IMPRS NeuroCom Summer School, Leipzig, Germany.
- 2017 **WPA XVII World Congress of Psychiatry Conference**, Berlin, Germany.
7th IMPRS NeuroCom Summer School, London, Great Britain.
23rd Annual Meeting of the Organization for Human Brain Mapping (OHBM), Vancouver, Canada.
- 2016 **Deutsche Gesellschaft für Psychiatrie und Psychotherapie, Psychosomatik und Nervenheilkunde Kongress 2016 (DGPPN), Psyche-Mensch-Gesellschaft**, Berlin, Germany.
10th International Conference on Frontotemporal Dementias (ICFTD), München, Germany.
6th IMPRS NeuroCom Summer School "What makes us human?", Leipzig, Germany.

Publications

- 2019 **Albrecht F**, Mueller K, Ballarini T, Lampe L, Diehl-Schmid J, Fassbender K, Fliessbach K, Jahn H, Jech R, Kassubek J, Kornhuber J, Landwehrmeyer B, Lauer M, Ludolph A C, Lyros E, Prudlo J, Schneider A, Synofzik M, Wiltfang J, Danek A, Otto M, FTLD-Consortium & Schroeter M L, *Predicting Corticobasal Syndrome and Alien/Anarchic Limb Syndrome From Structural Brain Imaging*, *Cortex* (2019), doi.org/10.1016/j.cortex.2019.02.015.
Albrecht F, Bisenius S, Neumann J, Whitwell J & Schroeter M L, *Atrophy in midbrain & cerebral/cerebellar pedunculi is specific for progressive supranuclear palsy - a cross-validation meta-analysis*, *NeuroImage: Clinical* (2019): 101722, doi.org/10.1016/j.nicl.2019.101722.
- 2018 **Albrecht F***, Ballarini T*, Neumann J, & Schroeter M L, *FDG-PET hypometabolism overcomes MRI atrophy in Parkinson's disease: A whole-brain multimodal imaging meta-analysis*, *NeuroImage: Clinical* (2018), doi:10.1016/j.nicl.2018.11.004.
Bezdicek O, Ballarini T, Buschke H, Ruzicka F, Roth J, **Albrecht F**, Ruzicka E, Karsten Mueller K, Schroeter M L & Jech R, *Memory impairment in Parkinson's disease: The retrieval versus associative deficit hypothesis revisited and reconciled*, *Neuropsychology* 33.3 (2019): 391, dx.doi.org/10.1037/neu0000503.
Ballarini T, Mueller K, **Albrecht F**, Ruzicka F, Bezdicek O, Ruzicka E, Roth J, Vymazal J, Jech R & Schroeter M L, *Regional gray matter changes and age predict individual treatment response in Parkinson's disease*, *NeuroImage: Clinical*, 101636 (2018), doi:10.1038/s41531-017-0012-6..
- 2017 **Albrecht F**, Bisenius S, Morales Schaack R & Schroeter M L, *Disentangling the neural correlates of corticobasal syndrome & corticobasal degeneration with systematic & quantitative ALE meta-analyses*, *npj Parkinson's Disease* 3, Article number: 12 (2017), doi:10.1038/s41531-017-0012-6..

Submitted Papers

- Stefanova E, Dubljevic O, Herbert C, Stern E, Urban S, Derntl B, Wiebking C, Brown C, Drach-Zahavy A, Loeffler L, Schroeter M L, **Albrecht F**, Fairfield B, Palumbo R & Leroy L, *Anticipatory feelings*, in revision *Neuroscience & Biobehavioral Reviews*.
- Bezdicek O*, Ballarini T*, **Albrecht F***, Libon D J, Lamar M, Ruzicka F, Roth J, Hurlestone M J, Karsten Mueller K, Schroeter M L & Jech R, *Serial Order Recall in Working Memory across the Cognitive Spectrum of Parkinson's Disease and Neuroimaging Correlates*, in submission *Neuropsychology*.

Publications as Part of Consortium for Frontotemporal Lobar Degeneration (FTLDC study group)

- 2018 Schoenecker S, Neuhofer C, Otto M, Ludolph A, Kassubek J, Landwehrmeyer B, Anderl-Straub S, Semler E, Diehl-Schmid J, Prix C, Vollmar C, Fortea J; Deutsches FTLD-Konsortium, Huppertz HJ, Arzberger T, Edbauer D, Feddersen B, Dieterich M, Schroeter ML, Volk AE, Fließbach K, Schneider A, Kornhuber J, Maler M, Prudlo J, Jahn H, Boeckh-Behrens T, Danek A, Klopstock T & Levin J, *Atrophy in the Thalamus But Not Cerebellum Is Specific for C9orf72 FTD and ALS Patients - An Atlas-Based Volumetric MRI Study.*, *Front Aging Neurosci.* 2018 Mar 15;10:45., doi: 10.3389/fnagi.2018.00045., eCollection 2018..

Steinacker P, Verde F, Fang L, Feneberg E, Oeckl P, Roeber S, Anderl-Straub S, Danek A, Diehl-Schmid J, Fassbender K, Fliessbach K, Foerstl H, Giese A, Jahn H, Kassubek J, Kornhuber J, Landwehrmeyer GB, Lauer M, Pinkhardt EH, Prudlo J, Rosenbohm A, Schneider A, Schroeter ML, Tumani H, von Arnim CAF, Weishaupt J, Weydt P, Ludolph AC, Yilmazer Hanke D, Otto M & FTLDc study group, *Chitotriosidase (CHIT1) is increased in microglia and macrophages in spinal cord of amyotrophic lateral sclerosis and cerebrospinal fluid levels correlate with disease severity and progression*, J Neurol Neurosurg Psychiatry. 2018 Mar;89(3):239-247., doi: 10.1136/jnnp-2017-317138.